Development of an Energy Module for the Multi-objective Optimisation of complex distillation Processes

This dissertation is approved by the Faculty of Environmental Sciences and Process Engineering at the Brandenburg University of Technology Cottbus in partial fulfillment of the requirement for the award of the academic degree of Doctor of Engineering (Dr.-Ing.) in Process Engineering

by

(M.Sc.)
Tijani, Alhassan Salami

from Accra, Ghana

Supervisor:	Prof. Dr.-Ing. Werner Witt
Supervisor:	Dr.-Ing. Jörg Schmuhl (Visiting Professor)

Date of oral examination: 4th June, 2010

Zur Entwicklung eines Energiemoduls für komplexer Destillations-Verfahren unter Berücksichtigung der multikriteriellen Optimierung

Von der Fakultät für Umweltwissenschaften und Verfahrenstechnik der Brandenburgischen Technischen Universität Cottbus zur Erlangung des akademischen Grades eines Doktor-Ingenieurs (Dr.-Ing.) genehmigte Dissertation

vorgelegt von

(M.Sc.)
Tijani, Alhassan Salami

aus Accra, Ghana

Gutachter:	Prof. Dr.-Ing. Werner Witt
Gutachter:	Dr.-Ing. Jörg Schmuhl (Gastprofessor)

Tag der mündlichen Prüfung: 4. Juni 2010

Declaration

I hereby declare that my Doctoral Thesis is the result of my research work under the supervision of Prof. Dr.-Ing. Wernerho is my main supervisor, and Visiting Professor Dr.-Ing. Jörg Schmuhl as my second supervisor. All literature sources used for the writing of this dissertation have been adequately referenced. Also justified is the fact that this work is in no way a reproduction in part or whole of any work ever presented for the award of a degree.

Sign……. Date……

Alhassan Salami Tijani

Faculty of Environmental Sciences and Process Engineering

Chair of Plant Design and Safety Technology, BTU Cottbus Germany

Acknowledgement

All praises be to Almighty Allah (God), the Creator and Sustainer of this universe, First of all, I praise and thank Almighty Allah for motivating and guiding me on the right path throughout my doctorate research work, I praise Him and further seek His help in any moment of my life. May the peace and choicest blessings of Allah be upon our Prophet Muhammad (saw), his family and companions Amin.

I will like to express my deepest appreciation and special thanks to my supervisor, Prof. Dr.-Ing. Werner Witt for his wonderful support and contributions towards the success of my doctorate research work. It has been a great pleasure to work with him. My dear mother, Alhaja Senabu Gbadamosi and my entire family would like to say a very big thanks to my supervisor. His contribution towards my success is very much appreciated. I would like to acknowledge and express my gratitude also to my advisor Dr.-Ing. L. Dietzsch for his important information and support during scientific and technical discussions.

I would like to thank Prof. Dr.-Ing. Jörg Schmuhl for taking over the role of second supervisor, his contributions and advices are most appreciated.

I will like to thank all my scientific research colleagues at the Chair of Plant Design and Safety Technology who did not hesitate to help me whenever the need arises.

I am particularly grateful to my parents and family for their love, encouragements and support they gave me. It is because of their prayers that enable me to complete this doctorate work.

Finally I would like to thank all my friends for their great love and encouragement during my stay in Cottbus.

Dedication

This scientific research work is dedicated to my Almighty Allah (God) and His Prophet Muhammad (SAW).

Table of Content

Nomenclature

Symbols	units	Description
A	m^2	area
c	\$/kg	specific cost
$\mathbf{C}^*_{cw}$	\$/kg	cooling water cost
$\dot{\mathbf{C}}$	\$/y	cost per year
C_{el}	\$/kWhr	electricity cost
D	m	diameter
$\dot{\mathbf{d}}$	1/y	depreciation factor
Ex	kJ	exergy
En	kJ	energy
$\mathbf{ex}^*$	MJ/kg	specific exergy
$\dot{\mathbf{F}}_j$	kmol/hr	molar flow rates of feed on stage j
F_M	-	material factor
F_{BM}	-	bare-module factor
h	kJ/kg	specific enthalpy
$\dot{\mathbf{L}}_j$	kmol/hr	molar flow rates of liquid on stage j
L	m	length
$\dot{\mathbf{M}}$	kg/hr	mass flow rate
N_{act}	-	number of trays
p	bar	pressure
$\dot{\mathbf{P}}$	kW	electrical power
R	kJ/kmol/K	gas constant 8,3124 kJ/kmol/K
s	$\mathbf{kJ/(K \cdot kg)}$	entropy
T	K	temperature
W_{min}	$kJ/kmol_{feed}$	minimum separation work
$\dot{\mathbf{Q}}$	kW	heat duty
PEI	(PEI/hr)	PEI due to energy consumption
$\boldsymbol{\psi}_{ki}$	PEI/MJ	normalized impact score for chemical k for category i
$\dot{\mathbf{Q}}_{En}$	MJ/hr	rate of energy consumption
$\dot{\mathbf{V}}_j$	kmol/hr	molar flow rates of vapour on stage j
$\tilde{\mathbf{x}}_{jF}$	kmol/kmol	mole fraction of component j in feed
$\tilde{\mathbf{x}}_{jD}$	kmol/kmol	mole fraction of component j in distillate
$\tilde{\mathbf{x}}_{jB}$	kmol/kmol	mole fraction of component j in bottom
$\tilde{\mathbf{z}}_{i,j}$	kmol/kmol	mole fraction of feed on stage j

Greek symbols

γ_{jF}	activity coefficient of component j in feed mixture
γ_{jD}	activity coefficient of component j in distillate/Head
γ_{jB}	activity coefficient of component j in bottom

Subscripts

act	active
B	bottom
col	column
cw	cooling water
compr	compressor
D	distillate
el	electricity
F	feed
FCI	fixed capital investment
TDC	total depeciable cost
Hp	horse power
Stm	steam
Reb	reboiler
Hx	heat exchanger
irr	irreversible
ch	chemical
p	potential
k	kinetic
ph	physical

Superscripts

En	energy
Ex	exergy
L	Liquid
V	vapour

Abstract

Reduction of energy consumption has increasingly come into sharp focus in the chemical process industry. This is of great value not only for existing plant but also for the development of new processes. Therefore, the challenge for process design engineers to develop an integrated chemical process that simultaneously satisfies economic and environmental objectives has increased considerably. Particularly, multi-objective optimization in the chemical industry has become increasingly popular during the last decade. The main problem lies, in selecting the alternative best design during decision making with multiple and often conflicting objectives.

This thesis work presents a methodology for the multi-objective optimization of process design alternatives under economic and environmental objectives and also to establish the linkage between exergy and the environment.

Four distillation units design alternatives with increasing level of heat integration were considered. Each design is analysed from exergy, potential environmental impact (PEI) and economic point of view. A non-dominated solution known as the “Pareto optimal solution” is generated for decision making. The thermodynamic efficiency indicates where exergy losses occur.

The demand for industrial process heat by means of solar energy has generated much interest because it offers an innovative way to reduce operating cost and improve clean renewable electric power. Concentrated Solar Thermal Power (CSP) can provide solution to global energy problems within a relatively short time and is capable of contributing to carbon dioxide reduction, which is an important step towards zero emissions in the process industries. This work provides an overview of a simulation model to evaluate the environmental and economic performance of two case studies of solar thermal power plants. A methodology is presented to integrate solar thermal power plant into industrial processes and this is then compared with an existing hydrocarbon recovery (HCR) plant that depends on coal as its energy source. The two process design alternatives where simulated using the process simulator Aspen Plus^{TM}. This thesis work also evaluates two types of power plants based on coal. The plants considered provide utility systems such as steam and electrical energy to the process plants. Exergy analysis was performed for each type of plant. The standard PEI calculation procedure has been modified for consideration of specific energy resources or power plants.

Kurzfassung

Die multikriterielle Optimierung hat in der chemischen Industrie eine zunehmende Bedeutung für die Entscheidungsfindung bei der Auswahl des besten Entwurfs erhalten. Gleichzeitig mehrere Ziele, wie z.B. Wirtschaftlichkeit und Umweltschutz zu verfolgen, ist eine Herausforderung für Verfahrensingenieure. Die Verminderung des Energieverbrauchs gewinnt in der chemischen Verfahrensindustrie zunehmend an Gewicht. nicht nur für existierende Anlagen, sondern auch für die Entwicklung von neuen Verfahren.

Die vorliegende Arbeit präsentiert einen Ansatz für eine multikriterielle Optimierung von Verfahrensentwurfsalternativen unter Betrachtung von Ökonomie und Umweltschutz als auch Exergy und der Umweltschutz. Vier Destillationsalternativen mit unterschiedlich intensiver Wärmeintegration wurden untersucht. Es wurden jeweils die Exergy, die potenzielle Umweltwirkung (PEI) und Ökonomie analysiert.

Die direkte Erzeugung von Dampf mittels Sonnenenergie (Concentrated Solar Thermal Power, CSP) hat viel Interesse erzeugt, weil dadurch Betriebskosten verringert und gleichzeitig Umweltbelastungen (Kohlendioxidemission) reduziert werden können. In dieser Arbeit wird beispielhaft anhand von zwei Fallstudien gezeigt, wie die Verknüpfung thermische Solarkraftwerke mit industriellen Prozessen vorgenommen werden kann. Die zwei Prozessalternativen wurden unter Verwendung des Prozesssimulators Aspen PlusTM und das Solarkraftwerk unter Einsatz von Genius simuliert. Für die Bewertung der Umweltbelastung nach dem PEI - Berechnungsverfahren wurden Alternativen entwickelt.

1 Introduction

As energy prices continue to rise, chemical companies are increasingly looking towards energy efficiency as a way to reduce production costs and improve their competitive edge. The challenge for today's chemical manufacturers is to effectively focus their resources on improving the equipment and processes that will produce the greatest benefits in energy use.

Distillation is still the major separation process used in the chemical processing industry because of its numerous advantages. However, one important drawback is its considerable energy consumption. Distillation can generate more than 50% of plant operating cost. Due to recent increase in energy cost and environmental concerns, improvement of distillation is important.

Exergy analysis is an efficient technique for the design of more efficient thermal systems by reducing inefficiencies. Al-Muslim et al. [1] conducted a thermodynamic analysis of distillation systems to study energy and exergy efficiencies for system analysis, performance evaluation and optimization. Recently, there has been increasing number of publications on the linkage between exergy and the environment (e.g. [2]). Significant attention has been directed towards the use of exergy analysis in the assessment of thermal and other industrial processes and their environmental impacts. The concept of the environment as it applies to exergy analysis is discussed in detail elsewhere [3], [4]**.** While some authors integrate environmental issues in the form of waste treatment and waste disposal costs into an objective function [5], [6], others propose the use of mass of waste as an environmental indicator and profit as an economic indicator [7]. Cano-Ruiz et al. [8] published a review paper about incorporating environmental issues into the design of new processes and manufacturing facilities. This review explains the need to view environmental issues as part of the design objectives rather than as constraints on operations. The application of multi-objective optimization in the chemical industry has become increasingly significant. Process optimization is aimed at significant optimizing economic as well as environmental benefits; this can be modelled as a multi-objective optimization (MOO).

In this work, a new methodology is presented to integrate solar thermal power plant into industrial processes. Two case studies of solar thermal power plants were considered, case I provides utility system such as steam and case II generates electrical power to operate the process units. Also in this work, the old method of energy generation via coal was performed. Two case studies of coal power plant were analyzed, it is assumed that both plants use the same quantity of coal to produce both electrical energy and steam. Energy/ exergy analysis as well as PEI of the two coal power plants where performed. The standard PEI calculation

procedure has been modified for consideration of specific energy resources. The overview of the goal of this study is shown in figure 1.1.

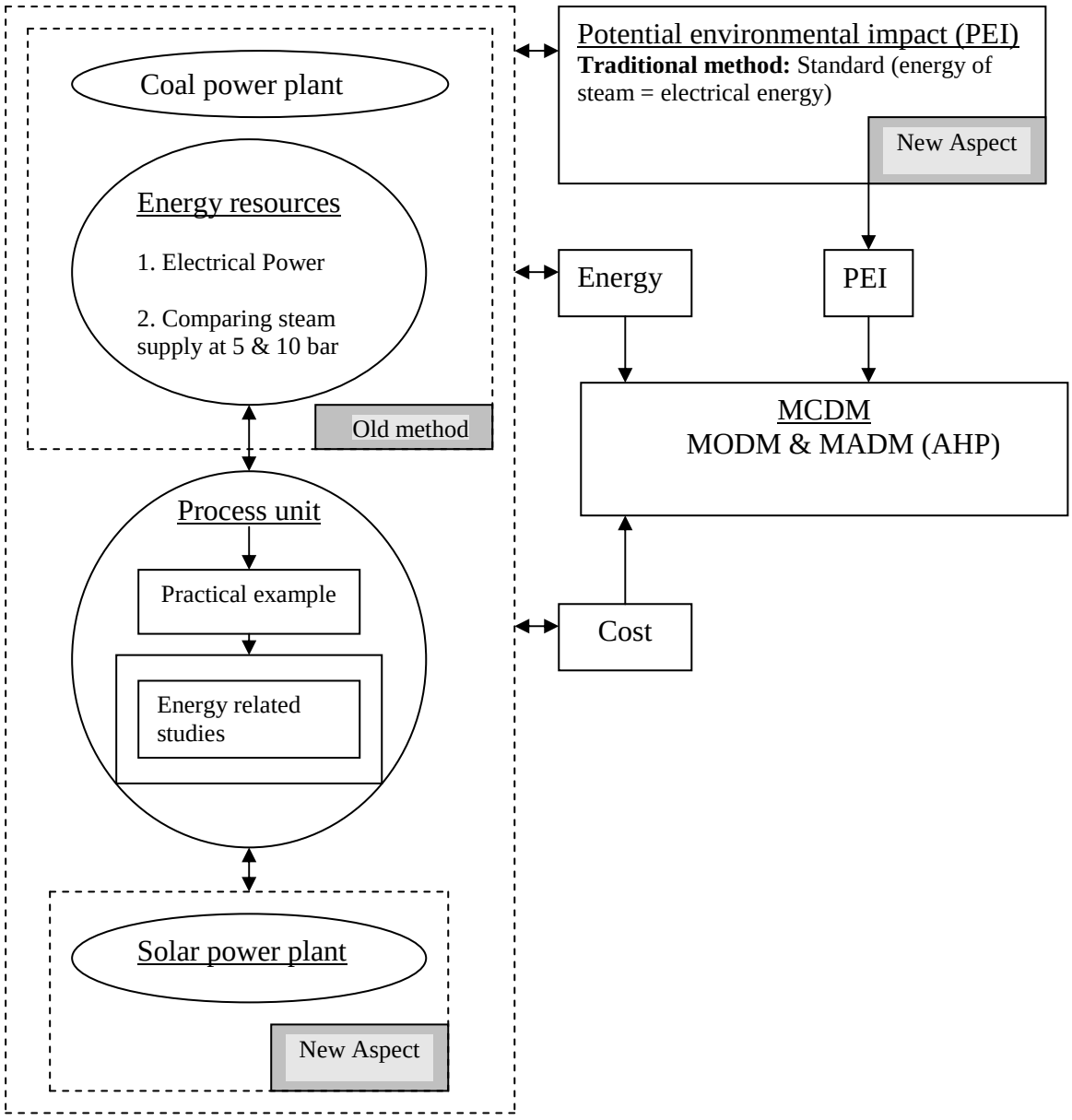

Figure 1.1. Overview of goal of study

In many applications, such as in the chemical process industry, the decision maker has multiple alternatives and multiple conflicting objectives. Therefore the existence of a number of criteria such as economic, potential environmental impact requires the use of a Multi-criteria decision making (MCDM) approach. The areas of MCDM applied in this work can be divided into two categories:

- Multiple Attribute Decision Making (MADM)

- Multiple Objective Decision Making (MODM)/Optimization

The goal of this work (refer to figure 1.1) is to present a methodology for the multi-objective optimization of process design alternatives under economic and environmental objectives and also to establish the linkage between exergy and the environment.

Various heat pumping schemes and pump around have been proposed as a means of saving energy in distillation. Of these schemes, the use of the column overhead vapour as the heat pumping fluid is usually the most attractive. In this work, the case studies presented are four design alternatives of distillation units with increasing levels of heat integration. The four process design alternatives were simulated using the process simulator Aspen Plus^{TM}. Because the main objective of this thesis is the development of a methodology for the multi-objective optimization of a chemical plant, the knowledge and discussion of the relevant fundamentals is a prerequisite of application of the method, this will be presented in the next chapter.

1.1 Motivation

Process energy integration and continuous improvement of process technology are important issues to ensure profitability of chemical productions. The complexity and challenges of today's production in the chemical industry is rapidly growing. This is because the number of performance criteria which have to be optimized are continuously increasing. Further more it is important to keep in mind that design problems may have solutions that are attractive and near the optimal solution. The integrated design process can be classified as a multiobjective optimization problem (see figure 1.2).

In standard optimization, the economic objective function is defined based on operating cost and Fixed Capital Investment (FCI) [9]-[13]. In order to achieve optimum results, appropriate independent or decision variables have to be selected. Modification of these variables must directly affect the objective function.

In the advanced optimization step, two objective functions are defined i.e. minimization of Economic and Potential environmental impact. These objectives are further classified into sub objectives which have to be considered, in order to reach the top goal of Multi-objective Optimization. These sub-objectives which are considered for process optimization are usually interlinked in a complex way and they include, heat integration, Potential environmental impact and safety etc.

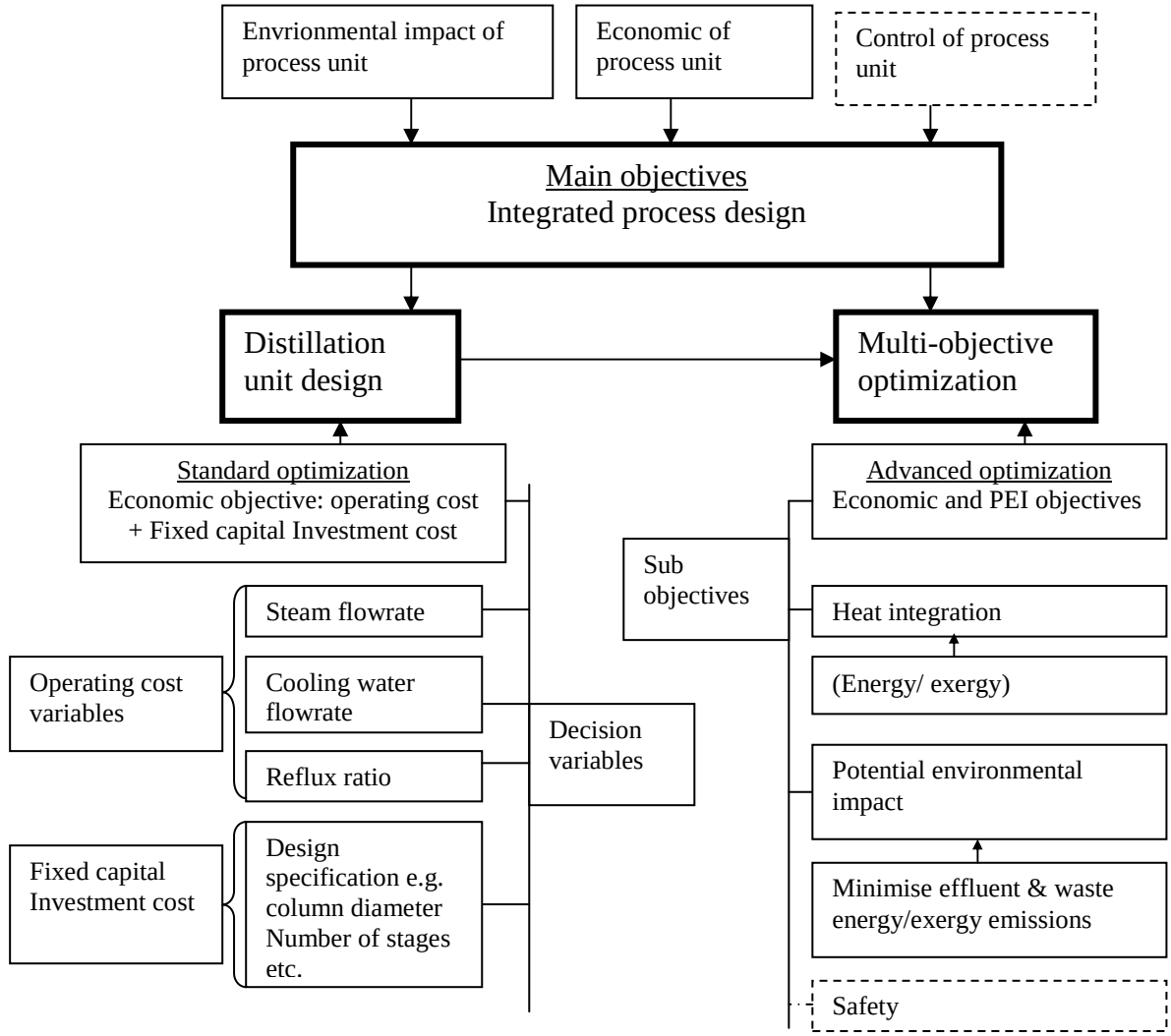

Figure 1.2. Structure of integrated process design

Applied in this work
Other possible applications tools

In terms of process analysis the sub objectives also represent the viewpoints under which production plant performance are measured. The above motivation gives the basis for objective of this work which is discussed in the next section.

1.2 Objectives

This thesis presents results of work on different aspects of computer aided mathematical models of process systems. The thesis concentrates on those mathematical models that consist mainly from a theory applied to a particular process system. Due to the challenges raised by the above criteria, the objectives of this thesis can be stated as follows:

- ✓ Developing exergy analysis method for optimization of distillation unit
- ✓ Improving the existing process with respect to performance criteria
- ✓ Minimizing energy and exergy consumption of the process plant
- ✓ Minimizing environmental impact due to energy and exergy of the process plant
- ✓ Improving thermodynamic efficiency of distillation
- ✓ Development of methodology for the multi-objective optimization of process design alternatives under economic and environmental objectives

Since distillation processes require large amount of energy, it is important to design and operate them as efficiently as possible in order to reduce their energy consumption. In this context it is important to note that not only energy costs are of interest but also the environmental aspects. Whenever fossil fuels are burned, CO_2 is emitted, contributing to global warming. The objective of this thesis is therefore to analyse the PEI of different power plants that produce steam and electrical power to operate distillation units. The reason for selecting distillation unit is that, like all other chemical process, distillation is known to have greatly contributed in many ways to the overall environmental impacts of separation processes because of its high energy consumption, because of this, potential environmental impact (PEI) has become an important criteria for the assessment of environmental performance of modern chemical industries. The overview of the objectives of this thesis that considered some new aspects is shown in figure 1.3.

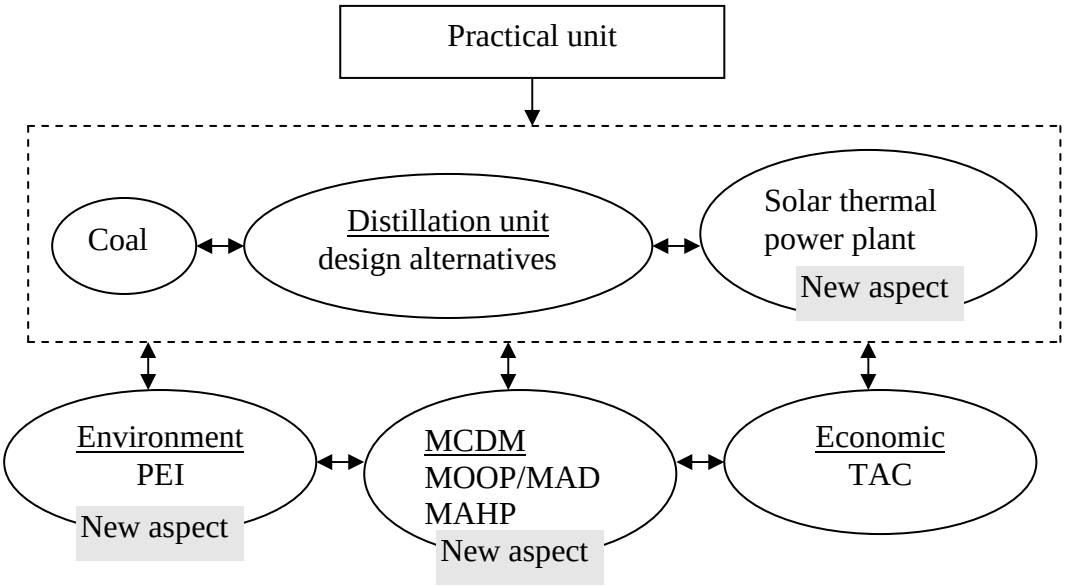

Figure 1.3. Objectives of thesis

1.3 Structure of this thesis

Process simulation in this work means, the application of deterministic modeling (i.e. models based on physical relationships). Over the last decades large deterministic models for distillation systems have been developed and applied to real world processes (see e.g. Skogestad [14] and Evans [15]). The advantage of deterministic models is the inclusion of physical and chemical knowledge, deterministic has the capability to predict trends and provides insights into the physical behaviour of the system. Often the understanding of the real process is improved, by developing and improving the simulation models.

All process models can be divided into steady state models and models which can represent the dynamic behaviour of the process. The real process plant is translated into a simulation model for the purpose of understanding the behaviour of the system. In the context of distillation processes, rigorous means, that the conditions on each tray in a column are determined by a system of ordinary differential and algebraic equations, further more, rigorous modeling implies accurate thermodynamic models, modeling fluid dynamics and good representation of heat and mass transfer. The mass transfer can be either modeled by assuming thermodynamic equilibrium, or with the inclusion of mass transfer laws. Following this introduction, this thesis is arranged into five chapters as follows:

Chapter one presents a brief discussion of the motivation and objective of this thesis.

Chapter two provides an overview of the fundamentals of the current state of the art methods for separating mixtures. A discussion of their strengths and drawbacks with respect to the design of processes for the separation of complex multi-components mixtures are presented. Detail theoretical discussions of energy/exergy consumption of these techniques are also presented. In section 2.4, the fundamental background of potential environmental impact objective as well as the linkage between exergy and the environment has been discussed. The theory and concept of the WAR algorithm and the potential environmental impact balance including energy and exergy is also described in this section. In section 2.5 the fundamentals of mathematical model of the main components of solar thermal power plant are described. Also in section 2.6, the fundamental design aspects of economic models which are implemented in the integrated methodology are discussed. Section 2.8 provides an overview of multi-criteria decision analysis (MCDA), also a Multiple Attribute Decision Making technique like AHP is applied in the ranking of alternatives.

In chapter three, some techniques that can be applied to improve the exergetic efficiency of distillation systems by integration of power plant and distillation are discussed. In this section

the theoretical approach (such as Carnot efficiency) as well as the practical approach of a heat pump distillation is discussed. Two main examples were studied:

- Combine power plant and heat pump (operated via electrical power)
- Combine power plant and distillation unit (operated via steam)

In Chapter four the standard PEI model is discussed, with some modification of the WAR algorithm. Different models were applied in calculating the PEI. The most significant modification to the WAR algorithm is the inclusion of exergy consumption into the potential environmental impact calculations. These models were further applied to power plant alternatives.

Chapter five discusses the different types of models that are used to compare different design alternatives of distillation units. The main models considered are:

- Economic Module
- Energy and exergy Module
- Environmental Module

A multiobjective optimization method is applied to each model to evaluate process improvement alternatives. Total annualized cost (TAC) and potential environmental impact (PEI) are taken as objective functions.

In Chapter six Two design alternatives that consist of integration of solar thermal power plant with distillation unit are discussed.

Chapter seven provides conclusions and recommendations for future work. A summary of the obtained results is given and the contributions of the thesis are highlighted.

2 Fundamentals

Distillation is still the most widely used separation technique in the chemical industry, in spite of its inherently low thermodynamic efficiency. In a more recent study, Humphrey and Siebert [16] stated that approximately 40,000 distillation units installed in the USA use 1.2 million barrels of crude oil daily. Energy–efficient design and operation are therefore important issues. Previous work has shown that potentially large savings could be obtained in the use of high quality energy (Rivero [17]). Kister [18] said that from thermodynamic viewpoint, a typical thermodynamic efficiency of a distillation system is about 10 %, this can be improved if intercondensers, interreboilers and heat pump are used. This chapter discusses the current state of the art methods for separating mixtures, with emphasis on energy consumption of these techniques.

2.1 Energy efficient distillation process design

Due to rising cost of energy, much attention has been given to the comparison of conventional distillation columns (see figure 2.1a) with other new design in order to achieve lower energy consumption. To improve distillation processes, three important areas can be identified.

- *Internals*: The energy efficiency can be improved with a better design of the column internals. By introducing packings, the number of theoretical stages in a given column can be increased, resulting in a lower reflux ratio and consequently in a lower energy requirement. With packings it is also possible to reduce the pressure drop in the column. This aspect is not covered in this work.
- *Heat integration*: Heat pump: various heat pumping schemes have been proposed as a means of saving energy in distillation. Of these schemes, the use of the column overhead vapour as the heat pumping fluid is usually the most attractive [19]-[20]. A detailed analysis of the applicability of vapour recompression has been published by many authors and recognized for its efficient application.

Null [21], Henley and Seader [22] have devoted a lot of attention to this subject. Null has discussed the different configurations of electrically driven heat pump-assisted distillation. The most widely used methods are: direct vapour recompression, external working fluid (closed cycle heat pump) and bottom flashing. In direct vapour recompression, the vapour leaving the top of a distillation column is compressed to a desired pressure/temperature, and is condensed in the reboiler of the same column, thus providing the heat needed for the generation of the required vapour flow rate along the column.

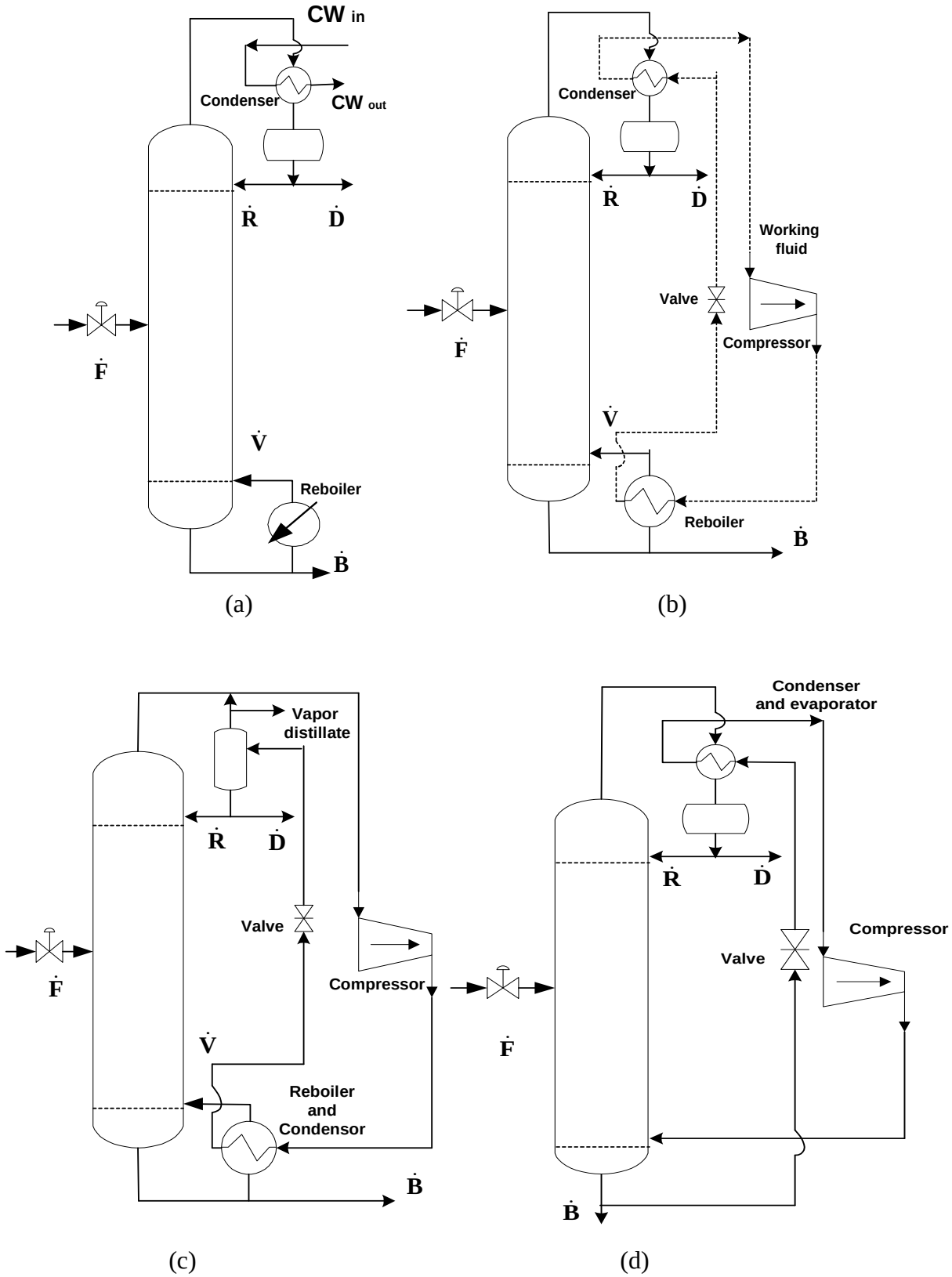

Figure 2.1. Simplified heat pump circuits: (a) Conventional distillation column, (b) Closed circuit heat pump, (c) Open circuit heat pump (compression of overhead vapor), (d) Open circuit heat pump (compression of reboiler evaporated stream). Source: King [23]

Such schemes are illustrated in figures 2.1 (b-d). In figure 2.1 b, an external heat pump (Closed circuit heat pump) is used, the heat taken from the condensers is raised to a high temperature by means of a compressor and then sent to the reboiler. In the alternative with compression of overhead vapour (see figure 2.1 c), the overhead vapour is heated up by compression and used to drive the reboiler. In the last configuration (see figure 2.1 d), the bottom product is vaporized by expansion through a valve, it is further evaporated by passing through the condenser.

- *Pumparound*: The purpose of the pump-around is to liquify part of the up flowing vapour by means of heat integration and to make useful heat available at the same time.

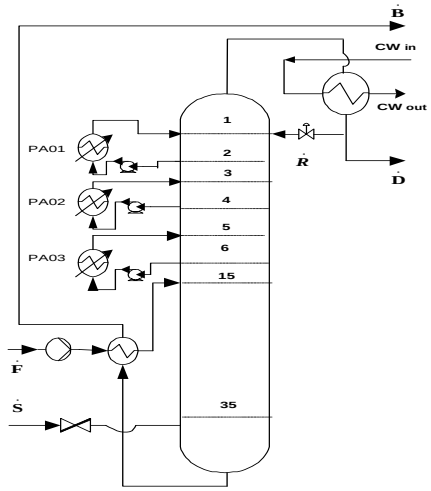

Figure 2.2. Pumparound distillation column

The pump-around circuit shown in figure 2.2 draws liquid from a tray, cools the liquid in a heat exchanger and returns the liquid to a tray above the original tray. The most important function of the pump-around is recovering heat to a process stream that would otherwise be lost to the cooling tower via the overhead condenser. Another purpose of the pump-around is to suppress top-tray flooding. In this work both the heat pump and the pumparound distillation columns are considered.

2.2 The use of energy as applied to distillation process

Distillation is the most used separation operation in chemical and petrochemical industries. Separation systems mainly involve interfacial mass and heat transfer as well as mixing. Heat is supplied from a higher temperature level at the reboiler and rejected in the condenser at a lower temperature level. It uses heat as the separating agent in a thermodynamically inefficient way.

This is why its ever-growing application is accompanied by a large increase in consumption of energy. According to the Gouy Stodola principle, high energy consumption in separation systems is due to irreversible processes of heat, mass transfer, and mixing, and is directly related to entropy production Demirel [24]. Zemp et al. [25] identified beneficial changes, like optimum feed stage, optimum feed thermal condition, as well as the possible benefits of using intermediate heat exchangers instead of changes in the thermal condition of the feed. On the basis of exergy analysis, Faria [26] used the exergy loss profile of a real column to correctly identify the optimum feed stage and thermal condition and other changes which improve column efficiency.

2.3 General fundamentals

Even though energy and exergy are expressed in the same unit, there exist significant differences.

Table 2.1. Energy vs. exergy

Energy	Exergy
The first law of thermodynamics	The second law of thermodynamics
Energy is a measure of quantity	Exergy is a measure of quality and quantity
Energy is always conserved, i.e., in total balance, it can neither be produced nor consumed.	Exergy is only conserved in a reversible process, but partly consumed in an irreversible process, i.e., real processes. Thus, exergy is never in balance for real processes

Source: Chamchine, [27]

2.3.1 Energy bandwidth analysis

Energy bandwidth analysis provides a measure of opportunities for energy savings through improvements in technology, process design and operating practices [28]. The bandwidth analysis quantifies the differences between process plant energy consumption levels as shown in figure 2.3. The current average process energy (Level 1) is based on the average energy consumption by a typical plant in today's manufacturing environment. A typical plant can reduce its process energy consumption by implementing best practices and incorporating existing state of the art equipment and process technologies and achieve the state of the art process energy (Level 2). A plant that has achieved the Level 2 is also referred to as a "World's Best Plant" [28] The practical minimum process energy (Level 3) is the industry average process energy

requirement for a typical plant after installation of new process technologies developed through applied research and development (R&D) beyond Level 2. The theoretical minimum energy (Level 4) is the absolute minimum process energy required by thermodynamics to convert raw materials into products under ideal conditions. It is important to note that the practical minimum energy is a "moving target" and its position depends on the level of technology R&D advancements

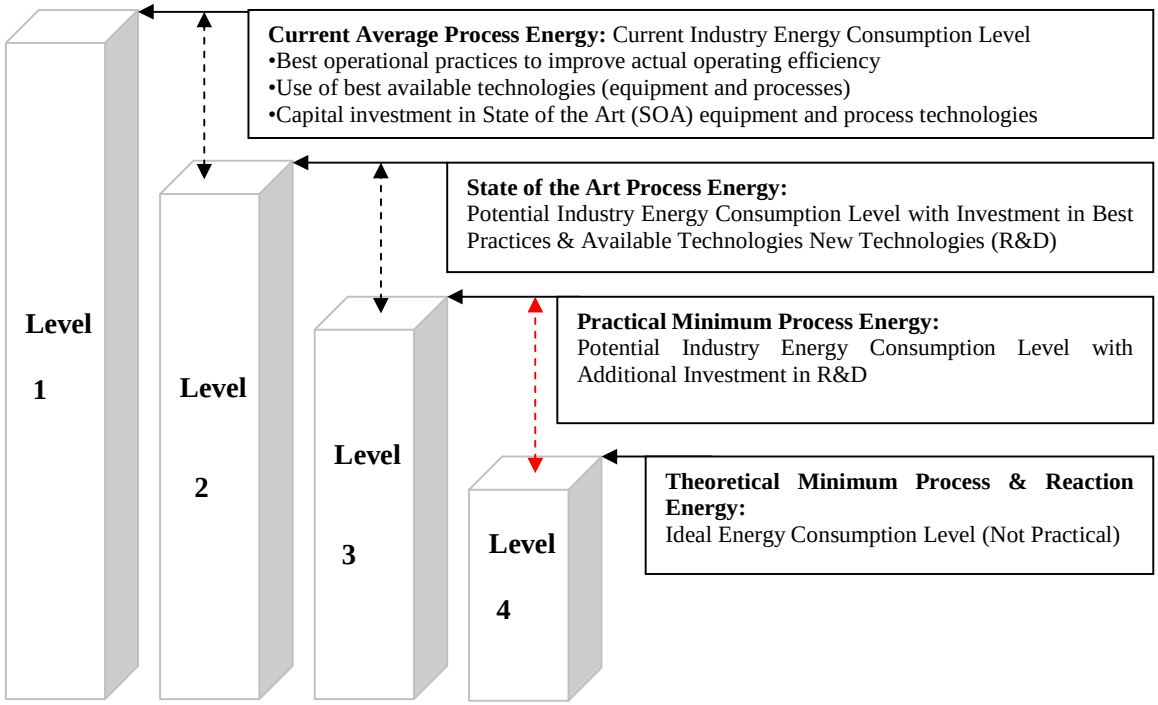

Figure 2.3. Typical Plant Process Energy Consumption Levels, Source: [28]

2.3.2 Minimum (reversible) work requirement for separation

There is a minimum amount of thermodynamic work involved in separating a mixture into its constituents regardless of the method of separation. The first step in such analysis is the determination of the minimum (reversible) work requirements for separation. Under isothermal conditions, the minimum work of separation is equal to the increase Gibbs free energy of the products compared with the feed. It is very important to determine the minimum (reversible)

work requirement for conducting a separation and to seek a practical process that approaches a limit or minimizes the use of expensive forms of energy. As a generalization of the thermodynamic analysis presented by Fratzscher et al. [29] and Robinson et al. [30], the minimum work requirement for separation of a mixture into pure products at constant pressure and temperature is given by:

$$\mathbf{w_{min} = \tilde{R} \cdot T_a \cdot \left[\sum_j \tilde{x}_{jF} \cdot \ln(\gamma_{jF} \cdot \tilde{x}_{jF}) - \frac{\dot{M}_D}{\dot{M}_S + \dot{M}_F} \cdot \sum_j \tilde{x}_{jD} \cdot \ln(\gamma_{jD} \cdot \tilde{x}_{jD}) - \frac{\dot{M}_B}{\dot{M}_S + \dot{M}_F} \cdot \sum_j \tilde{x}_{jB} \cdot \ln(\gamma_{jB} \cdot \tilde{x}_{jB}) \right]} \quad (2.1)$$

Equation (2.1) is applied to the case if the feed (F) is separated into two product streams i.e. distillate (D) and bottom (B). Mixtures with positive deviation from Raoult`s Law, i.e. mixtures with activity coefficient greater than 1, require lower minimum work for separation than do ideal solutions, the reverse is true for solutions with negative deviations [30].

Illustrative example of minimum (reversible) work calculation

Table 2.2 shows the stream properties of the distillation unit under study. These data together with other information (see appendix A.1) obtained from simulation are used to calculate the minimum work of the distillation unit. Since the separation process is a nonisothermal process;

Table 2.2. Stream properties of a distillation unit

Stream properties j	FEED	STEAM	BASE	HEAD
Total Flow kg/hr	4020	603	3672.1	950.90
Temperature ^{o}C	68	141	101.3	46.8
$\sum_j \tilde{x}_{jF} \cdot \ln(\gamma_{jF} \cdot \tilde{x}_{jF})$	-0,36362748	0	-0,10118988	-1,41643412

The reversible work $\mathbf{w_{min}}$ can be computed by first of all, finding the average temperature of separation (Robinson et. al. [30]) as follows:

$$\mathbf{T_a = \frac{T_B - T_D}{\ln \frac{T_B}{T_D}} = \frac{374.3 - 319.8}{\ln \frac{374.3}{319.8}} = 346.4\ K}$$

$$\mathbf{\tilde{R} = 8.3124 kJ/(kmol \cdot K)}$$

The reversible work $\mathbf{w_{min}}$ required per kmol of feed is calculated as follows:

$$\mathbf{w_{min} = 8.3124kJ/(kmol \cdot K) \cdot 346.4K \cdot \left[- 0.3636 - \left(\frac{950.904}{603 + 4020} \right) \cdot (-1.4164) - \left(\frac{3672.069}{603 + 4020} \right) \cdot (- 0.1012) \right]}$$

$$\mathbf{w_{min} = 23.305kJ/kmol_{feed}}$$

Numerical computations shows that the minimum separation power (4.2MJ/hr) is rather small compared to real energy input (7134 MJ/hr) of the example described.

$$\mathbf{\dot{p}_{min} = 23.205kJ/k\ mol \cdot 182.115\ kmol/hr}$$

$$\mathbf{\dot{p}_{min} = 4225kJ/hr}$$

2.3.3 Exergy

In this study, T_a is used as ambient temperature condition and T_o is used as lowest process temperature.

2.3.3.1 Exergy of flowing stream of matter

The exergy of a stream of matter is the maximum work (useful energy) that can be obtained from it in taking it to complete equilibrium (temperature and pressure) with the environment (Rivero 1993) [31]. For a stream of matter, the exergy flow can be expressed as:

$$\mathbf{\dot{E}x_S = \dot{E}x_k + \dot{E}x_p + \dot{E}x_{ph} + \dot{E}x_{ch}} \qquad (2.2)$$

Where $\mathbf{\dot{E}x_k}$ =Kinetic exergy, $\mathbf{\dot{E}x_p}$ =Potential exergy, $\mathbf{\dot{E}x_{ph}}$ =Physical exergy, $\mathbf{\dot{E}x_{ch}}$ =Chemical exergy. In this study $\mathbf{\dot{E}x_{ch}}$, $\mathbf{\dot{E}x_p}$, and $\mathbf{\dot{E}x_k}$ are assumed to be irrelevant, so only $\mathbf{\dot{E}x_{ph}}$ was considered, equation (2.2) therefore reduces to:

$$\mathbf{\dot{E}x_{ph} = (\dot{H} - \dot{H}_a) - T_a \cdot (\dot{S} - \dot{S}_a)} \qquad (2.3)$$

Where the subscript “a” indicates ambient conditions. The first term between brackets of the right-hand side of equation (2.3), represents the enthalpy flow rate and the second term entropy flow rate.

The above definition follows the 2nd Law of Thermodynamics, which states that not all heat energy can be converted to useful work. The portion that can be converted to useful work is referred to as exergy, while the remainder is called non-exergy input.

Today, engineers and scientists often use enthalpy (a thermodynamic quantity equal to the amount of energy in a system) or energy balances to evaluate the performance of chemical production processes and quantify energy losses [32]. However, this approach does not consider the quality of the energy loss or the actual energy potential associated with process streams.

Exergy analysis provides a powerful way for assessing the quality of energy and quantifying the portion of energy that can be recovered. For example, a large percentage of energy content can be extracted from flowing steam at high temperatures. As the steam temperature drops (e.g. after passing through a heat exchanger), the percentage of energy that can be recovered is reduced. This drop in energy quality is referred to as a loss of exergy or energy degradation. The concept of exergy and energy quality as applied to a chemical process is shown in figure 2.4.

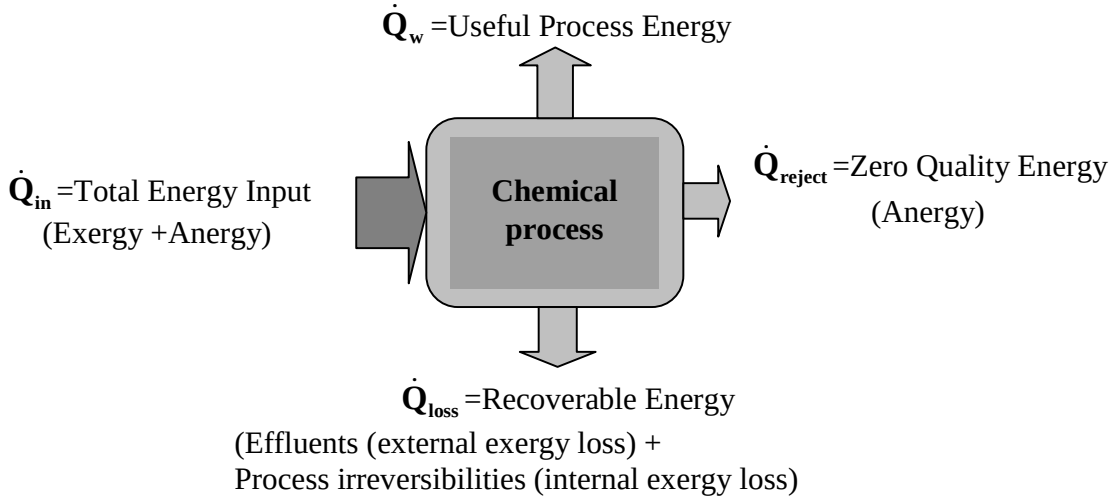

Figure 2.4. Energy vs. exergy, Source: [28]

Total energy input ($\dot{Q}_{in}$) consist of both exergy and non-exergy input. During the process, some of the total energy input (see equation (2.4)) is converted to some useful work ($\dot{Q}_w$), while some is lost due to internal and external energy loss factors ($\dot{Q}_{loss}$).

$$\dot{Q}_{in} = \dot{Q}_w + \dot{Q}_{loss} + \dot{Q}_{rejected} \quad (2.4)$$

The non-exergy component of total input energy has zero quality and is rejected ($\dot{\mathbf{Q}}_{\mathbf{rejected}}$).

2.3.3.2 Exergy of heat transfer

The amount of thermal exergy transfer associated with heat transfer $\dot{\mathbf{Q}}_{\mathbf{reb}}$ across the systems boundary at constant temperature T_s is:

$$\dot{\mathbf{E}}\mathbf{x}_{\mathbf{Q}_{\mathbf{reb}}} = \left(1 - \frac{\mathbf{T_a}}{\mathbf{T_s}}\right) \cdot \dot{\mathbf{Q}}_{\mathbf{reb}} \tag{2.5}$$

The term in the bracket is the Carnot efficiency factor. This equation implies that only a fraction of the energy content of a heat stream can be converted into work and this depends on the temperature of the source $\mathbf{T_s}$ and the ambient $\mathbf{T_a}$.

2.3.3.3 Exergy of electrical energy

The exergy associated with electrical energy is:

$$\dot{\mathbf{W}}_{\mathbf{el}} = \dot{\mathbf{E}}\mathbf{x}_{\mathbf{el}} \tag{2.6}$$

2.3.3.4 Exergy destructions in distillation columns

For real processes the exergy input Ex_{in} is always greater than the exergy output Ex_{out}, this unbalance is due to irreversibilities, which is also called exergy loss. The exergy loss and entropy production in distillation are related to each other according to Sato [34]:

$$\Delta\dot{\mathbf{E}}\mathbf{x}_{\mathbf{L}} = \mathbf{T_a} \cdot \Delta\dot{\mathbf{S}}_{\mathbf{irr}} = \dot{\mathbf{E}}\mathbf{x}_{\mathbf{in}}^{\mathbf{tot}} - \dot{\mathbf{E}}\mathbf{x}_{\mathbf{out}}^{\mathbf{tot}} \tag{2.7}$$

Where $\Delta\dot{\mathbf{S}}_{\mathbf{irr}}$ is the entropy production in the distillation unit.

2.3.3.5 Exergy efficiency

Exergy efficiency, which is also called second law efficiency, is usually defined, as the ratio of the total outgoing exergy flow to the total incoming exergy flow Sato [34]:

$$\xi = \frac{\dot{\mathbf{E}}\mathbf{x}_{\mathbf{out}}}{\dot{\mathbf{E}}\mathbf{x}_{\mathbf{in}}} = 1 - \frac{\Delta\dot{\mathbf{E}}\mathbf{x}^{\mathbf{L}}}{\dot{\mathbf{E}}\mathbf{x}_{\mathbf{in}}} \tag{2.8}$$

2.3.4 Balances

2.3.4.1 Energy balance

This section discusses some of the commonly used equation in thermodynamic applied to a control volume. For a steady state condition, the energy balance equation can be expressed as (Rivero, 1993) [31]:

$$\sum_{in} (\dot{H} + \dot{E}n_k + \dot{E}n_p)_{in} - \sum_{out} (\dot{H} + \dot{E}n_k + \dot{E}n_p)_{out} + \sum_{reb} \dot{Q}_{reb} - \dot{W} = 0 \qquad (2.9)$$

The energy balance is simplified by the assumption that changes in kinetic ($\dot{E}n_k$) and potential energy ($\dot{E}n_p$) are neglected.

2.3.4.2 Exergy balance

Unlike energy, exergy is not subject to a conservation law (except for ideal (reversible processes).

$$\sum_{in} \dot{E}x_s + \sum_{in} \dot{E}x_Q = \sum_{out} \dot{E}x_Q + \sum_{out} \dot{E}x_s + \dot{E}x_W + \Delta\dot{E}x_L \qquad (2.10)$$

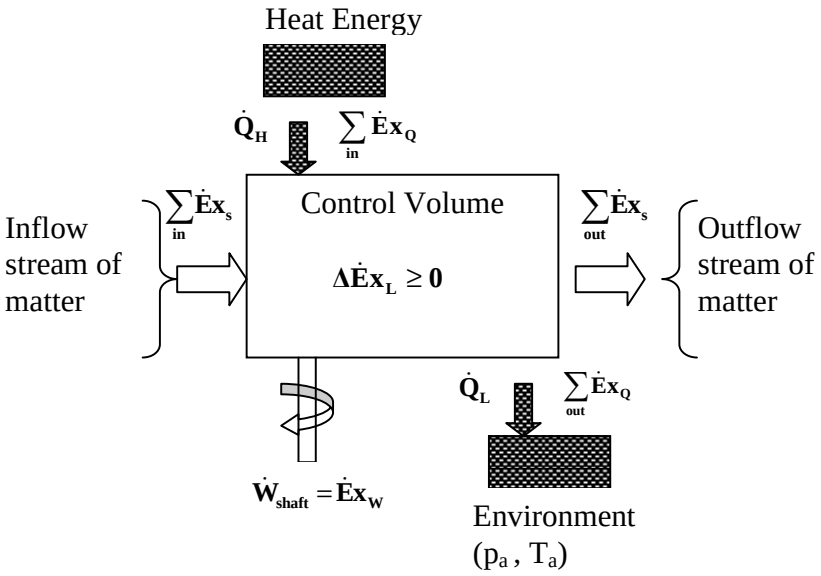

Figure 2.5. Exergy balance for a steady state process, Source: Tirandazi [33]

2.4 Environmental aspect in plant design

In this section, the fundamental background of the environmental objective aspect as well as the linkage between exergy and the environment has been discussed.

2.4.1 Potential Environmental Impacts (PEI)

The PEI of a given quantity of material and energy can be generally defined as the effect that this material or energy would have on the environment if they were to be emitted into the environment [35]**.** It is a conceptual quantity that cannot be measured directly but can be estimated from measurable or estimable quantities using functional relations between the two.

In recent times Potential Environmental Impacts (PEI) are not only used to quantify environmental effects caused by chemical industries but are also used as an optimization criteria alongside economic evaluations. This method of integrating environmental issues into distillation processes is because of the growing social concern on the dangerous pollutions emitted by this processes [8].

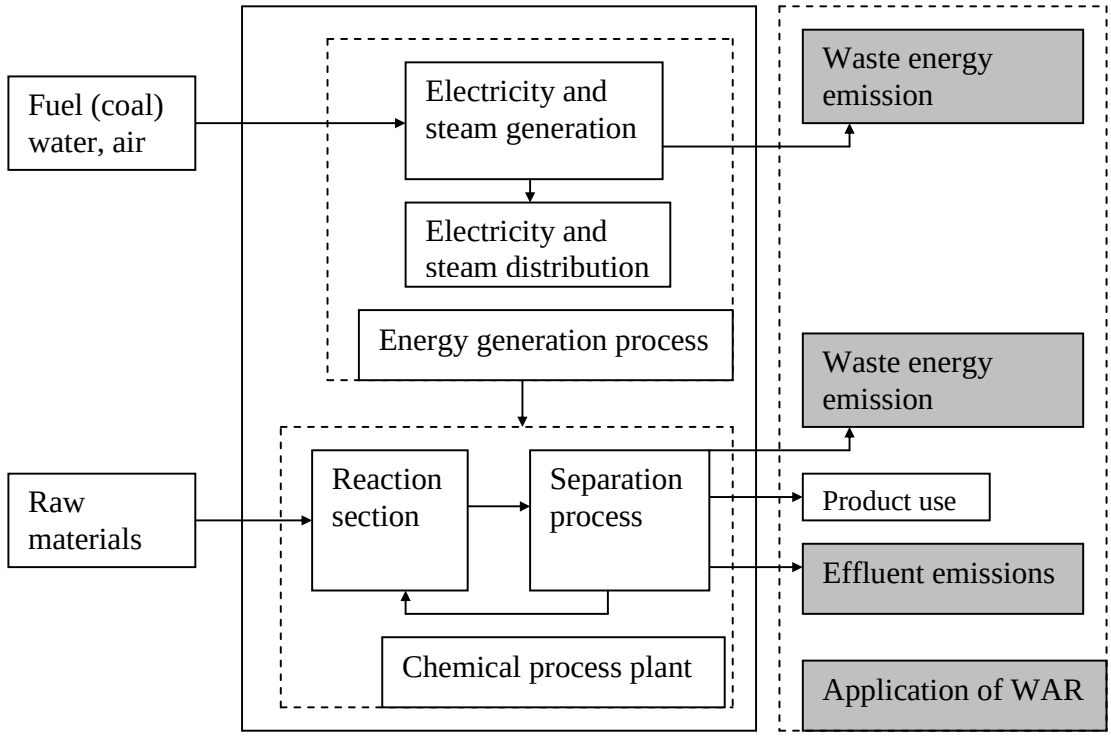

Figure 2.6. Systems boundaries for analysing potential environmental impact
Source: Douglas et al. [36] and Portha et al. [37]

A number of environmental methodologies such as Life cycle assessment (LCA), minimum environmental impact assessment (MEIM), and waste reduction algorithm (WAR) are available for evaluation of environmental performance of chemical processes. Figure 2.6 shows the system boundary around both the chemical process plant and the energy generation plant (electric power and steam generating utility). As shown in figure 2.6, the WAR algorithm considers only the waste energy emission and effluent streams emission. The material and energy flows that enter and leave the systems boundary include material and energy resources and waste energy and effluent stream emission. The theory and concept of the WAR algorithm and the potential environmental impact balance including energy and exergy is described in the next section.

2.4.1.1 The Waste Reduction Algorithm (WAR)

The Waste Reduction Algorithm Graphical User Interface (WAR GUI) was developed by Hilaly and Sikdar [38] to compare the environmental friendliness of chemical process designs. As an improvement upon the original WAR algorithm, Douglas et al. [36] extended the WAR Algorithm to include the consumption of energy by the chemical process into the environmental evaluation.

The WAR algorithm involves potential environmental impact (PEI) balances of mass and energy crossing a system´s boundary. Through the PEI balance, the generation of potential environmental impacts provides a relative indication of the environmental friendliness or unfriendliness of the system. Eight PEIs ranging from human and ecological toxicity to global warming potential are used in this algorithm. The intended use of the WAR Algorithm is therefore to provide a means for comparing the PEI of alternative designs for a process. Designs with lower PEI index values represent more environmentally desirable designs. The WAR algorithm is used to calculate the PEI with the help of eight potential environmental impact categories [35] that can be classified into:

i) Local:

- HTPI = Human Toxicity Potential by Ingestion
- HTPE = Human toxicity Potential exposure both dermal and inhalation

ii) Regional

- AP = Acidification Potential
- PCOP = Photochemical Oxidation Potential
- ATP = Aquatic Toxicity Potential

- TTP = Terrestrial Toxicity Potential And

iii) Global

- ODP = Ozone Depletion Potential
- GWP = Global Warming Potential

2.4.1.2 Simplified PEI balance for a chemical process

The WAR algorithm involves the concept of a Potential Environmental Impact (PEI) balance (analogous to a mass or energy balance) [39]. The balance involves the flow of environmental impact across system boundaries (as opposed to mass or energy).

The flow of impact can be due to mass or energy crossing the system boundaries (Douglas et al. [36]). From the PEI balance, PEI indexes are calculated which provide a relative indication of the environmental friendliness or unfriendliness of the chemical process. The PEI balance can be applied to a distillation unit as illustrated in Figure 2.7.

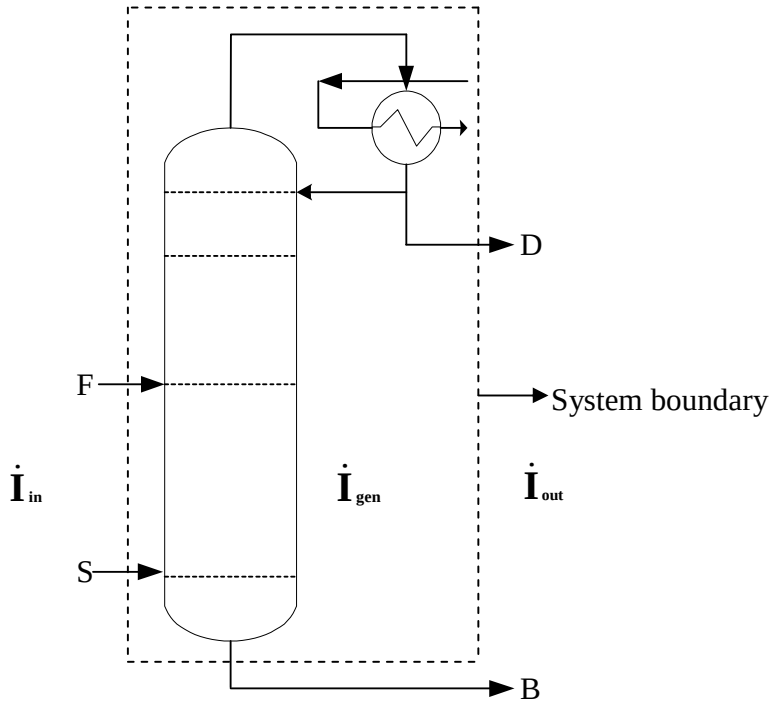

Figure 2.7. PEI balance for a distillation unit.

The potential environmental impact of the WAR algorithm is used as the environmental objectives in this thesis. For steady state processes the general potential environmental impact balance of mass and energy crossing the system boundary is as follows (Kim [40]):

$$\dot{I}_{in} = \dot{I}_{out} - \dot{I}_{gen} \quad (2.11)$$

Where:

$\dot{I}_{in}$ = Total input rate of PEI for mass (effluent stream) and energy

$\dot{I}_{gen}$ = Total rate of PEI for mass (effluent stream) and energy generated

$\dot{I}_{out}$ = Total output rate of PEI for mass (effluent stream) and energy

Because there is no reaction, $\dot{I}_{gen} = 0$, equation (2.11) is simplified to:

$$\dot{I}_{in} = \dot{I}_{out} \quad (2.12)$$

Also only the total output rate of PEI ($\dot{I}_{out}$) will be considered because $\dot{I}_{in} \approx 0$

Therefore the total output rate of PEI can be approximated by known and measurable quantities by:

$$\dot{I}_{out}^{total} = \dot{I}_{out}^{effluent} + \dot{I}_{out}^{energy} \quad (2.13)$$

Equation (2.13) can be simplified as follows:

$$\dot{I}_{i,out}^{effluent} = PEI_{std}^{eff} = \sum_{i}^{evncat} \alpha_i \cdot \sum_{j}^{streams} \dot{M}_{j,out}^{eff} \cdot \sum_{k}^{comps} x_{kj} \cdot \psi_{ki} \quad (2.14)$$

$$\dot{I}_{i,out}^{energy} = PEI_{std}^{En} = \sum_{i} \dot{Q}_{stm} \cdot \psi_{ki}^{En} \quad (2.15)$$

The overall total PEI is as follows:

$$\dot{I}_{out}^{total} = \sum_{i}^{evncat} \alpha_i \cdot \sum_{j}^{streams} \dot{M}_{j,out}^{eff} \cdot \sum_{k}^{comps} x_{kj} \cdot \psi_{ki} + \sum_{i} \dot{Q}_{stm} \cdot \psi_{ki}^{En} \quad (2.16)$$

Where:

PEI_{std}^{eff} = Rate of standard potential environmental impact of effluent stream (PEI/hr)

PEI_{std}^{En} = Rate of standard potential environmental impact due to energy consumption (PEI/hr)

α_i = Weighting factor for impact category i.

$\dot{M}_j^{eff}$ = Mass flow rate of the stream j (effluent stream) (kg/hr)

x_{kj} = Mass fraction of component k in stream j (kg/kg)

ψ_{ki} = Normalized impact score of component k for category i (PEI/kg)

ψ_{ki}^{En} = Normalized impact score of component k for category i due to energy (PEI/KJ)

$\dot{Q}_{stm}$ = Energy consumption (steam) for the separation task MJ

The detail expressions for the PEI due to energy and exergy will be discussion in the next section.

2.4.1.3 Integration of exergy into the WAR algorithm

The energy consumption of a process has an effect on the total potential environmental impact of a process. In general a reduction in the energy consumption of a process will also reduce the potential environmental impact of the process. In this thesis work, the impact due to the effluent stream of the distillation unit has not been considered. Because only the impact due to energy and exergy consumption was relevant. Cabezas et al. [39] have proposed that a potential environmental impact balance is required to incorporate environmental effect into process design. Douglas et al. [36] did improved on that balance by incorporating the consumption of energy into the PEI balance. The purpose of this section is to extend this analysis to include the PEI of the energy and exergy consumed by the energy generation (power plant) and chemical processes (distillation unit). In figure 2.8 an outline of the systems boundary is presented.

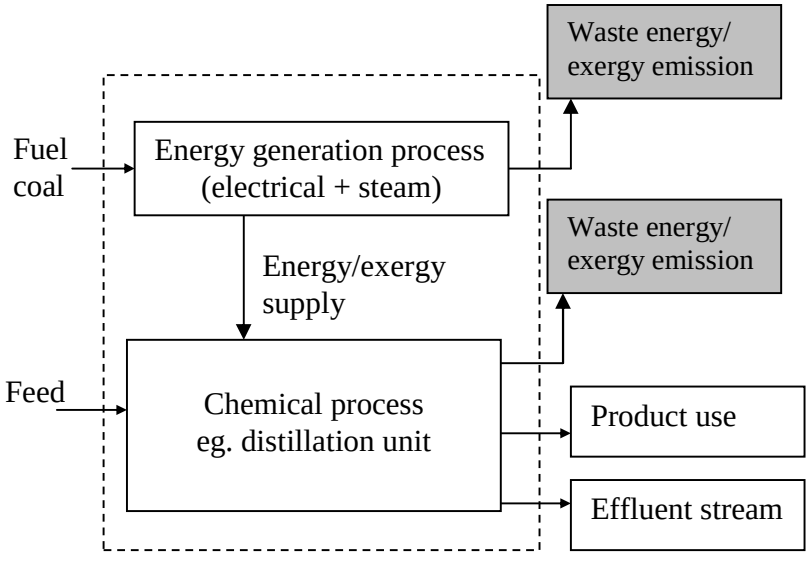

Figure 2.8. Integration of exergy into the PEI calculations

For the power plants alternatives discussed in this work, the PEI calculations were based on emissions rates of different chemicals such as (SO2, NO2, NO, HCL, HF, CO2 and CO) (USEPA [41]).

Table 2.3. Impact per unit energy (PEI /kWhr)

Category	Coal
HTPI	1.22E-06
TTP	7.83E-05
ATP	1.73E-02
GWP	1.93E-04
ODP	2.03E-09
PCOP	7.07E-08
AP	5.98E-03
$\sum \psi_{ki}^{En}$	0.02357

The standard model (PEI ($\mathbf{PEI}_{std}^{En}$)) is giving by:

$$\mathbf{PEI}_{std}^{En} = \sum \dot{\mathbf{Q}}_{coal} \cdot \psi_{ki}^{En}$$

The rate of PEI output due to exergy from source can be expressed as:

$$\mathbf{PEI}^{Ex} = \sum \left[(1 - \frac{\mathbf{T_a}}{\mathbf{T_p}}) \cdot \dot{\mathbf{Q}}_{stm} + \dot{\mathbf{W}}_{el} \right] \cdot \psi_{ki}^{Ex}, \text{ where: } \psi_{ki}^{Ex} = \frac{\psi_{ki}^{En}}{\eta_{el}}$$

Assuming that the emission rate of pollutants is directly proportional to the amount of energy required, one can obtain the impact rates for a given process by multiplying the impacts per unit energy by the energy input rate. The impacts per unit energy for coal and environmental impact category are given above in table 2.3.

The expression for normalized impact score for chemical k for category i due to energy or exergy input where computed for alternatives analysed in this work. The energy required to operate a process (distillation unit) was calculated by summing the entire energy requirement of the system. Included in the calculation is the energy or exergy input to the compressor.

2.5 Solar thermal power plant

The demand for industrial process heat by means of solar energy has generated much interest because it offers an innovative way to reduce operating cost and improve clean renewable electric power technologies. Many researches and publications (Price [42] and Kelly [43]) have been carried out in the areas of solar thermal energy utilization by the process industries. Other applications of parabolic trough collectors (PTCs) are reported by Bakos et al. [44] and Kalogirou et al. [45]. Integration of solar heat into industrial production process is a challenge to both the process engineer and the solar expert [solar heat for industrial processes]. A simulation tool can

be used to develop a solar collector that converts solar irradiation into thermal heat and a power conversion system that convert the heat to electricity. Recently, the German research laboratory Deutsches Zentrum fur Luft-und Raumfahrt e.V (DL) did developed new simulation tool “greenius” (www.greenius.net) for the technical and economical analysis of renewable power projects such as solar thermal or wind power plants (Quaschning [46]).

Recognising both the environmental and climatic hazards to be faced in the coming decades and the continue depletion of the world’s most valuable fossil energy resources, Concentrated Solar Thermal Power (CSP) can provide solutions to global energy problems within a relatively short time and is capable of contributing carbon dioxide reduction, which is an important step towards Zero emissions in the process industries.

In this section, a methodology is presented to integrate solar thermal power plants into industrial processes and these are then compared with an existing hydrocarbon recovery (HCR) plant that depends on coal as its energy source. All the process design alternatives where simulated using the process simulator Aspen Plus^{TM}. Whiles a state of the art parabolic trough power plant is analysed using the greenius simulation software. The mathematical model of each main component is carried out and the system simulation developed. The next section discusses the detail simulation models of the solar thermal power plant.

2.5.1 Greenius simulation environment

A number of computer simulations programs have been developed for modelling the performance of parabolic trough plants.

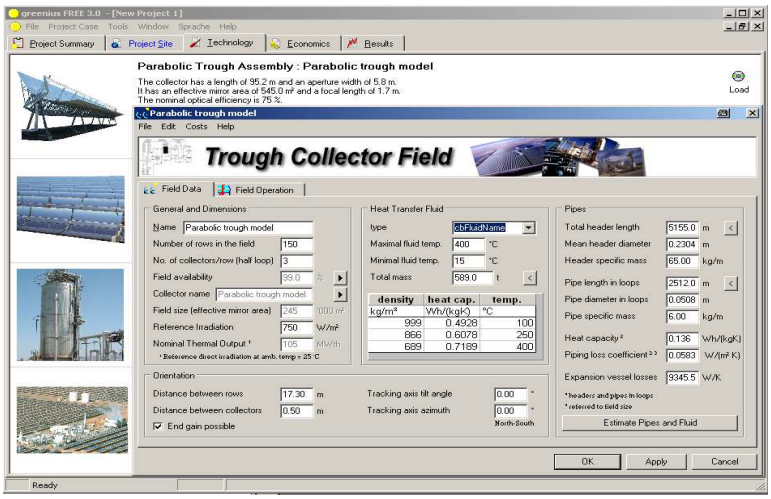

Figure 2.9. Interface of the greenius simulation tool

However most modern computer simulation tools only offer the possibility of technical analysis of the plant, also they have limited capability for modelling detailed technical as well as economical analysis of multiple technology types such as photovoltaic, wind energy and solar thermal power plants. In recent times the German research laboratory Deutsches Zentrum fur Luft-und Raumfahrt e.V (DLR) have developed a new simulation environment greenius that offers all these possibilities (Quaschning [46]).

The input for the simulation is hourly meteorological data of global irradiance, direct normal irradiance and ambient temperature. A screenshot of the project site interface is shown in figure. 2.9. With this meteorological data, site information, technical system data and economical specifications, the greenius simulation environment calculates the system output, system efficiencies and other technical parameters and provide various economical key values Quaschning et al., [47]. Due to its very rapid calculation ability and flexibility, the greenius simulation environment was used to perform the technical and economical calculations of thermal power plant in this work.

2.5.2 Technology selected and site location

The greenius simulation program allows the economic simulation of different technologies like Parabolic Trough Power Plant, Dish Stirling Systems, Grid Connected Photovoltaic Systems, Wind Power Park and Fuel Cell. The program automatically uses the location databases already installed; such as site coordinates, global irradiation, diffuse irradiation, azimuth angle calculations, energy costs, and economic tax information on site and temperature range, among others.

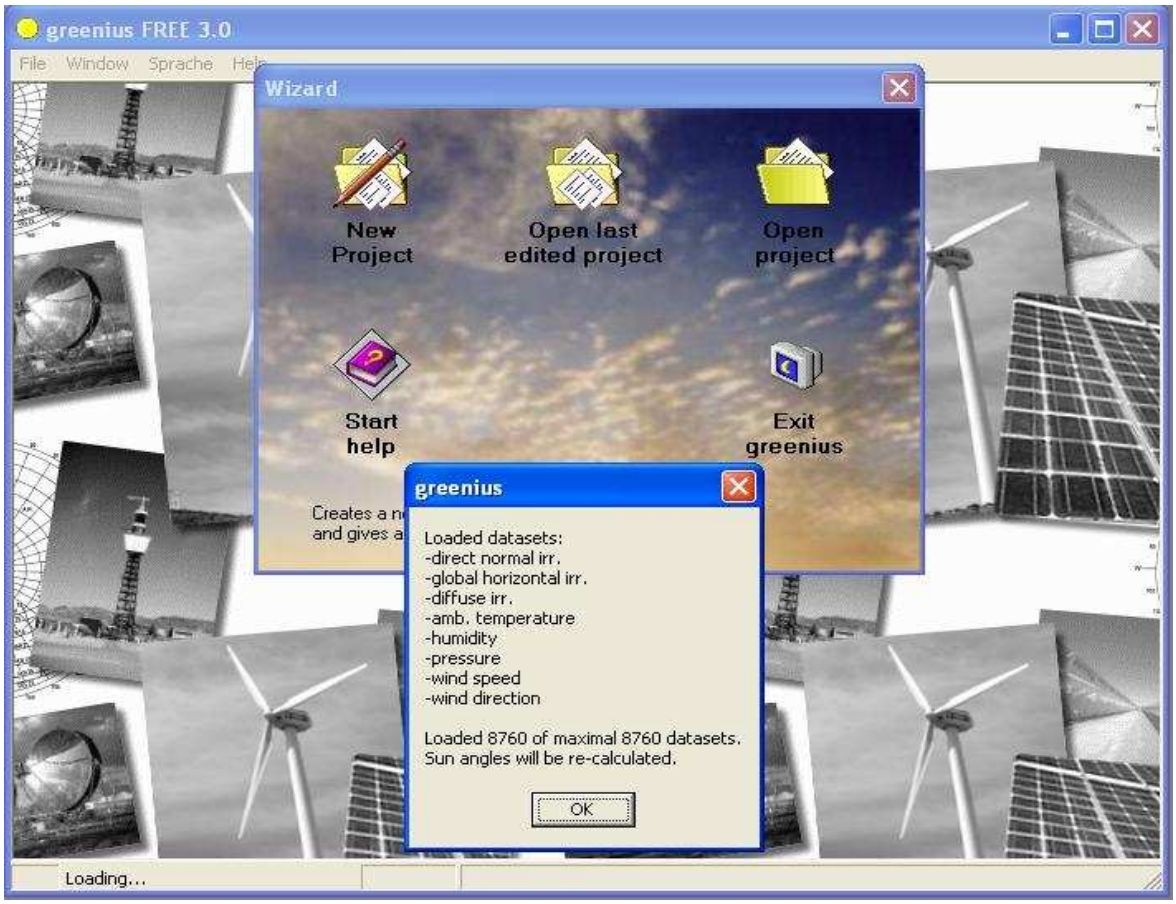

Figure 2.10. Start wizard in greenius[Free] (Source: greenius[Free] Simulation).

The first step in order to perform the simulation is to give the site location data to the program. Once the program is started, a new project is created (see figure 2.10) on the start wizard which loads the following data:

- Direct normal irradiation,
- Global horizontal irradiation
- Diffuse irradiation,
- Ambient temperature,
- Wind speed, and
- Wind direction.

The main meteorological data to be analyzed are the global horizontal irradiance (GHI), direct normal irradiance (DNI) and direct irradiance on collector plane (DNc).

i. **Direct normal irradiance (DNI)** or beam irradiance is the sun´s radiation measured on an imaginary surface directly facing the sun this measurement surface tracks it so that the direction of incident radiation is always normal (straight on) to it.

ii. **Direct horizontal irradiation (DHI)** differs from direct normal irradiance (DNI) because it is the measured incident on a flat horizontal plane. In this case, the DNI component is modified by the cosine of the angle of incidence (φ) at which it strikes the horizontal surface. Thus, it can be calculated as:

$$\mathbf{DHI} = \mathbf{DNI} \cdot \mathbf{cos}(\varphi)$$

iii. **Diffuse horizontal irradiation ($\mathbf{I_{diffuse}}$)** is the energy from the entire sky dome that falls on a horizontal surface, minus the effects of direct beam radiation as it hits the horizontal surface.

iv. **Global horizontal irradiation** (GHI) is defined as the sum of both the direct and diffuse components as measured incident on a flat horizontal plane. It is therefore the sum of the direct horizontal and diffuse horizontal values (Autodesk [48]).

$$\mathbf{GHI} = \mathbf{DHI} + \mathbf{I_{diffuse}} \text{ or } \mathbf{GHI} = \mathbf{DNI} \cdot \mathbf{cos}(\varphi) + \mathbf{I_{diffuse}}$$

A name has to be given to the new project and the program automatically shows a box asking for the technology to be used in the simulation. For this study, the Trough Power system is selected and the location of the project is selected as Almería, Spain. For the storage system, a two molten salt technology is to be used. The site location was selected according to the direct nominal irradiation on the site. As actual information shows that Almería is one of the world´s sites with high direct nominal irradiation. Almería has a direct annual insolation of over 1900 kWh/m^{2}y, with an average annual temperature of 17°C and a typical design irradiance of 950 W/m^2, which makes it an optimal location for a STP project (European Solar [49]]):

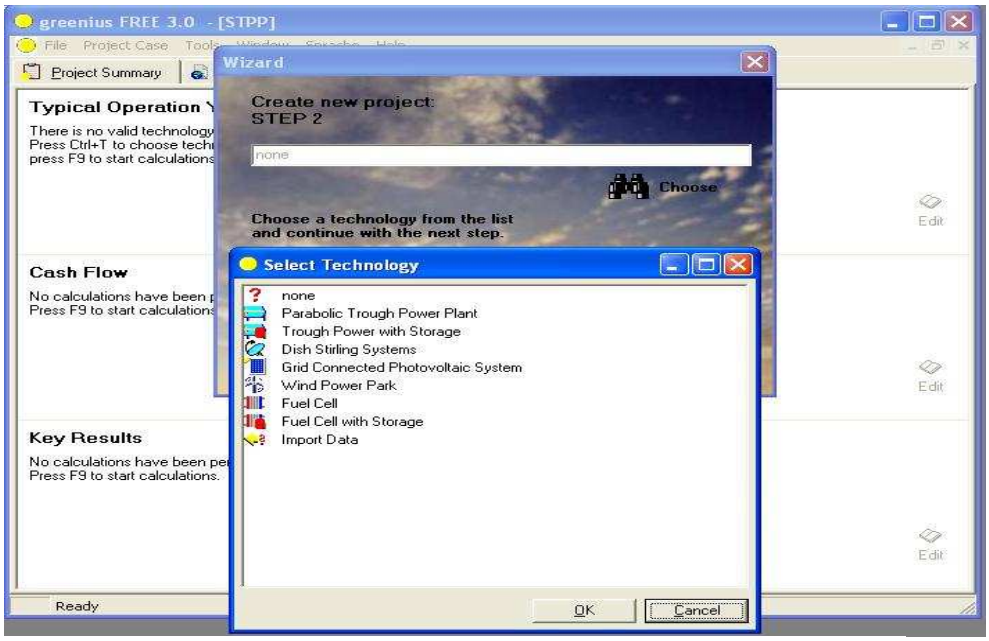

Figure 2.10. Technology selection in greenius^{Free} (Source: greenius^{Free} Simulation)

For the solar field, SKAL-ET 150 collectors are to be used for the STPP design. There are quite a variety of solar collectors that could be used and most of them perform in a similar way. The SKAL-ET 150 collector is optimum due to its high aperture area which irradiates more heat into the absorber. SKAL-ET 150 collector´s parameters used for the simulation are the shown in table 2.4.

Table 2.4. Scheme SKAL-ET 150 collector´s parameters (Source: AndaSol [50]).

Parameter	SKAL-ET 150
Focal length	1.71 m
Average distance to focus	2.12 m
Absorber Radius	3.5 cm
Absorber Length	4 m
Aperture width	5.77 m
Aperture area	817.5 m^2
Length	148.5 m
Number of Absorber Tubes	36
Overall Optical Efficiency	78%

These parameters have to be entered into the program in order to run the simulation, for the Parabolic Trough Assembly, Parabolic Trough Field, Thermal Storage and Power Block input data, see appendix B (figures B.2, B.3, B.4).

2.5.3 Storage system

In case there are strong fluctuations in the daily demand during operational periods or at night when there is no sunlight, thermal storage of solar energy is necessary, depending on the process heat demand profile (Goswami [51]).

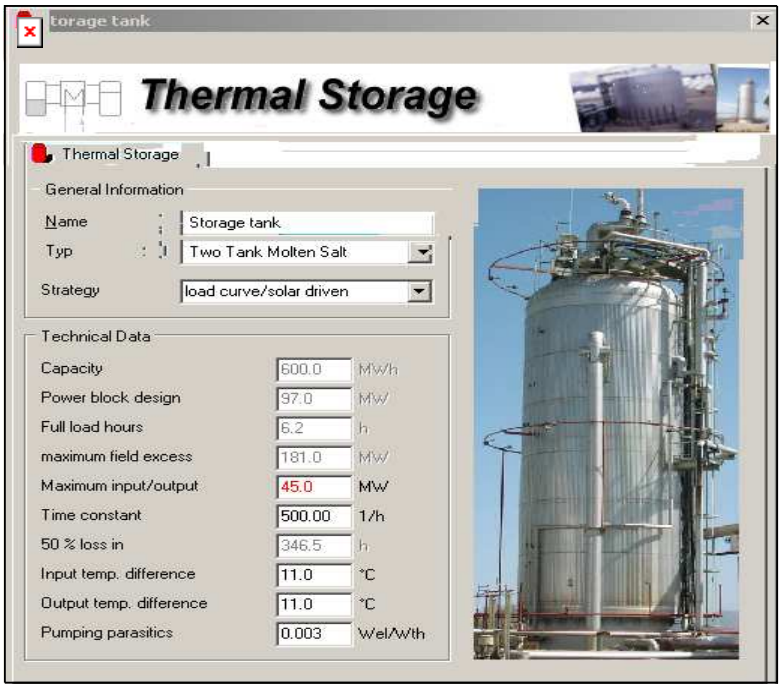

Figure 2.11. Scheme of a parabolic trough power plant with molten salt storage system

In this thesis two storage molten salts have been used (see figure 2.11). Molten salts are favoured central receiver coolants because of their high volume heat capacity, low vapor pressure, good heat transfer and low cost, which makes them economical enough to be used as a large bulk storage medium while their thermodynamic properties permit compact and efficient receivers (Winter et al. [52]**)**. The total molten salt storage capacity is 97 MWh with a 6.2 equivalent working hours and composed of 28,500 tons of the salt composite

2.5.4 Mathematical model and system simulation

The mathematical model of the main components of the Parabolic Trough Collector is described in this section. The system equations relevant to the configuration are expressed in the mathematical model next.

2.5.4.1 Concentration ratio C

An important parameter required for the design of a PTC is the geometric concentration ratio. Figure 2.12 shows the dimension of parabolic trough collector needed for the calculation of concentration ratio.

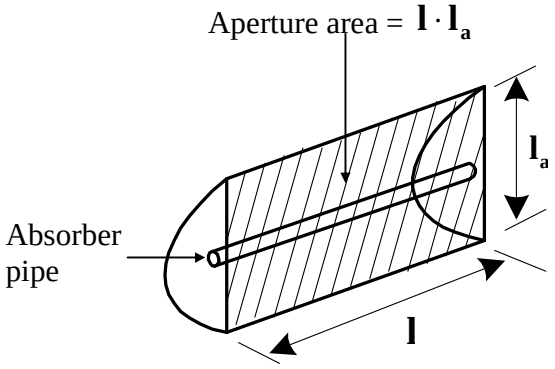

Figure 2.12. Concentration ratio of parabolic trough collector system

The concentration ratio, *C*, is given by:

$$C = \frac{l_a \cdot l}{\pi \cdot d_0 \cdot l} = \frac{l_a}{\pi \cdot d_0}$$

Where d_0 is the outer diameter of the receiver pipe, l is the collector length, and l_a is the parabola width. Usual values of the concentration ratio of PTCs are about 20, although the maximum theoretical value is on the order of 70.

2.5.4.2 Thermal energy of a parabolic trough collector

Figure 2.12 shows a schematic of a single parabolic trough collector system. The solar receiver is made of a copper tube and a glass envelope (PTC). The copper tube is coated with a heat resistant black paint and is surrounded by a concentric glass cover with an annular gap of 0.5 cm. Solar radiation is converted into heat by the Collector. Water from the recalculating pump is pumped through the copper tube. The concentrated radiation heats the water that circulates through the absorber pipe (copper tube), thus transforming the solar radiation into thermal energy. The rate of useful energy transferred to the heat transfer fluid (water) of a concentrating collector operating under steady-state conditions as described by Romero-Alvarez et al. [53] and Arasu et al. [54] is:

$$\dot{Q}_U = A_c \cdot E_d \cdot \cos(\varphi) \cdot \eta_{th} \tag{2.17}$$

Where: $\dot{Q}_U$ = rate of useful energy transferred to the heat transfer fluid (water).

Ac=collector aperture surface area

E_d=direct solar irradiance

φ = Incidence angle, η_{th} = Thermal efficiency

2.5.4.3 Losses in parabolic trough collectors

When direct solar radiation reaches the surface of a PTC, a significant amount of it is lost due to several different factors (Romero-Alvarez et al. [53]):

- Optical losses
- Thermal losses from the absorber pipe to the ambient
- Geometrical losses

i. Optical losses

The optical losses in a parabolic trough collector are associated with four parameters which are (see figure 2.13):

- Reflectivity (ρ)
- Interceptor factor (r)
- Transmissivity of the glass tube (τ) and
- Absorptivity of the absorber selective coating (α).

A brief explanation is given below.

- **Reflectivity (*ρ*):** Only a fraction of the incident radiation is reflected towards the receiver tube. Typical reflectivity values of clean silvered glass mirrors are around 0.93. After washing the mirrors, their reflectivity continuously decreases as dirt accumulates until the next washing.

- **Intercept factor (r):** A fraction of the direct solar radiation reflected by the mirrors does not reach the glass cover of the absorber tube due to either microscopic imperfections of the reflectors or macroscopic shape errors in the parabolic trough concentrators (e.g. imprecision during assembly). These losses are quantified by an optical parameter called the intercept factor, r, which is typically 0.95 for a collector properly assembled.

- **Transmissivity of the glass tube (τ):** A fraction of the direct solar radiation reflected by the mirrors and reaching the glass cover of the absorber pipe is not able to pass through it. The ratio between the radiation passing through the glass tube and the total incident radiation on it, gives transmissivity, τ, which is typically τ=0.93.

- **Absorptivity of the absorber selective coating (α):** This parameter quantifies the amount of energy absorbed by the steel absorber pipe, compared with the total radiation reaching the outer wall of the steel pipe. This parameter is typically 0.95 for receiver pipes with a cermet coating.

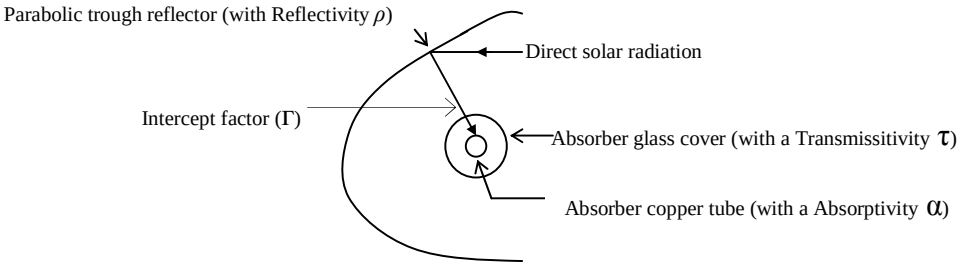

Figure 2.13. Optical parameters of a parabolic trough collector
Source: (Romero-Alvarez et al. [53]**)**

Multiplication of these four parameters when the incidence angle on the aperture plane is 0^0 gives what is called the peak optical efficiency of the PTC and this is expressed as in Reddy [55]:

$$\eta_{opt,0^0} = (\rho \cdot \gamma \cdot \tau \cdot \alpha)_{\varphi=0^0} \tag{2.18}$$

$\eta_{opt,0^\circ}$ is usually in the range of 0.70-0.76 for clean, good quality PTCs.

ii. Thermal losses from the absorber pipe to the ambient

The second type of losses is the thermal losses from the absorber pipe to the ambient. The total thermal loss in a PTC, $P_{Q,collector \rightarrow ambient}$, is due to a radiative heat loss from the absorber pipe to ambient, $P_{Q,absorber \rightarrow ambient}$, and convective and conductive heat losses from the absorber pipe to its ambient, $P_{Q,absorber \rightarrow glass}$. Although this heat loss is governed by the well-known mechanisms of radiation, conduction, and convection, it is a good practice to calculate them all together using the thermal loss coefficient, $U_{L)abs}$, according to (Arasu et al. [54]).

$$\mathbf{P_{Q,collector \rightarrow ambient} = U_{L)abs} \cdot \pi \cdot d_0 \cdot l \cdot (T_{abs} - T_{amb})} \quad (2.19)$$

The heat loss coefficient depends on the absorber pipe temperature and is found experimentally by performing specific thermal loss tests with the PTC operating at several temperatures within its typical working temperature range.

$$\mathbf{U_{L)abs} = a + b \cdot (T_{abs} - T_{amb}) + c \cdot (T_{abs} - T_{amb})^2} \quad (2.20)$$

iii. Geometrical losses

The third group of losses in a PTC is the geometrical losses that are due to the incidence angle, φ, of direct solar radiation on the aperture plane of the collector. The incidence angle is the angle between the normal to the aperture plane of the collector and the sun's vector, both contained on a plane perpendicular to the collector axis.

The incidence angle of direct solar radiation depends on PTC orientation and Sun position, which can be calculated by means of the azimuth (AZ) and elevation (EL) angles. The sun elevation angle is measured with respect to the horizon (positive upwards), while azimuth is 0° to the south and positive clockwise (Romero-Alvarez et al. [53]). Equation 2.21 is used for horizontal north-south orientation and equation 2.22 for east-west orientation (Romero-Alvarez et al. [53]).

$$\boldsymbol{\varphi = arc \cdot cos\left[1 - cos^2(EL) \cdot sin^2(AZ)\right]^{1/2}} \quad (2.21)$$

$$\boldsymbol{\varphi = arc \cdot cos\left[1 - cos^2(EL) \cdot cos^2(AZ)\right]^{1/2}} \quad (2.22)$$

2.5.4.4 Incidence angle modifier

The effect of the incidence angle on the optical efficiency is quantified by the incidence angle modifier K_n. The incidence angle modifier IAM is defined as the ratio of the collector output at a given incidence angle $\dot{Q}_u(\varphi_i)$ and the collector output at normal incidence $\dot{Q}_u(\varphi=0)$ (Fischer et al. [56]), see equation 2.23:

$$\mathbf{K_n = \frac{\dot{Q}(\varphi_i)}{\dot{Q}(\varphi = 0^0)}} \quad (2.23)$$

The performance measurements of PTC_s are normally taken with the solar isolation level measured perpendicular to the collector plane (i.e. facing the same direction as the collector). When the light shines on the collector from an angle the performance changes and this is what the IAM (Incidence Angle Modifier) values provide i.e., it is an angular performance factor.
The incidence angle modifier K_n can also be calculated as described by Brooks et al. [57].

$$\mathbf{K_n} = \frac{\boldsymbol{\eta}_{\varphi_i}}{\boldsymbol{\eta}_{\mathbf{opt},\,\varphi=0^0}} \tag{2.24}$$

Where

$\boldsymbol{\eta}_{\varphi_i}$ = The measured efficiency at a set value of φ_i

$\boldsymbol{\eta}_{\mathbf{opt},\,\varphi=0^0}$ = Peak optical efficiency at normal incidence

2.5.4.5 Global efficiency of PTC

The global efficiency can be calculated as the ratio between the net thermal output power delivered by the collector ($P_{Q,collector\rightarrow fluid}$) and the solar energy flux incident on the collector aperture plane ($P_{Q,sun\rightarrow collector}$). The global efficiency is given by:

$$\boldsymbol{\eta}_{\mathbf{global}} = \frac{\mathbf{P}_{\mathbf{Q,collector\rightarrow fluid}}}{\mathbf{P}_{\mathbf{Q,sun\rightarrow collector}}} \tag{2.25}$$

$$\mathbf{P}_{\mathbf{Q,sun\rightarrow collector}} = \mathbf{A_c} \cdot \mathbf{E_d} \cdot \mathbf{cos}(\boldsymbol{\varphi}) \tag{2.26}$$

$$\mathbf{P}_{\mathbf{Q,collector\rightarrow fluid}} = \mathbf{q_m} \cdot \left(\mathbf{h_{out}} - \mathbf{h_{in}}\right) \tag{2.27}$$

Where A_c = collector aperture surface, E_d = direct solar irradiance, φ = incidence angle, q_m = fluid mass flow through the absorber tube of the collector, h_{in} = fluid specific mass enthalpy at the collector inlet, and h_{out} fluid specific mass enthalpy at the collector outlet. The net output thermal power delivered by a PTC can be calculated, from a practical standpoint, calculation of the net thermal output power during the design phase is easier if thermal losses in the PTC, $P_{Q,collector\rightarrow ambient}$, are used instead of the thermal efficiency, η_{th}.

$$\mathbf{P}_{\mathbf{Q,collector\rightarrow fluid}} = \mathbf{A_c} \cdot \mathbf{E_c} \cdot \mathbf{cos}(\boldsymbol{\varphi}) \cdot \boldsymbol{\eta}_{\mathbf{opt},0^\circ} \cdot \mathbf{K}(\boldsymbol{\varphi}) \cdot \boldsymbol{\eta}_{\mathbf{th}} \cdot \mathbf{F_e} - \mathbf{U}_{\mathbf{L)abd}} \cdot \boldsymbol{\pi} \cdot \mathbf{d_0} \cdot \mathbf{l} \cdot (\mathbf{T_{abs}} - \mathbf{T_{amb}}) \tag{2.28}$$

F_e, which is $0 < F_e < 1$ and takes into account the progressive soiling of mirrors and glass tubes after washing. Usual values of F_e are around 0.97, which is equivalent to a mirror reflectivity of 0.90 for mirrors with a nominal reflectivity of 0.93 (Romero-Alvarez et al. [54]).

2.5.4.6 Operating conditions of the STPP

Once the input data are entered into the program, calculations are performed automatically by the program and key results are analyzed. The main operating conditions that were used for the simulation are shown in Table 2.5.

Table 2.5. Main operating conditions of simulated STP with a two molten salt tanks storage system (Source: greenius[Free] Simulation).

Meteorological Data:		
Direct horizontal irradiance	1164.8	kWh/(m²·y)
Diffuse horizontal irradiance (Diff)	647.6	kWh/(m²·y)
Global horizontal irradiance (GHI)	1812.4	kWh/(m²·y)
Direct normal irradiance (DNI)	1917.8	kWh/(m²·y)
Direct irradiance on collector plane (DNc)	1655.5	kWh/(m²·y)
Mean annual ambient temperature	17.6	°C
Location	Almería, Spain	
Collector type	SKAL-ET 150	
Number of collectors	690	
Effective Collector Area	510120	m²
Land use	710000	m²

2.5.5 Results and discussion of solar thermal power plant

2.5.5.1 Technological results/ Irradiation results

The main technology results of the simulated parabolic trough solar thermal power plant with a two molten salt tanks storage system are shown in Table 2.6.

Table 2.6. Main technology results of simulated STPP (Source: greenius[Free] Simulation).

Nominal thermal output	154.1	MW_{th}
Nominal electrical output	34.2	MW_{el}
Annual thermal field output	185986.2	MWh_{th}
Annual electrical output	56867.2	MWh_{el}
Annual gross output	61185.9	MWh_{el}
Specific thermal field output	546.9	kWh_{th}/m^2
Specific electrical output	155.5	kWh_{el}/m^2
Mean annual field efficiency	28.6	%
Mean system efficiency	8.1	%
Solar share	100	%
Full load hours	8000	hr/y
CO_2 Emissions	0	t CO_2

As seen in the Table 2.6 above, the simulated plant has a nominal electrical output of 34.2 MWh_{el} which is a good electricity production for the simulated plant. The AndaSol I plant is approximately of the same characteristics with a nominal electrical power of 49.9 MWh_{el} (Nava Paul [58]).

The main meteorological data to be analyzed are the global horizontal irradiance (GHI), direct normal irradiance (DNI) and direct irradiance on collector plane (DNc). Table 2.7 shows the simulation results for the specified site location (Almería). It also shows the effective operating range for a PTC with a maximum irradiation obtained in June for all the cases (GHI, DNI and DNc). The software automatically calculates the total GHI of 1812.4 kWh/ (m^2 y), DNI of 1917.8 kWh/(m^2 y), and a 1655.5 kWh/(m^2 y) for DNc.

Table 2.7. Simulation results for GHI, DNI and DNc in Almería, Spain (Source: greenius[Free] Simulation)

	GHI	DNI	DNc
	W/m²	W/m²	W/m²
Average	206.7	219.2	189.1
January	111.1	181.8	120.4
February	148.1	199.5	149.6
March	201.8	195.3	167.1
April	255.9	270.3	254.3
May	288	260.8	252.8
June	319.5	304.4	298.6
July	283.1	196.4	192.3
August	270.6	246.3	235.9
September	229.1	267.7	242
October	151.7	162.5	129.1
November	120.7	176.8	121.9
December	100.6	168	105.1

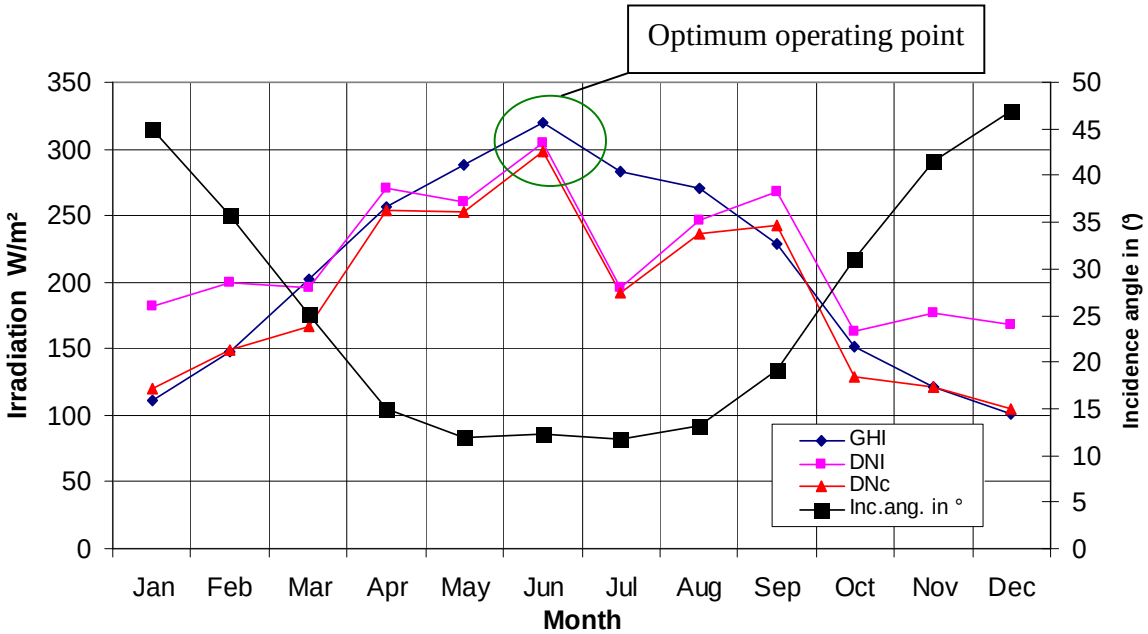

Figure 2.13. GHI, DNI and DNc irradiances in Almería, Spain (Source: greenius[Free] Simulation).

Figure 2.13 shows the meteorological results of irradiances distribution pattern at different times of the year for the site location considered in this study. It can be seen from figure 2.13 that the

DNI is the highest almost throughout the year except between April and August. The reason is that between January and April most of the solar irradiation are diffused back into the atmosphere and this reduces the GHI and the DN_C. Also as the incidence angle reduces, the GHI, DNI and DNc increase. The incidence angle however remains the same between May and August and the optimum values of GHI, DNI and DNc can be achieve in June. This result therefore gives the optimum operating condition at which the STPP can be operated.

2.5.5.2 Total efficiency and the total solar thermal output results

The efficiency of the STPP increases significantly from January up to a maximum of 12.78% in June which is the hottest month (see figure2.14), in this period a maximum solar thermal output of 45000 $MWhr_{th}$ was produced by the plant. After this as the efficiency start to decrease, the thermal output also decreases.

From this observation it will be more economical to operate the plant between March and September where the thermal output is good enough to produce electrical power. Also, the total solar energy produced in the field is an important variable to be considered when modeling the solar thermal power plant in Aspen Plus simulator.

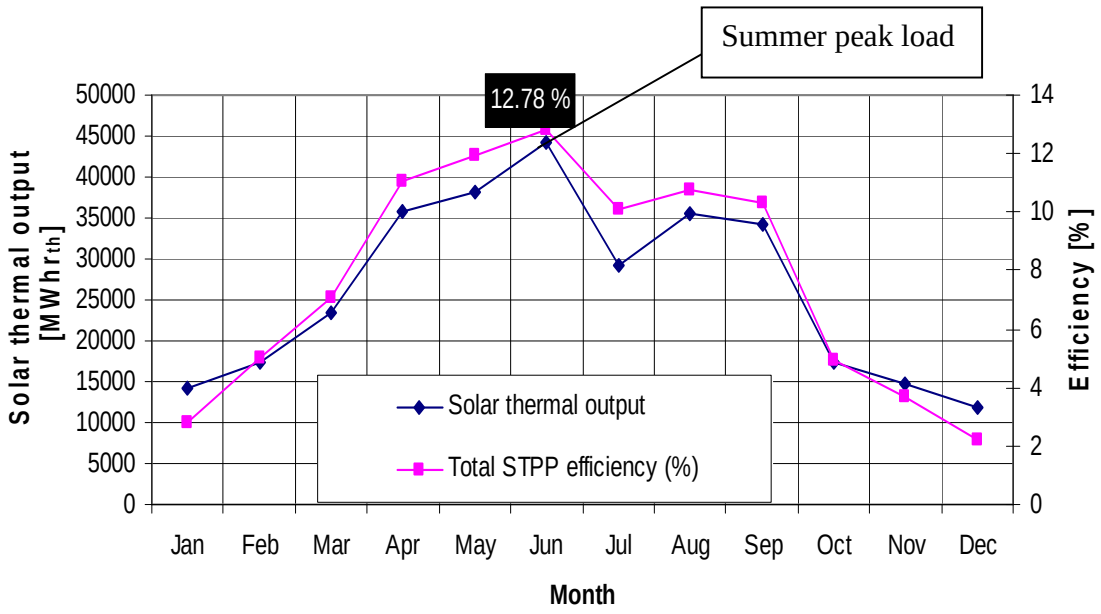

Figure 2.14. Total efficiency and total solar thermal results (Source: greenius[Free] Simulation)

2.5.6 Levelized electricity cost (LEC)

LEC is the sum of the annual fuel cost, annual operation and maintenance cost and the product of the capital cost times the fixed charge rate divided by annual energy produced [59]. One way to perform comparisons among different technologies is to use the levelized energy cost methodology [60], it allows to quantify the unitary cost of the electricity (kWh) generated during the lifetime of the power plant. LEC is widely used to compare competing energy sources [CDEF]. This thesis follows a methodology similar to that proposed by World Bank and European Commission report [61] and Kolb [62] to evaluate LEC. The levelized energy costs are calculated as follows:

$$\mathrm{LEC} = \frac{(FCR \cdot I) + OM + L - C}{E} \tag{2.29}$$

Where:

FCR- Fixed charge rate

I.- Installed capital cost

OM- Annual operated and maintenance cost in year zero,

L- Annual expenses for input energy

C- Annual CO_2 reduction credit

E- Energy produced

$$FCR = \sum_{t=1}^{n} \frac{1}{(1+k_d)^t} + p_1 ,$$

Where: n- Lifetime of the plant, k_d- Discount rate, p_I- Insurance rate.

Assumptions

The major economic assumptions that are employed in this analysis are described below.

Table 2.7 Economic assumptions

Item	Assumptions
n	25-year
Fuel Price	Coal prices are assumed to be $1.14/GJ
C	$7/ton of avoided CO_2 emissions is used
k_d	10%
p_I	1%
OM	55,383,225 €

2.5.6.1 Economic results of simulated STPP

The economic simulation results as shown in Table 2.8, show that the LEC value of the simulated STPP is around 0.155 €/kWh. The LEC value varies with the GHI, at higher GHI value, the corresponding LEC value is lower. With the help of greenius[Free] Software, it is possible to make a forecast graph for the LEC value.The economic key results are the following:

Table 2.8. Economic results of simulated STPP (Source: greenius[Free] Simulation).

Type of data		
Interest i	5	%
Number of years	25	y
Electricity Tariff	0.2	$/kWh
Required Tariff (LCOE)	0.161	€/kWh
Incremental LEC	0	€/kWh
Levelized Electricity Costs (LEC)	0.155	€/kWh
Cash flow	245, 417, 107	€
Total Investment Costs (IK)	160, 502, 448	€
Profit	84, 914, 659	€

LEC values are obtained after performing consecutive simulations for different GHI values in greenius[Free] Software. Table 2.9 shows the LEC values obtained after the simulations.

Table 2.9. LEC values obtained at different GHI (Source: greenius[Free] Simulation).

GHI	LEC
kWhr/m^2/y	€/kWhr
1929	0.145
1812	0.155
1767	0.194
1582	0.201
1570	0.228
1137	0.39
1088	0.491
993	0.538
948	0.6

After knowing the different values of LEC, the data is plotted and a trendline is graphed in order to forecast the LEC values for higher GHI.

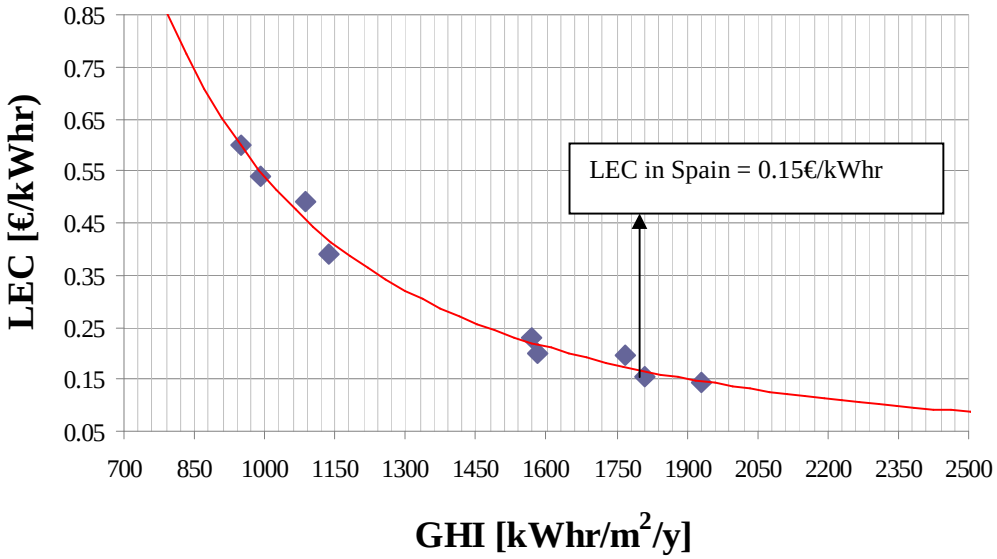

Figure 2.14. Plotted LEC values and GHI (Source: greenius[Free] Simulation)

Figure 2.14 shows that as the GHI is increased, the LEC also decreases. The LEC decreases sharply from 0.85 €/kWh to 0.15 €/kWh. This occurs between GHI of 850 to 900 kWhr/m^2/y. As indicated in the trendline, the LEC at a GHI of 1812 kWh/m^2 is of approximately 0.15 Eurocents per kWhr, which matches with the simulated data. If the STPP technology is operated at high GHI locations, the LEC achieved would be lower, which results in a lower cost per kWh of electricity produced.

2.5.6.2 Optimization of solar field collectors

The performance model was run with Spain (Almeria) insolation data to evaluate the optimum LEC for a particular number of collectors. Figure 2.15 shows that as the number of collectors increase, the LEC cost continue to decreases, the LEC however remain fairly constant with 690 number of collector. As the numbers of collectors continue to increase, it has little or no effect on LEC. In general the higher the number of collectors, the lower the LEC. The optimum value of the number of collectors corresponds to 690. Higher values of the number of collectors results in higher LEC because the capital investment increase more than the solar energy produced.

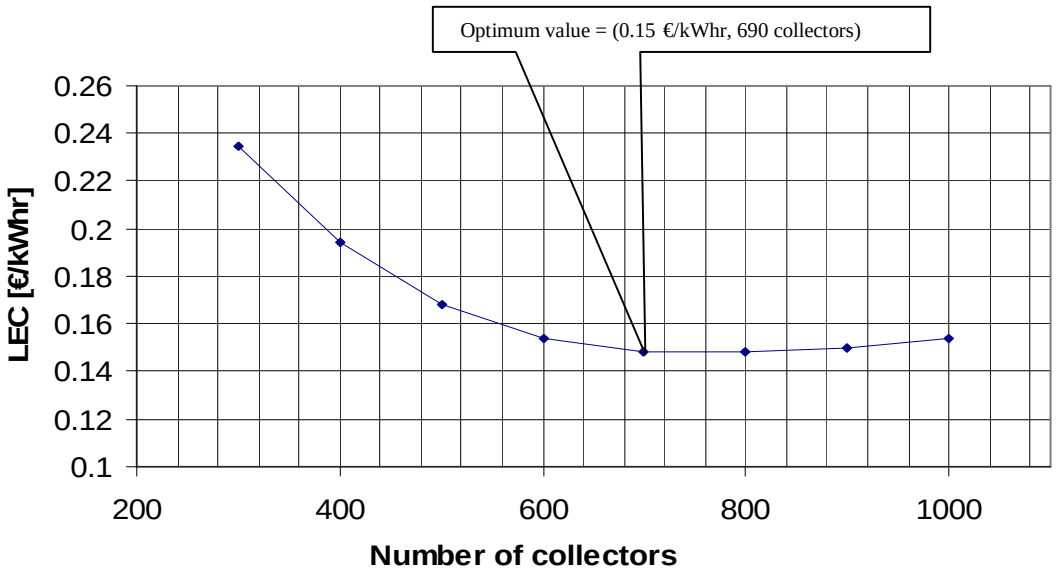

Figure 2.15. Optimization of number of solar collectors

2.5.6.3 Effect of optical efficiency on LEC

The main parameters affecting the optical efficiency are Reflectivity (ρ), Interceptor factor (ɾ), Transmissivity of the glass tube (τ) and Absorptivity of the absorber (α). Higher values of these factors can result in higher optical efficiency, which can lead to lower LEC. This is shown in figure 2.16. The plant in Spain is operating at approximately 85 % optical efficiency.

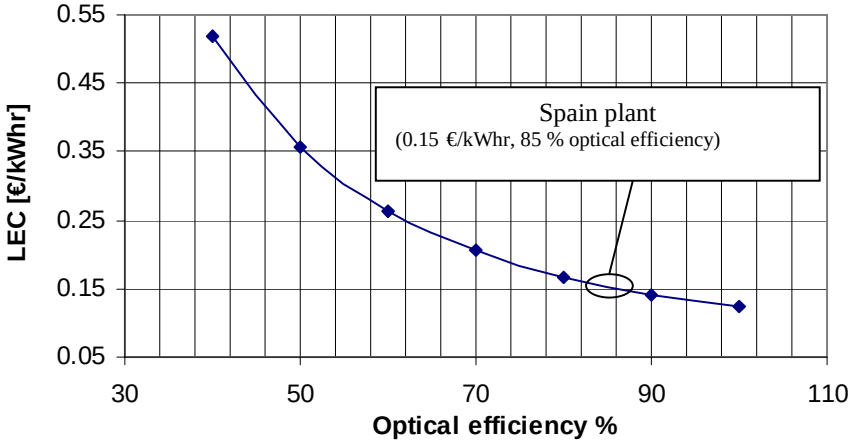

Figure 2.16. Effect of optical efficiency on LEC

2.5.6.4 LEC for different locations

Further simulations were made for different locations in Europe. Altogether these sites cover a Global annual irradiation range from 948 kWh/(m²y) in Germany (Hamburg) until 1812 kWh/(m² a) in Spain (Almeria). If the STPP technology is operated at high GHI locations, the LEC achieved would be lower, which results in a lower cost per kWh of electricity produced. Figure 2.17 shows that the solar thermal power plant can best be operated in areas with lowest LEC such as Spain (Almeria) and Italy (Gela).

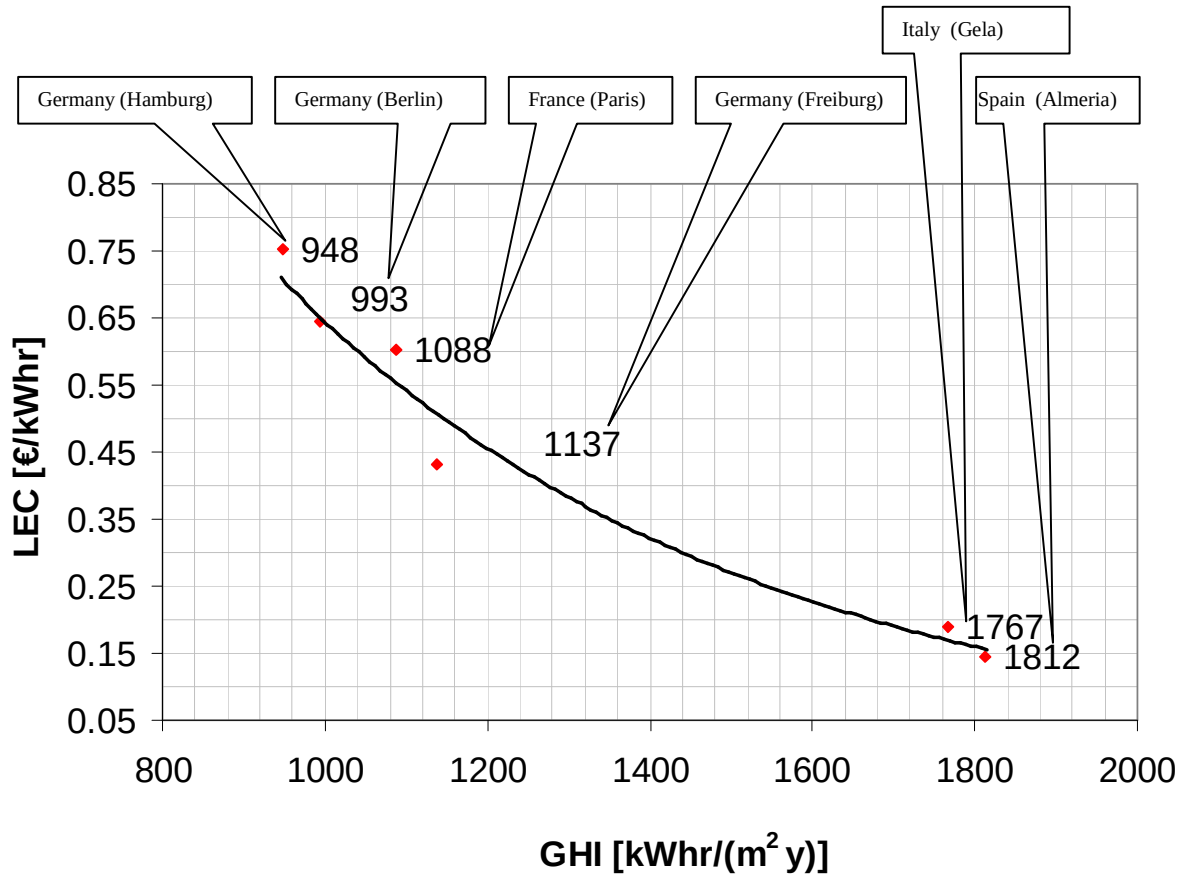

Figure 2.17. Global horizontal radiation or irradiance

2.5.6.5 Environmental impact of simulated STPP

Solar thermal power plant is a renewable technology which is completely environmentally friendly. As actual studies show, STPP are optimal energy sources that avoid the production of CO_2 and save tons of CO_2 produced during the year, which tends to help economically for the financing of the STPP.

Another important result from the simulation performed is the environmental impact of the STPP. As it can be seen in Table 2.10, the annual CO_2 reduction of the plant is of 66200 tons of CO_2 with an avoidance cost of 175.06 €/tonCO_2. That results into a total saving of 11,602,900.00 €/yr of CO_2 avoidance credit.

Table 2.10 Environmental impact of simulated STPP (Source: greenius[Free] Simulation).

Environmental Aspects		
Annual CO_2 avoidance	66200	tCO_2
CO_2 Avoidance Cost	175.06	€/tCO_2

2.6 Heat pump

In this section the theoretical approach (such as Carnot efficiency) as well as the practical approach of a heat pump distillation is discussed. The process temperature T_p of the heat pump distillation (see figure 2.18) becomes useful by increasing the outlet pressure of the compressor. In this example the distillation unit takes its energy source via the electrical power supplied to the compressor.

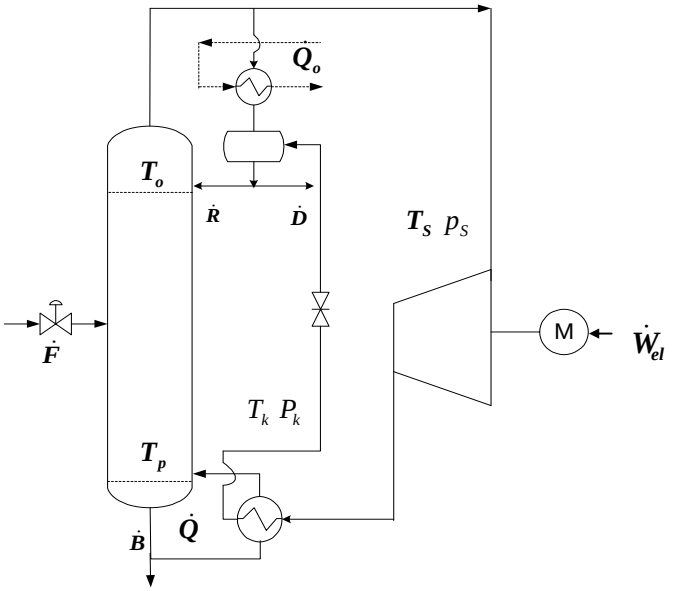

Figure 2.18. Electrically driven heat pump assisted distillation
(Compression of overhead vapor)

2.6.1 Energy efficiency

The energy efficiency of a heat pump is expressed interms of coefficient of performance which is indicated by the symbol ($\boldsymbol{\varepsilon}$). The coefficient of performance as expressed by Stockburger et al. [63], is the ratio of steam out put and the electrical power input to a compressor and is given by:

$$\boldsymbol{\varepsilon} = \frac{\dot{\mathbf{Q}}}{\dot{\mathbf{W}}_{\mathbf{el}}} \tag{2.30}$$

2.6.1.1 Coefficient of performance of a Carnot process

Figure 2.19 gives a brief explanation of the Carnot process cycle, from equation 2.30 the theoretical maximum coefficient of performance ($\boldsymbol{\varepsilon_C}$) of a Carnot process is given by:

$$\varepsilon_C = \frac{\dot{Q}}{\dot{Q} - \dot{Q}_o} = \frac{T_K \cdot \Delta S}{T_K \cdot \Delta S - T_s \cdot \Delta S} = \frac{T_K}{T_K - T_s} \tag{2.31}$$

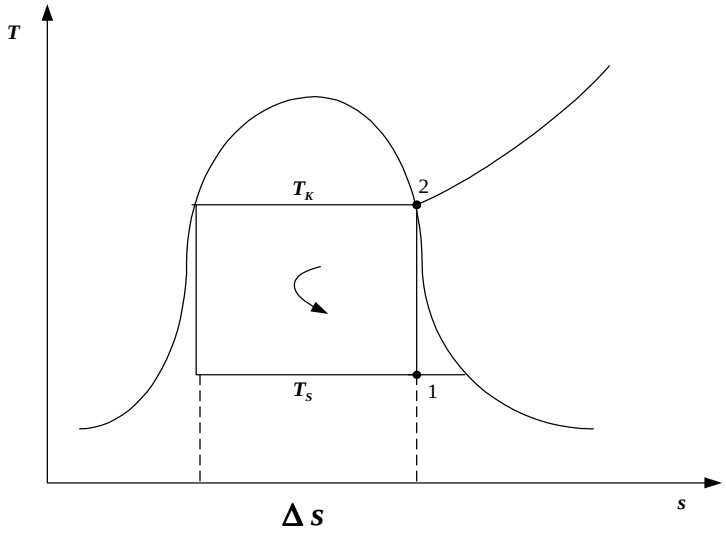

Figure 2.19. T S diagram of a standard cycle (CARNOT) process and real process

It can be shown from the second law of thermodynamic that no heat pump can be more efficient than a reversible heat pump working between the same temperature limits. Carnot showed that the most efficient possible cycle is one in which all the heat is supplied at one fixed temperature and all the heat is rejected at a lower fixed temperature (McConkey [64]). The cycle is most represented on a T-S diagram as shown in figure 2.20.

It is difficult in practice to device a system which can receive and reject heat at a constant temperature. A wet vapor is the only working substance which can do this conveniently, since for a wet vapor the pressure and temperature remain constant as the specific enthalpy of vaporization is supplied or rejected.

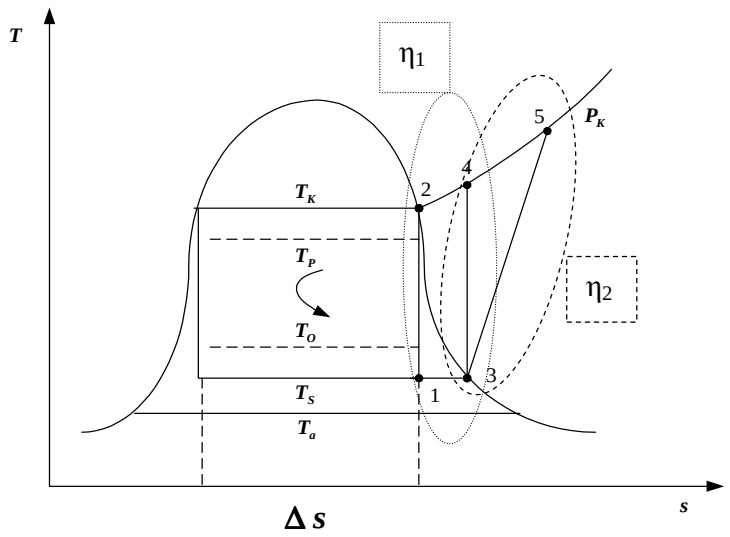

Figure 2.20. T S diagram of a standard cycle (CARNOT) process and real process
Source: Stockburger et al. [63]
Point 1→ Point 2 (Carnot process)
Point 3→ Point 4 (Isentropic process)
Point 3→ Point 5 (Real process)

2.6.1.2 Performance factors of a real process

There are other losses that occur in the case of real compression of the steam in a compressor, however these external losses have no effect on the working fluid. The mechanism of energy transfer from the source to the compressor is shown in figure 2.21.

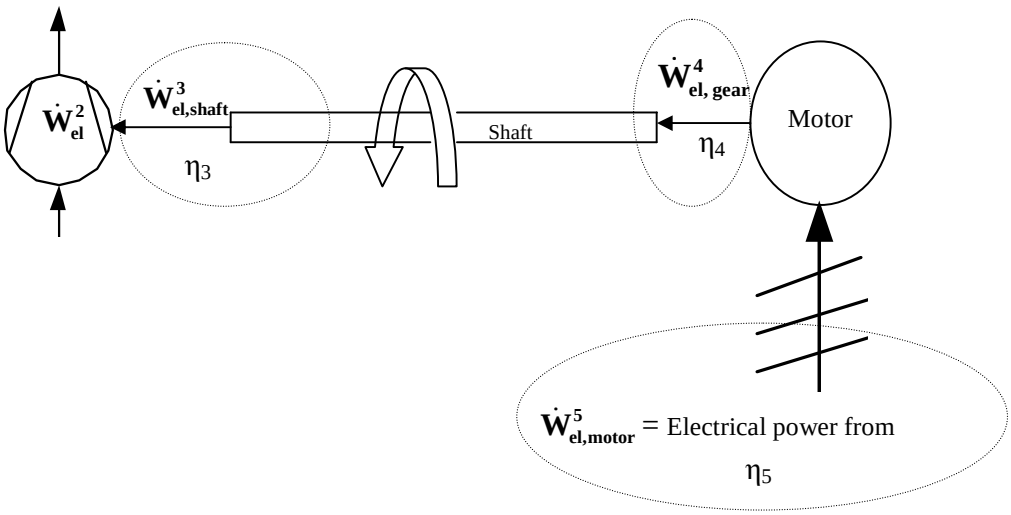

Figure 2.21. Mechanism of electrical power transfer to the compressor

The detail of the losses as discussed in (Stockburger et al. [63] is given by:

1. **Isentropic compression loss**

The real process is not a Carnot process. The real process moves gradually away from the Carnot cycle because of heat loses, frictional loses in the gear systems and loses in the compressor motor, so additional losses occur in the compression of the steam. Considering a saturated steam that is isentropically compressed from point 3 to 4 (superheated steam with pressure p_k) (refer to figure 2.20). The electrical power input to the compressor for this process (3 → 4) is given by $\dot{W}_{el}^{1}$. The performance factor η_1 of the two process i.e.

Point 1→ Point 2 (Carnot process)

Point 3→ Point 4 (isentropic process) is given by:

$$\eta_1 \equiv \frac{\dot{W}_{el}^{C}}{\dot{W}_{el}^{1}} \tag{2.32}$$

The specific isentropic compression work is given by (Stockburger et. al. [63]):

$$w_{isent} = \frac{\chi}{\chi - 1} \cdot \frac{R}{\tilde{M}} \cdot T_S \cdot \left\{ \left(\frac{P_K}{P_S} \right)^{\frac{\chi-1}{\chi}} - 1 \right\} \tag{2.33}$$

The specific enthalpy at point 4 is given by:

$$w_{isent} = \frac{\chi}{\chi - 1} \cdot \frac{R}{\tilde{M}} \cdot T_S \cdot \left\{ \left(\frac{P_K}{P_S} \right)^{\frac{\chi-1}{\chi}} - 1 \right\} \tag{2.34}$$

The heat transfer is given by:

$$h_4 = h_3 + w_{isent} \Rightarrow h_4 = h''(T_S) + w_{isent} \tag{2.35}$$

$$\dot{Q} = \dot{M} \cdot \Delta h \qquad \text{where } \Delta h = h_4 - h'(T_K) \tag{2.36}$$

$$\Delta h = h''(T_S) + w_{isent} - h'(T_K) \tag{2.37}$$

The coefficient of performance of the process with compression (3 →4) is given by: (Stockburger et al. [63]):

$$\varepsilon_1 = \frac{\dot{Q}}{\dot{W}_{el}^{1}} = \frac{\dot{M} \cdot \Delta h}{\dot{M} \cdot w_{isent}} \tag{2.38}$$

From equation 2.32, the performance factor η_1 of the two processes (i.e. Carnot and isentropic process) is given by:

$$\eta_1 = \frac{\varepsilon_1}{\varepsilon_C} = \frac{\dfrac{\dot{M} \cdot \Delta h}{\dot{M} \cdot w_{isent}}}{\dfrac{T_K}{T_K - T_s}} = \frac{h''(T_S) + w_{isent} - h'(T_K)}{w_{isent}} \cdot \frac{T_K - T_S}{T_K} \tag{2.39}$$

$$\eta_1 = \left[\frac{h''(T_S) - h'(T_K)}{w_{isent}} + 1\right] - \left[\frac{h''(T_S) - h'(T_K)}{w_{isent}} + 1\right] \cdot \frac{T_S}{T_K} \tag{2.40}$$

$$\eta_1 = \left[\frac{h''(T_S) - h'(T_K)}{\dfrac{w_{isent}}{T_S}} + T_S\right] \frac{1}{T_S} - \left[\frac{h''(T_S) - h'(T_K)}{\dfrac{w_{isent}}{T_S}} + 1\right] \cdot \frac{1}{T_K} \tag{2.41}$$

$$\eta_1 = \left[\frac{h''(T_S) - h'(T_K)}{\dfrac{\chi}{\chi - 1} \cdot \dfrac{R}{\tilde{M}} \cdot \left\{\left(\dfrac{P_K}{P_S}\right)^{\frac{\chi-1}{\chi}} - 1\right\}} + T_S\right] \cdot \left[\frac{1}{T_S} - \frac{1}{T_K}\right] \tag{2.42}$$

2. Irreversibility losses in compressor

The Compression from Point 3 P_S → Point 5 P_k is not an isentropic process due to irreversibility losses in the process such as inner losses. So the required electrical driving force increases due to further losses (refer to figure 2.21). These losses are considered through the inner efficiency. The inner efficiency η_2 is given by:

$$\eta_2 = \frac{\dot{W}_{el}^1}{\dot{W}_{el}^2} \tag{2.43}$$

3. Shaft losses

$$\eta_{3,\ \text{shaft}\ \text{mech.}} = \frac{\dot{W}_{el}^2}{\dot{W}_{el,\ shaft}^3} \tag{2.44}$$

4. **Gear systems losses**

$$\eta_{4,\,gear} = \frac{\dot{W}_{el}^{3}}{\dot{W}_{el,\,gear}^{4}} \tag{2.45}$$

5. **Motor losses**

$$\eta_{5,\,motor} = \frac{\dot{W}_{el}^{4}}{\dot{W}_{el,motor}^{5}} \tag{2.46}$$

Where $\dot{W}_{el,motor}^{5}$ is the available electrical power to drive the motor for the real process.

6. **Total performance factor**

The total efficiency of the compressor is given by:

$$\eta_{\Sigma} = \eta_1 \cdot \eta_2 \cdot \eta_3 \cdot \eta_4 \cdot \eta_5 \tag{2.47}$$

2.6.2 Exergy efficiency

The exergy efficiency is given by:

$$\xi \equiv \frac{\dot{E}x_{out}}{\dot{E}x_{in}} \tag{2.48}$$

2.6.2.1 Exergy efficiency of practical Carnot process

Considering the wet vapor region of the reversible cycle process shown in figure 2.20, the exergy efficiency of the Carnot process can be expressed as (Stockburger et al.[63]):

$$\xi_C = \frac{\dot{E}x_p}{\dot{E}x_o + \dot{W}_{el}^{C}} \tag{2.49}$$

The exergy transfer associated with the heating (reboiler) and cooling (condenser) streams are as follows:

$$\dot{\mathbf{E}}\mathbf{x}_{\mathbf{p}} = \dot{\mathbf{Q}} \cdot \left(\mathbf{1} - \frac{\mathbf{T}_{\mathbf{a}}}{\mathbf{T}_{\mathbf{p}}} \right) \tag{2.50}$$

$$\dot{\mathbf{E}}\mathbf{x}_{\mathbf{o}} = \dot{\mathbf{Q}}_{\mathbf{o}} \cdot \left(\mathbf{1} - \frac{\mathbf{T}_{\mathbf{a}}}{\mathbf{T}_{\mathbf{o}}} \right) \tag{2.51}$$

The heat transfer (heat duty) is given by:

$$\dot{\mathbf{Q}} = \dot{\mathbf{M}} \cdot \mathbf{T}_{\mathbf{K}} \cdot \boldsymbol{\Delta}\mathbf{s} \tag{2.52}$$

$$\dot{\mathbf{Q}}_{\mathbf{o}} = \dot{\mathbf{M}} \cdot \mathbf{T}_{\mathbf{o}} \cdot \boldsymbol{\Delta}\mathbf{s} \tag{2.53}$$

The electrical energy supplied to the compressor is responsible for the isentropic compression from point 1 to point 2 as shown in figure 2.20. The difference in the heating and cooling streams is equal to the electrical energy supplied to the compressor as shown below:

$$\dot{\mathbf{W}}_{\mathbf{el}}^{\mathbf{C}} = \dot{\mathbf{Q}} - \dot{\mathbf{Q}}_{\mathbf{o}} \tag{2.54}$$

The exergy balance of the heat pump is given by:

$$\dot{\mathbf{E}}\mathbf{x}_{\mathbf{p}} + \dot{\mathbf{E}}\mathbf{x}_{\mathbf{L}} = \dot{\mathbf{E}}\mathbf{x}_{\mathbf{o}} + \dot{\mathbf{W}}_{\mathbf{el}}^{\mathbf{C}} \tag{2.55}$$

Equation 2.49 becomes:

$$\xi_{\mathbf{C}} = \frac{\dot{\mathbf{E}}\mathbf{x}_{\mathbf{p}}}{\dot{\mathbf{E}}\mathbf{x}_{\mathbf{p}} + \dot{\mathbf{E}}\mathbf{x}_{\mathbf{L}}} \tag{2.56}$$

The exergy loss during the heat transfer of the heat streams $\dot{\boldsymbol{Q}}$ (reboiler) and $\dot{\boldsymbol{Q}}_{\boldsymbol{o}}$ (condenser) is given by:

$$\dot{\mathbf{E}}\mathbf{x}_{\mathbf{L}} = \dot{\mathbf{E}}\mathbf{x}_{\mathbf{L,k}} + \dot{\mathbf{E}}\mathbf{x}_{\mathbf{L,o}} \tag{2.57}$$

Where:

$$\dot{\mathbf{E}}\mathbf{x}_{\mathbf{L,k}} = \dot{\mathbf{Q}} \cdot \mathbf{T}_{\mathbf{a}} \cdot \left(\frac{\mathbf{T}_{\mathbf{k}} - \mathbf{T}_{\mathbf{p}}}{\mathbf{T}_{\mathbf{k}} \cdot \mathbf{T}_{\mathbf{p}}} \right) \tag{2.58}$$

$$\dot{\mathbf{E}}\mathbf{x}_{\mathbf{L,o}} = \dot{\mathbf{Q}}_{\mathbf{o}} \cdot \mathbf{T}_{\mathbf{a}} \cdot \left(\frac{\mathbf{T}_{\mathbf{o}} - \mathbf{T}_{\mathbf{s}}}{\mathbf{T}_{\mathbf{o}} \cdot \mathbf{T}_{\mathbf{s}}} \right) \tag{2.59}$$

Integrating equation 2.54 into 2.59 this gives:

$$\dot{\mathbf{E}}\mathbf{x}_{\mathbf{L,o}} = (\dot{\mathbf{Q}} - \dot{\mathbf{W}}_{\mathbf{el}}^{\mathbf{C}}) \cdot \mathbf{T}_{\mathbf{a}} \cdot \left(\frac{\mathbf{T}_{\mathbf{o}} - \mathbf{T}_{\mathbf{s}}}{\mathbf{T}_{\mathbf{o}} \cdot \mathbf{T}_{\mathbf{s}}} \right) \tag{2.60}$$

The exergy lost due to heat transfer by the reboiler (see figure 2.18) is given by:

$$\dot{\mathbf{E}}\mathbf{x}_{\mathbf{k}} = \dot{\mathbf{E}}\mathbf{x}_{\mathbf{p}} + \dot{\mathbf{E}}\mathbf{x}_{\mathbf{L,k}} \tag{2.61}$$

$$\dot{\mathbf{Q}} \cdot \left(\mathbf{1} - \frac{\mathbf{T}_{\mathbf{a}}}{\mathbf{T}_{\mathbf{K}}} \right) = \dot{\mathbf{Q}} \cdot \left(\mathbf{1} - \frac{\mathbf{T}_{\mathbf{a}}}{\mathbf{T}_{\mathbf{P}}} \right) + \dot{\mathbf{E}}\mathbf{x}_{\mathbf{L,K}} \tag{2.62}$$

$$\dot{\mathbf{E}}\mathbf{x}_{\mathbf{L,K}} = \dot{\mathbf{Q}} \cdot \left(\frac{\mathbf{T}_{\mathbf{K}} - \mathbf{T}_{\mathbf{a}}}{\mathbf{T}_{\mathbf{K}}} - \frac{\mathbf{T}_{\mathbf{P}} - \mathbf{T}_{\mathbf{a}}}{\mathbf{T}_{\mathbf{P}}} \right) \tag{2.63}$$

$$\dot{\mathbf{E}}\mathbf{x}_{\mathbf{L,K}} = \dot{\mathbf{Q}} \cdot \mathbf{T}_{\mathbf{a}} \cdot \left(-\frac{\mathbf{1}}{\mathbf{T}_{\mathbf{K}}} + \frac{\mathbf{1}}{\mathbf{T}_{\mathbf{P}}} \right) = \dot{\mathbf{Q}} \cdot \mathbf{T}_{\mathbf{a}} \cdot \left(\frac{\mathbf{T}_{\mathbf{K}} - \mathbf{T}_{\mathbf{P}}}{\mathbf{T}_{\mathbf{K}} \cdot \mathbf{T}_{\mathbf{P}}} \right) \tag{2.64}$$

Integrating equations 2.60 and 2.64 into 2.56 gives:

$$\xi_{\mathbf{C}} = \frac{\dot{\mathbf{Q}} \cdot \left(\mathbf{1} - \frac{\mathbf{T}_{\mathbf{a}}}{\mathbf{T}_{\mathbf{p}}} \right)}{\dot{\mathbf{Q}} \cdot \left(\mathbf{1} - \frac{\mathbf{T}_{\mathbf{a}}}{\mathbf{T}_{\mathbf{p}}} \right) + \dot{\mathbf{Q}} \cdot \mathbf{T}_{\mathbf{a}} \cdot \left(\frac{\mathbf{T}_{\mathbf{k}} - \mathbf{T}_{\mathbf{p}}}{\mathbf{T}_{\mathbf{k}} \cdot \mathbf{T}_{\mathbf{p}}} \right) + (\dot{\mathbf{Q}} - \dot{\mathbf{W}}_{\mathbf{el}}^{\mathbf{C}}) \cdot \mathbf{T}_{\mathbf{a}} \cdot \left(\frac{\mathbf{T}_{\mathbf{o}} - \mathbf{T}_{\mathbf{s}}}{\mathbf{T}_{\mathbf{o}} \cdot \mathbf{T}_{\mathbf{s}}} \right)} \tag{2.65}$$

$$\xi_{\mathbf{C}} = \frac{\left(\mathbf{1} - \frac{\mathbf{T}_{\mathbf{a}}}{\mathbf{T}_{\mathbf{P}}} \right)}{\left(\mathbf{1} - \frac{\mathbf{T}_{\mathbf{a}}}{\mathbf{T}_{\mathbf{p}}} \right) + \mathbf{T}_{\mathbf{a}} \cdot \left(\frac{\mathbf{T}_{\mathbf{k}} - \mathbf{T}_{\mathbf{p}}}{\mathbf{T}_{\mathbf{k}} \cdot \mathbf{T}_{\mathbf{p}}} \right) + (\mathbf{1} - \frac{\dot{\mathbf{W}}_{\mathbf{el}}^{\mathbf{C}}}{\dot{\mathbf{Q}}}) \cdot \left(\frac{\mathbf{T}_{\mathbf{o}} - \mathbf{T}_{\mathbf{s}}}{\mathbf{T}_{\mathbf{o}} \cdot \mathbf{T}_{\mathbf{s}}} \right)} \tag{2.66}$$

If the temperature difference i.e. $\mathbf{T}_{\mathbf{k}} = \mathbf{T}_{\mathbf{p}}$ and $\mathbf{T}_{\mathbf{o}} = \mathbf{T}_{\mathbf{s}}$, then exergy loss $\dot{\mathbf{E}}\mathbf{x}_{\mathbf{L}} = \mathbf{0}$

This means that the Carnot efficiency is $\xi_{\mathbf{C}} = \mathbf{1}$

The Carnot efficiency can be expressed in terms of only temperature as follows. Integrating equations 2.50, 2.60 and 2.64 into 2.56 gives (Stockburger et al. [63]):

$$\dot{W}_{el}^{C} = \dot{Q} - \dot{Q}_O \qquad \frac{\dot{W}_{el}^{C}}{\dot{Q}} = 1 - \frac{\dot{Q}_O}{\dot{Q}} \Rightarrow \left(1 - \frac{\dot{W}_{el}^{C}}{\dot{Q}}\right) = \frac{\dot{Q}_O}{\dot{Q}}$$

$\dot{W}_{el}^{C}$ is the electrical power input to the compressor for isentropic compression between point 1 and point 2 (see figure 2.20). Point 1 lies on the isothermal line T_S and point 2 lies on the isothermal line T_K, this means that:

$\dot{Q} = \dot{M} \cdot T_K \cdot \Delta S$ and $\dot{Q}_O = \dot{M} \cdot T_O \cdot \Delta S$ also $\frac{\dot{Q}_O}{\dot{Q}} = \frac{T_S}{T_K}$, integrating these into equation 2.66 gives the exergy efficiency of the Carnot process is (Stockburger et al. [63]):

$$\xi_C = \frac{\left(1 - \frac{T_a}{T_P}\right)}{\left(1 - \frac{T_a}{T_P}\right) + T_a \cdot \left(\frac{T_K - T_P}{T_K \cdot T_P}\right) + \frac{T_S}{T_K} \cdot \left(\frac{T_O - T_S}{T_O \cdot T_S}\right)} \tag{2.67}$$

$$\xi_C = \frac{\left(1 - \frac{T_a}{T_P}\right)}{\left(\frac{T_K}{T_K} - \frac{T_a}{T_P}\right) + T_a \cdot \left(\frac{T_K - T_P}{T_K \cdot T_P} + \frac{T_S}{T_K} \cdot \frac{T_O - T_S}{T_O \cdot T_S}\right)} \tag{2.68}$$

$$\xi_C = \frac{\left(1 - \frac{T_a}{T_P}\right)}{\frac{T_K}{T_K} - \frac{T_a}{T_P} + T_a \cdot \left(\frac{1}{T_P} - \frac{1}{T_K} + \frac{1}{T_K} - \frac{1}{T_K} \cdot \frac{T_S}{T_O}\right)} \tag{2.69}$$

$$\xi_C = \frac{\left(1 - \frac{T_a}{T_p}\right)}{\frac{T_k - T_a \cdot \frac{T_s}{T_o}}{T_k}} = \frac{T_k}{T_k - T_a \cdot \frac{T_S}{T_o}} \cdot \frac{T_p - T_a}{T_p} \tag{2.70}$$

2.6.2.2 Exergy efficiency of real process

The exergy efficiency of the real process including all losses is therefore shown as follows:

$$\xi_{real,HP} \equiv \frac{\dot{E}x_{out}}{\dot{E}x_{in}} = \frac{\dot{E}x_P}{\dot{E}x_P + \dot{E}x_L} = \frac{\dot{E}x_P}{\dot{E}x_P + \dot{E}x_{L,k} + \dot{E}x_{L,o,real} + \dot{E}x_{L,motor,real}} \tag{2.71}$$

Where:

a. Exergy transfer by (reboiler) to distillation unit

$\dot{E}x_p = \dot{Q} \cdot \left(1 - \frac{T_a}{T_p}\right)$ (refer to carnot)

b. Exergy loss from reboiler

$\dot{E}x_{L,k} = \dot{Q} \cdot T_a \cdot \left(\frac{T_k - T_p}{T_k \cdot T_p}\right)$ (refer to carnot)

c. Exergy loss from condenser

$\dot{E}x_{L,o,real} = \dot{Q}_o \cdot T_a \cdot \left(\frac{T_o - T_s}{T_o \cdot T_s}\right)$, Given that $\dot{W}_{el1,2} = \frac{\dot{W}_{el}^c}{\eta_1 \cdot \eta_2}$ and $\dot{W}_{el\,1,2} = \dot{Q} - \dot{Q}_o$

also $\eta_{1,2} = \eta_1 \cdot \eta_2$. The above equation becomes:

$\dot{E}x_{L,o,real} = (\dot{Q} - \frac{\dot{W}_{el}^C}{\eta_{12}}) \cdot T_a \cdot \left(\frac{T_o - T_s}{T_o \cdot T_s}\right)$

d. Exergy loss via motor

$\dot{W}_{el,motor}^5 \equiv \dot{W}_{el}^C + \dot{E}x_{L,motor,real}$, $\dot{W}_{el,motor}^5 = \frac{\dot{W}_{el}^C}{\eta_\Sigma}$, $\dot{E}x_{L,motor,real} = (\frac{1}{\eta_\Sigma} - 1) \cdot \dot{W}_{el}^C$

$\dot{E}x_{L,motor,real} == \frac{1 - \eta_\Sigma}{\eta_\Sigma} \cdot \dot{W}_{el}^C$

Equation 2.71 becomes:

$$\xi_{real,HP} = \frac{\dot{Q} \cdot \left(1 - \frac{T_a}{T_p}\right)}{\dot{Q} \cdot \left(1 - \frac{T_a}{T_p}\right) + T_a \cdot \dot{Q} \cdot \left(\frac{T_k - T_p}{T_k \cdot T_p}\right) + (\dot{Q} - \frac{\dot{W}_{el}^C}{\eta_{12}}) \cdot T_a \cdot \left(\frac{T_o - T_s}{T_o \cdot T_s}\right) + \dot{W}_{el}^C \cdot \frac{1 - \eta_\Sigma}{\eta_\Sigma}} \quad (2.72)$$

$$\xi_{real,HP} = \frac{\left(1 - \frac{T_a}{T_P}\right)}{\left(1 - \frac{T_a}{T_p}\right) + T_a \cdot \left(\frac{T_k - T_p}{T_k \cdot T_p}\right) + (1 - \frac{1}{\eta_{12} \cdot \varepsilon_C}) \cdot T_a \cdot \left(\frac{T_o - T_s}{T_o \cdot T_s}\right) + \frac{1}{\varepsilon_C} \cdot \frac{1 - \eta_\Sigma}{\eta_\Sigma}} \quad (2.73)$$

$$\xi_{real,HP} = \frac{1 - \frac{T_a}{T_P}}{1 - \frac{T_s \cdot T_a}{\eta_{12} \cdot T_k \cdot T_o} + T_a \cdot \frac{1 - \eta_{12}}{\eta_{12}} \left(\frac{1}{T_k} - \frac{1}{T_s} + \frac{1}{T_p} \right) + \frac{1 - \eta_{\Sigma}}{\eta_{\Sigma}} \cdot \frac{T_k - T_s}{T_k}} \tag{2.74}$$

$$\xi_{real,HP} = f\left(T_k, T_p, T_T, T_s, T_a, \eta_{12}, \eta_{\Sigma}\right)$$

Temperature relation is as follows:

T_k	>	T_p	>	T_o	>	T_s	>	T_a	
steam temp.(hotside)		**sump prod. temp.**		**top temp.(column)**		**compressor inlet temp.**		**ambient temp.**	

This is clearly a descriptive of a distillation column.

2.7 Distillation unit design aspect

For the rigorous modelling of a distillation column, models for the single stage will be discussed in this subchapter. A rigorous method describes a column as a group of equations and solves these equations to calculate the operating conditions of the column. The equations were first referred to as the MESH (Material, Equilibrium, Summation, Heat or enthalpy balance equations) equations by Wang and Henke [65].

2.7.1 Standard design procedure

2.7.1.1 Modelling of the equilibrium stage

For modelling of distillation column, the well known model of equilibrium stage is used. The general model of such an equilibrium stage is shown in figure 2.22.

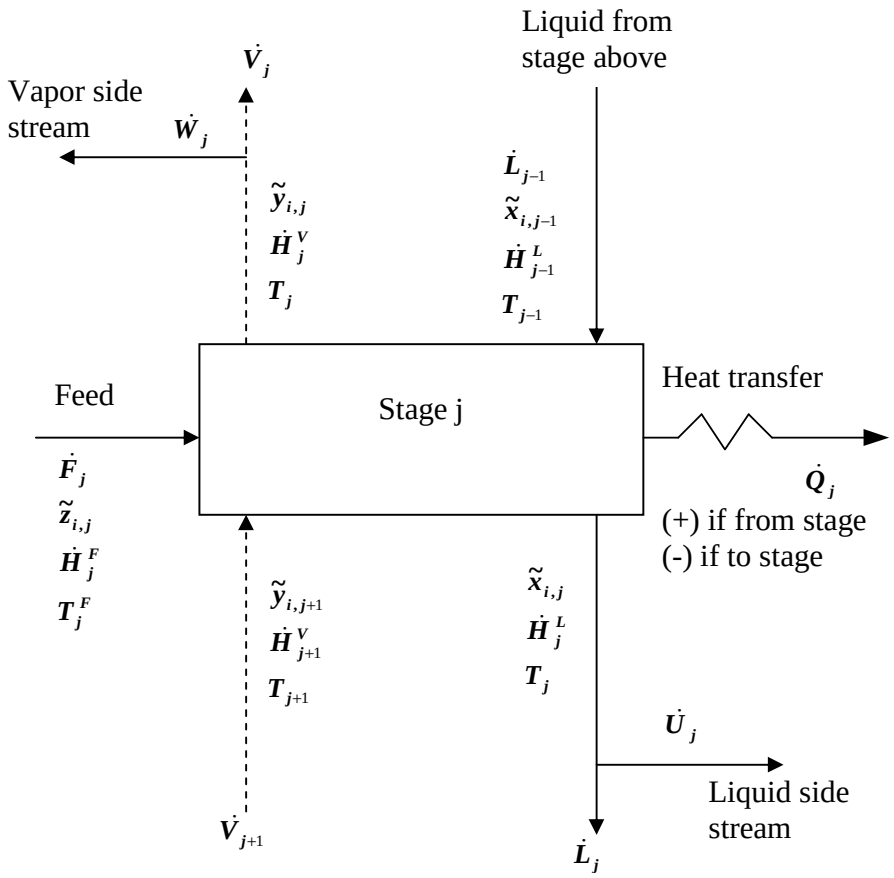

Figure 2.22. A general equilibrium stage for distillation. Source: Smith [66]

It allows for many design options other than simple columns with one feed and two products. On each stage, vapour flow of V_{j+1} and liquid flow of L_{j-1} enters the stage in counter current flow. The main assumptions of equilibrium stage analysis that leads to a constant molar overflow of the phases that leave the stage (Vj, Lj) is referred to as the McCabe – Thiele assumptions and these are (Smith [66]):

- The components have equal and constant molar enthalpies of vaporization (latent heats).
- The components sensible enthalpy changes $C_p \cdot \Delta T$ and heat of mixing are negligible compared to latent heat changes.
- The column is well insulated and heat loss is negligible.
- The pressure is uniform throughout the column.

Additionally there are side streams which can be withdrawn from the distillation column at intermediate stage as a liquid or vapor. Feed can enter, and heat can be transferred to or from the stage. A cascade of such equilibrium stages represents the most general form of a distillation column and on each stage, the so called MESH equations are solved (Brusis [67]) as follows.

Material balance for component i and stage j is:

$$\dot{L}_{j-1} \cdot \tilde{x}_{i,j-1} + \dot{V}_{j+1} \cdot \tilde{y}_{i,j+1} + \dot{F}_j \cdot \tilde{z}_{i,j} = (\dot{L}_j + \dot{U}_j) \cdot \tilde{x}_{i,j} + (\dot{V}_j + \dot{W}_j) \cdot \tilde{y}_{i,j} \tag{2.75}$$

Equilibrium relation for each component i is:

$$\tilde{y}_{i,j} = K_{i,j} \cdot \tilde{x}_{i,j} \tag{2.76}$$

Summation equation for each stage is given by:

For the vapour phase:

$$\sum_{i=1}^{NC} \tilde{y}_{i,j} = 1 \tag{2.78}$$

For the liquid phase

$$\sum_{i=1}^{NC} \tilde{x}_{i,j} = 1 \tag{2.77}$$

Heat or energy balance,

$$\dot{L}_{j-1} \cdot \dot{H}^{L}_{j-1} + \dot{V}_{j+1} \cdot \dot{H}^{V}_{j+1} + \dot{F}_{j} \cdot \dot{H}^{F}_{j} = (\dot{L}_{j} + \dot{U}_{j}) \cdot \dot{H}^{L}_{j} + (\dot{V}_{j} + \dot{W}_{j}) \cdot \dot{H}^{V}_{j} + \dot{Q}_{j} \quad (2.79)$$

There are many methods available for the evaluation of the above MESH-equations. For example Lewis and Matheson [68] developed the sequential methods for tray-to-tray calculation. RADFRAC model in Aspen Plus™ is used in this thesis. For process/economic optimization SQP is used.

2.7.2 Economic aspects

The purpose of chemical processes is to make profit. An understanding of process economics is therefore very important in process design. Excessive energy consumption by using hot and cold utilities influences the global cost of industrial processes. For this reason, one of the major worries of process design has been the reduction of utilities consumption, as well as the reduction of fixed capital investment (FCI) of the equipment. Process economics has three basic roles in process design (Smith [66]):

- *Evaluation of design alternatives*

In all stages of chemical design process, estimation of the fixed capital investment (FCI) and annual operating cost are very important for evaluation of processing alternatives.

- *Process optimization*

The setting of some process variables such as steam flow rate and reflux ratio can have a major influence on decision making in developing the flow sheet and on the overall profitability of the process. Optimization of such variables is very important

- *Profitability*

The economics of the chemical process is evaluated at different stages during the design to asses whether the project is economically viable.

2.7.2.1 Standard economic calculations

The cost effectiveness of a process can be evaluated by applying attributes such as cost, profit and profitability Brusis [67]. For optimization purposes, the estimation of fixed capital Investment (FCI) and operational cost ($\dot{\boldsymbol{C}}_{OC}$) is necessary. In this thesis, the evaluation of investment and operational cost of the different processes will be used for comparison between different process alternatives. In most cases if the investment costs are low, the operational costs are high and vice versa, so that there is economic optimum in between [68].
The cost of a process can be split into many different parts such as, capital, material, energy, labour, general plant, administration, sales and distribution and research and development costs [69].

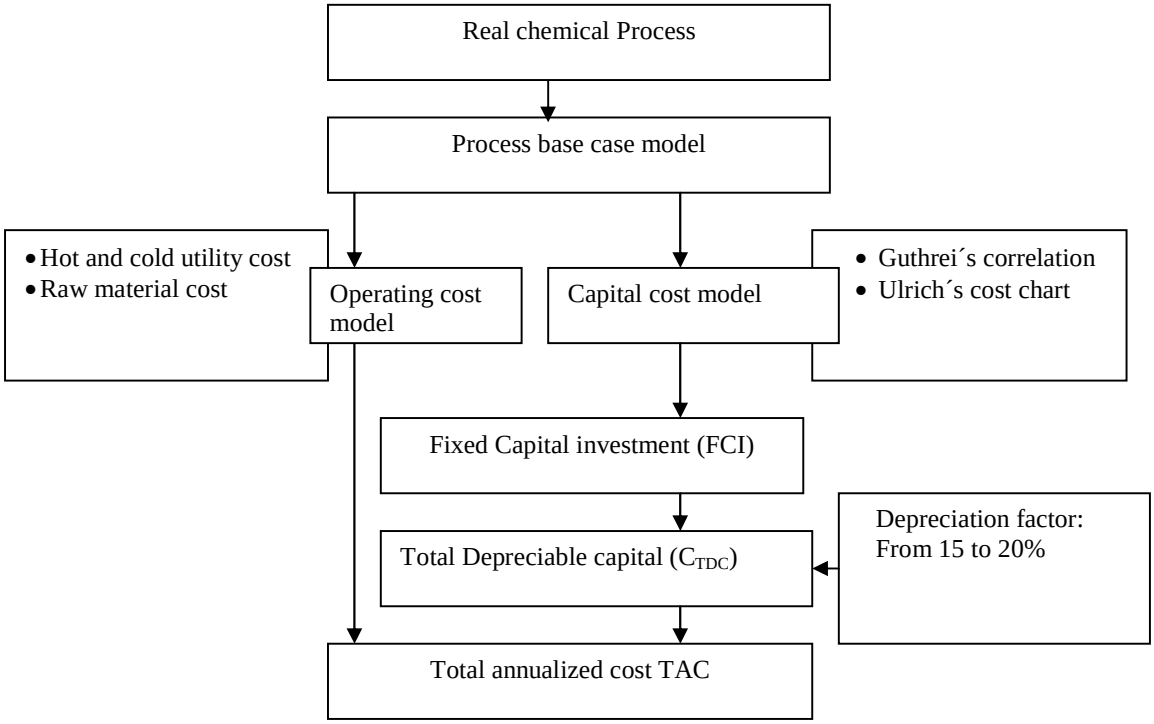

Figure 2.23. Standard cost model

The step in process simulation that produces the economic result is shown is figure 2.24.

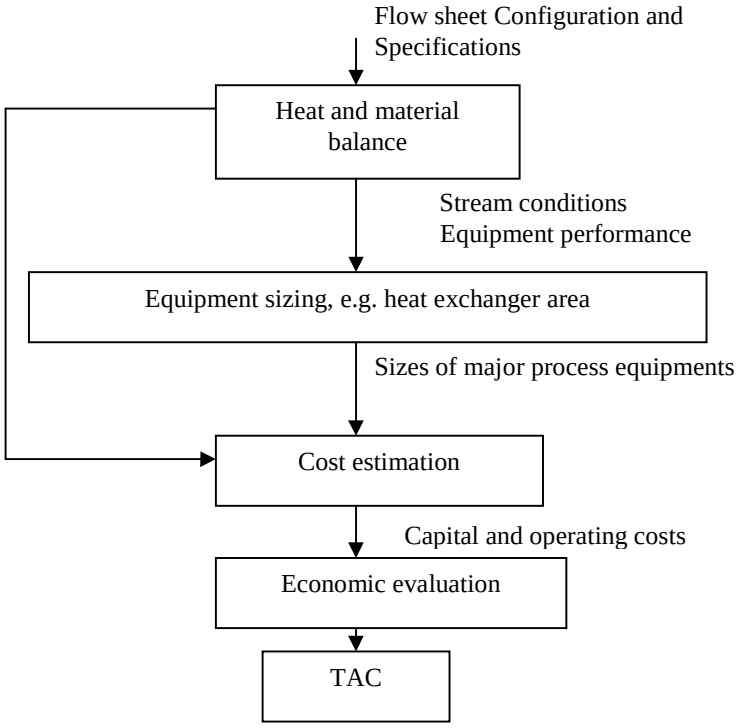

Figure 2.24. Steps in evaluating economic objective

In the context of optimization the relevant costs are mainly represented by fixed capital Investment (FCI) and operational costs for cooling and heating. In all stages of design process, estimation of Total annualized cost (TAC) is very important for the evaluation of process alternatives. In this thesis, Total annualized cost (TAC) is used as an indicator for economic objective for the evaluation of different process alternatives; a summary of the economic model is illustrated in figure 2.24. In the next subsection the various components of TAC are discussed.

2.7.2.2 Cost Index

The purchase cost of processing equipment is generally obtained from charts, equations or quotes from vendors. However, because of inflation, costs are not static, they generally increase with time. It is therefore necessary to update the cost data available from literature. This is done by the use of cost indices (Smith [66]):

$$\frac{\mathbf{C_1}}{\mathbf{C_2}} = \frac{\mathbf{Index_1}}{\mathbf{Index_2}} \qquad (2.80)$$

C1 = Cost of equipment in year 1

C2 = Cost of equipment in year 2

Index1 = Cost index in year 1

Index2 = Cost index in year 2

Some of the commonly used cost indices which are regularly published in chemical engineering magazines are:

- Marshall and Swift index
- Chemical engineering index
- Nelson and Farrar cost index (published in oil and gas journal).

2.7.2.3 Fixed capital investment (FCI)

From an economical point of view, according to Douglas [70], there are two methods to evaluate the costs of investments of equipment: to quote the costs of equipment and installations based on cost charts from vendor and to use cost correlation equations. Douglas [70] mentioned Guthrie's correlations, which calculate the purchase costs of process

equipment including installations very precisely. A lot of factors are used to calculate the installation costs, such as piping requirements, steel for structural supports, conventional instrumentation and controllers, installation of the auxiliary electrical equipment, insulation, painting, labour, freight, insurance, taxes, and other overhead expenses. In this thesis the bare-module concept introduced by Guthrei is used to estimate the installed cost of each process unit.

2.7.2.4 Operating cost

Among the evaluation of fixed capital investment cost, it is necessary to evaluate the operational costs ($\dot{C}_{OC}$). According to Peters and Timmerhaus [71] the operating costs of a chemical plant can be divided into two:

- Fixed operating cost
- Variable operating cost

The Fixed operating cost is independent of the rate of production and they include:

- Maintenance cost
- Salaries- operating labour cost
- Supervision cost
- Capital charges
- Taxes
- Insurance
- Licence fees and royalty payments.
- Plant overheads (e.g. safety services, Laboratory cost, administrative services)

Variable operating cost depends on the rate of production and include:

- Raw material cost
- Energy (utility- fuel, steam, electricity, cooling water process water, etc.) cost.
- Chemicals and catalysts consumed during manufacturing (other than raw materials).

Also, with respect to the variable operating cost, only the utility cost is considered for optimization, i.e. operating cost is estimated in terms of utility cost of cooling water, steam and electrical energy.

$$\dot{\mathbf{C}}_{\mathbf{OC}} = \dot{\mathbf{C}}_{\mathbf{utility\ cost}} \tag{2.81}$$

2.7.2.5 Capital cost

For the purpose of optimization and cost comparison of different design alternatives, the fixed Capital Investment (FCI) have to be annualized to guarantee a similar basis of time for both fixed capital investment (FCI) and operating cost. Annualization of the fixed capital investment (FCI) gives the total depreciable capital cost:

$$\dot{\mathbf{C}}_{\mathbf{TDC}} = \mathbf{(FCI)} \cdot \dot{\mathbf{d}} \tag{2.82}$$

Where $\dot{d}$ is the depreciation or capital recovery factor and normally varies from 15 to 20%.

2.7.2.6 Total annualized cost (TAC)

The Total annualized cost (TAC) is calculated as follows:

$$\mathbf{TAC} = \dot{\mathbf{C}}_{\mathbf{TDC}} + \dot{\mathbf{C}}_{\mathbf{OC}} \tag{2.83}$$

2.8 Multicriteria/Multiobjective Decision Making

In many fields of engineering particularly chemical process design, major decisions affecting the entire process lifecycle are done during early stages of the process design. The criteria used are not any more only economic but also environmental aspects are also taken into consideration. In many applications, such as in the chemical process industry, the decision maker has multiple alternatives and multiple conflicting objectives. For example, process heat integration of different design alternatives of distillation units can reduce the energy consumption which can lead to less potential environmental impact, but on the other hand heat integration can also increase the economic criteria due to increase number of process equipments such as heat exchanger area and pumps etc. Therefore the existence of a number of criteria requires the use of a Multi-criteria decision making (MCDM) approach.

MCDM techniques allow decision makers to choose or rank alternatives on the basis of several criteria. Decisions are made based on trade-offs or compromises among a number of criteria that are in conflict with each other (Colson [73] and Zeleny [74]).

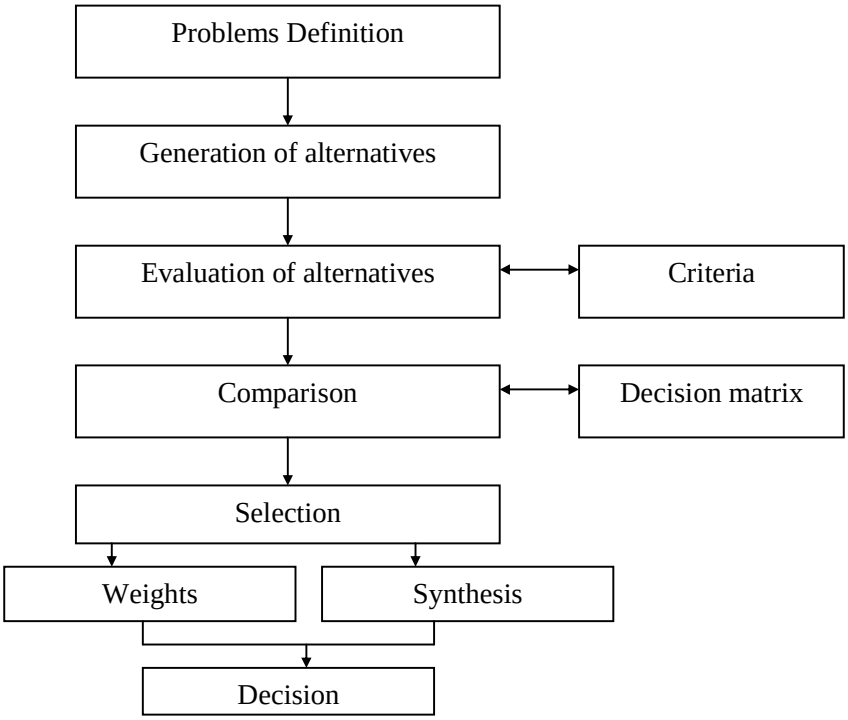

Figure 2.25. Multi-criteria decision support frame work. Source: Linkov [78]

There are many decision-making tools discussed by Hobbs [75], Zanakis et al.[76] and Triantaphyllou [77]. Among them, multi-criteria decision analysis (MCDA) is one of the most widely used decision methodologies.

MCDA can help to improve the quality of decisions by making decision-making more explicit, rational, and efficient. The main steps of multicriteria decision making have been summarized in figure 2.25.

According to Triantaphyllou [77] , the areas of MCDM can be divided into two categories:

- Multiple Attribute Decision Making (MADM)
- Multiple Objective Decision Making (MODM)

2.8.1 Multi-criteria decision making methods

Multi-criteria decision making methods are classified into two main groups as shown in figure 2.26.

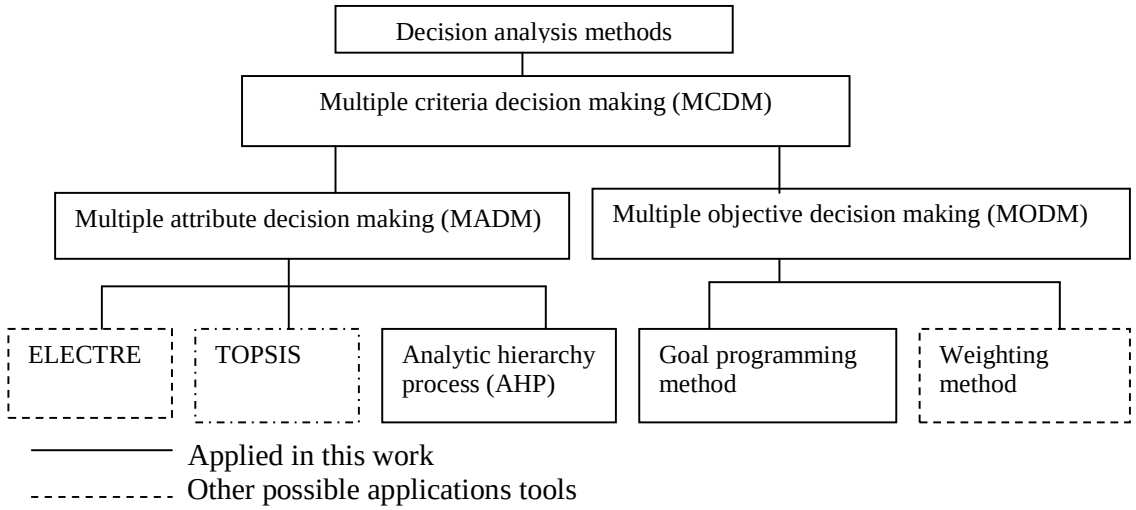

Figure 2.26. Classification of decision analysis methods. Source: Zhou [80]

Multiple Objective Decision Making (MODM) methods are multiple objective mathematical programming models in which a set of conflicting objectives are optimized and subjected to a set of mathematically defined constraints. MODM concentrate on problems where the alternatives are not predetermined i.e. MODM assumes continuous solution space. The purpose is to choose the ‘‘best’’ among all the alternatives [79]. Each alternative is defined implicitly in terms of the decision variables and evaluated by means of objective functions (see table 2.12).

A special case of MODM is the multiple objective linear programming (MOLP) where the objective functions and constraints are linear functions.

Multiple Attribute Decision Making (MADM) method refers to making preference decisions by evaluating all the alternatives that are usually characterized by multiple conflicting attributes. MADM studies problems where the decision space is discrete i.e. these problems have a limited number of alternatives and they have already been predetermined. In a general way it can be said that MADM selects the best alternative among a finite number whiles MODM designs the best alternative.

Table 2.12. Comparison of MODM and MADM Approaches (Hwang and Yoon [81])

	MODM	MADM
Criteria defined by	Objectives	Attributes
Objectives defined	Explicitly	Implicitly
Attributes defined	Implicitly	Explicitly
Alternatives defined	Implicitly	Explicitly
Number of alternatives	Infinite (large)	Finite (small)
Relevant to	Design/search	Evaluation/choice

2.8.2 MADM methods

Figure 2.26 shows some of the most widely used MADM methods. The basic principle of TOPSIS (technique for order preference by similarity to an ideal solution) method is that, the chosen alternative should have the shortest distance from the ideal solution and the farthest distance from the negative-ideal solution, but it does not consider the relative importance of these distances (Hwang and Yoon [81]). The ELECTRE (elimination and choice translating reality) method was first introduced by Benayoun et al. [82]. The method is based on an outranking concept by using pairwise comparison of alternatives under each of the criteria. It is a comprehensive evaluation approach in that it tries to rank a number of alternatives each one of which is described in terms of a number of criteria.

The analytic hierarchy process (AHP), developed by Saaty [83] is designed to solve complex problems involving multiple criteria. The process requires the decision maker to provide judgments about the relative importance of each criterion. It specifies preference on each criterion for each decision alternative. Although MCDM methods are widely diverse, many

of them have certain aspects in common, the main steps of MCDM are as follows (Linkov [78]):

I. Determine the relevant criteria and alternatives,
II. Attach numerical measures to the relative importance of the criteria and to the impacts of the alternatives on these criteria and
III. Process the numerical values to determine a ranking of each alternative

In section 2.8.3 the AHP method is presented in details with an illustrative example.

2.8.2.1 Basic properties of MADM methods

Although MCDM methods could be very different, most of the following terms are used in common:

- **Alternatives:** In this thesis, alternatives are the different designs of distillation units available for consideration.
- **Attributes:** Attributes represents the different dimensions from which alternatives can be viewed e.g. economic and environmental attributes. Attributes are also referred to as “goals” or “decision criteria”.
- **Objectives:** It is the statement about the desired state of the system under consideration. It indicates the directions of improvement of one or more attributes. Objectives are functionality related to a set of attributes.
- **Conflict among Criteria:** Since different criteria represent different dimensions of the alternatives, they may conflict with each other. For instance, economic may conflict with environmental criteria.
- **Decision weights:** Most of the MCDM methods require that the criteria be assigned weights of importance usually these weights are normalized to add up to one. How these weights can be determined is described in section 2.7.3.1 of this thesis.
- **Decision matrix:**

The starting point for modeling a discrete decision problem under multiple objectives is that, the set of alternatives and decision criteria must be defined as follows:

Alternative: A_i (i = 1, . . . , m),

Decision criteria: C_j (j= 1, . . . , m).

The typical MCDM problem is concerned with the task of ranking a finite number of decision alternatives, each of which is explicitly described in terms of different characteristics (also

often called attributes, decision criteria, or objectives) which have to be taken into account simultaneously. Usually, the performance values a_{ij} and the criteria weights w_j are viewed as the entries of a decision matrix defined as follows:

A decision matrix **A** is an (m x n) matrix in which element a_{ij} indicates the performance of alternative A_i when it is evaluated in terms of decision criteria Cj. It is assumed that the decision maker has determined the weights of relative performance of the decision criteria (denoted as $w_{j,}$ for j= 1, . . . , m).

This information is best summarized in figure 2.35 according to Zimmermann [84]:

	Criteria				
	C_1	C_2	C_3	. . .	C_n
Alternative	w_1	w_2	w_3	. . .	w_n
A1	a_{11}	a_{12}	a_{13}	. . .	a_{1n}
A2	a_{21}	a_{22}	a_{23}	. . .	a_{2n}
.	.	.	.	. . .	.
.	.	.	.	. . .	.
.	.	.	.	. . .	.
A_m	a_{m1}	a_{m2}	a_{m3}	. . .	a_{mn}

Figure 2.27. A typical decision matrix

In general, the problems considered in discrete MADA methods is to judge the attractiveness of alternatives on the basis of the scores of the decision criteria $C_j(a_j)$. Depending upon the multiple-criteria aggregation procedure applied, a MADA method can identify the following (Janssen [85]):

A complete ranking: $\boldsymbol{A_1 > A_2 \geq A_3 > A_4}$

The best alternative: $\boldsymbol{A_1 > (A_2, A_3, A_4)}$

A set of acceptable alternatives: $\boldsymbol{(A_1 A_2, A_3) > A_4}$

An incomplete ranking of alternatives: $\boldsymbol{[A_1 > (A_2, A_3, A_4)]}$ or $\boldsymbol{[(A_1, A_2) > (A_3, A_4)]}$

These procedures create complete pre-orders, complete orders, or partial orders. In a complete order, all alternatives are ranked relative to one another, and no two alternatives are regarded as equal. The order is pre-order if some alternatives are regarded as equal. In partial orders, some alternatives may not be ranked relative to others. In the next section the AHP method is presented in details with an illustrative example.

2.8.3 Application of the Analytic Hierarchy Process (AHP)

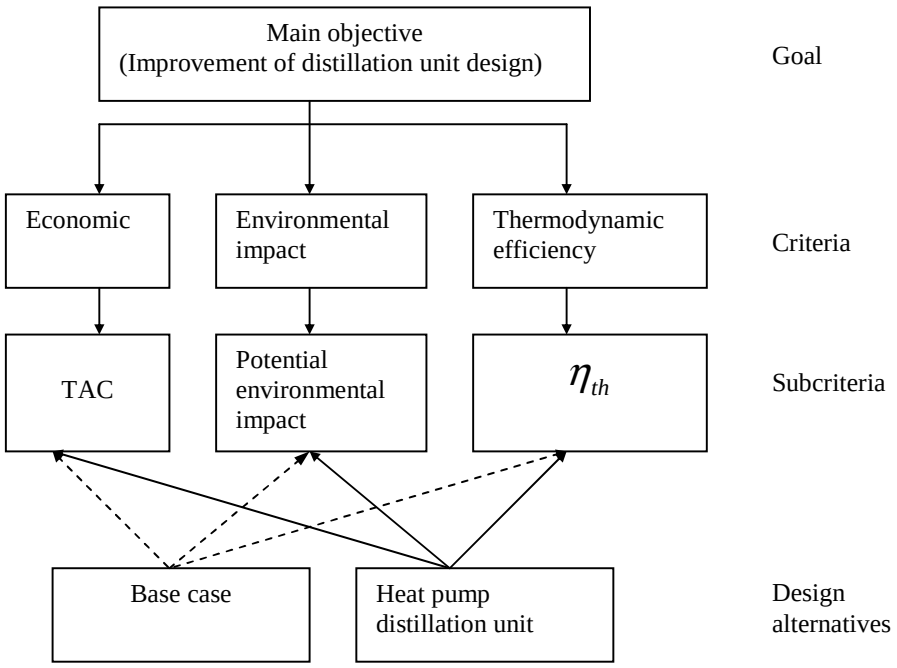

Figure 2.28. Decision Hierarchy based on (Forman et al.[86])

The Analytic Hierarchy Process (AHP) is a tool for analyzing a problem with several criteria with multiple conflicts among them Saaty [83]. It is a multi-attribute decision aiding model that allows decision makers to model a complex problem in a hierarchical structure. For example referring to figure 2.28, from top to bottom, we have the goal (main objective), criteria, sub- criteria and alternatives. The AHP begins with the choice of the problem to analyze and the identification of objectives (factors that influence the problem) and alternatives that can satisfy these objectives. They are then structured in the hierarchy.

On the top of the hierarchy as shown in figure 2.28, the Improvement of distillation unit design is the overall objective to be achieved. The criteria (i.e. economic, environment and thermodynamic efficiency) are also called attribute. On a level below we can have sub-criteria, and on the lowest level we have the alternatives, that are the available options.

2.8.3.1 AHP method

After decomposition of an AHP problem into a hierarchical structure as discussed in the previous section, the next step is to construct a pairwise comparison matrix. The matrix takes pairwise comparisons as input and produces relative weights as output. The pairwise

comparison is quantified by using a scale proposed by Saaty [83]. The values of the pairwise comparison are determined according to the instructions presented in Table 2.13.

Table 2.13. Scale for pairwise comparison (Saaty [83])

Intensity of importance	Definition	Explanation
1	Equal importance	Two criteria contribute equally to the objective
3	Weak importance of one over another	Experience and judgment slightly favour one criteria over another.
5	Strong importance	Experience and judgment strongly favour one criteria over another.
7	Very strong importance	An criteria is strongly favoured and it's dominance is demonstrated in practice
9	Extreme importance	The evidence favouring one criteria over another is of the highest possible order of affirmation
2,4,6,8	Intermediate values between the two adjacent judgments	When compromise is needed
Reciprocals	If activity i has one of the above numbers assigned to it when compared with activity j , then j has the reciprocal value when compared with i	

Once the pairwise comparison is determined by using a scale, they are processed in order to derive the final values. These values are estimates of the relative weights of importance of the criteria being compared. An element of matrix **X** (see table 2.14), x_{ij} may be assigned any value from the AHP original measurement scale containing the integers from 1 to 9.

Table 2.14. Pairwise comparison matrix X

Criteria	X_1	X_2	X_3
X_1	x_{11}	x_{12}	x_{13}
X_2	x_{21}	x_{22}	x_{23}
X_3	x_{31}	x_{32}	x_{33}

Where X_1 = Economic, X_2 = Environment, X_3 = η_{th}

The particular number, usually selected by a decision maker, is used to express the relative importance of a particular criterion when compared across different alternatives. For example if we are comparing the criteria X_1 and X_3 and we think X_1 has a strong importance over X_3, then the element (x_{13}) of this matrix X is 5 i.e. $x_{13}=5$.

The following condition should always be fulfilled when making pairwise comparison:

$$\mathbf{x_{ij} = \frac{1}{x_{ji}} if\ i \neq j\ otherwise\ x_{ii} = 1} \tag{2.84}$$

Equation 2.87 applies to the case when we are comparing the criteria X_3 and X_1, the reciprocal rating is assigned i.e. $x_{31}=1/5$.

The normalized matrix $\mathbf{X}_{norm}$ is obtained by dividing each element of matrix **X** in column *i* by the sum of all elements in the same column *i* as follows:

$$\mathbf{r_{ij} = \frac{x_{ij}}{\sum_{i=1}^{N} x_{ij}} \quad where\ i = 1,2,....,\ N.} \tag{2.85}$$

Next, the matrix of weights, **w** is computed. For example, the weight for the i^{th} row of the matrix **w**, w_i is determined as the average of elements in row i of the matrix $\mathbf{X}_{norm}$ as follows:

$$\mathbf{w_i = \frac{\sum_{j=1}^{N} r_{ij}}{N} \ for\ j = 1,2,....,\ N.} \tag{2.86}$$

2.8.3.2 Illustrative example of AHP method

This section is only concerned with the way the AHP method is applied to a real industrial problem. Optimization was performed to evaluate process improvement of a base case and heat pump distillation units. The main criteria considered in this example are economic, environment and thermodynamic efficiency η_{th} criteria. Modifications where made to each alternative and the optimization results are shown in table 2.15.

The optimization results in table 2.15 shows that there exists a trade off between the objective criteria. The problem is to select the best alternative based on the three criteria. As part of the AHP method, the values of the pairwise comparison are determined first by using a scale proposed by (Saaty [83]).

Table 2.15. Optimization results

Alternatives studied	Base case	Heat pump
Reflux ratio	0.585	0.620
Steam rate kg/hr	573.36	315.56
Electricity consumed kW	-	43
TAC \$/y x 10^3	279	302
η_{th} %	0.31	0.27
Exergy Loss kW	58.32	71.11
$\boldsymbol{PEI}_{std}^{En}$ PEI/hr	49	29

The numerical values of this scale are used to calculate the priority weights of each criteria. As shown in Table 2.16, economic criteria has strong importance than thermodynamic efficiency, a score of 5 is therefore given i.e. we put x_{13} =5, also economic criteria has weak importance over environmental criteria, so a score of 3 is awarded i.e. x_{12} =3.

Table 2.16. Pairwise comparison matrix X

	Economic	Environment	η_{th}
Economic	1	3	5
Environment	1/3	1	3
η_{th}	1/5	1/3	1
sum	1.53	4.3	9

Applying equation 2.85 to the pairwise comparison matrix X (table 2.16), the following normalized results can be obtain for column one of table 2.16 as follows:

Given that

$$\mathbf{r_{ij}} = \frac{\mathbf{x_{ij}}}{\sum_{i=1}^{N} \mathbf{x_{ij}}} \qquad \mathbf{r_{21}} = \frac{\frac{1}{3}}{1.53} = \mathbf{0.22}$$

$$\mathbf{r_{11}} = \frac{1}{1.53} = \mathbf{0.65} \qquad \mathbf{r_{31}} = \frac{\frac{1}{5}}{1.53} = \mathbf{0.13}$$

The same normalization procedure is applied to columns 2 and 3 of table 2.16, the complete results is shown in table 2.17.

Table 2.17. Normalized Pairwise comparison matrix $\mathbf{X}_{norm}$

	Economic	Environment	η_{th}
Economic	0.65	0.70	0.55
Environment	0.22	0.23	0.33
η_{th}	0.13	0.07	0.11

Applying equation 2.86 to the Pairwise comparison matrix X (table 2.17), the matrix of weights (w_i) can be constructed as shown in table 2.18.

Table 2.18. Matrix of weights (w_i)

	Economic	Environment	η_{th}	Sum	Average (w_i)
Economic	0.65	0.70	0.55	1.9	0.63
Environment	0.22	0.23	0.33	0.78	0.26
η_{th}	0.13	0.07	0.11	0.31	0.11

w_i is determined as the average of elements in row i of the matrix $\mathbf{X}_{norm}$ as follows:

$$\mathbf{w_i} = \frac{\sum_{j=1}^{N} \mathbf{r_{ij}}}{\mathbf{N}}$$

$$\mathbf{w_1} = \frac{\mathbf{0.65 + 0.70 + 0.55}}{\mathbf{3}} = \mathbf{0.63}$$

$$\mathbf{w_2} = \frac{\mathbf{0.22 + 0.23 + 0.33}}{\mathbf{3}} = \mathbf{0.26}$$

$$\mathbf{w_3} = \frac{\mathbf{0.13 + 0.07 + 0.11}}{\mathbf{3}} = \mathbf{0.11}$$

The result of the pairwise comparison shows that economic, environment and η_{th} criteria have the following weights; 0.63, 0.26 and 0.12 respectively. The decision matrix for each alternative is shown in Table 2.19.

Table 2.19. Criteria matrix

	Criteria		
Alternative	Economic	Environment	η_{th}
Weights (w_i)	0.63	0.26	0.11
Base case (A_1)	279	49	31
Heat pump (A_2)	302	29	27

The entry $a_{ij,}$ represents the relative value of alternative A_i when it is considered in terms of criteria C_j . The columns in the decision matrix have been normalized to add up to one (see table 2.20).

Table 2.20. Normalized criteria matrix

	Criteria		
Alternative	Economic	Environment	η_{th}
Weights (w_i)	0.63	0.26	0.11
Base case (A_1)	279/581	49/78	31/58
Heat pump (A_2)	302/581	29/78	27/58

According to AHP the best alternative is indicated by:

$$\mathbf{A_{AHP-score} = \max_i \sum_{j=1}^{n} a_{ij} \cdot w_j, \qquad for\ i = 1,2,3,\ldots\ldots\ldots m} \tag{2.87}$$

When equation 2.87 is applied to the data of table 2.20, the following scores can be calculated for each alternative:

$$\mathbf{A_{1,\,AHP-score} = \left(\frac{279}{581}\right)\cdot 0.63 + \left(\frac{49}{78}\right)\cdot 0.26 + \left(\frac{31}{58}\right)\cdot 0.11 = 0.53}$$

$\mathbf{A_{2,\,AHP-score} = \left(\frac{302}{581}\right)\cdot 0.63 + \left(\frac{29}{78}\right)\cdot 0.26 + \left(\frac{27}{58}\right)\cdot 0.11 = 0.47}$, $A_{1,\,AHP\text{-}score}$= 0.53, $A_{2,\,AHP\text{-}score}$= 0.47, Therefore the best alternative is alternative A_1 (base case) because it has the highest AHP.

2.8.4 Multiple Objective Decision Making

Multiple Objective Decision Making (MODM) is a MCDM approach. Many real world applications involve several objective functions that need to be optimized simultaneously. It is extremely rare to have one feasible solution which simultaneously optimizes all of the objective functions. So, optimizing one of the objective functions has the effect of moving another objective function away from its most desirable value. These are the usual conflicts among the objective functions in multi-objective models. There are several publications (Volker et al. [87] and Rajesh et al. [88]) that have addressed multi-objective optimization problem in the field of chemical engineering. Edgar and Himmelblau [89] did give extensive discussion on multiobjective optimization issues in the chemical process industry.

2.8.4.1 Definition of multiobjective optimization problem

Multi-Objective Optimization is the process of minimizing or maximizing a desired objective functions. The problem usually has a number of constraints which any feasible solution (including the optimal solution) must satisfy. The general form of the multiobjective optimization problem can be stated as follows (Deb [90]):

$$\begin{aligned} &\textbf{min} \quad \mathbf{F(X)} = [\mathbf{f}_1(\mathbf{x}), \mathbf{f}_2(\mathbf{x}), ..., \mathbf{f}_m(\mathbf{x})]^T \\ &\quad \textbf{w.r.t.} \quad \mathbf{x} \\ &\textbf{subject to} \\ &\mathbf{g}_j(\mathbf{X}) \geq \mathbf{0} \qquad \mathbf{j = 1, 2, ..., J} \\ &\mathbf{h}_k(\mathbf{X}) = \mathbf{0} \qquad \mathbf{k = 1, 2, ..., K} \\ &\mathbf{x}_i^L \leq \mathbf{x}_i \geq \mathbf{x}_i^U \qquad \mathbf{i = 1, 2, ..., n} \end{aligned} \tag{2.88}$$

Where *f* is a vector of economic and environmental objective functions. X is a vector of n decision variables (such as, process variables (e.g. steam flow rate, feed flow rate, reflux ratio, product purity etc), design variables or process configuration (column diameter, number of trays etc)) $X = [\mathbf{x}_1, \mathbf{x}_2, ..., \mathbf{x}_n]^T$. The constraints associated with the problem are j inequality constraints $g_j(X)$ related to the process variables such as product purity and k equality constraints $h_k(X)$ associated with the process design variables (e.g. column diameter) and process model equations (e.g. mass and energy balance). The last sets of constraints are called variable bounds, restricting each decision variable x_i to take a value within a lower $x_i^{(L)}$ and upper bound $x_i^{(U)}$. The solution to the multi-objective optimization is not a single solution, but rather it is the nondominated set, also known as the Pareto set after

the French-Italian economist and sociologist Vifredo Pareto [91]. The set is a collection of alternatives that represent potential compromise solutions among the objective functions. For each solution in the decision space there exist points in the objective space denoted by:

$$\mathbf{Z = F(X) = [z_1, z_2, ..., z_m]^T}$$

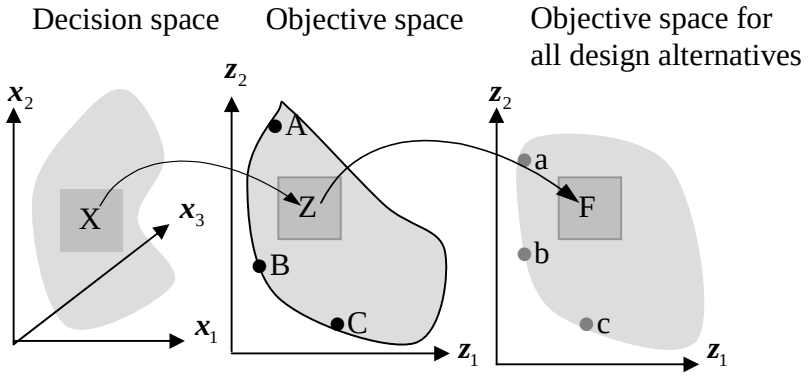

Figure 2.29. An illustration of a multi-objective optimization problem with decision variable space X mapping into objective space Z. Source: Deb [90]

Figure 2.29 illustrates these two spaces and the link between them. The objective vectors (z_1, z_2) at points A, B and C are nondominated set also known as the Pareto set. The best nondominated solutions are the relevant design alternatives for the decision-maker. In relation to the case study to be discussed later, the following definitions are necessary.

Definitions:

i. Decision Space X: This consist of the process and design variables (e.g. steam flow rate, reflux ratio, cooling water rate, column diameter, product purity)

ii. Objective Space Z: This consist of the feasible criterion space (i.e. z_1=TAC, z_2=PEI).

iii. Objective space for all alternatives F: This is the feasible objective space with respect to each design alternative (e.g. a = base case, b = heat pump and c = pump-around)

Procedure: The feasible region of the decision space is first located. The shaded region in the objective space corresponds to the feasible solutions in decision space. Since all Pareto optimal points lie on the boundary of the feasible objective space Z, the Pareto optimal points are used to locate the nondominated solutions (e.g. points A, B, C in fig.

2.29) in the objective space. Each design alternative is further located by means of the feasible objective space for all design alternatives.

2.8.4.2 Iterative procedure of numerical optimization

Process simulation in this work means, the application of deterministic modeling (i.e. models based on physical relationships). The process is represented by a collection of models. The models consist of equations. The model depends on the initial values of the variables to simulate the process and calculates results (see figure 2.30).

Figure 2.30. A typical process model

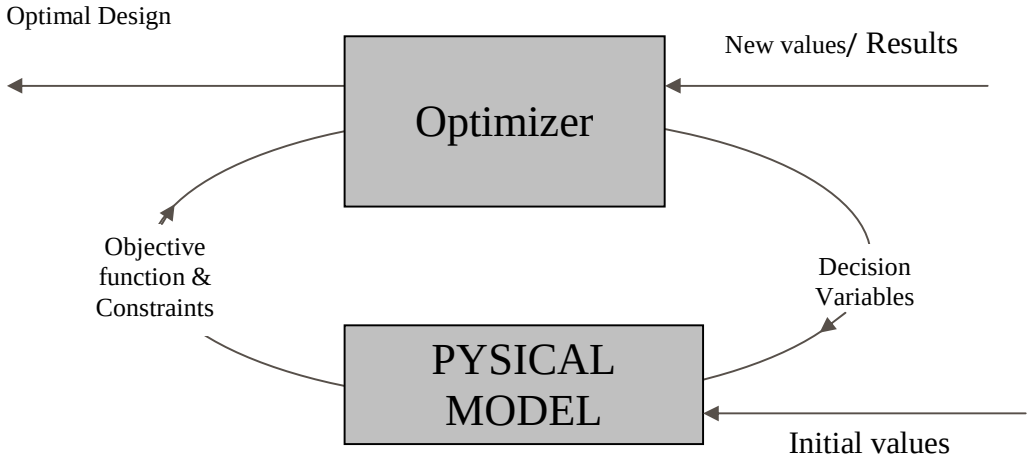

Figure 2.31. Representation of numerical optimization framework.
Source: Diwekar [92]

Figure 2.31 illustrates schematically the iterative approach applied in a numerical optimization technique. The optimizer generates a set of values for the decision variables x. The model simulates the process and calculates the data for the objective function under consideration of constraints. This information is used by the optimizer to calculate a new set of decision variables. This iterative sequence is continued until the optimization criteria pertaining to the optimization algorithm are satisfied.

3 Combination of distillation and power plant

Distillation remains the most used separation method, but it has a low thermodynamic efficiency in stand-alone operation. Therefore energy saving in distillations is a main topic in integrated process design. In this chapter some techniques that can be applied to improve the energetic efficiency of distillation systems by integration of the power plant and distillation is discussed. Generation of heat can be done in different ways, the importance of using a particular method can be established by comparing different options. Morosyuk [93] suggested that different options can be compared in the following order: comparison of energy performance parameters under theoretical conditions (such as Carnot efficiency); comparison of such parameters against those obtained under real practical process condition, with nonrecoverable energy losses, losses due to friction, losses due to irreversibility in the process, mechanical and gear losses etc. The main product of a power station is electrical power, this means that the primary energy input is a direct function of the electrical power produced i.e. see figure 3.1.

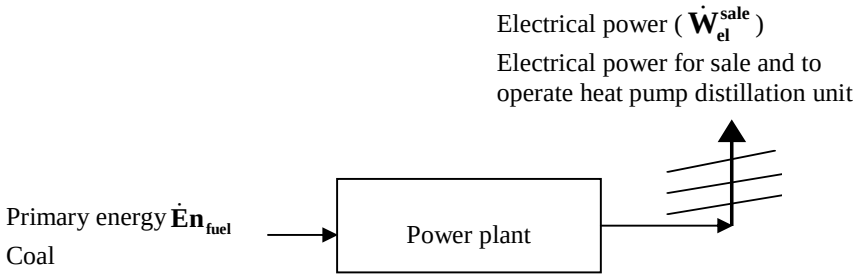

Figure 3.1. Electrical power production

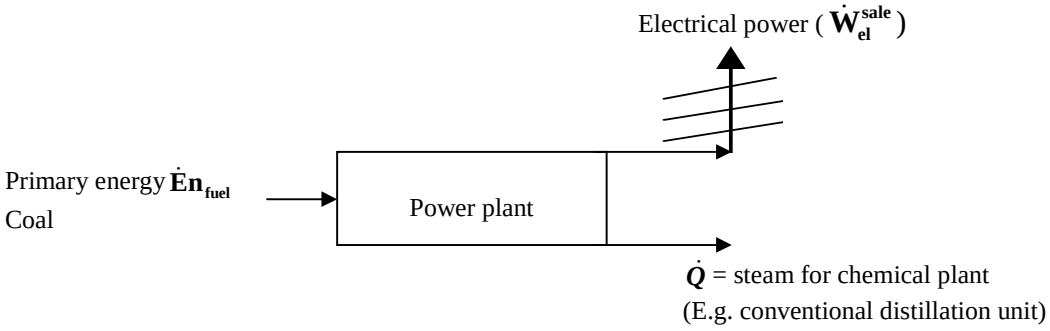

Figure 3.2. Electrical power and steam production

In the chemical industry, both electrical power and process steam is needed to operate the process plant, in this case the primary energy is a function of both the electrical power and the steam produced i.e. $\dot{\mathbf{E}}\mathbf{n}_{\mathbf{fuel}} = \mathbf{f}(\dot{\mathbf{W}}_{\mathbf{el}} + \dot{\mathbf{Q}})$ see figure 3.2 for illustration.

3.1 Via electrical power (heat pump)

3.1.1 Method

Given that $\dot{W}^{5}_{el,motor}$ is the available electrical power from the source to drive the compressor motor for the real process (refer to figure 2.21). $\dot{W}^{5}_{el,motor}$ is a function of fuel consumed, i.e. $\dot{W}^{5}_{el,motor} = f(\dot{E}x_{fuel})$. If T_o is used as the process reference temperature, a relationship can be developed between the useful exergy and the primary exergy input. For a power plant with a condensing turbine (only electrical power is produced, no steam production), the exergy efficiency is given by (Stockburger et al.[36]):

$$\xi_{\mathbf{real,fuel,HP}} = \frac{\dot{\mathbf{E}}\mathbf{x}_{\mathbf{p}}(\mathbf{T_o})}{\dot{\mathbf{E}}\mathbf{x}_{\mathbf{fuel}}} = \frac{\dot{\mathbf{E}}\mathbf{x}_{\mathbf{p}}(\mathbf{T_o})}{\dot{\mathbf{W}}^{\mathbf{5}}_{\mathbf{el,motor}}} \cdot \frac{\dot{\mathbf{W}}^{\mathbf{5}}_{\mathbf{el,motor}}}{\dot{\mathbf{E}}\mathbf{x}_{\mathbf{fuel}}} = \frac{\dot{\mathbf{E}}\mathbf{x}_{\mathbf{p}}(\mathbf{T_o})}{\dot{\mathbf{W}}^{\mathbf{5}}_{\mathbf{el,motor}}} \cdot \boldsymbol{\eta}_{\mathbf{cpp}} \tag{3.1}$$

$$\dot{E}x_{fuel} \approx \dot{M}_{fuel} \cdot H_l$$

Where H_l =lower heating value of the fuel.

The steam produced via the reboiler and the exergy losses are equal to the electrical power input and this is given by:

$$\dot{E}x_p(T_o) + \dot{E}x_L(T_o) = \dot{W}^{5}_{el,motor} \tag{3.2}$$

If T_o is used as the reference temperature instead of T_a equations 3.1 can be expressed as:

$$\xi_{real,fuel,HP} = \frac{\dot{E}x_p(T_o)}{\dot{E}x_p(T_o) + \dot{E}x_L(T_o)} \cdot \eta_{cpp} \tag{3.3}$$

$$\xi_{real,fuel,HP} = \frac{1 - \frac{T_o}{T_p}}{1 - \frac{T_S}{\eta_{12} \cdot T_k} + T_o \cdot \frac{1-\eta_{12}}{\eta_{12}} \left(\frac{1}{T_k} - \frac{1}{T_s} + \frac{1}{T_o} \right) + \frac{1-\eta_{\Sigma}}{\eta_{\Sigma}} \cdot \frac{T_k - T_s}{T_k}} \cdot \eta_{cpp} \tag{3.4}$$

If sale of electrical energy has to be considered, the numerator and denominator of equation 3.4 is extended by the factor: $\frac{W_{el}^{sale}}{\dot{Q}} = \frac{\dot{m}_{st} \cdot n(p_{st})}{\dot{m}_{st} \cdot \Delta h(p_{st})}$ and this gives:

$$\xi_{real,fuel,HP} = \frac{1 - \frac{T_o}{T_P} + \frac{n(p_{st})}{\Delta h(p_{st})}}{1 - \frac{T_S}{\eta_{12} \cdot T_K} + T_o \cdot \frac{1-\eta_{12}}{\eta_{12}} \left(\frac{1}{T_K} - \frac{1}{T_S} + \frac{1}{T_o} \right) + \frac{1-\eta_{\Sigma}}{\eta_{\Sigma}} \cdot \frac{T_K - T_S}{T_K} + \frac{n(p_{st})}{\Delta h(p_{st})}} \cdot \eta_{cpp} \qquad (3.5)$$

3.1.2 Application

In this section, heat pump is used as a means of saving primary energy. The heat pump is operated via electrical power from the power plant (see figure 3.3). The exergy efficiency of the fuel is calculated for different operating range of the heat pump. The detail numerical calculations are given below (refer to table 3.1)

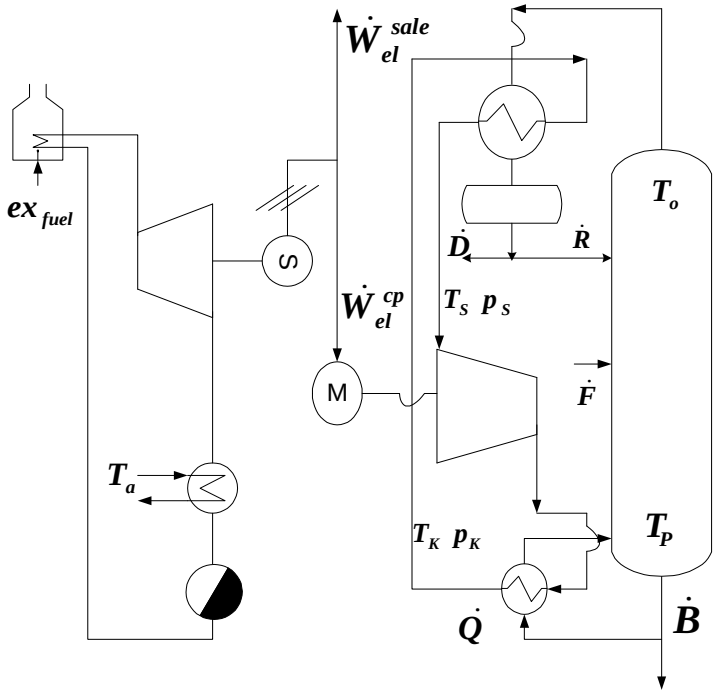

Figure 3.3. Integration of heat pump distillation unit with condensing power plant

The following numerical values are defined for equation 3.5.

Given that $T_s = T_o - 10K$, $T_k = T_p + 10K$; $\chi = 1.3$; $\tilde{M}$ =20 kg/kmol; η_2 =0.72; $\eta_{12} = 0.72 \cdot \eta_1$;

η_3 =0.90 η_4 =0.95; η_5 =0.90; $\eta_{\Sigma} = 0.554 \cdot \eta_1$; η_{cpp} =0.35 η_1 is calculated from equation 2.42

Table 3.1. Simulation results of exergy efficiency of heat pump combine with power plant

T_o	[K]	328 →							
$T_P - T_o$	[K]	10	20	30	40	50	60	70	80
T_P	[K]	338	348	358	368	378	388	398	408
T_s	[K]	318							
T_k	[K]	348	358	368	378	388	398	408	418
P_s	[bar]	0.1 →							
P_k	[bar]	0.39	0.58	0.85	1.21	1.69	2.32	3.13	4.15
$h''(T_s) - h'(T_k)$	[kJ/kg]	2269	2227	2185	2143	2100	2058	2015	1972
η_1		1.01	0.98	0.95	0.922	0.899	0.882	0.863	0.847
η_{12}		0.728	0.709	0.692	0.664	0.647	0.635	0.621	0.61
η_{Σ}		0.56	0.541	0.531	0.511	0.498	0.488	0.478	0.469
$n(p_{stm})/\Delta h_{stm}$		0.461 →				0.37 →			
$\zeta_{real,\ fuel,\ HP}$		0.325	0.272	0.262	0.259	0.241	0.236	0.231	0.225

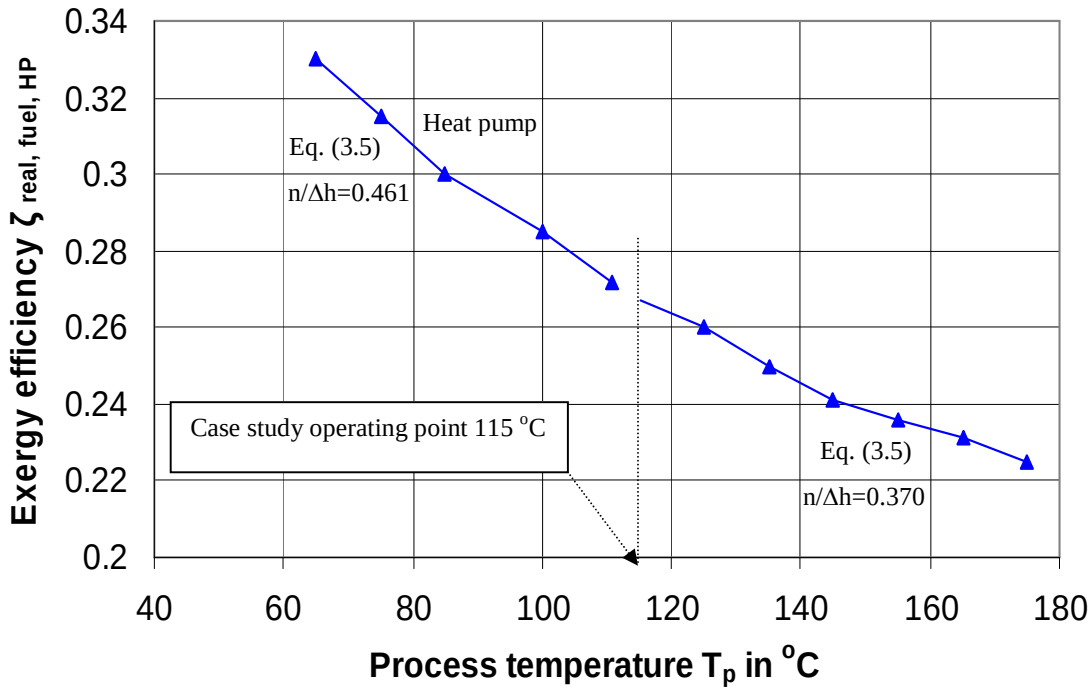

Figure 2.13. Exergy efficiency of combination of power plant and heat pump, T_o=55 °C

Figure 2.13 shows that as the process bottom temperature difference ($\mathbf{T_p}$) increase, the exergy efficiency decreases. With consideration of temperature at the top (T_o), the lower the temperature difference ($\mathbf{T_p - T_o}$) is, the higher is the exergy efficiency of the heat pump.

3.2 Via steam

3.2.1 Method

In this section, a conventional distillation unit (see figure 3.4) that depends on saturated steam from a power plant as source of energy is analysed.

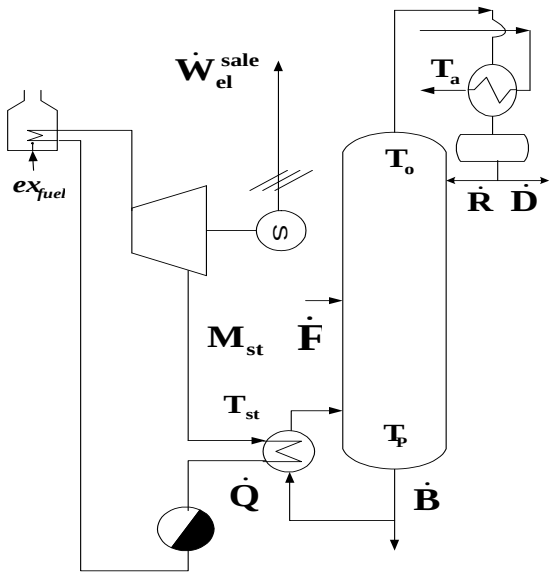

Figure 3.4. Steam and electrical power from power plant (back pressure turbine)

Considering the saturated steam from the power plant with the following properties, $\mathbf{P_{st}}$, $\mathbf{T_{st}}$ and $\mathbf{\Delta h_{st}}$, the mass flow rate of the saturated steam from the turbine can be calculated as follows:

$$\dot{\mathbf{M}}_{st} = \frac{\dot{\mathbf{Q}}}{\Delta \mathbf{h}_{st}(\mathbf{p}_{st})} \tag{3.6}$$

From equation 3.6, the exergy transfer to the distillation process can be calculated as follows:

$$\dot{\mathbf{E}}\mathbf{x}_{st}(\mathbf{T_o}) = \dot{\mathbf{M}}_{st} \cdot \Delta \mathbf{h}_{st}(\mathbf{p}_{st}) \cdot \left(1 - \frac{\mathbf{T_o}}{\mathbf{T}_{st}}\right) \tag{3.7a}$$

The exergy input is:

$$\dot{E}x_p(T_o) = \dot{M}_{st} \cdot \Delta h_{st}(p_{st}) \cdot \left(1 - \frac{T_o}{T_p}\right) \tag{3.7b}$$

For any given steam flow rate from the power plant (see figure 3.4), there is a corresponding electrical power generation and the ratio of these two parameters is given by:

$$n(p_{st}) = \frac{\dot{W}_{el}^{sale}}{\dot{M}_{st}} \Rightarrow \dot{W}_{el}^{sale} = n(p_{st}) \cdot \dot{M}_{st} \tag{3.8}$$

$n(p_{st})$ indicates the amount of electrical power produced per ton of net steam from the power plant (steam turbine). Given that the exergy of fuel input to power plant is $\dot{E}x_{fuel}$, the corresponding exergy of steam and electrical power produce are as shown below:

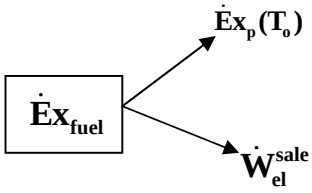

For the process operating on a saturated steam from the power plant, the exergy efficiency is given by:

$$\xi_{real,fuel,stm} = \frac{\dot{E}x_p(T_o) + \dot{W}_{el}^{sale}}{\dot{E}x_{fuel}} \tag{3.9}$$

Equation 3.7b with Equations 3.8 + 3.9 gives:

$$\xi_{real,fuel,stm} = \left[\Delta h_{st}(p_{st}) \cdot \left(1 - \frac{T_o}{T_p}\right) + n(p_{st})\right] \cdot \frac{1}{\frac{\dot{E}x_{fuel}}{\dot{M}_{st}}} \tag{3.10}$$

$\frac{\dot{E}x_{fuel}}{\dot{M}_{st}} = ex_{bpp}$ = the specific exergy input to the power plant (back pressure turbine) per ton of steam produced.

The main idea of this section is to study how the outlet steam of the turbine can be used to operate the distillation column. From equation 3.10 if p_{st} and $n(p_{st})$ are predefined, the efficiency $\xi_{real,fuel,stm}$ increases with increasing process temperature T_p. This means that when using steam from a power plant to heat a process stream, it is better to maintain a smaller

temperature difference ($\mathbf{T_{st} - T_p}$) between the power plant and the process plant. But sufficient temperature difference ($\mathbf{T_{st} - T_p}$) is required to achieve heat transfer.

3.2.2 Application

The simulation results are shown in figure 3.5 and table 3.2.

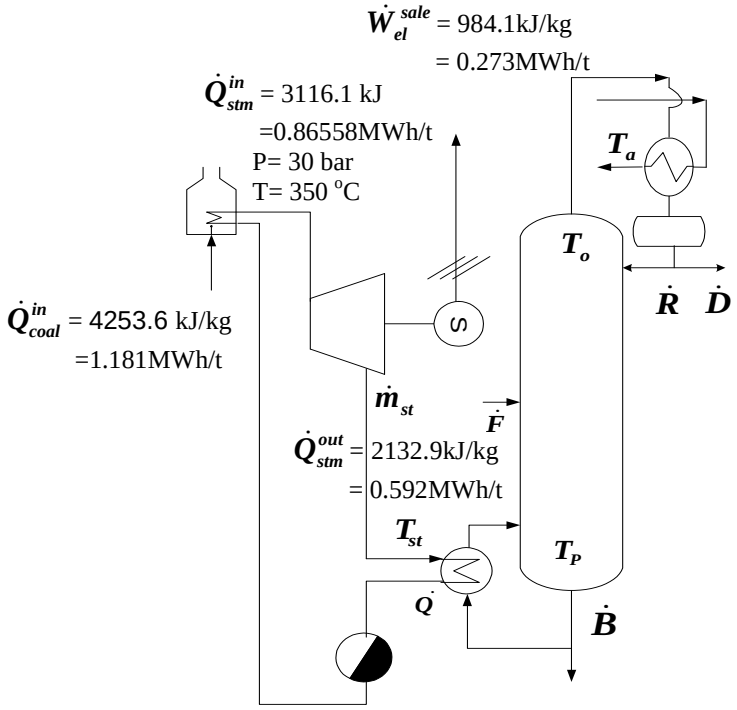

Figure 3.5. Integration of conventional distillation unit with back pressure power plant

Table 3.2 Simulation results

$\mathbf{p_{st}}$	bar	4	10
$\mathbf{T_{st}}$	^{o}C	143	180
$\dot{\mathbf{M}}_{\mathbf{st}}$	kg/hr	1000	1000
$\mathbf{n(p_{st})}$	MWh/t	0.273	0.20
$\mathbf{\Delta h_{st}(p_{st})}$	MWh/t	0.592	0.54
$\mathbf{T_o}$	^{o}C	55.34	55.34
T_P	^{o}C	101	135
$T_P - T_o$	^{o}C	45.6	80

Exergy efficiency calculations as function of $\mathbf{T_p}$ is illustrated in figure 3.6 for steam quality of 4 bar and 10 bar (using equations 3.11 and 3.12):

$$\xi_{real,fuel,stm}(p_{st} = 4bar) = 0.732 - \frac{164.58}{T_p}; T_p \text{ in } K \tag{3.11}$$

$$\xi_{real,fuel,stm}(p_{st} = 10bar) = 0.626 - \frac{150}{T_p}; T_p \text{ in } K \tag{3.12}$$

A graphical illustrative example of the calculation is given below.

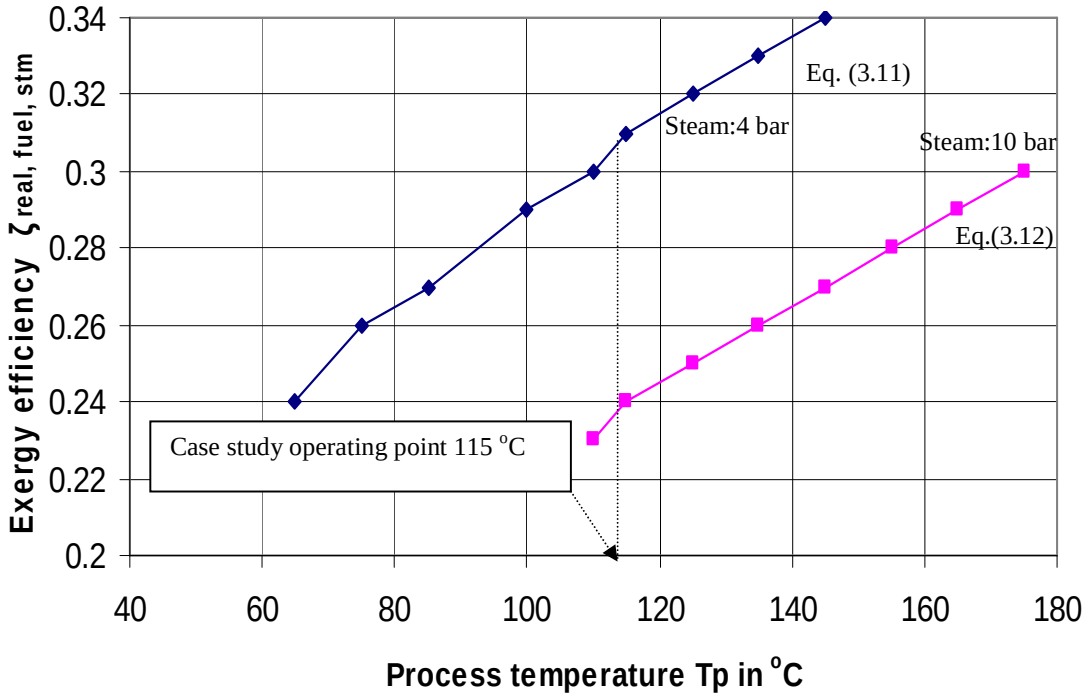

Figure 3.6. Exergy efficiency as a function of the process temperature T_p, T_o=55 °C

From figure 3.6 it can be observed that if $\mathbf{T_p}$ is increased, $\xi_{real,fuel,stm}$ increases. This condition gives lower values of $(T_{st} - T_p)$. If the outlet pressure $\mathbf{p_{st}}$ of the turbine is increased, the specific electrical energy $\mathbf{n(p_{st})}$ decreases. This effect is shown in figure 3.6 via the difference of the 4 bar and 10 bar pressures $(T_p - T_o)$

3.3 Comparison of the alternatives

In order to compare the two processes (i.e. conventional distillation and heat pump), it is also necessary to consider the exergy efficiency of the heat pump which is operated via electrical power output of the power plant (see figure 2.17).

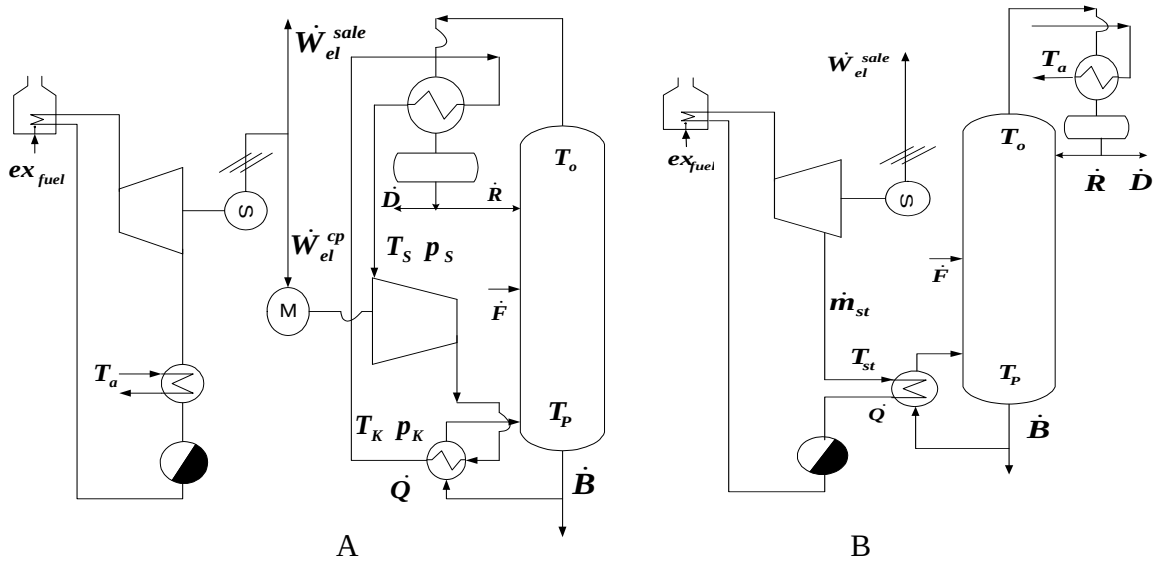

Figure 3.7. A: Combine power plant and heat pump (operated via electrical power)
B: Combine power plant and distillation unit (operated via steam)

Example

Exergy efficiency calculations as function of $\mathbf{T_p}$ is illustrated in figure 3.8 for steam quality of 4bar and 10 bar (using equation 3.7): A graphical illustrative example of the calculation is given below.

$$\xi_{real,fuel,stm}(p_{st} = 4bar) = 0.732 - \frac{164.58}{T_p}; T_p \text{ in K} \tag{3.13}$$

$$\xi_{real,fuel,stm}(p_{st} = 10bar) = 0.626 - \frac{150}{T_p}; T_p \text{ in K} \tag{3.14}$$

$$\xi_{real,fuel,HP} = \frac{1 - \frac{T_o}{T_P} + \frac{n(p_{st})}{\Delta h(p_{st})}}{1 - \frac{T_S}{\eta_{12} \cdot T_K} + T_o \cdot \frac{1-\eta_{12}}{\eta_{12}} \left(\frac{1}{T_K} - \frac{1}{T_S} + \frac{1}{T_o} \right) + \frac{1-\eta}{\eta} \cdot \frac{T_K - T_S}{T_K} + \frac{n(p_{st})}{\Delta h(p_{st})}} \cdot \eta_{cpp} \qquad (3.15)$$

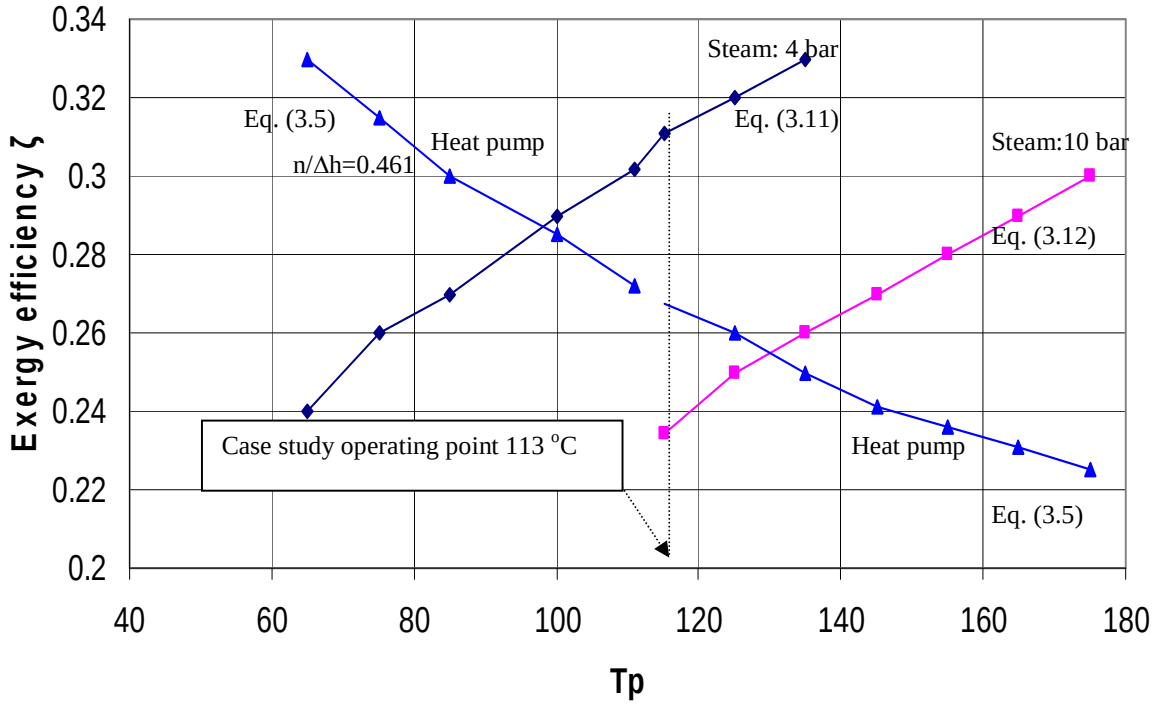

Figure 38. Comparison of exergy efficiency of the two processes, T_o=55 °C

3.4 Conclusion

Figure 3.8 shows that the higher the process temperature the greater is the exergy efficiency of steam combination but lower is the exergy efficiency of the heat pump combination. On the other hand the lower is the difference between steam and process temperature is, the better will be the steam combination. The heat pump combination is better because higher exergy efficiency is achieved with smaller process temperature difference.

4 Potential Environmental impact models (PEI-models)

4.1 Development of new PEI-models

For the alternatives discussed in this work, the PEI calculations were based on waste stack gas and waste energy released to the atmosphere by the energy generation unit. The energy generation unit is an electric power generation unit as illustrated in the outline of the system boundary in Figure 4.1 This thesis follows a methodology proposed by Douglas et al.[36] which relates PEI to measurable quantities such as energy consumption rate and potential environmental impact score (ψ_{ki}) of chemical k for category i. Due to the limitations imposed on the WAR-algorithm, coal is assumed to be the source of energy for steam and/or electrical energy production.

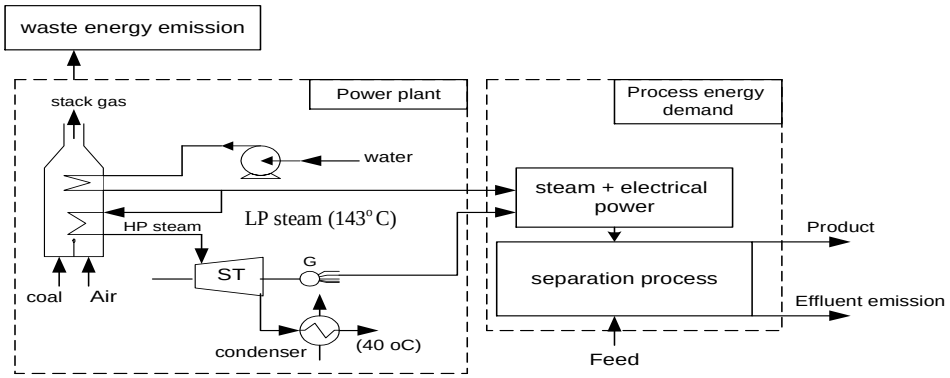

Figure 4.1. Combine heat & power plant (no HRSG) providing utility for separation (Smith [66])

With some modification of the methodology, different models were applied in calculating the PEI. Aspen plus was used to simulate the processes to provide data for the analysis. Impact due to effluent (base stream) of the distillation process was not considered in this study.

4.1.1 PEI due to energy consumption: Energy model^{standard}

The energy consumed by the separation task can be expressed as in Douglas et al. [36] :

$$\dot{E}n = \sum(\dot{Q}_{stm} + \dot{W}_{el}) \tag{4.1}$$

The efficiency values for conversion of chemical energy in coal to steam or electrical power are assumed to be 100 % and these are considered as follows:

$$\dot{\mathbf{Q}}_{\mathbf{coal}} = \dot{\mathbf{Q}}_{\mathbf{stm}} \tag{4.2}$$

$$\dot{\mathbf{Q}}_{\mathbf{coal}} = \dot{\mathbf{W}}_{\mathbf{el}} \tag{4.3}$$

In the standard model (PEI ($\mathbf{PEI}_{\mathbf{std}}^{\mathbf{En}}$)), coal combustion is assumed to be the source of energy production. Therefore environmental effect considered is based on coal combustion.

$$\mathbf{PEI}_{\mathbf{std}}^{\mathbf{En}} = \sum \dot{\mathbf{Q}}_{\mathbf{coal}} \cdot \boldsymbol{\psi}_{\mathbf{ki}}^{\mathbf{En}} \tag{4.4}$$

i. Calculation example for heat pump

The heat pump alternative is used to illustrate the PEI calculation procedure for the amount of energy consumption. Given the following data for the heat pump alternative shown in figure 4.2.

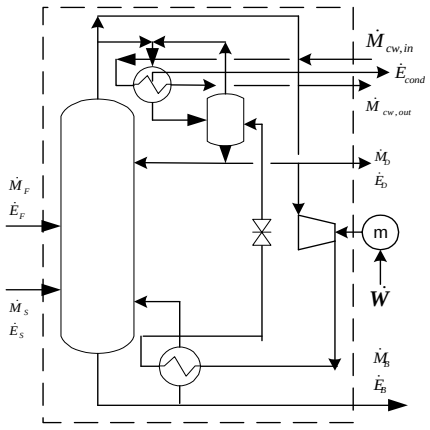

Figure 4.2. Balance for heat pump alternative

$\dot{\mathbf{Q}}_{\mathbf{coal,1}} = \dot{\mathbf{Q}}_{\mathbf{stm}}$ = 213 kW, $\dot{\mathbf{Q}}_{\mathbf{coal,2}} = \dot{\mathbf{W}}_{\mathbf{el}}$ = 43 kW, $\boldsymbol{\psi}_{\mathbf{ki}}^{\mathbf{En}} = \mathbf{0.02357PEI/kWhr}$

The $\mathbf{PEI}_{\mathbf{std}}^{\mathbf{En}} = \sum(\dot{\mathbf{Q}}_{\mathbf{coal,1}} + \dot{\mathbf{Q}}_{\mathbf{coal,2}}) \cdot \boldsymbol{\psi}_{\mathbf{ki}}^{\mathbf{En}} = \mathbf{(213\ kW + 43\ kW) \cdot 0.02357PEI/kWhr}$

Therefore the $\mathbf{PEI}_{\mathbf{std}}^{\mathbf{En}}$ for heat pump is 6 PEI/hr.

4.1.2 PEI due to energy from source: Energy model[modified]

With some modification of the standard method, actual quantity of coal is used to produce both steam and electrical energy. This means that the energy from the source is considered in the PEI index calculations. The basis that was considered for the analysis is illustrated in figures 4.3 and 4.4.

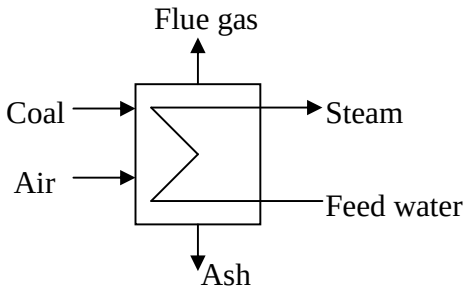

Figure 4.3 Conventional boiler

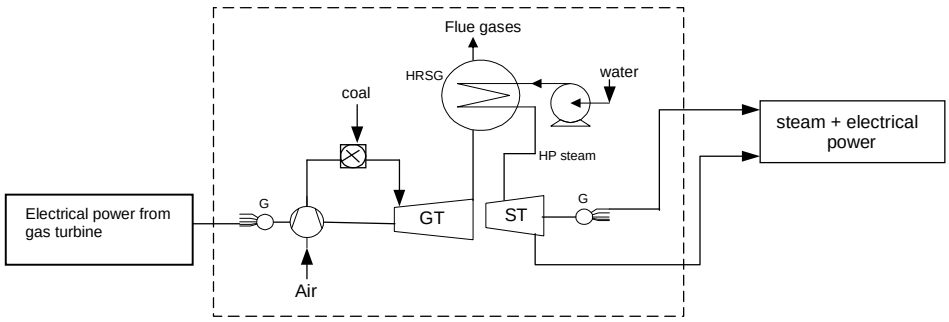

Figure 4.4 Power plant with gas and steam turbine

The efficiency with which steam and electrical power are generated from the combustion of coal can be defined as (Smith [66]):

$$\eta_{stm} = \frac{\dot{Q}_{stm}}{\dot{Q}_{coal,1}} \tag{4.5}$$

$$\eta_{el} = \frac{\dot{W}_{el}}{\dot{Q}_{coal,2}} \tag{4.6}$$

Where:

$$\dot{Q}_{stm} = H_{stm} \cdot \dot{M}_{stm} \text{ and } \dot{Q}_{coal} = H_{coal} \cdot \dot{M}_{coal}$$

H_{stm}=Enthalpy of steam used, H_{coal}=Higher heating value of coal =34MJ/Kg (Smith [66])

Equations 4.5 and 4.6 integrated into equation 4.4 gives:

$$\mathbf{PEI}^{\mathbf{En}}_{\mathbf{mod}} = \sum \left(\frac{\dot{\mathbf{Q}}_{\mathbf{stm}}}{\boldsymbol{\eta}_{\mathbf{stm}}} + \frac{\dot{\mathbf{W}}_{\mathbf{el}}}{\boldsymbol{\eta}_{\mathbf{el}}}\right) \cdot \psi^{\mathbf{En}^{*}}_{\mathbf{ki,\,j}} \tag{4.7}$$

Where j in this term ($\psi^{\mathbf{En}^{*}}_{\mathbf{ki,\,j}}$) can be 1 or 2

$$\boldsymbol{\psi}^{\mathbf{En}^{*}}_{\mathbf{ki,1}} = \boldsymbol{\psi}^{\mathbf{En}}_{\mathbf{ki}} \cdot \boldsymbol{\eta}_{\mathbf{stm}} \quad (j=1) \tag{4.8}$$

For real process conditions, $\boldsymbol{\eta}_{\mathbf{stm}}$ has not to be considered in this context.

$$\boldsymbol{\psi}^{\mathbf{En}^{*}}_{\mathbf{ki,2}} = \boldsymbol{\psi}^{\mathbf{En}}_{\mathbf{ki}} \qquad (j=2) \tag{4.9}$$

Integrating equation (4.8) and (4.9) separately into equation (4.7) gives the following:

1. Energy source: steam via coal, electrical power via coal

$$\mathbf{PEI}^{\mathbf{En}}_{\mathbf{mod\ 1}} = \sum \left(\frac{\dot{\mathbf{Q}}_{\mathbf{stm}}}{\boldsymbol{\eta}_{\mathbf{stm}}} + \frac{\dot{\mathbf{W}}_{\mathbf{el}}}{\boldsymbol{\eta}_{\mathbf{el}}}\right) \cdot \psi^{\mathbf{En}}_{\mathbf{ki}} \cdot \boldsymbol{\eta}_{\mathbf{stm}} \quad \text{(for comparison with } \mathbf{PEI}^{\mathbf{En}}_{\mathbf{std}}\text{)} \tag{4.10}$$

$$\mathbf{PEI}^{\mathbf{En}}_{\mathbf{mod2}} = \sum \left(\frac{\dot{\mathbf{Q}}_{\mathbf{stm}}}{\boldsymbol{\eta}_{\mathbf{stm}}} + \frac{\dot{\mathbf{W}}_{\mathbf{el}}}{\boldsymbol{\eta}_{\mathbf{el}}}\right) \cdot \psi^{\mathbf{En}}_{\mathbf{ki}} \tag{4.11}$$

$\mathbf{PEI}^{\mathbf{En}}_{\mathbf{mod1}}$ - (this term considers the environmental effect of electrical power production from source)*

$\mathbf{PEI}^{\mathbf{En}}_{\mathbf{mod2}}$ - (this term considers the real effect of electrical power production and the real environmental effect of steam production from source)*.

*Refer to figure 4.3 and 4.4 for the basis.

Equation (4.10) indicates that environmental effect of steam is the same as before (i.e. the standard PEI). The terms in the bracket of equation (4.11) gives the real quantity of coal used to produce both steam and electrical power.

ii. Calculation example for heat pump (see figure 4.2*)*

By assuming an efficiency of steam generation of 85% and distribution losses of 10%, the overall efficiency $\boldsymbol{\eta}_{\mathbf{stm}}$ of steam generation and distribution is 75%. Electrical power generation is assumed to have overall efficiency $\boldsymbol{\eta}_{\mathbf{el}}$ of 30%. Given the following data:

$\dot{\mathbf{Q}}_{\mathbf{stm}}$ = 213 kW, $\dot{\mathbf{W}}_{\mathbf{el}}$ = 43 kW, $\boldsymbol{\psi}^{\mathbf{En}}_{\mathbf{ki}} = \mathbf{0.02357PEI/kWhr}$.

$$\left(\frac{\dot{\mathbf{Q}}_{\mathbf{stm}}}{\boldsymbol{\eta}_{\mathbf{stm}}} + \frac{\dot{\mathbf{W}}_{\mathbf{el}}}{\boldsymbol{\eta}_{\mathbf{el}}}\right) = \frac{\mathbf{213\,kW}}{\mathbf{0.75}} + \frac{\mathbf{43\,kW}}{\mathbf{0.3}} = \mathbf{327\,kW}$$

$$\psi^{En^*}_{ki,1} = \psi^{En}_{ki} \cdot \eta_{stm} = 0.02357 PEI/kWhr \cdot 0.75 = 1.77 \cdot 10^{-2}\ PEI/kWhr$$

$$PEI^{En}_{mod,j} = \sum \left(\frac{\dot{Q}_{stm}}{\eta_{stm}} + \frac{\dot{W}_{el}}{\eta_{el}}\right) \cdot \psi^{En}_{ki} \cdot \eta_{stm,j}$$ gives i,

$$PEI^{En}_{mod1} = \left(\frac{213\,kW}{0.75} + \frac{43\,kW}{0.3}\right) \cdot 0.02357 PEI/kWhr \cdot 0.75$$ = 7.6 PEI/hr.

$$PEI^{En}_{mod2} = \left(\frac{213\,kW}{0.75} + \frac{43\,kW}{0.3}\right) \cdot 0.02357 PEI/kWhr$$ = 10 PEI/hr.

PEI^{En}_{mod1} is close to the standard value (PEI^{En}_{std}) = 7.6 PEI/hr because steam effect has not been changed. $PEI^{En}_{mod\,2}$ includes efficiency values observed in practice for the arrangements described in figures 4.3 and 4.4.

4.1.3 PEI due to source exergy: Exergy $model^{modified}_{stream}$

Exergy analysis uses parameters such as temperature and pressure to determine energy quality. The quality of steam can be expressed via temperature level or exergy. The drop in energy quality is referred to as exergy loss or energy degradation. Decreasing exergy loss of a process means lower fuel consumption; this will in turn reduce emissions and waste heat to the environment. As shown in figure 4.5, a process stream at 523K is used to produce steam to operate a distillation unit. Also in figure 4.6, electrical power is produced via direct combustion of coal. The PEI analysis interms of exergy is performed for these two situations.

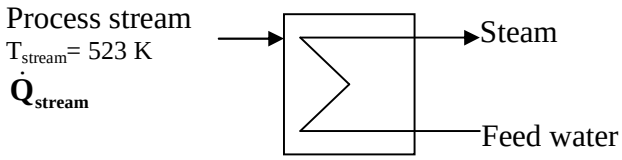

Figure 4.5 Steam production via process stream

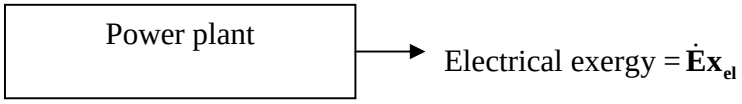

Figure 4.6 Electrical energy via coal

The rate of PEI output due to exergy production from source can be expressed as:

$$PEI^{Ex} = \sum (\dot{E}x_{stream} + \dot{E}x_{el}) \cdot \psi^{Ex}_{ki,j} \qquad (4.12)$$

The exergy of a heat stream can be calculated by:

$$\dot{\mathbf{E}}\mathbf{x}_{\mathbf{stream}} = (\mathbf{1} - \frac{\mathbf{T_a}}{\mathbf{T_{stream}}}) \cdot \dot{\mathbf{Q}}_{\mathbf{stream}} \tag{4.13}$$

The term in the bracket is the *Carnot efficiency factor*. This equation implies that only a fraction of the energy content of a heat stream can be converted into work and this depends on the temperature of the source $\mathbf{T_{stream}}$ and the ambient $\mathbf{T_a}$. Substituting (4.13) into (4.12), the rate of potential environmental impact output due to exergy consumption can be expressed as:

$$\mathbf{PEI}^{\mathbf{Ex}} = \sum \left[(\mathbf{1} - \frac{\mathbf{T_a}}{\mathbf{T_{stream}}}) \cdot \dot{\mathbf{Q}}_{\mathbf{stream}} + \dot{\mathbf{W}}_{\mathbf{el}} \right] \cdot \psi^{\mathbf{Ex}}_{\mathbf{ki,j}} \tag{4.14}$$

Where:

j in this term ($\psi^{\mathbf{Ex}}_{\mathbf{ki,j}}$) can be 1 or 2 i.e.:

$$\psi^{\mathbf{Ex}}_{\mathbf{ki,1}} = \frac{\psi^{\mathbf{En}}_{\mathbf{ki}}}{\eta_{\mathbf{el}}} \tag{4.15}$$

Integrating equations (4.15) into (4.14) give:

1. Energy source: steam via process stream, electrical energy via coal

$$\mathbf{PEI}^{\mathbf{Ex}}_{\mathbf{1}} = \sum \left[(\mathbf{1} - \frac{\mathbf{T_a}}{\mathbf{T_{stream}}}) \cdot \dot{\mathbf{Q}}_{\mathbf{stream}} + \dot{\mathbf{W}}_{\mathbf{el}} \right] \cdot \frac{\psi^{\mathbf{En}}_{\mathbf{ki}}}{\eta_{\mathbf{el}}} \tag{4.16}$$

iii. Calculation example from figure 4.2

Given the following data: T_a = 293 K, T_p=523 K, $\dot{\mathbf{Q}}_{\mathbf{stm}}$=213 kW, $\dot{\mathbf{W}}_{\mathbf{el}}$ = 43 kW, $\psi^{\mathbf{En}}_{\mathbf{ki}} = \mathbf{0.02357PEI/kWhr}$, $\boldsymbol{\varepsilon}$ = 0.297 (Source: [27])

$$\eta_{\mathbf{carnot}} = (\mathbf{1} - \frac{\mathbf{T_a}}{\mathbf{T_{stream}}}) = (1\text{-}293/523) = 0.44$$

Considering the practical Carnot efficiency of steam from the source at temperature 250^{o}C

$$\eta_{\mathbf{carnot,steam}} = (\mathbf{1} - \frac{\mathbf{T_a}}{\mathbf{T_{stream}}}) = (\mathbf{1} - \frac{\mathbf{293}}{\mathbf{250 + 273}}) = \mathbf{0.44} \tag{4.17}$$

$$\eta_{\mathbf{electrical}} = \mathbf{0.3} \qquad \text{Smith [66]} \tag{4.18}$$

Integrating the coefficient of performance ε into equation 4.16 gives:

$$(1-\frac{T_a}{T_{stream}})\cdot\varepsilon\cdot\dot{Q}_{stream}+\dot{W}_{el}=0.44\cdot 297\cdot 213\ kW+43\ kW=70.8\ kW$$

$$PEI_{PS}^{Ex}=\sum\left[(1-\frac{T_a}{T_{stream}})\cdot\varepsilon\cdot\dot{Q}_{stream}+\dot{W}_{el}\right]\cdot\frac{\psi_{ki}^{En}}{\eta_{el}}=70.8kW\cdot 0.0786PEI/kWhr=5.6\ PEI/hr$$

iv. Further discussion

Given that the source temperature is at 1000^{o}C, the PEI can be calculated as follows:

$$PEI_{PS}^{Ex}=\sum\left[(1-\frac{T_a}{T_{stream}})\cdot\varepsilon\cdot\dot{Q}_{stream}+\dot{W}_{el}\right]\cdot\frac{\psi_{ki}^{En}}{\eta_{el}}$$

$$PEI_{PS}^{Ex}=\sum\left[(1-\frac{293}{1000+273})\cdot 0.297\cdot 213+43\right]\cdot\frac{0.02357}{0.3}=3.8PEI/hr$$

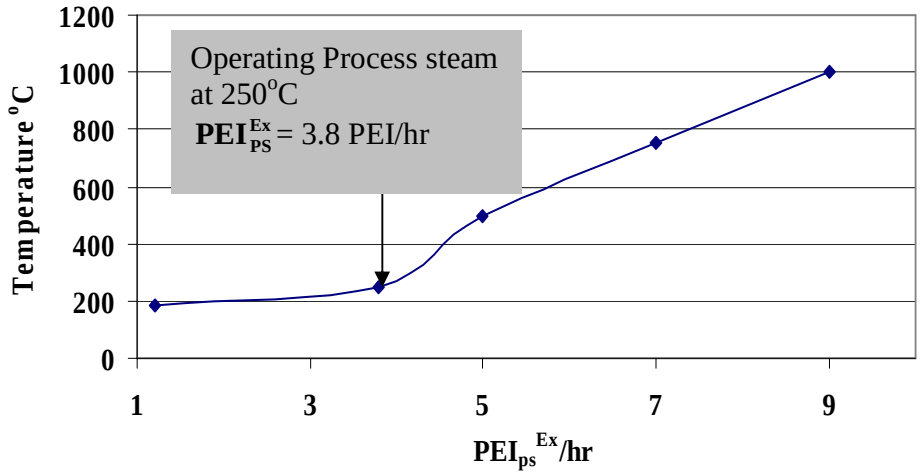

Figure 4.7. PEI VS source temperature

Figure 4.7 shows that as the temperature of the source is increased, the PEI index also increases, this is due to consumption of more coal at the source.

4.1.4 PEI for combine power plant Exergy model$_{CPP}^{modified}$

In process industry, distillation units are usually operated by means of an industrial power plant. The fuel (e.g. coal) is preliminary used in order to produce electrical power via pressurized gas required by the gas turbine (GT) and superheated steam (steam at high temperature and pressure) required by the steam turbine (ST) (see figure 4.8).

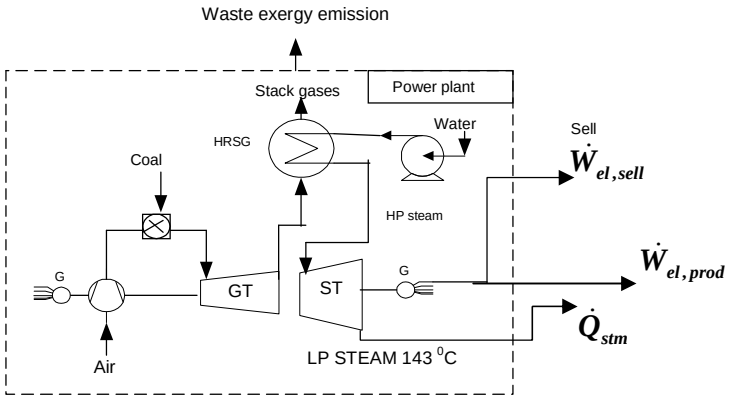

Figure 4.8. Combine heat and power plant (with HRSG) system providing utility for separation process (Smith [66]):

The exhaust gases leaving the gas turbine enter the HRSG at temperature of about 600 ^{o}C. A heat recovery steam generator (HRSG) system is used to recover the waste energy from the flue gas. HP- steam is produced and expanded in a steam turbine. The LP steam (at about 143 ^{o}C) from the steam turbine is sent to the distillation process.

Aspen plus flowsheet Simulator, a commercial software for steady-state chemical/power system simulation is used in this work for simulating the performance of the power plants. This software calculates thermodynamic variables such as mass flow rate, temperature, pressure, enthalpy, entropy, and the amount of electrical power produced. The calculation of the real efficiency ($\boldsymbol{\eta}_{\mathbf{real}}$) value for this power plant is as follows:

$$\dot{\mathbf{Q}}_{\mathbf{coal}} - \frac{\dot{\mathbf{W}}_{\mathbf{el,sale}}}{\boldsymbol{\eta}_{\mathbf{el}}} = \frac{\dot{\mathbf{E}}\mathbf{x}_{\mathbf{stm}} + \dot{\mathbf{W}}_{\mathbf{el,cons}}}{\boldsymbol{\eta}_{\mathbf{real}}} \tag{4.19}$$

Where:

$\dot{\mathbf{Q}}_{\mathbf{coal}}$ = Equivalent total quantity of coal consumed by the power plant

$\frac{\dot{W}_{el,sale}}{\eta_{el}}$ = Equivalent quantity of coal used to produce electrical power ($\dot{W}_{el,sale}$) for sale

$\frac{\dot{E}x_{stm} + \dot{W}_{el,cons}}{\eta_{real}}$ = Equivalent quantity of coal used to produce electrical power and steam to operate the distillation unit.

$\dot{E}x_{stm}$ = Exergy of steam consume by the distillation unit

$\dot{W}_{el,cons}$ = Electrical power consume by the distillation unit

$$\dot{Q}_{coal} - \frac{\dot{W}_{el,sell}}{\eta_{el}} = \frac{(1 - \frac{T_0}{T_s}) \cdot \dot{Q}_{stm} + (\dot{W}_{el,produce} - \dot{W}_{el,sale})}{\eta_{real}} \quad (4.20)$$

$$\eta_{real} = \frac{(1 - \frac{T_0}{T_s}) \cdot \dot{Q}_{stm} + (\dot{W}_{el,prod} - \dot{W}_{el,sell})}{\dot{Q}_{coal} - \frac{\dot{W}_{el,sell}}{\eta_{el}}} \quad (4.21)$$

$$PEI_{CPP}^{Ex} = \left[\dot{E}x_{stm} + \dot{W}_{el,cons}\right] \cdot \frac{\psi_{ki}^{En}}{\eta_{real}} \quad (4.22)$$

Example: $\eta_{real} = \frac{\left[(1 - \frac{293}{416}) \cdot 213 + (65 - 22)\right]}{\left[318 - \frac{22}{0.3}\right]} = 0.43$

$PEI_{CPP}^{Ex} = \left[(1 - \frac{293}{416}) \cdot 213 + 43\right] \cdot \frac{0.02357}{0.43}$ = 5.7 PEI/hr

The results shows that the PEI index is much lower when chemical plants (distillation unit) take their energy source directly from the power plant.

4.1.5 Discussion of new aspect

The most significant modification to the WAR algorithm is the inclusion of both energy production and energy consumption into the potential environmental impact calculations. The energy consumed by the process unit (heat pump) comes directly from a power generating facility, from the above calculations it was observed that the $\mathbf{PEI}^{En}_{std}$ = 6 PEI/hr.

$\mathbf{PEI}^{En}_{mod,1}$ = 7.6 PEI/hr
$\mathbf{PEI}^{En}_{mod,2}$ = 10 PEI/hr
} Energy source: Steam via coal; electrical power via coal

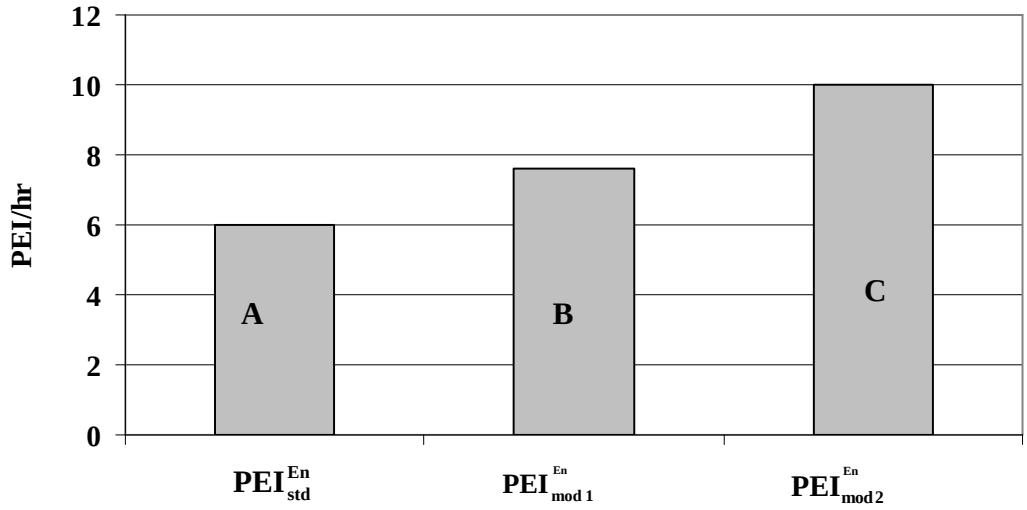

Figure 4.9. Comparison of the different PEI-models
A: PEI based on 100 % efficiency for steam and electrical power
B: PEI includes lower efficiency of electrical power
C: PEI includes real efficiency values for steam and electrical power

Figure 4.9 shows that the PEI index for the standard case is lower than the other models because the other models consider both actual quantity of coal used from the source.

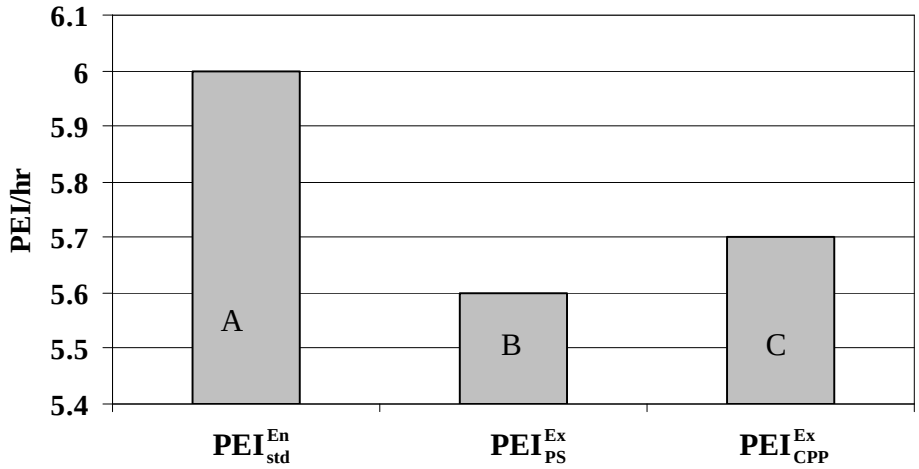

Figure 4.10. Comparison of the different PEI-models

A: Source: - Coal power plant, Standard: 100% efficiency for coal and steam

B: Source: - Process stream and coal power plant with real efficiency for electrical power, exergy of steam is low

C: Source: - Combine power plant, real efficiency, sale of electrical power causes low PEI

In reference to figure 4.10, $\mathbf{PEI}^{\mathbf{Ex}}_{\mathbf{PS}}$=5.6 PEI/hr- Energy source: steam via process stream; electrical energy via coal, this value is about 6 % reduction of PEI index compare to the standard PEI. On the other hand the $\mathbf{PEI}^{\mathbf{Ex}}_{\mathbf{CPP}}$ for the combine power plant is 5.7, this is about 5 % reduction in PEI compared with the standard case. This results shows that heat integration via process stream is more environmentally friendly than all other alternatives.

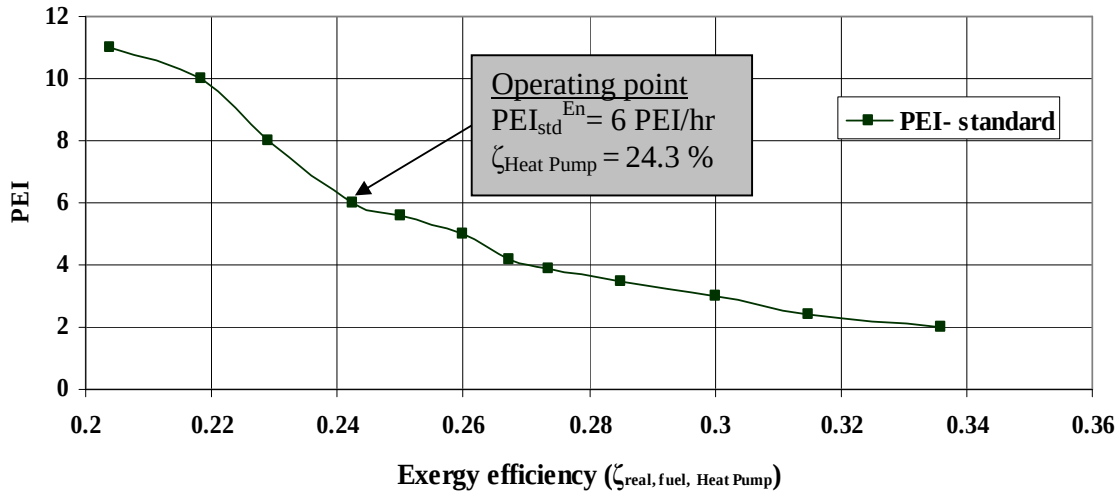

Figure 4.11. PEI- due to energy consumption versus exergy efficiency of heat pump

The inclusion of exergy into the WAR algorithm's calculations provides a more realistic view of the PEI generated by a chemical processing unit. Figure 4.11 shows that as the exergy efficiency of the process unit increases as the PEI decreases. The increase in the exergy efficiency is caused by less fuel utilization which gives less exergy consumption by the distillation unit and also less PEI.

5 Multi-Criteria Decision Making (MCDM)

5.1 Proposed methodology

In order to describe and predict the behaviour of a complex chemical process plant, it is often necessary to use mathematical modeling. In the same way, identification of the optimum operating conditions that will ensure improve process performance usually makes the use of optimization techniques very important.

Chemical process design problems are multi-objective in nature, i.e. several objectives are required to be satisfied, maximized or minimized, simultaneously within a specified range of constraints. The proposed optimization methodology presented in this thesis formulates the decision maker preferences into mathematical forms. In the next section a detail discussion of the methodology is presented.

5.1.1 Systematic procedure

Figure 5.1 describes the proposed methodology's structure, showing the inter-linking of the software tools used and the flow of data between them. The methodology consists of the following steps:

1. Definition of problem and system boundary and data gathering
2. Generation of base case flowsheet and simulation model
3. Generation of proposed alternatives
4. Evaluation of alternatives (Comparison between the modified and the base case interms of objectives).
5. Multiobjective optimization on environmental and economics objectives

5.1.1.1 Step 1: Definition of problem and system boundary and data gathering

As a first step in the design methodology, the design starts with:

- Framing of the problem

  The primary attributes of the problem are identified and classified according to the following quantities: equipment design variables, operational variables, physical properties, process parameters and the lower and upper bounds of the parameters, as well as mass and energy balance information are gathered.

- Definition of the scope of the study and key assumptions such as production target (e.g., the quality of streams).

- Definition of the functional units on which all calculations are based
- Finally the preferences of the decision makers should be defined, and corresponding objectives should be defined. To make these objectives operational, they have to be transformed into indicators (e.g. in this thesis work, environmental objective is transformed into PEI and economic objective is transformed into TAC).

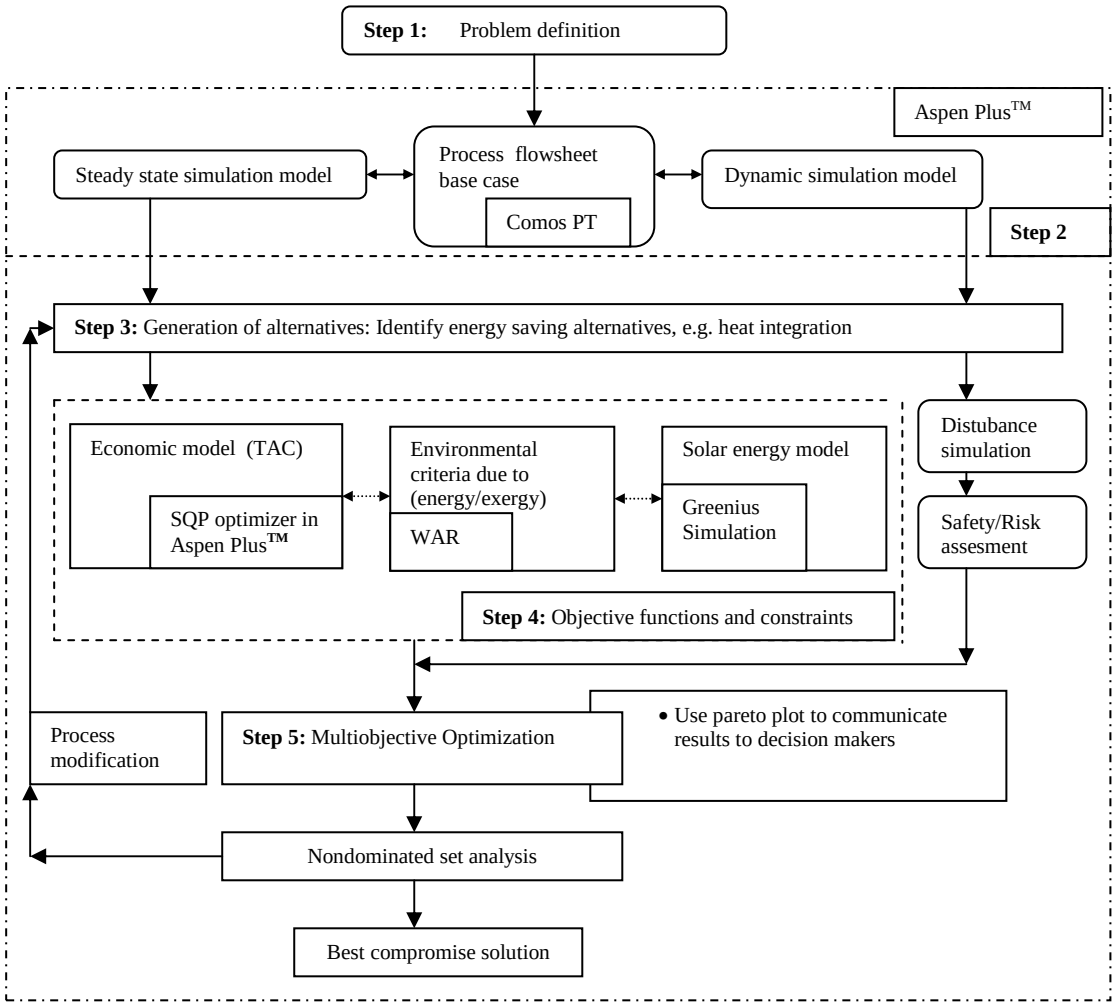

Figure 5.1. Steps of proposed methodology

5.1.1.2 Step 2: Generation of base case flowsheet and simulation model

In the next step, the detailed process unit diagram for the base case design is presented with some support from step 1. As is the case with all computer aided engineering (CAE) support tools, Comos [PT] is used for the rapid and effective development of the base case flowsheet and process flow diagrams as well as piping and instrumentation diagrams. No process data is computed or created in Comos [PT]. This task is usually performed by "simulators". Comos [PT] only imports data to or from simulators (Comos [PT] [94]). Based on the data extracted from

step 1 and the complete base case flowsheet, a representative steady state simulation models are configured in Aspen Plus. Also alternative models are generated and this is discussed in more detail in step 3.

5.1.1.3 Step 3: Generation of proposed alternatives

For the generation of alternatives, a number of methods have been suggested, of which hierarchical approaches (Douglas [95]**,** Douglas [96], Rossiter et al. [97], Kirkwood et al. [98], Rajagopal et al.[99]), and mathematical programming techniques (Grossmann,[100], El-Halwagi [101] Papalexandri [102]) are among the most prominent. Mathematical programming techniques, frequently implemented as mixed-integer nonlinear problems (MINLP), can identify the optimal solution out of a number of alternatives. Usually, however, they suffer from the fact that very detailed unit operation models are necessary to obtain this optimal solution. On the other hand it is simple to use the hierarchical procedure to identify energy saving and potential pollution problems and to identify process alternatives that can be used to eliminate these problems. This thesis follows a general hierarchical procedure developed by Douglas [95] (see table 5.1) for the generation of process design alternatives.

Table 5.1. Hierarchical Procedure for Process synthesis. Source: Douglas [95]

level 1	Input information: type of problem
level 2	Input-output structure of the flowsheet
level 3	Recycle structure of the flowsheet
level 4	Specification of the separation system
level 5	Heat integration
level 6.	Evaluation of alternatives

5.1.1.4 Step 4: Evaluation of alternatives

After generation of alternatives, the objective functions as well as constraints are defined and exploited. Data are transferred from each process model into WAR algorithm for evaluation of environmental objective of each process alternative. In this thesis work, the successive quadratic programming algorithm (SQP) of Lang and Biegler [103] which is available in Aspen Plus^{TM} has been adopted for economic optimization.

Modification is made to the base case by generation of the proposed alternative (solar model). The solar model is first developed by means of the Greenius simulation tool. On the basis of

the data extracted from the Greenius simulation model, a representative simulation model is built in Aspen Plus^{TM}. In the optimization step, a number of runs are carried out in order to optimize the various factors (i.e. process variables) affecting the performance of the unit. Finally the best compromised alternative from a range of optimum solutions are evaluated.

5.1.1.5 Step 5: Multiobjective optimization on environmental and economics objectives

In step 5, the multiobjective optimization method is applied to locate the nondominated or pareto surface which map the optimal solutions of decision variables such as steam flow rate, reflux ratio to the objective functions. It is suggested here to communicate the results to the decision makers in a two-dimensional Pareto plot as discussed earlier in section 2.4.8 (also refer to figure 2.29). This graphic representation serves two purposes: On the one hand, it shows the position of all alternatives with respect to both objective functions. On the other hand, usually several decision makers are involved in the selection of a process alternative. In many cases, these decision makers exhibit different sets of values and prefer different objective functions. Consequently, the Pareto plot can be used as a communication tool enabling the decision makers to discuss the implications of their decisions and thus aids in coming to more reliable decisions. In the next section the mathematical modules used for the evaluation of economic, energy/exergy and environmental objectives are presented.

5.1.2 Models

The foundation of a system consists of mathematical modules of the system to be designed (in this case a chemical process), these models are expressed in terms of equations or constraints that must be solved to predict the performance of the system under study. The next section discusses the different types of models that are used to compare different design alternatives of distillation units. The main models considered are:

- Economic Model
- Energy and exergy model
- Environmental model
- Solar energy model

5.1.2.1 Economic models

The cost effectiveness of operating a process plant can be evaluated by applying attributes like cost, return on investment and total annualized cost (TAC) Ahmad [104]. For

optimization, the estimation of investment and operational cost is necessary. In this work TAC is used as an economic objective function. Given the purchase cost of each process unit, the installed cost is obtained by adding the cost of installation. The cost of installation of each unit is estimated using factored-cost methods based on free on board purchase cost (f.o.b) of the process equipment. For each equipment (such as column, tray, heat exchanger), Guthrie (see e.g. Seider [105]) provides factors to estimate the direct costs of materials (i.e. piping, concrete, steel, instruments and controllers) as well as indirect costs (i.e. insurance, taxes) involved in the installation procedure. When these costs are added to the purchased cost, Guthrie calls the result as bare-module cost. The bare-module concept introduced by Guthrie was used in the estimation of the installed cost of each process unit.

5.1.2.1.1 Installed cost

i. Installed cost of heat exchanger

For a shell and tube heat exchanger, the installed cost $\mathbf{C_{Inst}^{Hx}}$ is calculated using the bare-module cost (C_{BM}), The bare-model cost is the same as the installed cost of the heat exchanger because the bare-model cost accounts for the installation factor and is given by:

$$\mathbf{C_{BM} = C_{Inst}^{Hx} = C_p \cdot F_{BM} \cdot \left[\frac{I_{2005}}{I_{base}}\right]}$$

Where F_{BM}= bare-model factor for heat exchanger

Where C_p= free on board (f.o.b) purchase cost

$\left[\frac{\mathbf{I_{2005}}}{\mathbf{I_{base}}}\right]$ = correction factor for cost index necessary to increase the given installation factor to its present value, details of the cost index used can be found in table 5.2

$$\mathbf{C_{Inst}^{Hx} = [450 \cdot A^{0.7} \cdot (1.65 + 1.22 \cdot F_M \cdot p^{0.09})] \cdot F_{BM} \cdot \left[\frac{I_{2005}}{I_{base}}\right]} \quad (5.1)$$

Where:

A = Area in m^2

F_M = material factor (carbon steel (cs) is used in this calculation)

P = pressure in bar

These factors are shown in table 5.2.

Table 5.2. Correlation for correction factors for heat exchangers as in Seider [105]

F_M (cs)	1
F_{BM}	3.17
Cost Index data	
I_{base}	CE plant cost Index= 315 (mid 1982)
I_{2005}	CE plant cost Index= 468.2 (mid 2005)

ii. Installed cost of column

The installed cost of the column is calculated in terms of the bare-model cost C_{BM}:

$$\mathbf{C_{BM} = C_{Inst}^{col} = 1780 \cdot L^{0.87} \cdot D^{1.23} \cdot \left[2.86 + 1.694 \cdot F_M \cdot (10.01 - 7.408 \cdot lnp + 1.395 \cdot (lnp)^2)\right] \cdot \left[\frac{I}{I_{base}}\right]} \quad (5.2)$$

Where:

L= length (m)

D= diameter (m)

F_M = material factor (carbon steel (cs) is used in this calculation)

P = pressure in bar

Table 5.3. Correlation for correction factors for column as in Seider [105]

P in bar	1bar
F_M (cs)	1
F_{BM}	4.16
Cost Index data	
I_{base}	CE plant cost Index= 315 (mid 1982)
I_{2005}	CE plant cost Index= 468.2 (mid 2005)

iii. Installed cost of trays

The installed cost of the column is calculated in terms of the bare-model cost C_{BM}:

$$\mathbf{C_{Inst}^{tray} = (193.04 + 22.72 \cdot D + 60.38 \cdot D^2) \cdot F_{BM} \cdot N_{act} \cdot f_q \cdot \left[\frac{I}{I_{base}}\right]} \quad (5.3)$$

Where:

D= diameter (m)

F_{BM}= bare-model factor for trays

N_{act}= actual number of trays

f_q= quantity factor, f_q=1 when N_{act} >20 trays

Table 5.4. Correlation for correction factors for trays as in Seider [105]

F_{BM}	4.16
Cost Index data	
I_{base}	CE plant cost Index= 315 (mid 1982)
I_{2005}	CE plant cost Index= 468.2 (mid 2005)

iv. Installed cost of pump

The free on board purchase cost (f.o.b) of a pump is given by:

$$\mathbf{C_p = F_M \cdot C_B}$$

Where:

C_p= free on board (f.o.b) purchase cost

F_M = material factor (carbon steel (cs) is used in this calculation)

C_B= Base cost, $\mathbf{C_B = [exp\left\{7.3883 + 0.26986\left[\ln\left(\dot{P}_{hp}\right)\right] + 0.06718\left[\ln\left(\dot{P}_{hp}\right)\right]^2\right\}}$

The installed cost for pump is given by $\mathbf{C_{Inst}^{pump} = F_M \cdot C_B \cdot F_{BM} \cdot \left[\frac{I}{I_{base}}\right]}$

$$\mathbf{C_{Inst}^{pump} = [exp\left\{7.3883 + 0.26986\left[\ln\left(\dot{P}_{hp}\right)\right] + 0.06718\left[\ln\left(\dot{P}_{hp}\right)\right]^2\right\}] \cdot F_M \cdot F_{BM} \cdot \left[\frac{I}{I_{base}}\right]} \quad (5.4)$$

Where:

$\dot{P}_{hp}$ = power (horse power)

The cost index data used fort the calculation can be found in table 5.5.

Table 5.5. Correlation for correction factors for pump as in Seider [105]

F_M (cs)	1
F_{BM}	3.30
Cost Index data	
I_{base}	CE plant cost Index= 394 (mid 2000)
I_{2005}	CE plant cost Index= 468.2 (2005)

v. Installed cost of compressor

The free on board purchase cost (f.o.b) of a compressor is given by:

$$\mathbf{C_p = F_M \cdot C_B}$$

Where:

C_p= free on board (f.o.b) purchase cost

F_M = material factor (carbon steel (cs) is used in this calculation)

C_B= Base cost, $\mathbf{C_B = exp\left\{7.7661 + 0.7243 \cdot \left[\ln\left(\dot{P}_{hp}\right)\right]\right\}}$

$$\mathbf{C_{Inst}^{Compr} = \left[exp\left\{7.7661 + 0.7243 \cdot \left[\ln\left(\dot{P}_{hp}\right)\right]\right\}\right] \cdot F_M \cdot F_{BM} \cdot \left[\frac{I}{I_{base}}\right]} \quad (5.5)$$

Where $\dot{\mathbf{P}}_{\mathbf{hp}}$ = power (horse power)

The cost index data used for the calculation can be found in table 5.6

Table 5.6. Correlation for correction factors for pump as in Seider [105]

F_M (cs)	1
F_{BM} (cs)	2.15
Cost Index data	
I_{base}	CE plant cost Index= 394 (mid 2000)
I_{2005}	CE plant cost Index= 468.2 (2005)

5.1.2.1.2 Fixed capital investment (FCI)

Fixed capital investment was obtained by summing all the installed cost of the equipments as shown below:

$$\mathbf{C}_{\mathbf{FCI}} = \boldsymbol{C}_{Hx} + \boldsymbol{C}_{col} + \boldsymbol{C}_{tray} + \boldsymbol{C}_{pump} + \boldsymbol{C}_{compr} \tag{5.6}$$

5.1.2.1.3 Depreciation cost

The depreciation cost is estimated as a percentage per year of the total depreciable capital. The total depreciable capital considered in this work does consider only FCI.

$$\dot{\mathbf{C}}_{\mathbf{TDC}} = [\boldsymbol{C}_{Hx} + \boldsymbol{C}_{col} + \boldsymbol{C}_{tray} + \boldsymbol{C}_{pump} + \boldsymbol{C}_{compr}] \cdot \dot{\boldsymbol{d}} \tag{5.7}$$

Where $\dot{d}$ is the depreciation or capital recovery factor and normally varies from 15 to 20% per year (0.15/yr < $\dot{d}$ >0.20/yr).

5.1.2.1.4 Operating cost

In this work operating cost is estimated in terms of utility cost of cooling water, steam and electrical energy. The operating cost is formulated as follows:

$$\dot{\boldsymbol{C}}_{utility} = \boldsymbol{c}_{\boldsymbol{S}} \cdot \dot{\boldsymbol{M}}_{\boldsymbol{S}} \cdot (8000\,\boldsymbol{hr/y}) + \boldsymbol{c}^{*}_{cw} \cdot \dot{\boldsymbol{M}}_{cw} \cdot (8000\,\boldsymbol{hr/y}) + \boldsymbol{c}_{el} \cdot \dot{\boldsymbol{P}}_{el} \cdot (8000\,\boldsymbol{hr/y}) \tag{5.8}$$

The operating cost is estimated using the following utility prices. For the examples studied in this thesis, low pressure steam as well as cooling water costs data are taken from Douglas [70] and are assumed to be available as shown in table 5.7.

Table 5.7. Economic data considered (source: Douglas [70])

Utility	Cost
Cooling water c_{cw}	$0.07 \cdot 10^{-3}$ ($/kg)
Low-pressure steam (150 psi) c_S	$8.8 \cdot 10^{-3}$ ($/kg)
Electricity c_{el}	0.04 ($/kWhr)
Operating hours per year	8000 (hr/y)

5.1.2.1.5 Total annualized cost

TAC (Operating cost + $\dot{\mathbf{C}}_{\mathbf{TDC}}$) is considered in this paper as the economic objective function and is given by:

$$\dot{C}_{TAC} = \dot{C}_{utility} + \dot{\mathbf{C}}_{\mathbf{TDC}} \tag{5.9}$$

In the next section detail discussion of application of energy and exergy models that is relevant to this work is given.

5.1.2.2 Energy and exergy models

Recently, significant attention has been directed towards the use of exergy analysis in the assessment of thermal and other industrial processes since exergy analysis is effective both for achieving efficient energy utilization and for providing optimum designs and operation. The use of irreversible thermodynamics is relatively new to the field of distillation, and is still under development (Taprap [106]). The pillar of irreversible thermodynamics is the entropy production rate. So, it is by origin suitable for processes where second law analysis and optimization are important. In this study, a thermodynamic analysis of a distillation unit is presented and different configurations of the distillation unit are analysed. Evaluation of how much energy each configuration requires from the utility system (steam) are also presented. Maximum efficiency corresponding to minimum entropy production in the column is found.

5.1.2.2.1 Methodology for calculating exergy

Figure 5.2 represents the proposed methodology's structure showing the inter-linking of the software tools used to analyse thermodynamic efficiency in this work. The process is modeled using Aspen Plus^{TM} simulator.

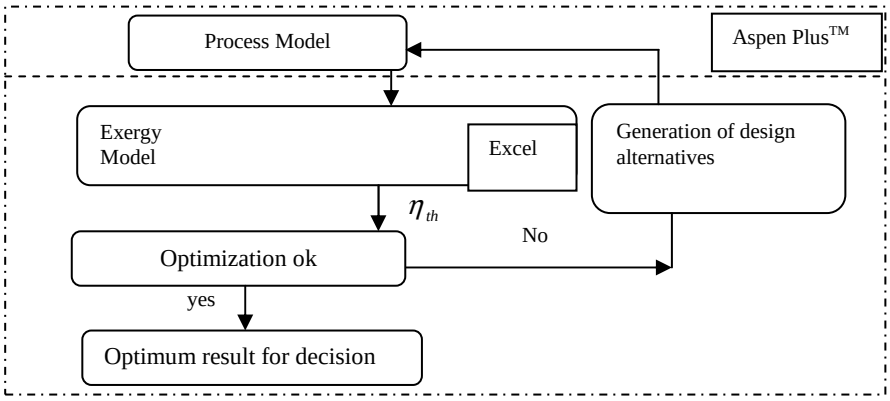

Figure 5.2 Methodology

Mass and energy data from the Aspen Plus^{TM} model are transferred to MS-Excel© to compute the exergy of the streams and thermodynamic efficiency of the distillation unit under study. The base case is improved by generating structural alternatives such as variation of feed stage and side stream withdrawal.

5.1.2.2.2 Column exergy balance

In this section the conservation of energy equations and rate of exergy losses and thermodynamic efficiency as discussed in the previous section have been applied to each design alternative.

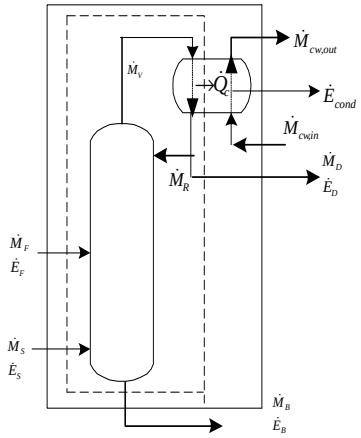

Figure 5.3 Balance for base case

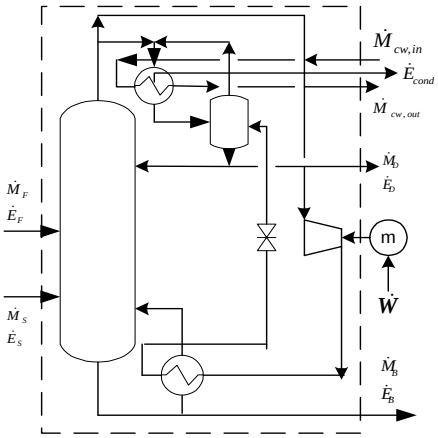

Figure 5.4. Balance for heat pump alternative

Figures 5.3 and 5.4 show the balance regions of the base case distillation unit under study and the heat pump alternative. Energy and exergy balance as well as the minimum work for the base case and heat pump can be stated as follows: (consider that $\dot{\mathbf{E}}_\mathbf{D} = \dot{\mathbf{M}}_\mathbf{D} \cdot \mathbf{e}_\mathbf{D}^*$)

i. *Base case*

Energy balance

$$\dot{\mathbf{M}}_\mathbf{F} \cdot \mathbf{h}_\mathbf{F} + \dot{\mathbf{M}}_\mathbf{S} \cdot \mathbf{h}_\mathbf{S} - \dot{\mathbf{M}}_\mathbf{D} \cdot \mathbf{h}_\mathbf{D} - \dot{\mathbf{M}}_\mathbf{B} \cdot \mathbf{h}_\mathbf{B} = \dot{\mathbf{Q}}_\mathbf{c} \tag{5.10}$$

Exergy balance

$$\dot{\mathbf{E}}\mathbf{x}_\mathbf{F} + \dot{\mathbf{E}}\mathbf{x}_\mathbf{S} = \dot{\mathbf{E}}\mathbf{x}_\mathbf{D} + \dot{\mathbf{E}}\mathbf{x}_\mathbf{B} + \dot{\mathbf{E}}\mathbf{x}_\mathbf{cond} + \Delta\dot{\mathbf{E}}\mathbf{x}_\mathbf{L} \tag{5.11}$$

Assuming $\dot{E}_{cond}$ =0

$$\dot{\mathbf{W}}_\mathbf{min} = \dot{\mathbf{M}}_\mathbf{D} \cdot \mathbf{ex}_\mathbf{D}^* + \dot{\mathbf{M}}_\mathbf{B} \cdot \mathbf{ex}_\mathbf{B}^* - \dot{\mathbf{M}}_\mathbf{F} \cdot \mathbf{ex}_\mathbf{F}^* + \dot{\mathbf{M}}_\mathbf{S} \cdot \mathbf{ex}_\mathbf{S}^* \tag{5.12}$$

ii. Heat pump
Energy balance

$$\dot{\mathbf{M}}_\mathbf{F} \cdot \mathbf{h}_\mathbf{F} + \dot{\mathbf{M}}_\mathbf{S} \cdot \mathbf{h}_\mathbf{S} + \dot{\mathbf{W}}_\mathbf{el} - \dot{\mathbf{M}}_\mathbf{D} \cdot \mathbf{h}_\mathbf{D} - \dot{\mathbf{M}}_\mathbf{B} \cdot \mathbf{h}_\mathbf{B} = \dot{\mathbf{Q}}_\mathbf{cond} \tag{5.13}$$

Exergy balance

$$\dot{\mathbf{E}}\mathbf{x}_{\mathbf{F}} + \dot{\mathbf{E}}\mathbf{x}_{\mathbf{S}} + \dot{\mathbf{W}}_{\mathbf{el}} = \dot{\mathbf{E}}\mathbf{x}_{\mathbf{D}} + \dot{\mathbf{E}}\mathbf{x}_{\mathbf{B}} + \dot{\mathbf{E}}\mathbf{x}_{\mathbf{cond}} + \Delta\dot{\mathbf{E}}\mathbf{x}_{L} \tag{5.14}$$

Assuming $\dot{E}x_{cond}$ =0

$$\dot{\mathbf{W}}_{\mathbf{min}} = \dot{\mathbf{M}}_{\mathbf{D}} \cdot \mathbf{ex}_{\mathbf{D}}^{*} + \dot{\mathbf{M}}_{\mathbf{B}} \cdot \mathbf{ex}_{\mathbf{B}}^{*} - \dot{\mathbf{M}}_{\mathbf{F}} \cdot \mathbf{ex}_{\mathbf{F}}^{*} - \dot{\mathbf{M}}_{\mathbf{S}} \cdot \mathbf{ex}_{\mathbf{S}}^{*} - \dot{\mathbf{W}}_{\mathbf{el}} \tag{5.15}$$

5.1.2.2.3 Stage exergy loss

Exergy loss is a measure of irreversibility in the column due to momentum loss (pressure driving force), thermal loss (temperature driving force/mixing), and chemical potential loss (mass transfer driving force/mixing). In the column there is entropy production due to heat and mass transfer between the fluid streams. In the condenser there is entropy production due to heat transfer only. The exergy loss on tray n ($\dot{E}x_{n,tray}^{loss}$) as in Sato [34] is calculated with an exergy balance over the tray (see fig.5.5) for symbols and numbering. The terms to the right of equation 5.16 represents the exergy carried in and out with the mass flow.

$$\dot{\mathbf{E}}\mathbf{x}_{\mathbf{n,tray}}^{\mathbf{loss}} = \dot{\mathbf{N}}_{\mathbf{n+1}}^{\mathbf{V}} \cdot \mathbf{ex}_{\mathbf{n+1}}^{\mathbf{V}} + \dot{\mathbf{N}}_{\mathbf{n-1}}^{\mathbf{L}} \cdot \mathbf{ex}_{\mathbf{n-1}}^{\mathbf{L}} - \dot{\mathbf{N}}_{\mathbf{n}}^{\mathbf{V}} \cdot \mathbf{ex}_{\mathbf{n}}^{\mathbf{V}} - \dot{\mathbf{N}}_{\mathbf{n}}^{\mathbf{L}} \cdot \mathbf{ex}_{\mathbf{n}}^{\mathbf{L}} \tag{5.16}$$

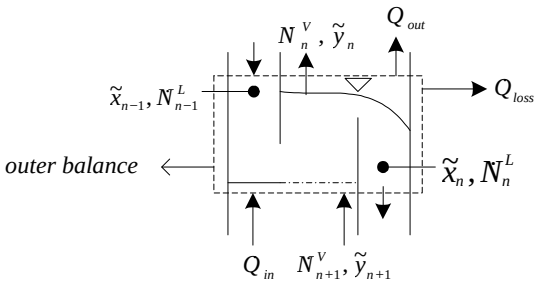

Figure 5.5. Component balance on tray

5.1.2.2.4 Minimum work and thermodynamic efficiency

To calculate the thermodynamic efficiency, the basic concepts of energy and exergy described previously were applied to the distillation unit. The minimum amount of work required for separation can be calculated as follows.

$$\dot{\mathbf{W}}_{\mathbf{min}} = \dot{\mathbf{M}}_{\mathbf{D}} \cdot \mathbf{ex}_{\mathbf{D}}^{*} + \dot{\mathbf{M}}_{\mathbf{B}} \cdot \mathbf{ex}_{\mathbf{B}}^{*} - \dot{\mathbf{M}}_{\mathbf{F}} \cdot \mathbf{ex}_{\mathbf{F}}^{*} - \dot{\mathbf{M}}_{\mathbf{S}} \cdot \mathbf{ex}_{\mathbf{S}}^{*} \tag{5.17}$$

The thermodynamic efficiency of the column can be express as.

$$\eta_{\mathbf{th}} = \frac{\dot{\mathbf{W}}_{\mathbf{min}}}{\dot{\mathbf{W}}_{\mathbf{min}} + \dot{\mathbf{E}}\mathbf{x}_{\mathbf{loss}}^{\mathbf{total}}} \tag{5.18}$$

The methodology for calculating thermodynamic efficiency is as shown in figure 5.6. Where

n = number of alternatives.

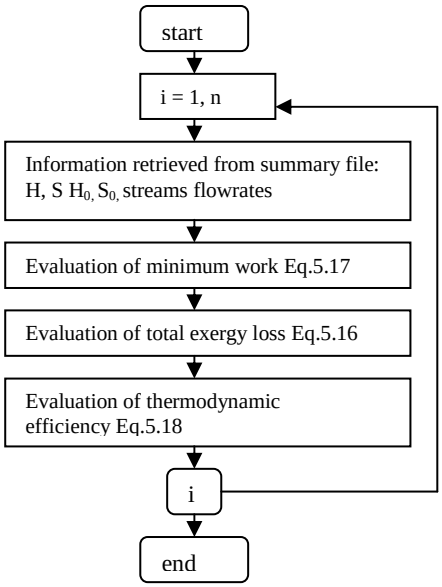

Figure 5.6. Calculation procedure of thermodynamic efficiency

5.1.2.3 Environmental model

In this section, a methodology for integration between the chemical process and potential environmental impact is discussed. An integrated framework that combines alternative generation capabilities and the WAR algorithm is proposed. The methodology consists of the following steps, as shown in Figure 5.7:

(i) Problem definition

(ii) Flowsheet diagram representing the base case

(iii) Base case simulation model using Aspen Plus^{TM} process simulator

(iv) Environmental impact calculation using WAR algorithm

(v) Generation of proposed alternatives

(vi) Comparison between the modified and the base case

As a first step in the design methodology, the design starts with framing of the problem. The primary attributes of the problem are identified and classified according to the following quantities: equipment design variables, operational variables, physical properties, process parameters and the lower and upper bounds of the parameters, as well as mass and energy balance information are gathered. In the next step, the detailed process unit diagram for the base case design is presented. In the third step, the steady state material and energy balances of the distillation unit are performed using Aspen Plus^{TM} process simulator.

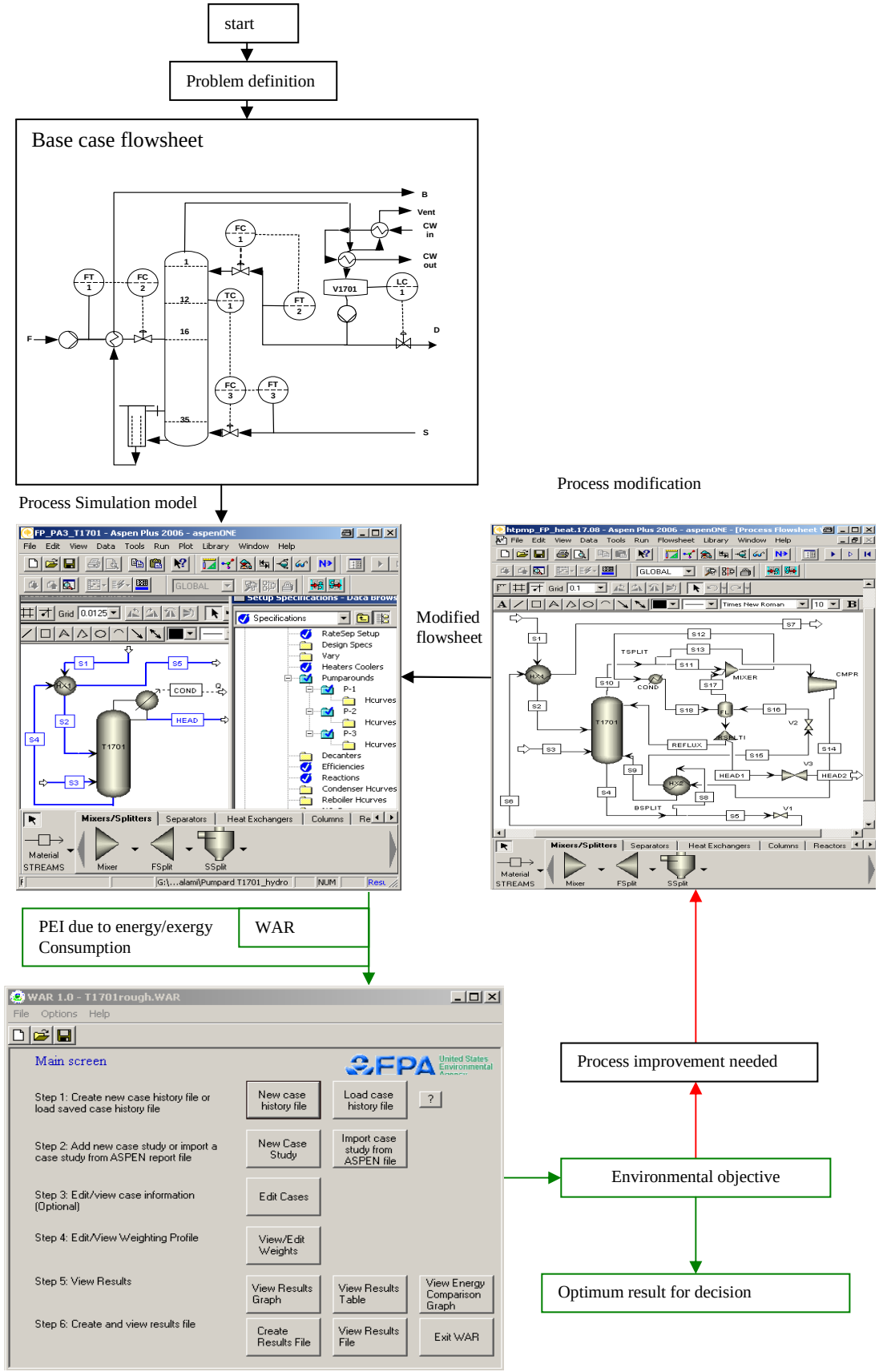

Figure 5.7. Methodology for analyzing Environmental Criteria

Based on the simulation results, the process data from Aspen PlusTM are entered into the WAR GUI in order to compute the PEI due to energy/exergy consumption of the base case model. The process data information includes the chemicals used, the flow rates of the streams entering and leaving the process, and the energy usage of the process.
Modification is made to the base case by generation of the proposed alternative. In the optimization step, a number of runs are carried out in order to optimize the various factors (i.e. process variables) affecting the performance of the unit. Finally the decision makers choose the best compromise alternative from a range of optimum solutions.

5.1.2.3.1 Modification of Standard Potential Environmental Impact model

In this section, the main environmental models that were considered in this thesis are defined, detail discussion of the individual models can be found in chapter 4. In the standard model, standard PEI ($\mathbf{PEI}^{\mathbf{En}}_{\mathbf{std}}$) of coal combustion is assumed to be the source of energy for steam and/ or electrical energy production and these can be expressed as follows:

$$\mathbf{PEI}^{\mathbf{En}}_{\mathbf{std}} = \sum \dot{\mathbf{Q}}_{\mathbf{coal}} \cdot \psi^{\mathbf{En}}_{\mathbf{ki}} \tag{5.19}$$

With some modification of the standard model, new alternative models were developed in this thesis to calculate PEI which is closed to the real environmental effect, which depends on the energy source. These are stated as follows:
Energy source: steam via coal; electrical via coal

$$\mathbf{PEI}^{\mathbf{En}}_{\mathbf{mod}_1} = \sum \left(\frac{\dot{\mathbf{Q}}_{\mathbf{stm}}}{\eta_{\mathbf{stm}}} + \frac{\dot{\mathbf{W}}_{\mathbf{el}}}{\eta_{\mathbf{el}}}\right) \cdot \psi^{\mathbf{En}}_{\mathbf{ki}} \cdot \eta_{\mathbf{stm}} \qquad \text{(for comparison with } \mathbf{PEI}^{\mathbf{En}}_{\mathbf{std}}\text{)} \tag{5.20}$$

$$\mathbf{PEI}^{\mathbf{En}}_{\mathbf{mod2}} = \sum \left(\frac{\dot{\mathbf{Q}}_{\mathbf{stm}}}{\eta_{\mathbf{stm}}} + \frac{\dot{\mathbf{W}}_{\mathbf{el}}}{\eta_{\mathbf{el}}}\right) \cdot \psi^{\mathbf{En}}_{\mathbf{ki,2}} \tag{5.21}$$

Energy source: steam via process stream; electrical energy via coal

$$\mathbf{PEI}^{\mathbf{Ex}}_{\mathbf{PS}} = \sum \left[\left(1 - \frac{\mathbf{T}_0}{\mathbf{T}_s}\right) \cdot \varepsilon \cdot \dot{\mathbf{Q}}_{\mathbf{stm}} + \dot{\mathbf{W}}_{\mathbf{el}} \right] \cdot \frac{\psi^{\mathbf{En}}_{\mathbf{ki}}}{\eta_{\mathbf{el}}} \tag{5.22}$$

5.2 Application of the proposed methodology

Mathematical modeling makes use of computer simulation as the main tool of investigation.
A systematic design deals mainly with the identification of two steps:

- Modeling in which each element of the system is described and criteria for measuring performance are assigned.

- Optimization, in which adjustable parameters are set in a way that gives the best performance of the whole system.

In this section, the detail description of the process plant under investigation is presented (see figure 5.8).

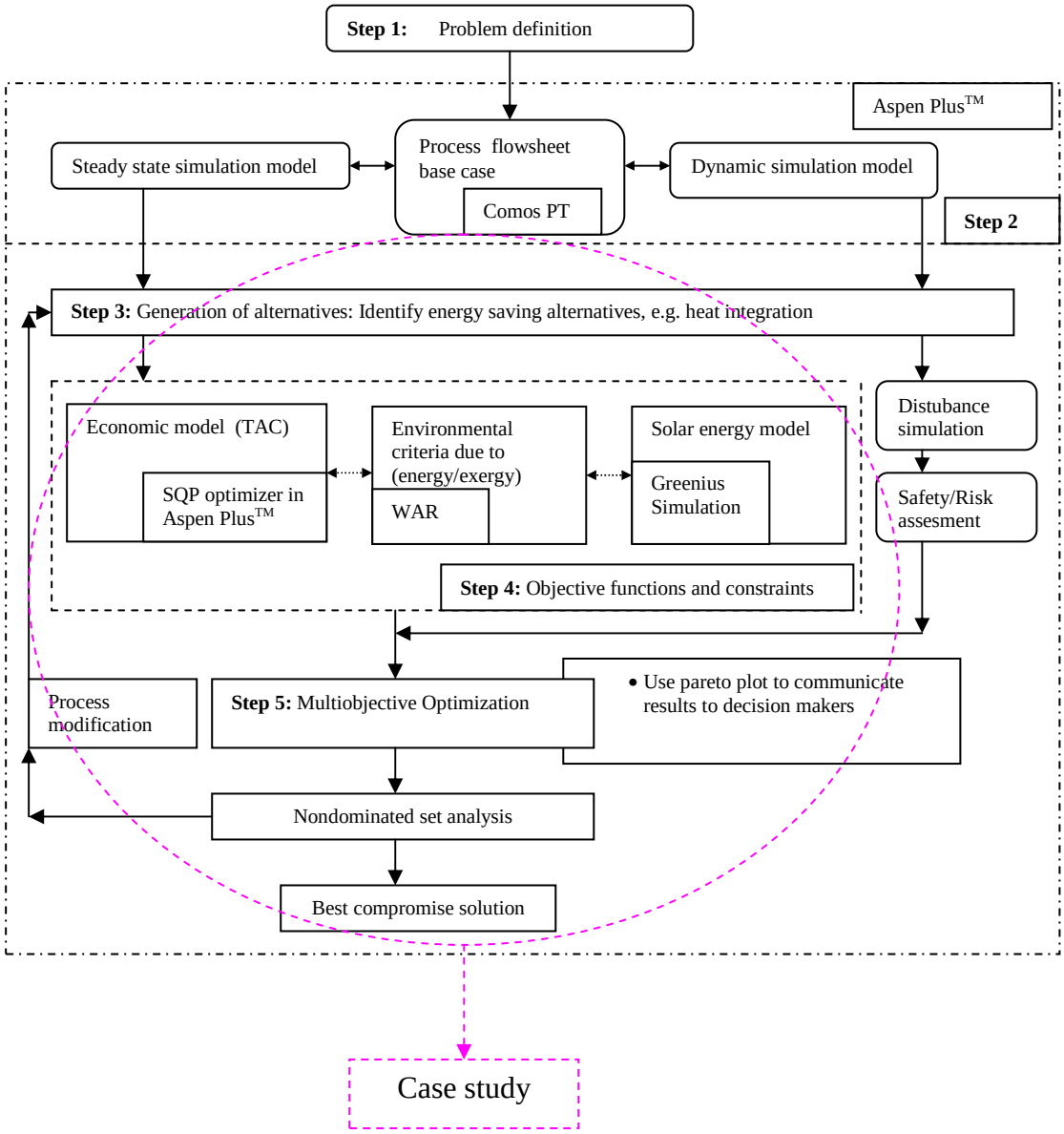

Figure 5.8. General concept of the case studies discussed

5.2.1 Step 1: Definition of problem

Rigorous column simulation requires specifying the operating conditions of the column. The feed composition, flow, pressure and temperature are usually specified. Also the specifications for the products are usually known. One of the main operating parameters to be selected during design is reflux ratio.

- Reflux ratio

Reflux ratio is one of the variables that need to be set for distillation. For a stand alone distillation unit (see figure 5.9) which uses utility for both reboiling and condensing, there is a capital energy trade off.

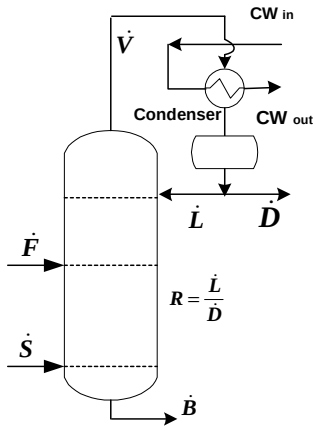

Figure 5.9. Distillation unit model

As reflux ratio is reduced towards the minimum, the capital investment cost of the column increases because more trays are required. But the energy consumption decreases as the reflux ratio is reduced because energy is directly related to vapour boil up and vapour rates decreases as reflux ratio is decreased.

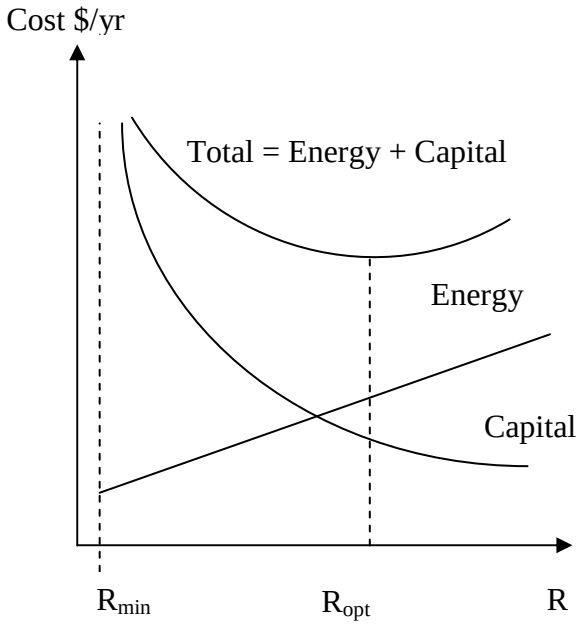

Figure 5.10. The capital energy trade-off for a distillation

This is evident from the equation $\dot{\mathbf{V}} = \dot{\mathbf{L}} + \dot{\mathbf{D}}$: distillate flow rate D is fixed for a given separation, but $\dot{\mathbf{L}}$ decreases as reflux ratio is reduced. On the other hand as reflux ratio is

reduced, energy operating cost decreases, but capital investment costs increases. The optimum reflux ratio is the one that minimizes total cost (operating cost plus annual investment depreciation, see figure 5.10).

5.2.2 Step 2: Generation of base case flowsheet

This thesis work concentrates on the stripping column which is part of a Hydrocarbon Recovery (HCR) unit (see figure 5.11). The hydrocarbons and solvents in the reactor Offgas are removed by adsorption on beds of activated carbon.

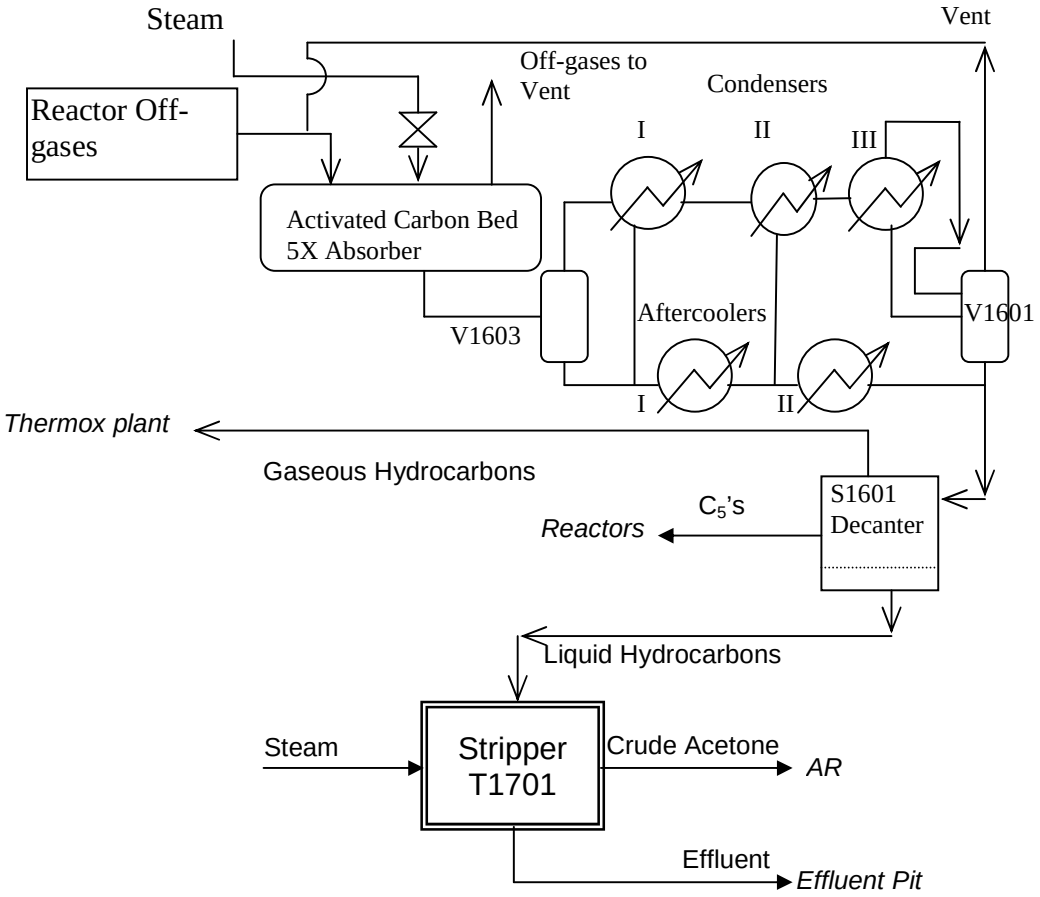

Figure 5.11. Block diagram of the Hydrocarbon Recovery (HCR) Process plant

The hydrocarbons and solvents are further desorbed by using live steam which is cooled down by a series of condensers before entering the decanter. All gases leave the process in order to be burned at the Thermox plant. The liquid hydrocarbon phase is returned to the reactors and the liquid aqueous solvent phase is transferred continuously to the stripper column T1701 (see figure 5.12). The solvents are stripped from the aqueous phase by using live steam and pumped to one of the AR plants. The effluent water leaves T1701 through a stand pipe to the in-plant effluent pit.

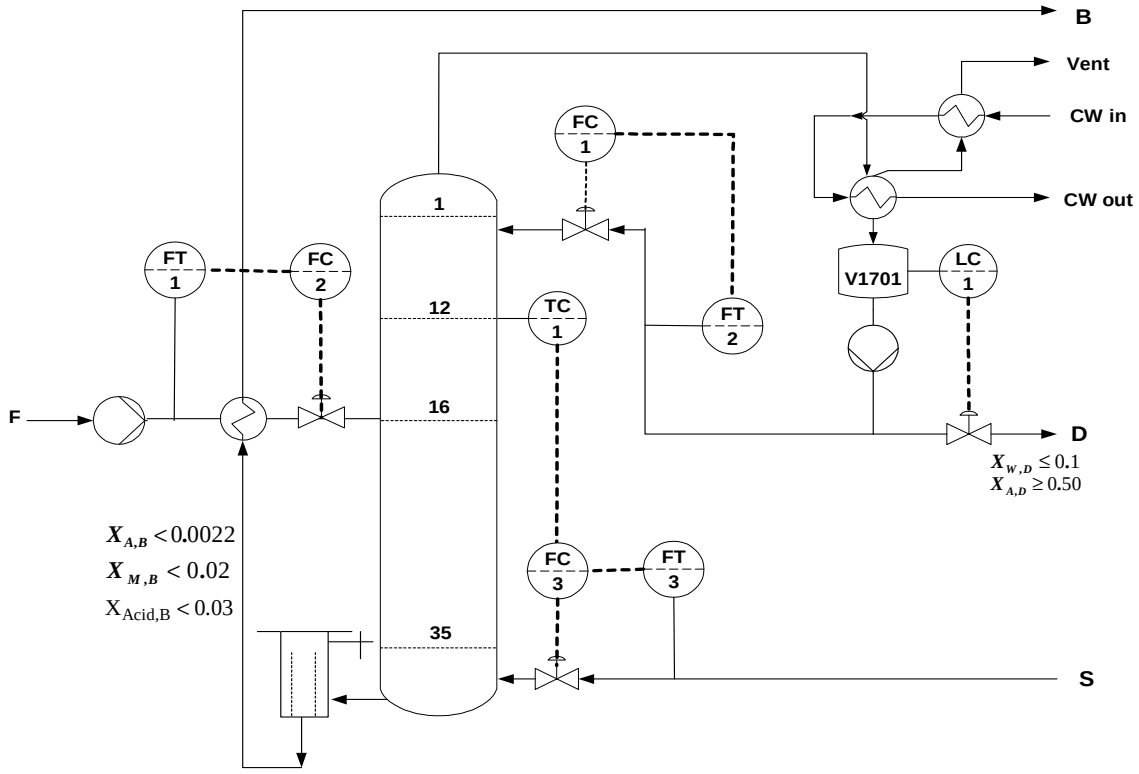

Figure 5.12. Process flow diagram of column T1701

5.2.3 Step 3: Generation proposed alternatives

Figure 5.13 (a) provides a simple schematic illustration of a distillation column (steam stripping column) unit from a real chemical plant. The main components of the feed stream are water, acetone, methanol, and acetic acid etc (see table 5.6).

The feed stream, which is close to its bubble point enters the stripping column normally on tray 15. The column has a diameter of 0.728 m and 35 trays, where the rectifying section includes trays 1-15 and the stripping section 16-35. The column is operated with live steam (700 kg/hr, 140^{o}C and 3.75 bars) injection into the base below stage 35. The top pressure is 1.01 bar, reflux ratio 0.7 (operating plant) and the feed flow rate 4000 kg/hr. Figures 5.14 b, c and d shows the alternatives studied in this work.

The operating targets are as shown below (mass %).

Distillate: $x_{Water} < 10$ %, $x_{Acetone} > 50$ %,

Base: $x_{Acidity} < 3$ %, $x_{Acetone} < 0.22$ %, $x_{Methanol} < 2$ %

The acidity is the sum of the mass fraction of the acids i.e. acetic acid, formic acid and propionic acid. Acetone is the key component for the base and head qualities.

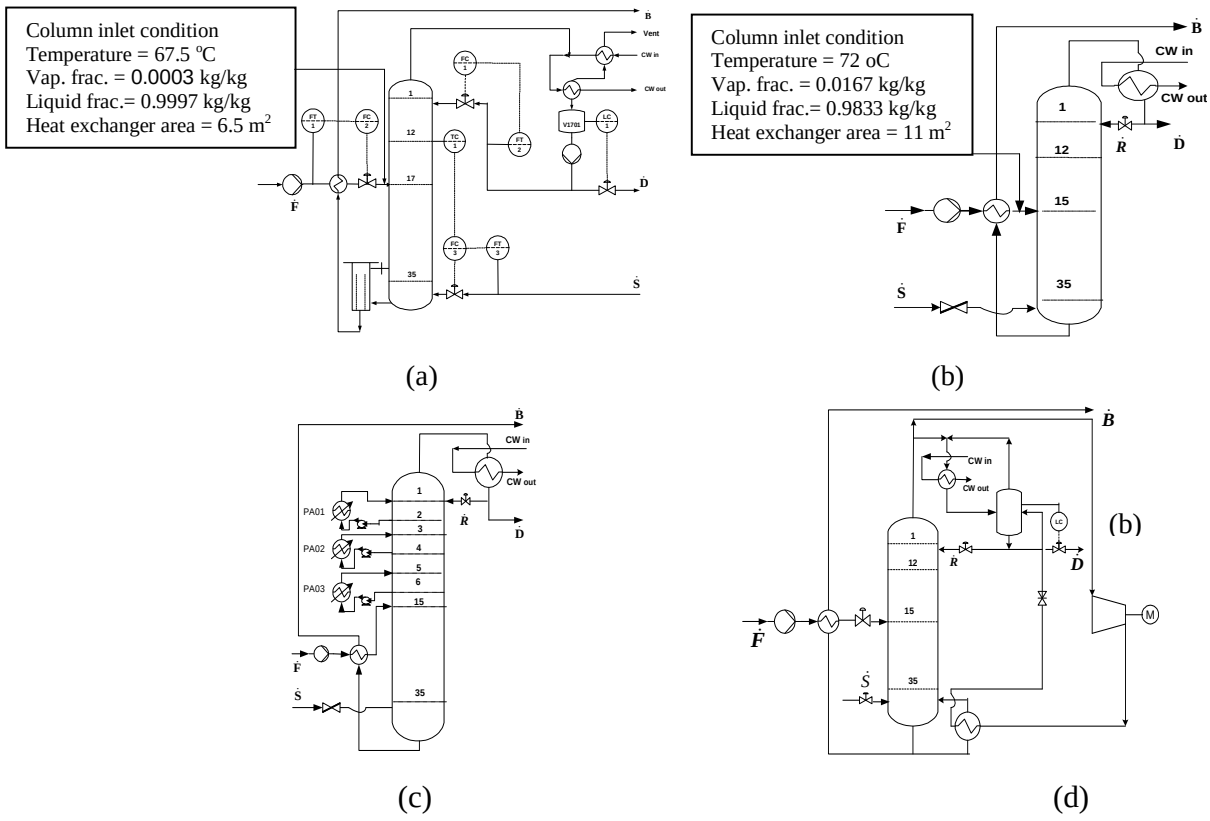

Figure 5.13. Energy integration alternatives: (a) base case (b) extended feed preheat (c) pump-around (d) heat pump

Table 5.8. Typical Stream Compositions

Component	Feed [wt-%]	Head [wt-%]	Base [wt-%]
Methanol	1.65	4.62	0.55
Acetaldehyde	2.21	8.84	0
Methyl Formate	3.77	15.03	0.01
Ethanol	1.06	4.13	0.03
Acetone	13.11	52.36	0.01
Methyl Acetate	2.34	9.33	0.01
Methyl Ethyl Ketone	0.57	2.26	0
Ethyl Acetate	0.25	0.98	0
DiEthyl Ketone	0,1	0.39	0
Water	72.68	2.06	96.89
Acetic Acid	1.75	0	1.94
Formic Acid	0.37	0	0.41
Propionic Acid	0.14	0	0.15
sum	100	100	100

Plant Operating conditions vs. simulation

This section gives an overview of design details and plant equipment specification of the base case model (see table Tables 5.9 and 5.10).

Table 5.9. Detail plant design specification

column	Value
Height (m)	13.118
Diameter (m)	0.8
Design pressure (bar)	2.76
Trays	Value
Number of stages	35
Feed stage	16
Tray spacing (m)	0.3
Design pressure (bar)	1.9

Table 5.10. Design Data

Section	Material	Height	Diameter	Trays	Spacing	Valves	Active Area
Rectifying	S. Steel[1]	5.4 m	0.8 m	16-35	0.3 m	55	0.4693 m^2
Stripping	S. Steel	4.5 m	0.8 m	1-15	0.3 m	46	0.3939 m^2

[1]Stainless Steel

Simulation models of Design alternatives

In this section, the process models are presented, first the detail simulation models are presented.

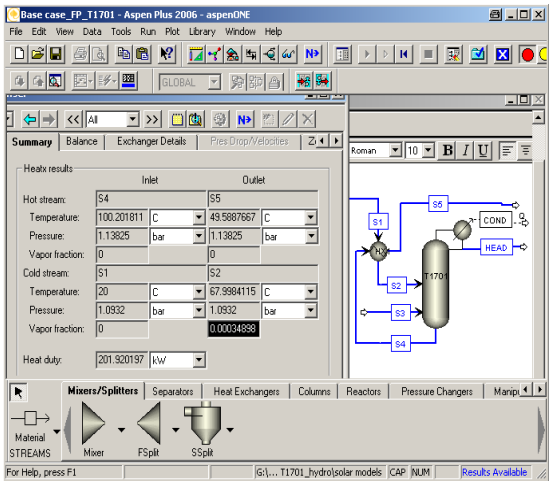

(a)

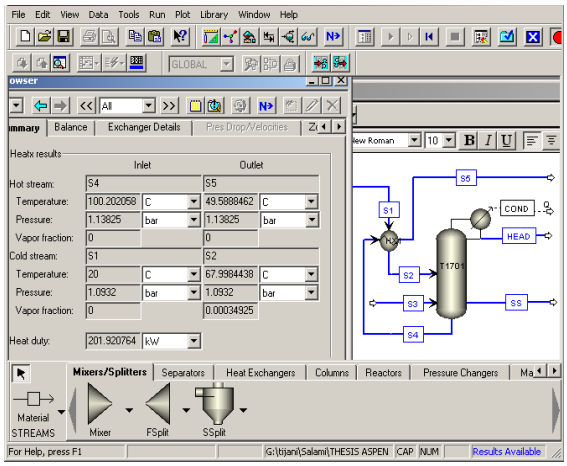

(b)

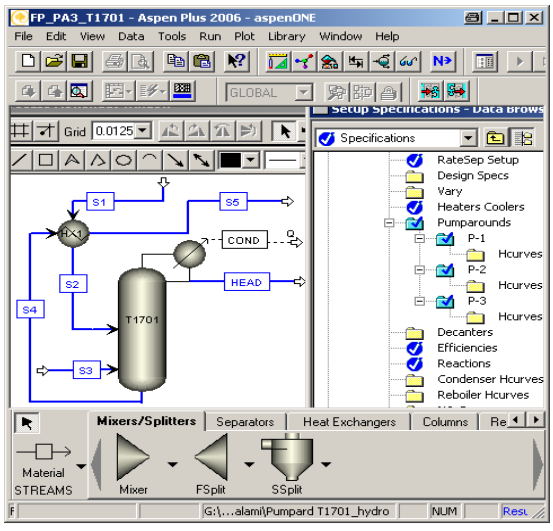

(c)

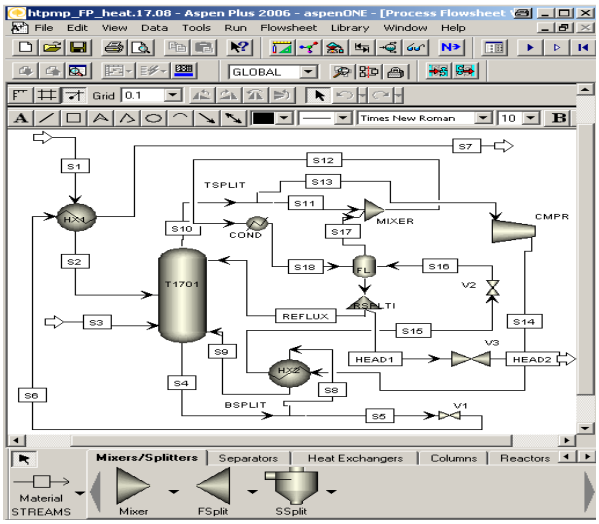

(d)

Figure 5.14 Aspen model for alternatives: (a) base case (liquid) and extended feed preheat (b) Side stream (c) pump-around (liquid) (d) heat pump (liquid)

Computer simulations of the actual plant help to identify new solutions for column operations. The RADFRAC models (figure 5.14) were selected in Aspen Plus™ for the analysis.

The results of the steady state simulation for the base case model are compared with the plant data as shown in tables 5.11 and 5.12. Table 5.11 shows the operating conditions with the optimum steam rate of 539 kg/hr whiles table 5.12 gives the quality of the head product.

Table 5.11. Operating conditions

	Operating plant data	Aspen Plus™ simulation*	Aspen Plus™ simulation (optimum)**
Steam flow rate (kg/hr)	700	574	539
Feed flow rate (kg/hr)	4000	4000	4000
Reflux ratio	0.7	0.7	0.54
Distillate flow rate (kg/hr)	1068	922	924
Base flow rate (kg/hr)	3632	3652	3615

Table 5.12. Product quality (simulation based on theoretical stages, $\mathbf{E_{MG,i,j}} = 1{,}0$ *)*

Components	Plant data for head quality	Simul. result head quality*	Simul. result head quality (optimum)**
	Mass fract.	Mass fract.	Mass fract.
Methanol	0.04	0.01	0.01
Acetaldehyde	0.08	0.09	0.10
Methyl Formate	0.15	0.16	0.14
Ethanol	0.04	0.01	0.01
Acetone	0.52	0.56	0.55
Methyl Acetate	0.09	0.10	0.10
Methyl Ethyl Ketone	0.02	0.03	0.03
Ethyl Acetate	0.01	0.01	0.01
DiEthyl Ketone	0.01	0.01	0.01
Water	0.02	0.02	0.02
Acetic Acid	0	0	0
Formic Acid	0	0	0
Propionic Acid	0	0	0

* Modification of plant operating conditions and simulated in Aspen Plus™

** Results for optimum operating conditions for the plant

E_{MG} : Murphre tray efficiency

Considering the simulation results in table 4, Murphre tray efficiency was assumed to be equal to 1 that is why there is no big variation in the mass fraction of the components of actual plant when compared with simulation results.

5.2.4 Step 4: Evaluation of alternatives

5.2.4.1 Design alternatives

i. Side stream

The exergy calculation methodology is illustrated with the help of a distillation column unit. The base case was modified by introducing a side stream at tray 30, see figure 5.15. This modification contributed to energy saving.

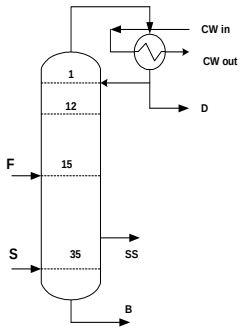

Figure 5.15. Design alternative (with side stream)

The steady state simulation model is configured in Aspen Plus^{TM} using RADFRAC method. Detailed degree of freedom analysis is performed for determining the number of decision variables (independent variables we can affect) needed to execute the simulation. With given values for feed composition, feed flow rate, operating pressure, total number of trays, feed tray location, the distillation unit has two degrees of freedom (steam flow rate and reflux ratio). Thus, these decision variables are used for optimization and satisfaction of purity constraints which are product key component composition. Table 5.13 shows optimum operating conditions and purity achieved for base case and side stream case. There is a slight change in the product purity of the base case compared with side stream case (see table 5.13).

Table 5.13. Simulation results for optimal operating conditions

	Reflux ratio	Steam flow kg/hr	Distillate comp. mass %		Base comp. mass %		
			x_{water}	$x_{acetone}$	$x_{methanol}$	$x_{acidity}$	$x_{acetone}$
Base case	0.635	569	2.16	55.0	1.49	2.48	0.219
Side stream case	0.580	513	2.10	54.3	1.35	2.49	0.220

The side stream case favours energy reduction (see table 5.13). The other advantage of the side stream case is that it removes the middle boiling components. The main results of the simulation are summarized in table 5.14. As shown in table 5.14 the base case design gives higher irreversibility loss (exergy loss) compared with the side stream case. This results to higher thermodynamic efficiency. The reason is that the side stream design has less separation work.

Table 5.14. Simulation Results

	Base case	Side stream
Reflux ratio	0.635	0.580
$\dot{Q}_{cond}$ MJ/hr	-807.37	-764.23
$\dot{M}_s$ kg/hr	569	513
$\dot{E}_{Total}^{Loss}$ MJ/hr	185	170
$\dot{W}_{min}$ MJ/hr	250	222
η_{th} %	27.29	29.52

Exergy loss is greatest at the base of the column (stage 35) for base case with 103MJ/hr of exergy loss, whiles the side stream has 93 MJ/hr of exergy loss.

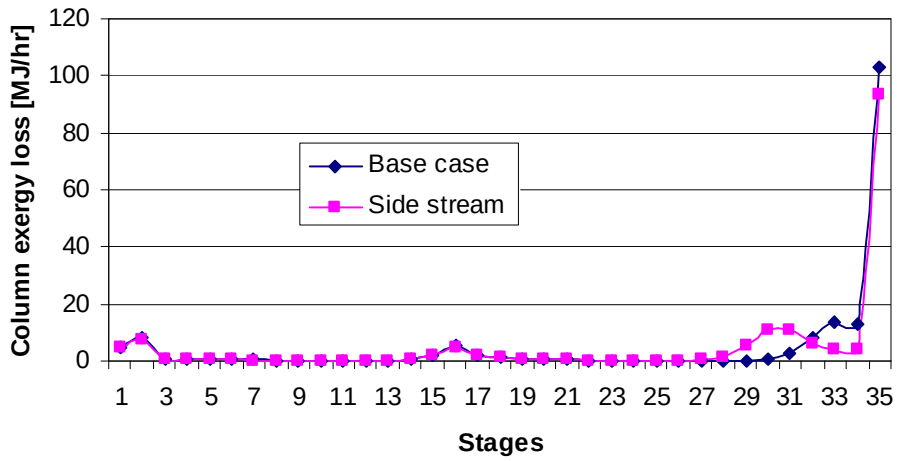

Figure 5.16. Exergy loss profiles in columns (steam 141^{o}C)

This situation is illustrated in Figure 5.16. In terms of thermodynamic efficiency, energy consumption, the side stream solution should be preferred. The main contribution to the exergy loss within the distillation unit is therefore is due to steam condition (too high temperature).

Table 5.15. Results of product quality for steam at 110^0C

	Reflux ratio	Steam flow kg/hr	Distillate comp. mass %		Base comp. mass %		
			x_{water}	$x_{acetone}$	$x_{methanol}$	$x_{acidity}$	$x_{acetone}$
Base case	0.635	564	2.11	55.0	1.48	2.48	0.22

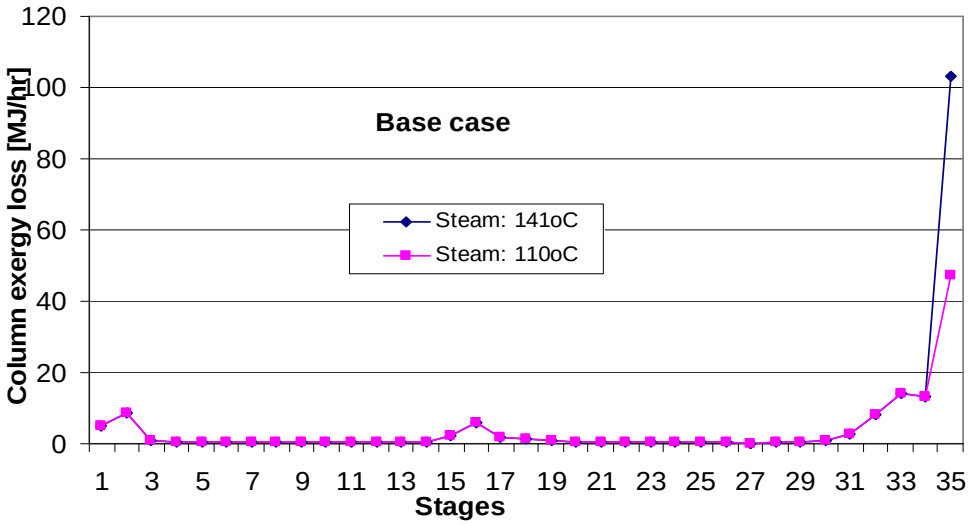

Figure 5.17. Exergy loss profiles in column (steam at 110^0C vs. 141^0C)

In order to reduce the exergy loss at the bottom of the column, the steam condition was changed. The temperature of entering steam was reduced from 141^0C to 110^0C. Figure 5.17 shows the resulted exergy profile. The exergy loss of steam inlet decreased by approximately a factor of 3 while product quality remains the same (see table 5.15).

ii. Extended feed preheat

Figure 5.18 shows the exergy content of the bottom streams of the distillation column, it can be observed, that the bottom stream has high exergy content. In the original plant, a heat exchanger is used to preheat the feed stream via the bottom stream. The effect is shown in figure 5.18. Because of the exergy level of bottom stream (hot stream) to the heat exchanger (feed preheat), there is some potential for optimization. The distillate stream is send to the acetone recovery plant. Because of this, it is not considered in the further analysis of this study. As shown in figure

5.19 about 6.4% of the exergy content of the bottom stream was recovered through feed preheat and this was further improve to 10 % of exergy recovery using extended feed preheat.

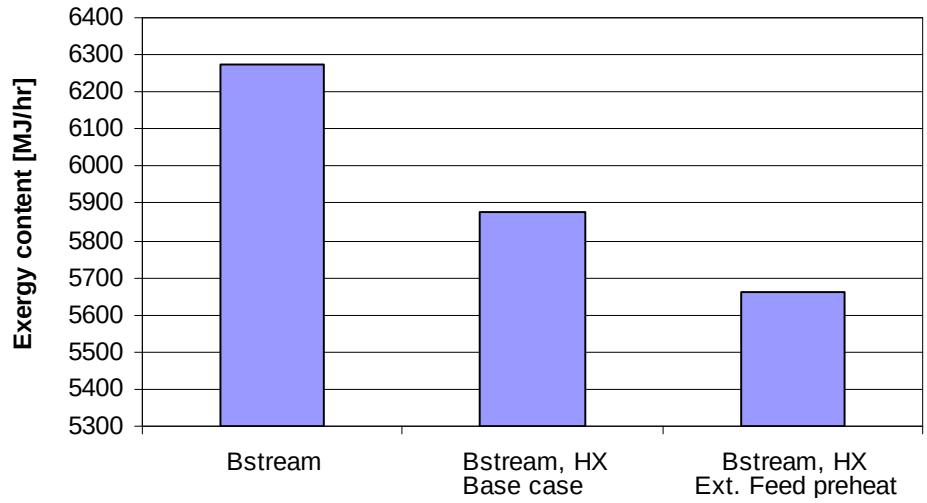

Figure 5.18. Distribution of exergy of streams for base case design and extended feed preheat
B_{strm} - exergy of bottom stream, $B_{strm, Hx}$ - exergy of bottom stream after integrating it with heat exchanger to preheat feed stream

The exergy loss profiles of Figure 5.19 show that the reduction in exergy loss at the feed stage is about 60% with values of 5.74 MJ/hr in base case and 2.34 MJ/hr in extended feed preheat. Also, the exergy loss on stage 35 decreases by 15.6 %, and becomes 103 MJ/hr in base case and 86.9 MJ/hr in extended feed preheat.

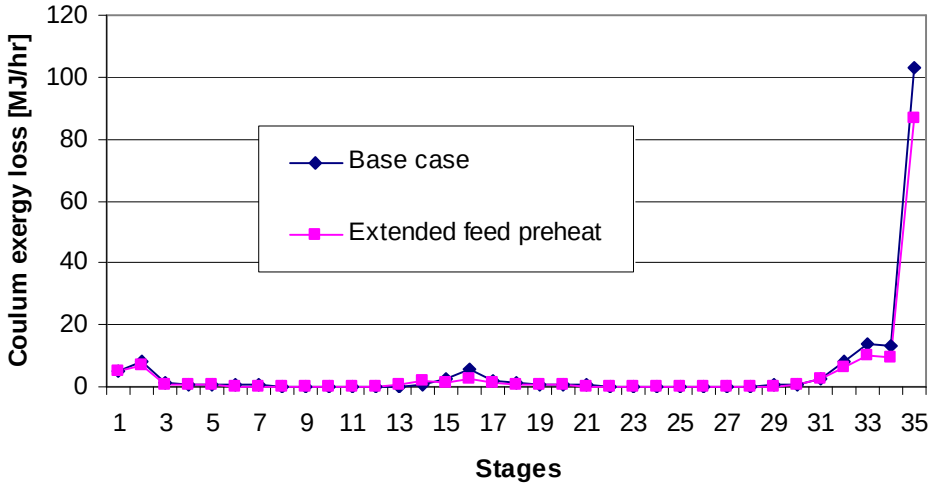

Figure 5.19. Exergy loss profiles in column (steam at 141^0C)

iii. Pump around

Pump around installation may be of value if the heat transferred can be used as a heat source. Another purpose of the pump-around is to suppress top-tray flooding. The pump-around circuit shown in figure 5.14 c has been observed to be most advantageous (see table 5.16). In this case liquid is drawn from a tray, cools the liquid in a heat exchanger and returns the liquid to a tray above the original tray. The results of the simulation are shown in table 5.16. A maximum heat recovery of 415 kW was achieved with three pump-around.

Table 5.16 Pump-around (PA) simulation results (liquid from tray)

No. of PA[a]	Withdraw tray	Return tray	Steam rate (kg/hr)	PA[a]. duty (kW)	Cond. duty (kW)	Reflux ratio
1	2	1	523.30	320	-184	0.51
2	2	1	541	382	-174	0.49
	4	3				
3	2	1	565	415	-170	0.48
	4	3				
	6	5				

PAa : Pump-around

A simulation study was further analyses with saturated vapour removed from tray (see table 5.17). The stream leaving the column is saturated vapour and the stream re-entering the column is condensed liquid.

Table 5.17. Pump-around (PA) simulation results (saturated vapour from tray)

No. of PA[a]	Withdraw tray	Return tray	Steam rate (kg/hr)	PA[a]. duty (kW)	Cond. duty (kW)	Reflux ratio
1	2	1	570.30	528.3	-121	0.47
2	2	1	583.82	545	-129	0.43
	4	3				
3	2	1	623	573	-146	0.40
	4	3				
	6	5				

PAa : Pump-around

It was found out that this option was better than the liquid removal from the tray, because a maximum heat recovery of 573 kW was achieved with three pump-around which gives about

27.6% increase in heat recovery when compared with the liquid removal. The advantage of the vapour removal ensures that heavy components are not transferred up the tray. The pump-around alternative is operated at lower reflux ratio compared to other alternatives, this is due to the fact that heat removal by the pump-around creates an additional intermediate PA duty. The steam flow rate increases because of less active tray above the pump around.

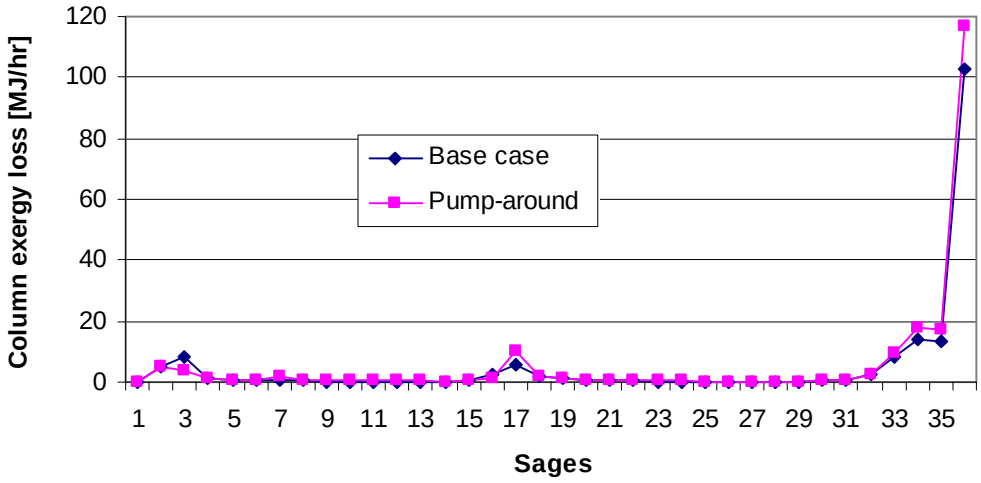

Figure 5.20. Exergy loss profiles in column (steam at 141^{0}C)

Figure 5.20 shows the exergy loss profile of the pump around compared with the base case. It can be shown that exergy loss of the pump around on stage 35 is the highest because the exergy loss on stage 35 increases by 13.2 %, and becomes 103 MJ/hr in base case and 116.6 MJ/hr in pump around. This is also due to high steam rate of the pump around. The only region in which the exergy loss of the pump around was lowest is at the condenser, which is 8.5 MJ/hr and 3.9 MJ/hr for base case. The reduction in the exergy loss is due to the lower heat duty of the pump around condenser.

iv. Heat pump

The exergy loss profiles of Figure 5.21 show that the increase in exergy loss at the feed stage is about 50% with values of 5.74 MJ/hr in base case and 11.8 MJ/hr in heat pump. Also, the exergy loss on stage 35 decreases by 20.8 %, and becomes 103 MJ/hr in base case and 81.5 MJ/hr in heat pump.

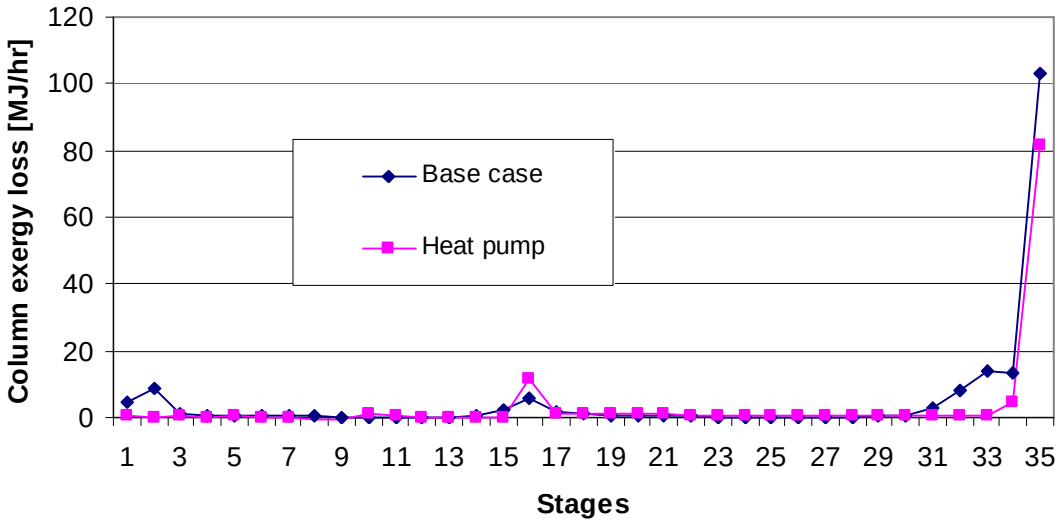

Figure 5.21. Exergy loss profiles in column (steam at 141^{0}C)

5.2.4.2 Comparison of alternatives studied

Figure 5.22 compares the exergy loss profiles in all the alternatives. The pump around design operates with rather large exergy losses of 116MJ/hr at stage 35 (see figure 5.22). The reason is due to it's high steam consumption. Also the feed stage exergy loss was highest for heat pump alternative and lowest for extended feed preheats. The heat pump alternative however reduces the total exergy losses by about 35.6%, and hence save a considerable amount of the available energy and also it gives it the highest thermodynamic efficiency.

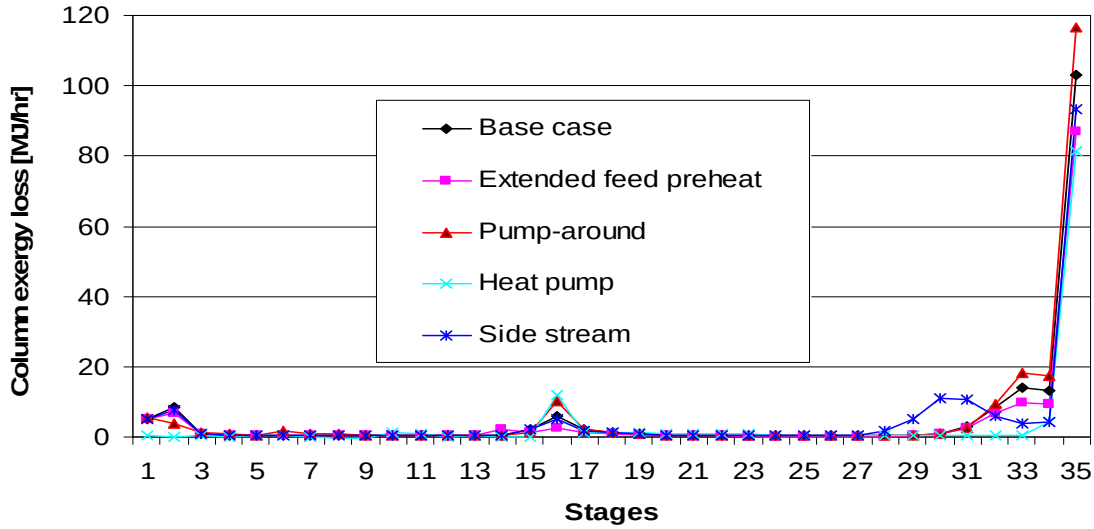

Figure 5.22. Comparison of exergy loss profiles in all the alternatives

As Table 5.18 shows, the reduction in the total exergy loss is 18.8 % with the total column exergy losses of 175 MJ/hr and 142 MJ/hr in base case and extended feed preheat respectively

Table 5.18. Comparison of operating parameters design alternatives

	Base case	Extended Feed preheat	Pump-around (Vapour)	Heat pump	Side stream
Reflux ratio	0.635	0.58	0.7	0.52	0.59
Feed stage 16 temperature (^{o}C)	68.6	72.1	68	65	66
$\dot{Q}_{cond}$ MJ/hr	-807.37	-758.61	-622.31	-543	-722
$\dot{M}_{s}$ kg/hr	569	481	623 (-152)	357	513
Electrical input MJ/hr	-	-	-	154	-
Exergy loss due to electrical input $\dot{E}_{el}^{Loss}$	-	-	-	20	-
Exergy loss feed stage 16 MJ/hr	5.74	2.34	10	11.86	4.9
Exergy loss on stage 35 MJ/hr	103	86.9	116	81	93.8
$\dot{E}_{Total}^{Loss}$ MJ/hr	185	142	201(-40) =161	111 (+23)=134	170
η_{th} %	27.29	32.2	23.4(+8) =31.4	38(-5)=33	29.52

Conclusion

The exergy loss profiles are plotted by calculating the exergy loss at each stage of the column, taking into account all entering and leaving material and heat streams. In general, the exergy loss profile was used as a tool to examine the irreversibility in each design alternative. It is found that the column configuration with least exergy losses have the highest thermodynamic efficiency of 33 % (Heat pump alternative), this is an improvement over the base case with efficiency of 27.29 %.

5.2.5 Step 5: Multi-objective optimization

i. Objective function

In this work multi-objective optimization is performed to evaluate process improvement alternatives. Total annualized cost (TAC) and potential environmental impact (PEI) are taken as objective functions. The SQP method was used for the economic (TAC) objective. It can

converge tear streams, equality and inequality constraints simultaneously with the optimization problem. The WAR algorithm was used to evaluate the PEI of each design alternative. The optimization problem can be formulated as follows:

$$\min.(TAC) = c_S \cdot \dot{M}_S \cdot (8000\,hr/y) + c^*_{cw} \cdot \dot{F}_{cw} \cdot (8000\,hr/y) + c_{el} \cdot \dot{P}_{el} \cdot (8000\,hr/y) + \dot{C}_{TCI}$$

$$\min.PEI^{En}_{mod\,2} = \sum\left(\frac{\dot{Q}_{stm}}{\eta_{stm}} + \frac{\dot{W}_{el}}{\eta_{el}}\right) \cdot \psi^{En}_{ki} \quad \text{or} \quad \min.PEI^{Ex}_{PS} = \sum\left[\left(1 - \frac{T_a}{T_{stream}}\right) \cdot \varepsilon \cdot \dot{Q}_{stream} + \dot{W}_{el}\right] \cdot \frac{\psi^{En}_{ki}}{\eta_{el}} \qquad (5.23)$$

ii. Constraints

The appropriate decision variables which are used in the minimization of the objective functions are selected and the modification of these variables must directly affect the objective functions.

Table 5.19. Plant operating constraints

Equality constraint	Design variables	Process variables
	- Number of trays = 35 - Feed location =15 - Column diameter = 0.8m - Tray spacing = 0.3m	- Column pressure (top) =1.032 bar - Feed flow rate = 4000 kg/hr - Reflux ratio = 0.7
Inequality constraint		- Distillate comp. (mass %): $x_{Ac.} > 50$ % - Bottom comp. (mass %): $x_{Ac.} < 0.22$ % - Steam flow rate < 700kg/hr

Table 5.20. Simulation constraint

Equality constraint	Design variables	Process variables
	- Number of trays =35 - Optimum feed stage = 15 - Column diameter = 0.8m - Tray spacing = 0.3m	- Column pressure (top) = 1.032bar - Feed flow rate = 4000 kg/hr - Mass & energy balance equations
Inequality constraint		- Distillate comp. (mass %): $54 < x_{Ac.} < 56$ [(1)] - Bottom comp. (mass %): $0.20 < x_{Ac.} < 0.22$ [(1)] - Steam rate (kg/hr) $340 <$ steam < 620 [(2)] - Reflux ratio $0.45 < RR < 1.3$ [(2)]

[(1)] Small range of Key component, because utility consumption depends on bottom and distillate key components. [(2)] Simulation constraints.

5.2.5.1 Results and discussion of objective cost

The comparison of design alternatives is based on a small range of simulation constraints of the key components and the same feed flow rate. Table 5.21 shows that based on the data used and assumptions made, the extended feed preheat did result in lowest TAC. The TAC of the heat pump is the highest. This is due to the additional process machinery (i.e. compressor) and process equipment (heat exchangers).

Table 5.21. Optimization results

Alternatives	Base case	Extended Feed preheat	Pump-around (Vapour)	Heat pump
Condenser duty kW	-224	-209	-170	-125
Steam flowrate kg/hr	555	481	623 (-152)	357
Heat input via steam [kW]	331	286	371 (-90)	213
Cooling water flowrate [kg/hr]	12, 400	12, 323	9, 246	5, 319
steam produced [kg/hr]	-	-	143	-
Electricity consumed [kW]	-	-	-	43
Operating cost [$/y]	**45, 048**	**40, 801**	**48, 691 –23%**	**40, 788**
Heat exchanger HX1 cost [$]	10, 893	15, 743	10, 893	10, 893
Heat exchanger HX2 cost [$]	-	-	-	45, 436
Compressor cost [$]	-	-	-	56, 803
Pump cost [$]	-	-	21, 004	-
Heat exchanger (Pumprd.) cost [$]	-	-	32, 679	-
Condenser cost [$]	40, 884	40, 684	40, 102	36, 248
Column cost [$]	262, 819	262, 819	262, 819	262, 819
Tray cost [$]	17, 490	17, 490	17, 490	17, 490
Fixed Capital Investment cost [$]	332, 086	336, 736	374, 094	429, 689
Depreciation cost [$/y]	66, 417	67, 347	74, 818	85, 937
TAC [$/y]	**111, 465**	**108, 148**	**112, 311**	**126, 725**
Feed rate [kg/hr]	4000	4000	4000	4000
Reflux ratio	0.635	0.58	0.7	0.52
Distillate comp. Mass %				
x_{water} < 10 %	2.0	2.1	2.1	2.0
(key component) 56 < $\mathbf{x_{acetone}}$ <54%	55.0	55.0	55.0	55.0
Base comp. Mass %				
$x_{methanol}$ < 2 %	1.49	1.47	1.31	1.60
$\mathbf{x_{acidity}}$ < 3 %	2.50	2.54	2.49	2.50
(key component) 0.20 < x_{aceton} < 0.22 %	0.22	0.22	0.22	0.22

For other alternatives steam cost is the most relevant variable. The high steam flow rate (623kg/hr) of the pump-around alternative gives it the highest operating cost. But considering the positive aspect of using the heat (152kg/hr steam) recovered by the pump-around to heat up other process streams, this reduced the operating cost of the pump-around by $ 11, 198 i.e. 23% .

5.2.5.2 Objective of potential environmental impact

The result for each alternative can be found in table 5.22, Table 5.22 shows that the PEI for $\mathbf{PEI}^{\mathbf{En}}_{\mathbf{mod\,2}}$ was the highest in all the cases, this is because the real effect of electrical energy and steam was considered in this model. Also the standard $\mathbf{PEI}^{\mathbf{En}}_{\mathbf{std}}$ and the $\mathbf{PEI}^{\mathbf{En}}_{\mathbf{mod}_1}$ effect are the same for all the cases except that of heat pump, this is because the effect of electrical energy consumption was considered only for heat pump.

Table 5.22. Comparison of potential environmental impact of alternatives

Alternatives	Base case	Extended feed preheat	Pump-around	Heat pump
Energy content of steam [kW]	331	286	371 (-90)	213
PEI analysis				
$\mathbf{PEI}^{\mathbf{En}}_{\mathbf{std}}$ (1)	7.8	6.74	8.74 (-2.12)	6
$\mathbf{PEI}^{\mathbf{En}}_{\mathbf{mod1}}$ (1)	10.4	9.0	11.7(-2.8)	7
$\mathbf{PEI}^{\mathbf{En}}_{\mathbf{mod\,2}}$ (1)	10.4	9.0	11.7(-2.8)	10
$\mathbf{PEI}^{\mathbf{Ex}}_{\mathbf{PS}}$ (2)	3.4	2.9	3.8(-1.6)	5 (3)

(1) Coal power plant

(2) Process stream

(3) Heat pump based on coal power plant

5.2.5.3 Analysis of individual design alternative

The most important variable that was considered for the optimization is reflux ratio (RR). This is illustrated in figure 5.3a. Each point on the graphs (see figures 5.23 to 5.26) corresponds to a specific reflux ratio as well as a set of objective function (TAC_{min}, PEI_{min}). Referring to figure 5.23a, as reflux ratio is decreased from 0.68 to 0.52, the TAC increases, this is due to increase in number or size of process equipment (such as number of plates) which have direct effect on the capital cost. On the other hand as the reflux ratio is decrease the energy consumption (steam rate) decreases because less reboiling and is required, the effect is that the PEI index also decreases.
In order to communicate the results to the decision maker, two-dimensional Pareto plots were obtained for each alternative (see figures. 5.23 to 5.26).

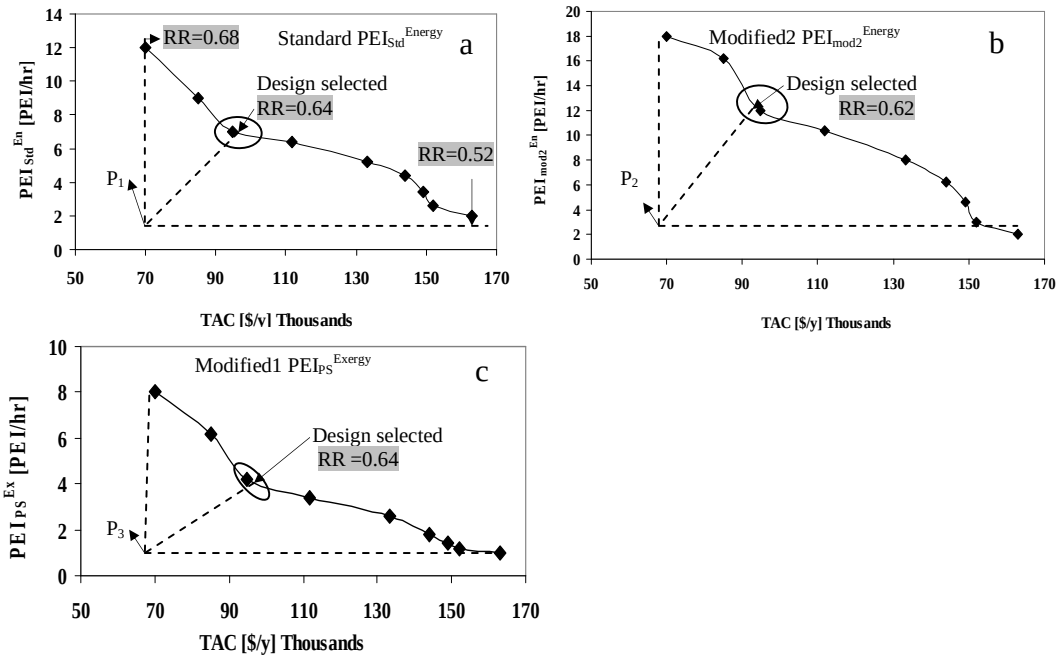

Figure. 5.23. Pareto trade off surfaces for base case

Figure 5.23 shows the pareto trade-off surface for the base case alterative. The minimum value P (TAC_{min}, PEI_{min}) of each objective function corresponds to the ideal objective vector which is a non-existent solution; this is represented by P_1, P_2 and P_3 in figures. 5.23 a, b and c respectively. In this case, the ideal objective vector is used to find the best solution along the pareto surface. Considering that the ideal objective vector P_1 = (TAC_{min}, PEI_{min}) in figure 5.23a is the point

corresponding to minimum TAC and minimum PEI, it is clear from figure 5.23a that the Pareto optimal solutions are closer to the ideal objective vector. This procedure is applied to all the alternatives. The decision maker has to select the best solution depending on the importance of objectives.

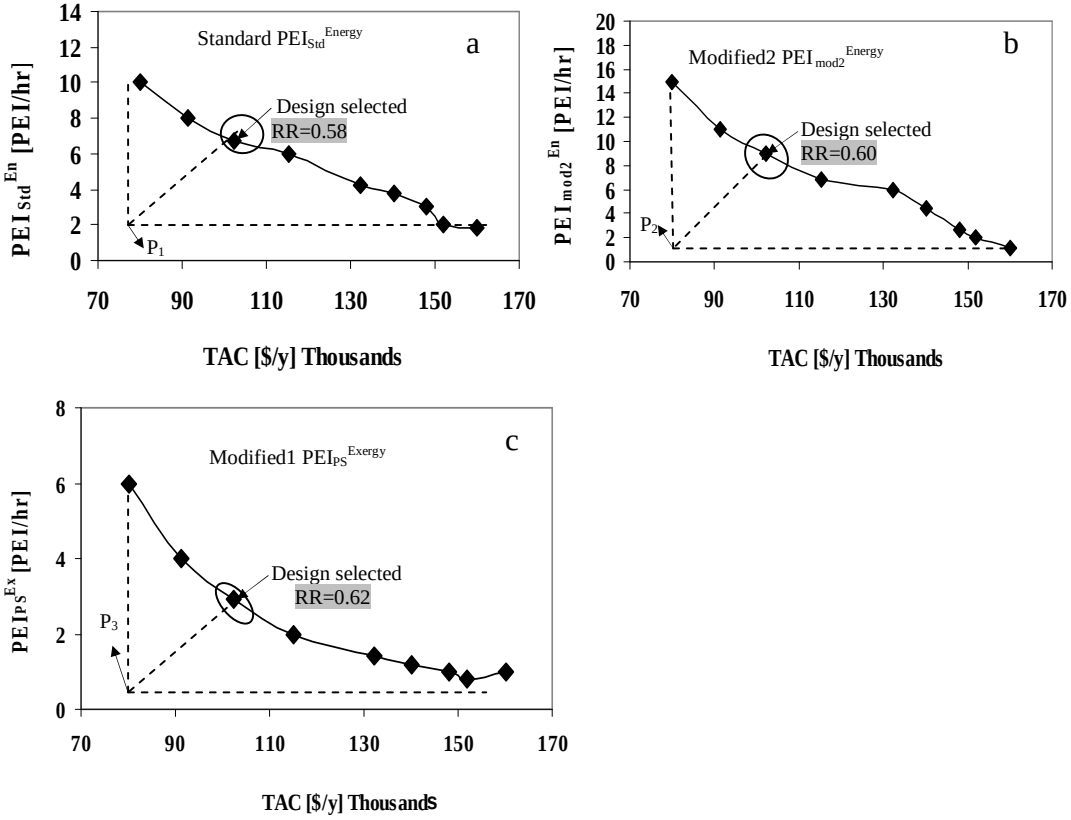

Figure 5.24. Pareto trade off surfaces for extended feed preheat

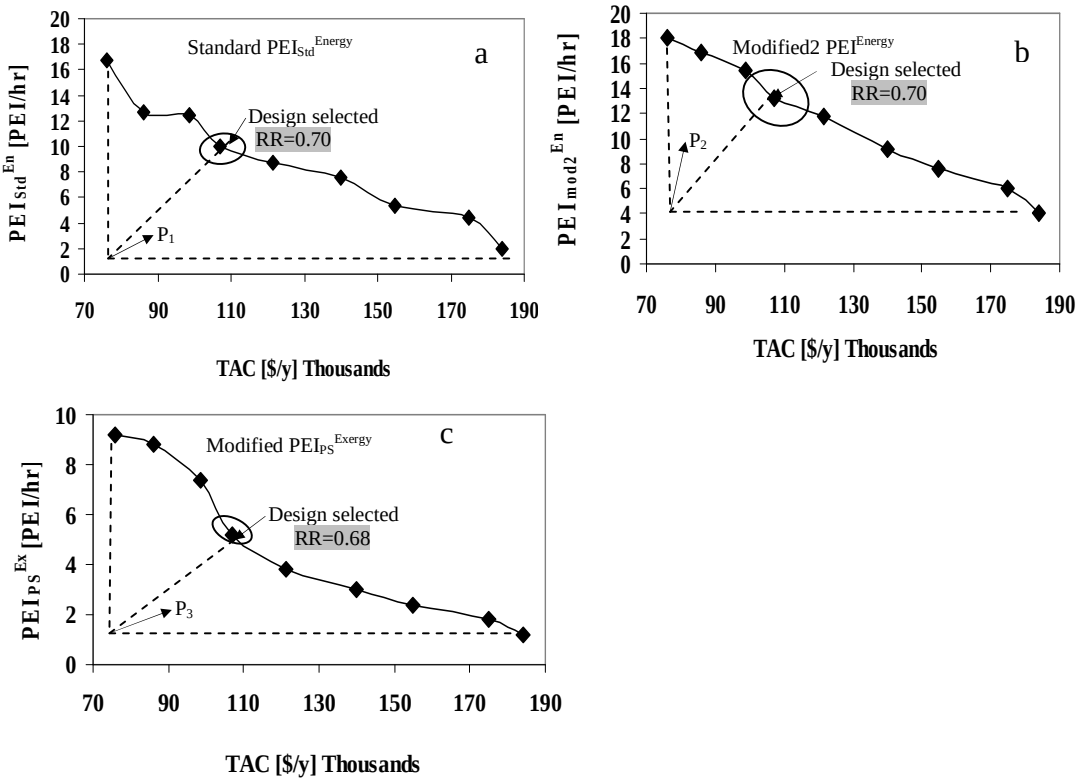

Figure 5.25.Pareto trade off surfaces for pump-around

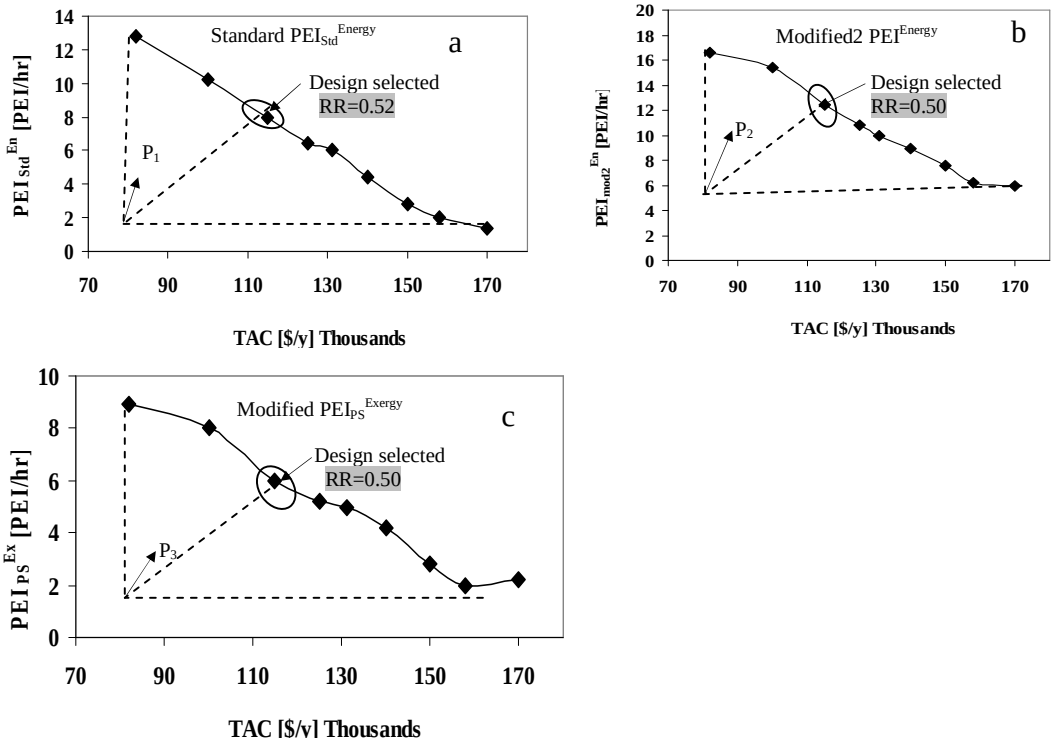

Figure 5.26. Pareto trade off surfaces for heat pump

5.2.5.4 Best alternative

In order to communicate the results to the decision maker, two-dimensional Pareto plot was obtained for all the alternatives (see figure 5.27).

In this analysis only three of the PEI models were considered (i.e. $\mathbf{PEI}_{std}^{En}$, $\mathbf{PEI}_{mod2}^{En}$ and $\mathbf{PEI}_{1}^{Ex}$).

Figure 5.27 shows that there are trade-offs in the evaluation of Potential environmental impacts and TAC of each design alternative. As the level of heat integration increases, the PEI of each alternative reduces. Any two solutions can be picked from the feasible objective space and Compared.

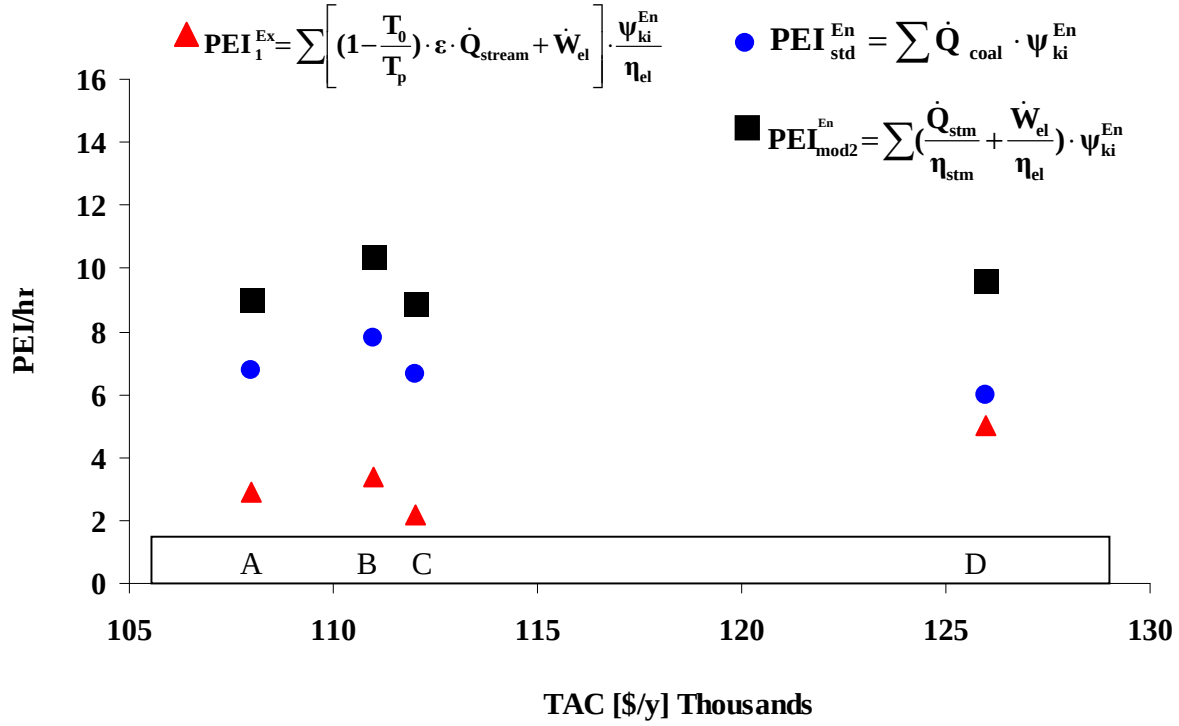

Figure 5.27. Nondominated set analysis of each alternative
(A) Extended feed preheat (B) Base case (C) pump around (D) heat pump

The PEI due to energy consumption in the case of modified2 was the highest for all the alternatives as show in figure 5.27, the reason is that, the equation corresponding to the modified2 PEI gives the actual quantity of coal that was used for steam and electrical energy production. The standard PEI is based on assumption that coal is the source of energy for steam

and/or electrical energy production that is why it has the lowest PEI for the alternatives. The preferred set of alternatives in figure 5.27 is known as the nondominated set. This set represents potential compromise solutions among the objectives. Consider the solutions B and C that corresponds to base case and pump around alternative in figure 5.27, solution C is better than solution B in the PEI-objective whiles solution C is inferior to solution B in TAC-objective. Based on this observation, it can be concluded that the base case and pumparound alternatives constitute a nondominated or pareto set which can be used for decision making. The same procedure is applied to remaining alternatives

5.2.5.5 Cost trade-offs for extended feed preheat

The investment in the heat exchanger of the extended feed preheat are plotted in figure 5.28.

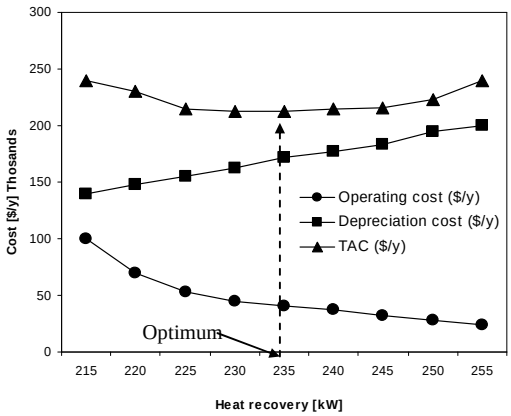

Figure 5.28. Recovery of heat from waste stream (bottom product)
involves trade-off between reduce operating cost and depreciation cost.

As the amount of heat recovery increases, the operating cost for the distillation process decreases. On the other hand the depreciation cost increases due to increase in heat exchanger size. The TAC shows a minimum of $ 212,000 at optimum heat recovery of 235kW.

5.2.5.6 Thermodynamic efficiency comparison of design alternatives

Figure 5.29 shows the thermodynamic efficiency associated with the hydrocarbon recovery design options considered in this study.

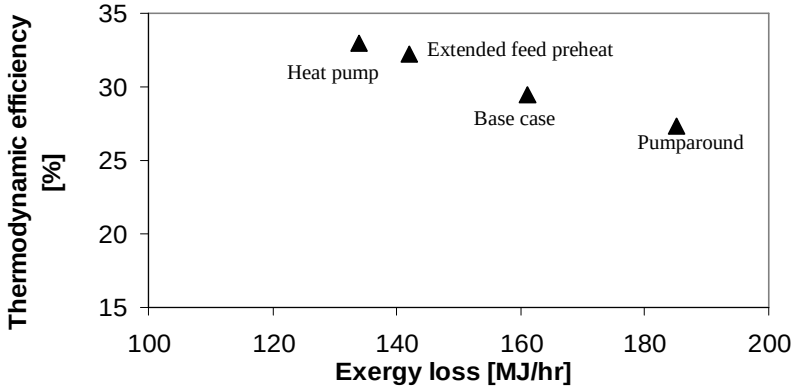

Figure 5.29 Thermodynamic efficiency associated with different design alternatives

It may be observed that increasing thermodynamic efficiency reduces exergy losses.

5.2.6 Conclusions

Exergy balance is powerful for energy optimization. In other words, exergy analysis can reveal whether or not and by how much it is possible to design more efficient energy systems by reducing inefficiencies in existing systems. In this work the concept of exergy loss Profiles was considered for improving thermodynamic efficiency of distillation column T1701. The 27.29 % thermodynamic efficiency of the base case distillation unit indicates that much exergy supplied by the steam is wasted or loss at stage 35 and the feed stage. It is obvious that a large amount of energy is lost at the steam inlet. The exergy loss profiles obtained by these balances were useful in identifying beneficial changes in the column layout from the point of view of exergy consumption.

Also in this study, a methodology for multiobjective optimization algorithm is performed interms of TAC and PEI through four examples of hydrocarbon recovery process. The multiobjective optimization gives a set of optimizaion results known as the Pareto optimal solutions. The rate of potential environmental impact output due to energy/exergy consumption for the separation task where evaluated using the WAR algorithm. The solution to the multi-objective optimization was

not a single solution, but rather is the nondominated set, this set represent potential compromise solutions among the alternatives. The optimization result show that the base case and heat pump alternatives constitute a nondominted or pareto set which can be used for decision making.

6 Combination of solar thermal power plant and distillation unit

6.1 Procedure

In this work, an integrated methodology that combines potential environmental impact and economic analysis as well as alternative generation capabilities of the greenius simulation tool is proposed. The methodology consists of the following steps as illustrated in figure 6.1:

I. Problem definition
II. Flow sheet diagram representing the base case
III. Base case simulation model using Aspen Plus™ process simulator
IV. Environmental impact calculation using WAR algorithm and process economic analysis using Aspen Plus™
V. Generation of proposed alternative (solar model)
VI. Comparison between the modified and the base case interims of Environmental impact and economics

As a first step in the design methodology, the design starts with framing of the problem. The primary attributes of the problem are identified and classified according to the following quantities: equipment design variables, operational variables, physical properties, process parameters and the lower and upper bounds of the parameters, as well as mass and energy balance information are gathered.

In the next step, the detailed process unit diagram for the base case design is presented. The distillation unit flow sheet diagram represents the flow of material to and from the unit as illustrated in figure 6.1.

In the third step, the steady state material and energy balances of the distillation unit are performed using Aspen Plus™ process simulator. Based on the simulation results, the process data from Aspen PlusTM are entered into the WAR GUI in order to compute the PEI due to energy/exergy consumption of the base case model.

The process data information includes the chemicals used, the flow rates of the streams entering and leaving the process, and the energy usage of the process.

Modification is made to the base case by generation of the proposed alternative (solar model).

The solar model is first developed by means of the Greenius Simulation tool. On the basis of the data extracted from the Greenius Simulation model, a representative simulation model is built in

Aspen Plus^{TM}. In the optimization step, a number of runs are carried out in order to optimize the various factors (i.e. process variables) affecting the performance of the unit. Finally the decision makers choose the best compromise alternative from a range of optimum solutions.

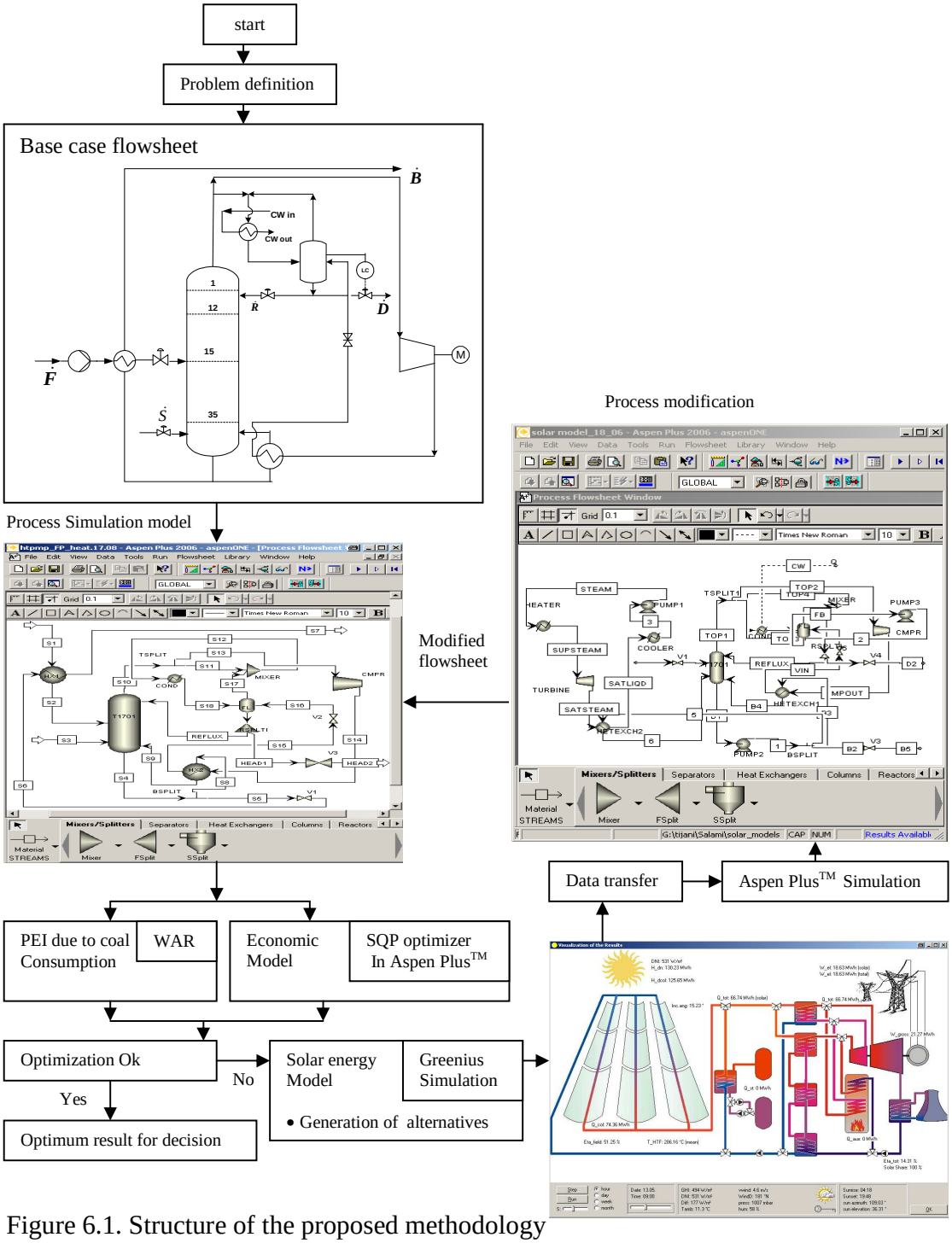

Figure 6.1. Structure of the proposed methodology

6.2 Solar thermal power plant

A simplified scheme of a typical solar thermal power plant using parabolic troughs integrated in a Rankine water/steam power cycle is shown in figure 6.2. It consists of an arrangement of parabolic trough collectors, high and low pressure steam turbines and recalculating pump. This solar thermal power plant is similar to that of conventional Rankine power plant, except for the heat source. The main technical parameters concerning flow rates, pressures and temperatures are given. The steam leaving the HP-turbine goes to the LP-turbine stage. After this stage the steam is condensed and the condensate is then pumped through the cycle again.

Integration of a solar steam generation system to a given industrial process involves a simple plant interface to feed steam directly into the existing process (distillation). Two design alternatives that consist of integration of solar thermal power plant with distillation unit will be discussed in the next section

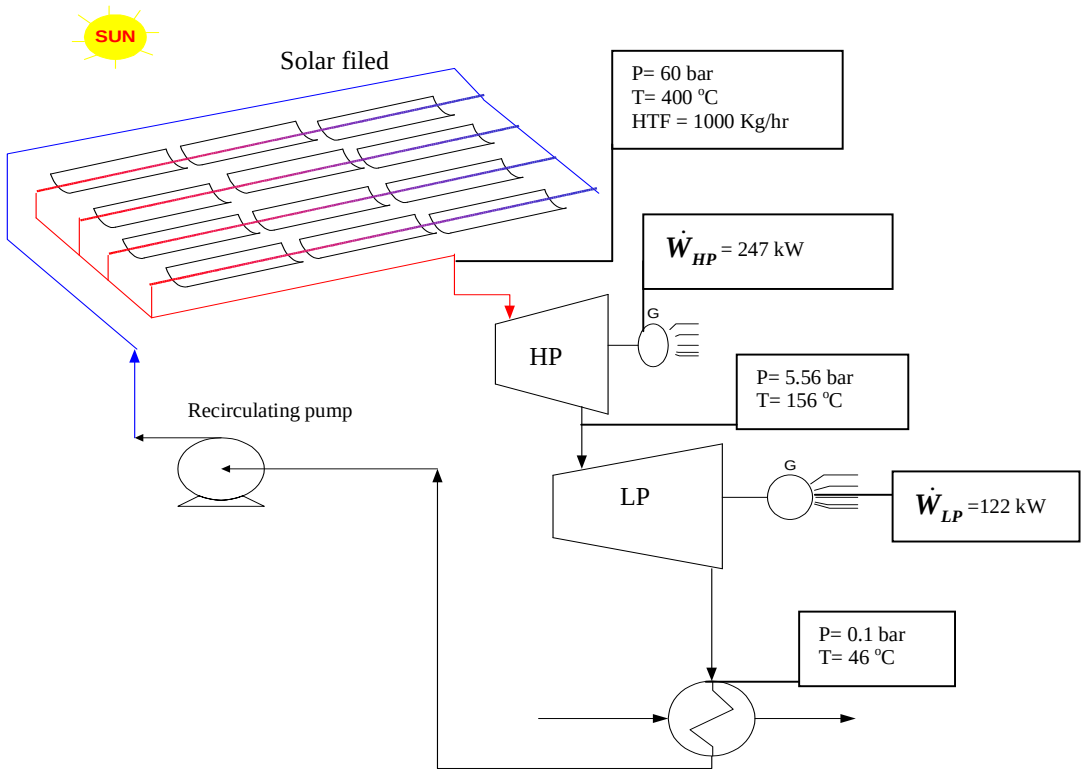

Figure 6.2. Flowsheet of standard solar thermal power block

6.2.1 Simulation model

As seen in the previous chapters, the following data are the main results from the simulation performed. Simulation in greenius[Free] software was performed according to real data and meteorological conditions in Almería, Spain. After performing the simulation, the following visualization results were obtained.

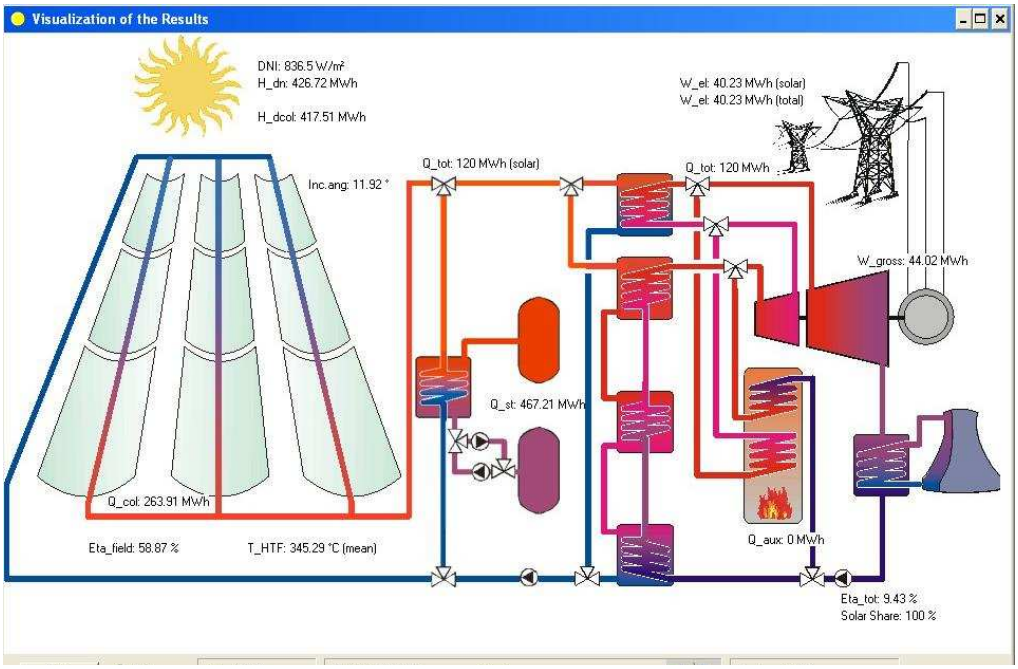

Figure 6.3. STPP visualization results (Source: greenius[Free] simulation).

The nominal electrical power output of the simulated STPP is 34.2 MW_{el}. The annual electrical production is of 110 GWh_{el}, while that of ANDASOL 1 is 179 GWh_{el}, according to the European Commission [107]. The STPP of ANDASOL 1 has an average efficiency between 10 and 15 %, while the simulated STPP has an average efficiency of 10.6 %, with peak efficiency of 12.78 % in the month of July, according to the simulation results.

6.3 Solar thermal power plant and distillation unit

6.3.1 Aspen simulation model

6.3.1.1 Case I: Solar and heat pump model (Operating process plant via electric power)

The concept of the solar thermal power plant is that, the solar field collects the solar energy available in the form of direct solar radiation and converts it into thermal energy (superheated steam). A heat transfer fluid (HTF- water) is circulated through the collector field for the generation of superheated steam (400^{o}C). The superheated steam is expanded in steam turbines (high and low pressure turbine) that drive electricity generator.

The solar thermal power plant is simulated with the greenius simulation tool. The results are then transferred to Aspen plus simulation tool. Due to the limitations of Aspen plus, the solar energy source is expressed via a heater model. The main parameters transferred into Aspen plus simulation are the operating pressure (65 bar) and temperature (408 ^{o}C). Figure 6.4 shows the modified solar thermal power plant combined with a heat pump distillation unit. In this alternative, the electrical power produced by the LP-turbine is used to operate the compressor of the heat pump (Case I).

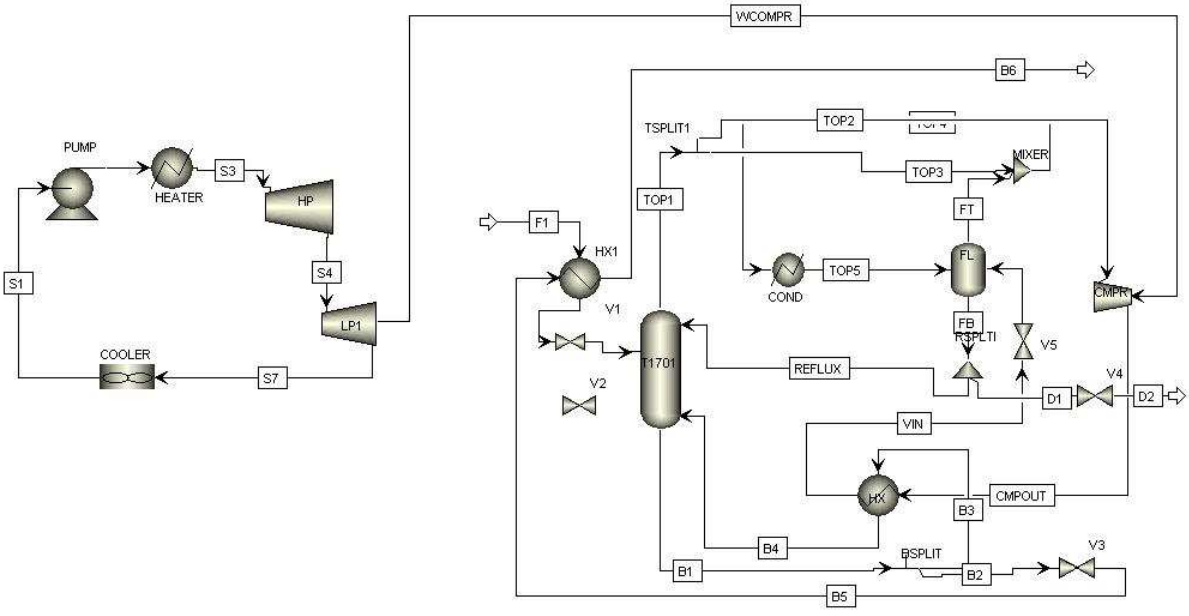

Figure 6.4. Case I: Heat pump model (Source: Aspen Plus simulation).

6.3.1.2 Case II: Solar and heat integration model (Operating process plant via steam)

In case II, a medium pressure steam turbine is integrated into the plant (see figure 6.5). Waste steam (118^{o}C, 1.7 bar) from the MP-turbine is passed through a heat exchanger to produce saturated steam (112^{o}C, 1.29bar) and then send into the distillation column for separation process. Practically, a side stream can be withdrawn from the LP-pressure turbine to operate the distillation column, in that case there is no need to install the MP-turbine.

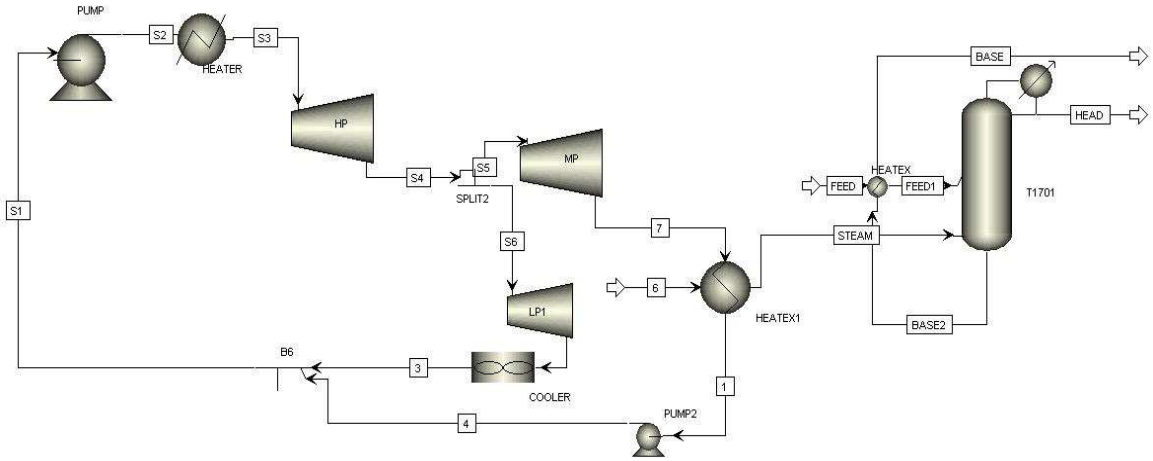

Figure 6.5. Case II: heat integration model (Source: Aspen Plus simulation).

6.3.1.3 Application

Figures 6.6. and 6.7. Shows simulation result for case I and II.

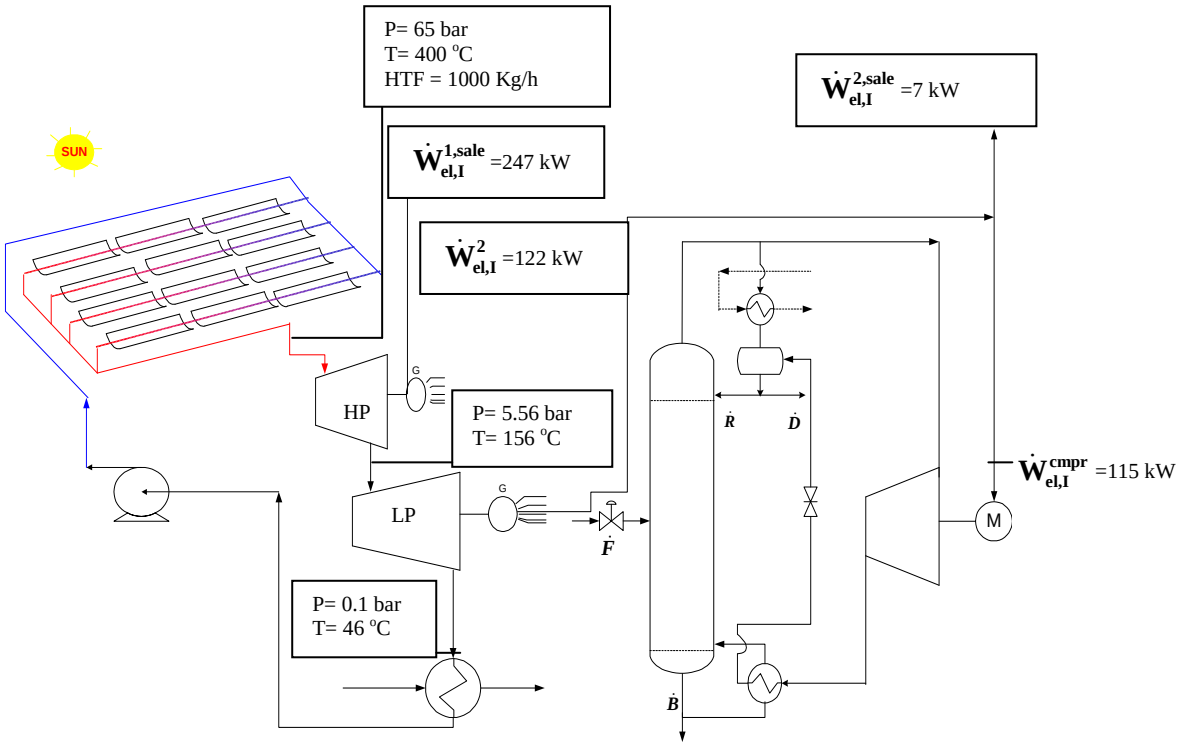

Figure 6.6. Case I: Solar-distillation system (operating process plant via electric power)

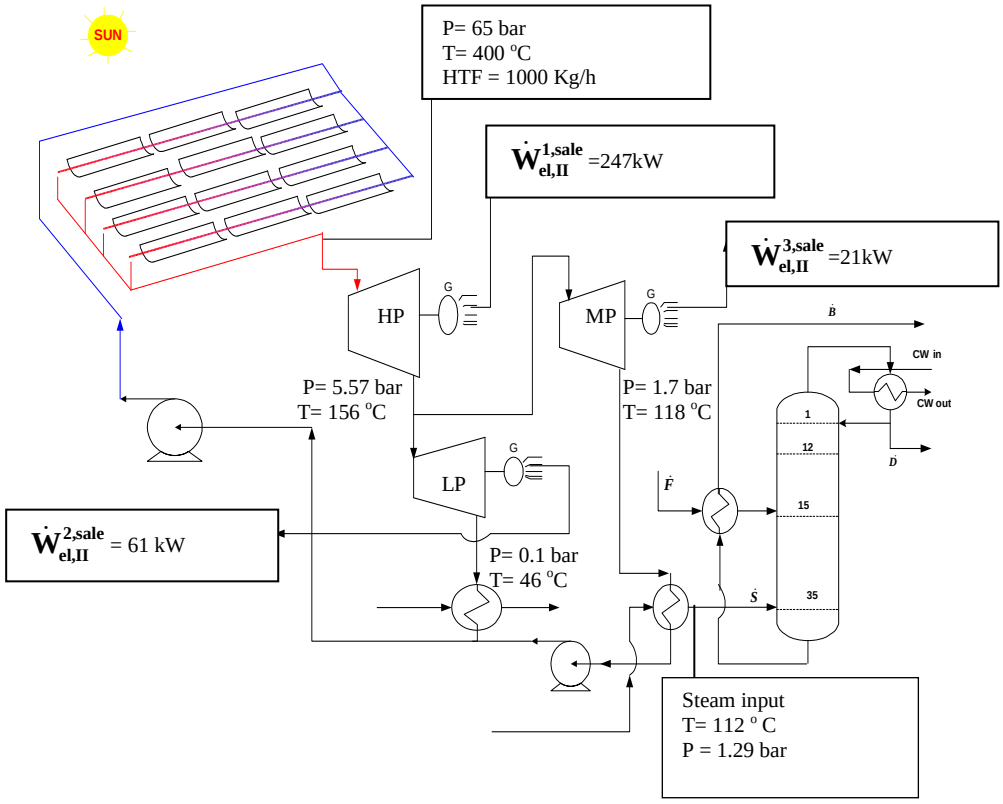

Figure 6.7. Case II: Solar-distillation system (operating process plant via steam)

6.3.1.3.1 Electrical power balance for cases I

After performing the Aspen Plus simulation, the electrical power delivered to the heat pump distillation unit can be seen in figure 6.6. As shown in figure 6.6, electrical power is used to operate the distillation. The total electrical power produced by the solar power plant can be calculated as:

$\dot{W}_{el,I,total}^{solar} = \dot{W}_{el,I}^{1,sale} + \dot{W}_{el,I}^{1,2} = 247\,kW + 122\,kW$ =369 kW

The total electrical power for sale can be calculated, knowing the compressor´s electrical power consumption: $\dot{W}_{el,I}^{cmpr}$ = 115 kW

$\dot{W}_{el,I}^{sale} = \dot{W}_{el,I,total}^{solar} - \dot{W}_{el,I}^{cmpr} = 369\,kW - 115\,kW = 254\,kW$

6.3.1.3.2 Electrical power balance for cases II

Considering case II, the total electrical power produced by the solar power plant can be stated as follows: $\dot{W}_{el,II,total}^{solar} = \dot{W}_{el,II}^{1,sale} + \dot{W}_{el,II}^{2,sale} + \dot{W}_{el,II}^{3,sale}$

$\dot{W}_{el,II,total}^{solar} = 247\,kW + 61\,kW + 21\,kW = 329\,kW$, The difference in electrical power produced of both cases (heat pump and heat integration distillation) can be stated as:

$\Delta\dot{W}_{el} = 369\,kW - 329\,kW = 40\,kW$

The difference in electrical power produced $\Delta\dot{W}_{el}$ is 40 kW, and this is equivalent to the amount of steam used to operate the distillation column of case II. This conclusion is made because both cases I and II have the same in output condition (i.e. P= 65 bar T= 400 ^{o}C, HTF = 1000 Kg/hr) from the solar thermal power plant.

6.3.2 Total Annualized Cost

i. Total installed cost comparison.

Table 6.1 shows the comparative values of the installed costs for the equipment used in both base case and alternative cases. Only the components relevant to the distillation unit are considered in the cost analysis.

As seen in Table 6.1, the Installed Cost of the different models varies according to the equipment used. The base case model uses less equipment than the other models, so the installed cost is less. For the heat pump model, the installed cost increases due to the use of the compressor. It can also be seen that the Steam distillation model has the higher cost due to the use of the pump to

recycling the water into the solar field. For the heat pump model, the installed cost increases due to the use of the compressor.

Table 6.1. Total installed cost comparison.

Energy source		Coal	Solar thermal power plant	
Alternatives		Base case	Case I: Heat pump	Case II: Steam distillation
Heat exchanger	[$]	10, 893	40, 436	55, 124
Column	[$]	262, 819	262, 819	262, 819
Column trays	[$]	17, 490	17, 490	17, 490
Condenser	[$]	35, 600	18, 300	35, 600
Reflux drum	[$]	12, 100	12, 100	12, 100
Compressor	[$]	-	56, 803	-
Pump	[$]	-	-	10, 000
Total Installed Cost	[$]	338, 902	407, 948	393, 209
Depreciation factor	[1/y]	0.2	0.2	0.2
Depreciation cost	[$/y]	67, 780	81, 589	78, 641

ii. Electricity cost data

The basis for calculating the utility cost of electrical energy of the plants is taken from the economic data of the simulated solar thermal power plant as shown in figure 6.8. The LEC is based on the annual GHI from the sun. Figure 6.8 shows that as the GHI increases the LEC reduces and it was found that the LEC of the Spain plant is 0.155 Euro/kWhr which corresponds to annual GHI of 1812 kWhr/(m^2 y). A range of values of LEC from 0.201 to 0.098 can be used for comparison of the different alternatives of the solar thermal power plant. But in the illustration calculations, only the LEC of Spain is considered.

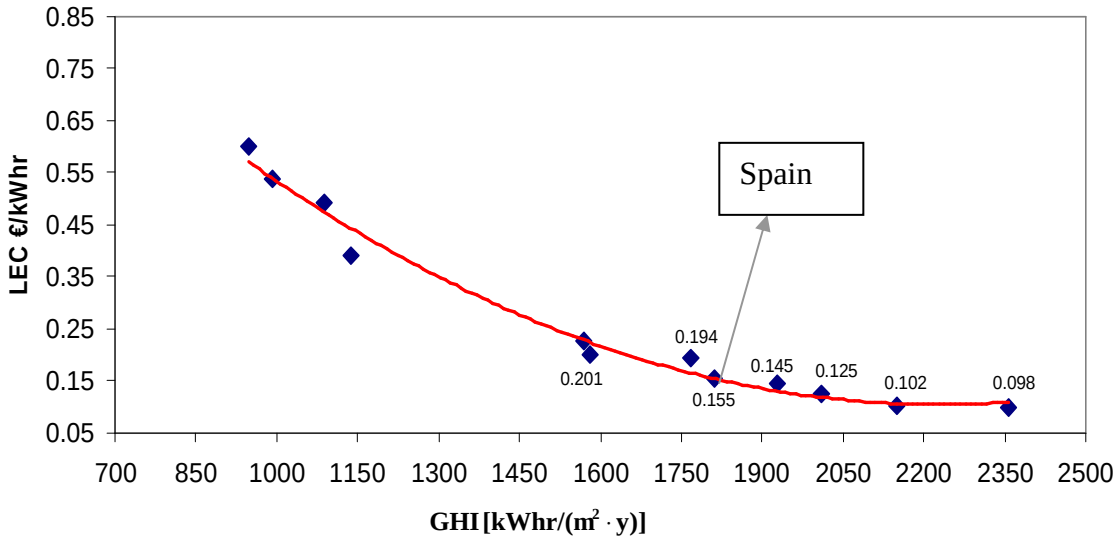

Figure 6.8. Annual global horizontal irradiation as a function of LEC

iii. Operating cost

This section outlines the typical operating costs of a conventional distillation unit (base case) operated via steam input and distillation unit (Case I and II) operated via solar thermal power plant. The economic analysis of all the alternatives follows a methodology similar to that proposed by Kolb [62] and World Bank [108]. The operating parameters are listed in table 6.3. With reference to the data given in table 6.3, the operating cost of each alternative is estimated in terms of utility cost of steam and electrical energy and using operating cost factor in figure 6.8 and table 6.3 as in Kolb [62]:

a. Operating cost for base case

This is calculated in terms of steam and cooling water flow rate and is given by:

$$\dot{\mathbf{C}}_{\mathbf{op,basecase}} = \mathbf{c_S} \cdot \dot{\mathbf{M}}_{\mathbf{S}} \cdot \mathbf{(8000\,hr/y)} + \mathbf{c}^{*}_{\mathbf{cw}} \cdot \dot{\mathbf{M}}_{\mathbf{cw}} \cdot \mathbf{(8000\,hr/y)} \quad (6.1)$$

$$\dot{\mathbf{C}}_{\mathbf{op,basecase}} = \mathbf{8.8 \cdot 10^{-3}\$/kg \cdot 555kg/hr \cdot (8000\,hr/y) + 0.7 \cdot 10^{-4}\$/kg \cdot 12400kg/hr \cdot (8000\,hr/y)}$$

$$\dot{\mathbf{C}}_{\mathbf{op,basecase}} = \mathbf{46,\,016\ \$/y}$$

b. Operating cost for Case I: Heat pump (LEC of Spain plant 0.155 $/kWhr)

This is calculated in terms of electrical energy consumption by the compressor and cooling water flow rate. Given that LEC of Spain is 0.155 $/kWhr (assuming that dollar rates are same)

$$\dot{\mathbf{C}}_{\mathbf{op,CaseI}} = \mathbf{c}^{*}_{\mathbf{cw}} \cdot \dot{\mathbf{M}}_{\mathbf{cw}} \cdot \mathbf{(8000hr/y)} + \mathbf{c_{el}} \cdot \dot{\mathbf{P}}_{\mathbf{el}} \cdot \mathbf{(8000\,hr/y)} \quad (6.2)$$

$$\dot{\mathbf{C}}_{\mathbf{op,CaseI}} = \mathbf{0.7 \cdot 10^{-4}\$/kg \cdot 4200\,kg/hr \cdot (8000hr/y) + 0.155\$/kWhr \cdot 115kW \cdot (8000\,hr/y)}$$

$$\dot{\mathbf{C}}_{\mathbf{op,CaseI}} = 144,\,953\ \$/y$$

c. Operating cost for Case II: Steam distillation (LEC of Spain plant 0.155 $/kWhr)

The difference in electrical power produced ($\Delta \dot{W}_{el}$ = 40kW), this is equivalent to the amount of steam used to operate the distillation column of case II. The operating cost is therefore calculated in terms of electrical power and cooling water flow rate and is given by:

$$\dot{\mathbf{C}}_{\mathbf{op,CaseII}} = \mathbf{c_{el}} \cdot \dot{\mathbf{P}}_{\mathbf{el}} \cdot \mathbf{(8000\,hr/y)} + \mathbf{c}^{*}_{\mathbf{cw}} \cdot \dot{\mathbf{M}}_{\mathbf{cw}} \cdot \mathbf{(8000\,hr/y)} \quad (6.3)$$

$$\dot{\mathbf{C}}_{\mathbf{op,CaseII}} = \mathbf{0.155\$/kWhr \cdot 40kW \cdot (8000\,hr/y) + 0.4 \cdot 10^{-4}\$/kg \cdot 12{,}323kg/hr \cdot (8000\,hr/y)}$$

$$\dot{\boldsymbol{C}}_{\boldsymbol{op,Case\,II}} = 56,\,500\ \mathbf{\$/y}$$

As seen from the above results, the operating cost for the base case is much lower than the other alternatives. Using the above operating cost, the TAC_{Spain} for Spain was calculated and the summary of the results is shown in table 6.2.

Table 6.2. Summary of TAC_{Spain} for Spain plant using LEC of 0.155 $/kWhr

Energy source	Coal	Solar thermal power plant	
Alternatives	Base case	Case I: Heat pump	Case II: Steam
Operating cost [$/y]	46, 016	144, 953	56, 500
Depreciation cost [$/y]	67, 780	81, 589	78, 641
$TAC_{Spain\ 1}$ [$/y]	**113, 796**	**226, 542**	**135, 141**

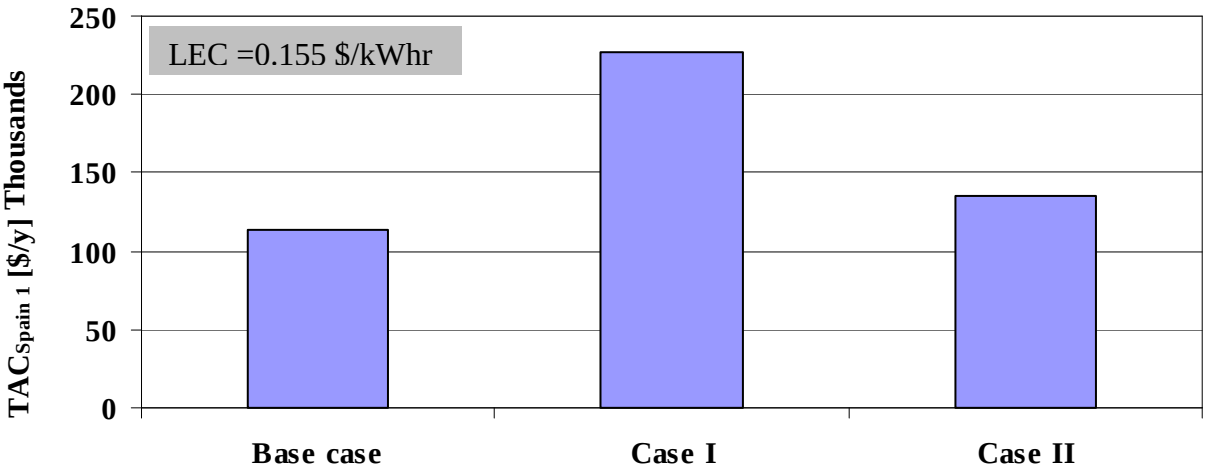

Figure 6.9. Comparison of TAC_{Spain} of alternatives

Figure 6.9 shows that it is cheaper to operate case II in Spain due to it´s lower TAC. Similar calculations were performed for LEC between 0.098 - 0.201 and the results are illustrated in table 6.3.

Table 6.3. Operating parameters and results

Alternatives	Base case	Case I: Heat pump	Case II: Steam
System design			
Actual electrical output [kW_{el}]	-	369	329
Depreciation factor [1/y]	0.2	0.2	0.2
Operating hours [hr/y]	8000	8000	8000
Steam cost [$/ton]	8.8		
Cooling water cost [$/ton]	0.07	0.07	0.07
Fuel			
Fuel source	Coal	solar	solar
Steam input [kg/hr]	555	-	555
Cooling water flowrate kg/hr	12, 400	4,200	12, 323
Compressor work [kW]		115	
Electricity cost (LEC) [$/kWhr]	-	0.098 - 0.201	0.098 - 0.201
Operating cost [$/y]	46, 016	**92, 512 -187, 272**	**38, 260 - 71, 220**
$TAC_{Spain\ 2}$ [$/y]	**113, 796**	**174, 101 - 268, 861**	**116, 901 - 149, 861**

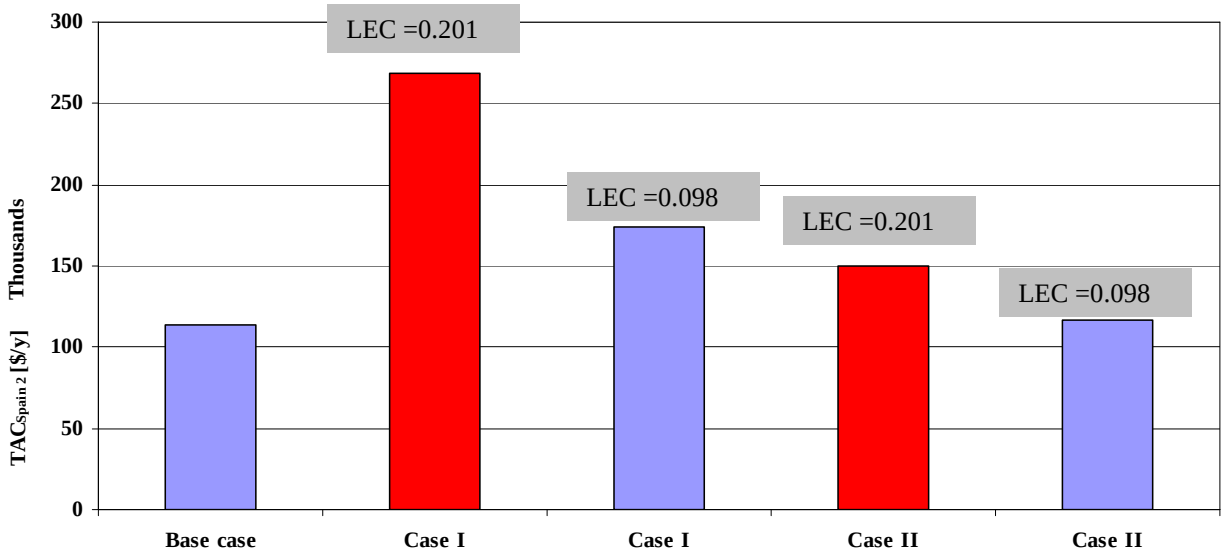

Figure 6.10. Comparison of $TAC_{Spain\ 2}$ of alternatives

Figure 6.10 shows that if the future LEC is reduced to 0.098 $/kWhr, this can reduce the TAC of both case I and Case II, for example With LEC decreasing from 0.201 to 0.098, the $TAC_{Spain\ 2}$ of case I (heat pump) is reduced by about 42 % i.e. from 268, 861 $/y to 174, 101 $/y. Similar situation did occur for case II (steam distillation). In general, if the LEC is reduced, the TAC also decreases. In the next section the environmental effect of the solar thermal power plant as well as the base case will be discussed.

6.3.2.1 Discussion of cost and environmental aspect

In this section two basic methods were used in the calculation of environmental effect of Co_2, method 1 considers the Co_2 emission cost whilst method 2 considers the Co_2 avoidance cost. Since the base case is operated by means of steam, the cost of Co_2 emitted to the environment due to heat produced to operate the base case is considered using method 1.

a. Method 1: Cosideration of emission cost

$$\mathbf{TAC} = \dot{\mathbf{C}}_{\mathbf{TDC}} + \dot{\mathbf{C}}_{\mathbf{OC}} + \mathbf{CO}_2\,\mathbf{emission\ cost} \qquad (6.4)$$

Equation 6.4 therefore shows the TAC for the base case. The Co_2 emission cost for the base case is illustrated below

i. Carbon dioxide emission cost calculation for bas case

Steam flow rate for base case= 555 kg/hr, Co_2 emission from steam= 0.345 $kgCo_2$/kWhr [109]

Δh^{GL} =2200 kJ/kg, $\dot{Q}_{steam} = 2200\,kJ/kg \cdot 555\,kg/hr = 1221\,MJ/hr$

The rate of Co_2 emission is given by

$\dot{M}_{Co_2,hr} = 1221\,MJ/hr \cdot 0.345\,kg/3.6\,MJ = 117\,kgCo_2/hr$

The annual Co_2 emission is

$\dot{M}_{CO_2,y} = 117\,kgCo_2/hr \cdot 8000\,hr/y = 936\,tonCo_2/y$

$\textbf{Annual Co}_2\textbf{ emission cost} = 936\ tonCo_2/y \cdot 7\ \$/tonCo_2 = 6{,}552\ \$/y$

Annual Co_2 emission cost due to steam production is 6,552 $/y. This results is a negative effect because 6,552 $/y needs to be paid annually for causing emission to the environment

b. Method 2: Cosideration of avoidance cost

Also since there is Co_2 reduction from the operation of the solar thermal power plant, method 2 was used in the calculation of Co_2 avoidance cost. Equation 6.5 therefore shows the TAC for the alternative case.

$$\textbf{TAC} = \dot{C}_{TDC} + \dot{C}_{OC} - \textbf{Co}_2\textbf{ avoidance cost} \qquad (6.5)$$

The Co_2 avoidance cost for both case I and case II using method 2 is illustrated below:

ii. Carbon dioxide avoidance calculation for case I

$\textbf{Annual avoided co}_2\textbf{ emission} = \dot{W}^{solar}_{el,I,total} \cdot \textbf{specific emission factor (Em}_{fact}\textbf{)}$

$\textbf{Annual avoided Co}_2\textbf{ emission} = 0.115\ MW \cdot 0.827\ ton\,Co_2/MWhr \cdot 8000\ hr/y$

$\textbf{Annual avoided Co}_2\textbf{ emission} = 760\ ton\,Co_2/y$

$\textbf{Annual Co}_2\textbf{ credit} = \textbf{Annual avoided emission} \cdot \textbf{Co}_2\textbf{ emission credit}$

$\textbf{Annual Co}_2\textbf{ credit} = 760\,ton\,Co_2/y \cdot 7\ \$/tonCo_2$

$\textbf{Annual Co}_2\textbf{ credit} = 5{,}325\ \$/y$

iii. Carbon dioxide credit calculation for case II

$\textbf{Annual avoided Co}_2\textbf{ emission} = \dot{W}^{solar}_{el,II,total} \cdot \textbf{specific emission factor (Em}_{fact}\textbf{)}$

$\textbf{Annual avoided Co}_2\textbf{ emission} = 0.040\ MW \cdot 0.827\ ton\,Co_2/MWhr \cdot 8000\ hr/y$

$\textbf{Annual avoided Co}_2\textbf{ emission} = 265\ ton\,Co_2/y$

$\textbf{Annual Co}_2\textbf{ credit} = \textbf{Annual avoided emission} \cdot \textbf{co}_2\textbf{ emission credit}$

$\textbf{Annual Co}_2\textbf{ credit} = 265\ tonCo_2/y \cdot 7\ \$/ton\ Co_2$

$\textbf{Annual Co}_2\textbf{ credit} = 1{,}852\ \$/y$

The results of both case I and II indicates that both cases have positive effect interms of environmental impact because their operation gives annual Co_2 creadit which can lead to a reduction in TAC. Eventhough both methods 1 and 2 can be used for further environmental analysis of all the alternatives, only method 2 is considered futher because of its positive effect on the environment.

Table 6.4. Effect of Co_2 credit and LEC

Energy source		Coal	Solar thermal power plant			
Alternatives		Base case	Case I: Heat pump		Case II: Steam	
LEC $/kWhr		-	0.155			
Steam cost	[$/ton]	8.8	-		-	
Operating cost	[$/y]	46, 016	144, 953		56, 500	
Depreciation cost	[$/y]	67, 780	81, 589		78, 641	
TAC_{Spain}	**[$/y]**	**113, 796**	**226, 542**		**135, 141**	
Co_2 credits	[$/ ton$Co_2$]	-	7	40	7	40
Co2 reduction credit	[$/y]	-	5, 325	30, 400	1, 852	10, 600
$TAC_{Spain, Env1}$	**[$/y]**	**113, 796**	**221, 217**	**196, 142**	**133, 289**	**124, 541**
LEC $/kWhr		-	0.098			
Operating cost	[$/y]	-	92, 512		38, 260	
$TAC_{Spain, Env2}$			**168, 776**	**143, 701**	**115, 049**	**106, 501**
LEC $/kWhr			0.201			
Operating cost	[$/y]		**187, 272**		**71, 220**	
$TAC_{Spain, Env3}$			**263, 536**	**238, 461**	**148, 009**	**139, 261**

Table 6.4 shows the calculations of the effect of Co_2 credit and LEC on TAC, calculations were performed for LEC of 0.155 $/kWhr for Spain plant and also different values of 0.098 $/kWhr and 0.201$/kWhr were also used for the calculation and the results are illustrated in table 6.4.

A study was conducted for the spain plant with steam cost increasing from 8.8 $/ton to 20 $/ton, the results are shown in table 6.5.

Table 6.5. Effect of steam cost on Spain plant

Energy source		Coal	Solar thermal power plant	
Alternatives		Base case	Case I: Heat pump	Case II: Steam
LEC $/kWhr		-	0.155	
Steam cost	[$/ton]	8.8	-	-
Operating cost	[$/y]	46, 016	144, 953	56, 500
Depreciation cost	[$/y]	67, 780	81, 589	78, 641
TAC_{Spain}	**[$/y]**	**113, 796**	**226, 542**	**135, 141**
Co_2 credits	[$/ ton$Co_2$]		7	
$TAC_{Spain, steam,1}$		**113, 796**	**221, 217**	**133, 289**
Steam cost	[$/ton]	20		
Operating cost	[$/y]	**95, 744**	-	-
Co_2 credits	[$/ ton$Co_2$]	-	40	
$TAC_{Spain, steam,2}$		**163, 524**	**196, 142**	**124, 541**

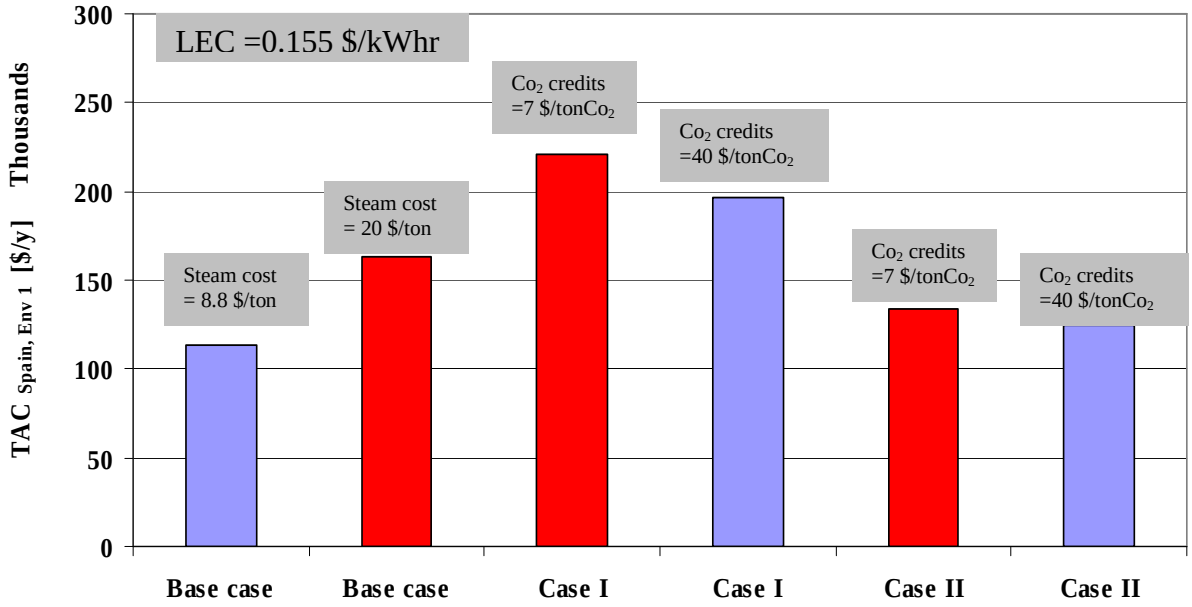

Figure 6.11. Comparison of $TAC_{Spain,\ Env\ 1}$ of alternatives

Figure 6.11 shows an increase in TAC_{Spain} of the base case by about 30 % , this increase is because of the increase in future price of steam from 8.8 $/ton to 20 $/ton. Figure 6.14 also shows that Case II is the best of all the alternatives because it has the lowest TAC. Figure 6.11 also shows that if the future cost of Co_2 credit is increase to 40 $/ton$Co_2$ this can give a significant reduction in $TAC_{Spain,\ Env\ 1}$, for example the $TAC_{Spain,\ Env\ 1}$ of Case I is reduced by about 11.4 % .

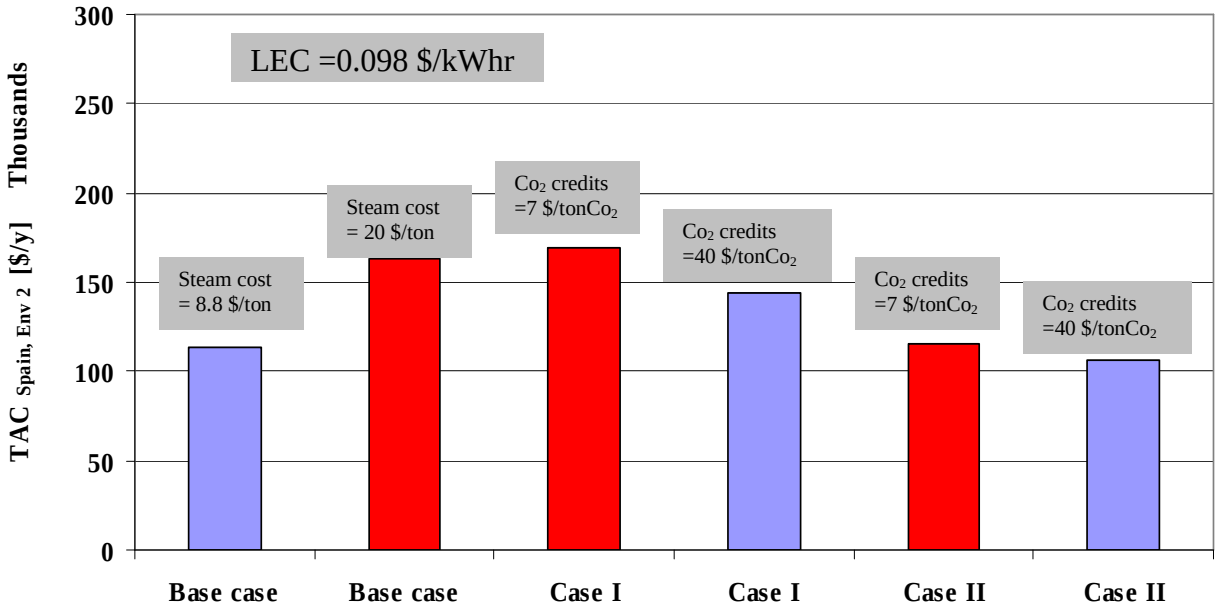

Figure 6.12. Comparison of $TAC_{Spain,Env\ 2}$ of alternatives

Figure 6.12 shows that further reduction in $TAC_{Spain,Env\ 2}$ can be achieved if the future LEC is equal to 0.098 $/kWhr.

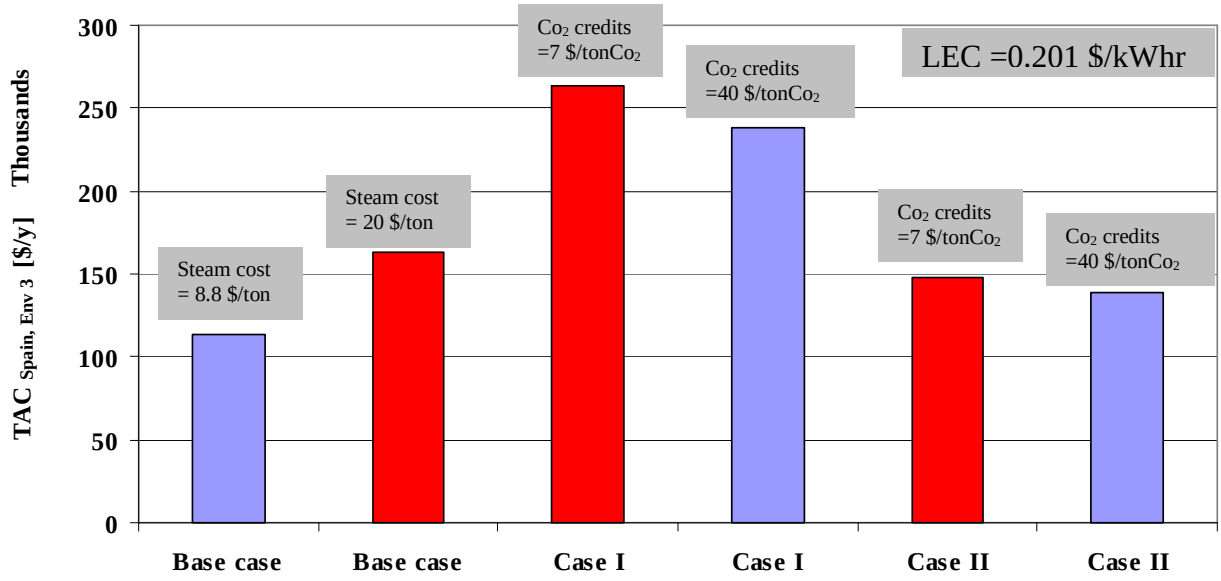

Figure 6.13. Comparison of $TAC_{Spain,Env\ 3}$ of alternatives

On the other hand figure 6.13 shows a higher increase in TAC for all the alternatives, the only factor reduce the TAC is the Co2 credits.

6.3.2.2 Conclusions

It can be concluded that the steam alternative is more environmentally friendly because it operates via only steam. That is the STPP produces 329 kW of electricity and 40 kW of steam is used to operate the distillation in Spain. On the other hand the STPP of the heat pump produces 369 kW of electricity and 115kW is used to operate the heat pump. Also when the futre TAC of case II: steam distillation (124, 541 $/y) is considered, it can be found that it is closed to that of the base case which is 113, 796 $/y, this show that solar thermal power plant can replace coal power in future.

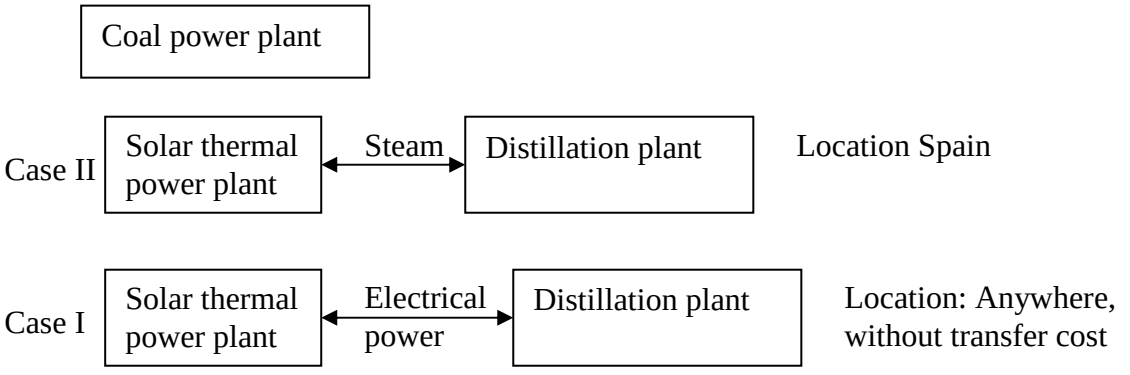

7 Conclusion and recommendations

The chemical industry has undergone significant changes due to the increased cost of energy, increasingly stringent environmental regulations. One of the most important engineering tools for addressing these issues is optimization. Modifications in plant design and operating procedures have been implemented to reduce costs and meet constraints, with an emphasis on improving efficiency. Process simulation is used to predict the behaviour of a process by using basic engineering relationships, such as mass and energy balances, and phase and chemical equilibrium. Given reliable thermodynamic data, realistic operating conditions, and rigorous equipment models, it is possible to simulate actual plant behaviour. Today major chemical plants are built by first simulating the process on a computer. In this thesis work is a model base optimization framework has been used for the efficient solution of large scale optimization problems in the field of energy/exergy, environmental and economic objectives.
In the optimization step, a number of runs are carried out in order to optimize the various factors (i.e. process variables e.g. reflux ratio, steam flow rate) affecting the performance of the unit. Finally the best compromised alternative from a range of optimum solutions are evaluated.

7.1 Environmental model

This thesis introduces a new framework for the conceptual design and environmental screening of separation processes. It is based on the targeting of key environmental performance objective for each unit contain within the flowsheet of the process alternative. The important areas of consideration in the environmental models are the theory and concept of the WAR algorithm. The WAR algorithm was used to compute standard potential environmental impact. In this thesis work, the impact due to the effluent stream of the distillation unit has not been considered, only the impact due to energy and exergy consumption was relevant. The standard potential environmental impact was extended to include the PEI of the energy and exergy consumed by the energy generation (power plant) and chemical processes (distillation unit). The major emissions from the combustion of fuel are Co_2, the products of combustion are best minimized by making the process efficient in it´s use of energy through efficient heat recovery.

7.2 Energy/exergy model

A variety of different alternatives and approaches have been proposed to modify the structure or change the operating parameters of distillation column in other to reduce losses and increase column efficiency. In this thesis, energy and exergy analyses of distillation units have been conducted to study thermodynamic efficiency of the units. A systematic procedure for exergy analysis as well as thermodynamic efficiency have been proposed and demonstrated by four case studies. It is found that the column configuration with least exergy losses have the highest thermodynamic efficiency of 33 % (Heat pump alternative), this is an improvement over the base case with efficiency of 29.29 %.

7.3 Multiobjective optimization

The methodology for multiobjective optimization algorithm has been demonstrated in terms of TAC and PEI with four examples of hydrocarbon recovery process. Multiobjective optimization gives a set of optimization results known as the Pareto optimal solutions. The rate of potential environmental impact output due to energy/exergy consumption for the separation task were evaluated using the WAR algorithm. The optimum solution may change due to variation of energy costs and/ or depreciation factors.

Multiple Attribute Decision Making technique like AHP is applied in this thesis for ranking of alternatives. The AHP method was applied to real industrial problems. Optimization was performed to evaluate process improvement of a base case and heat pump distillation unit.

7.4 Solar and distillation

The utilization of waste energy is of primary important in process plants because it leads to economical savings and energy process recovery. An example of recovery waste energy is the use of turbine´s output steam for industrial purposes. As seen in the chapter 6, STPP is a renewable energy source that is contemporarily being implemented in many Mediterranean countries where solar radiation reaches more than 1000 W/m^2. Heat recovery from STPP can be used for many industrial processes in the food, washing and other processes where temperatures between 200-400°C are being used. As seen in the past pages, waste energy is possible to be used in industrial processes, specifically in the distillation process, with the help of heat exchange.

Today's technologies of solar thermal power plants are operated in the cost range of 15 -20 $/kWhr [108]. The LEC results achieved for this study is 0.155 $/kWhr which falls within the expected operating range. The Co_2 avoidance cost was calculated for all the solar thermal

power plant alternatives, the Co_2 reduction credit factor of 7 \$/ tonCo_2 did not have much effect on the TAC, however when a future credit factor of 40 \$/ tonCo_2 was used, there were a considerable reduction in TAC, for example a reduction of about 14 % (i.e from 226, 542 \$/y 196, 142 \$/y) was obsereved in Case I: Heat pump. Aslo there were a significant reduction of TAC for case II: steam distillation (i.e from 135, 141 \$/y to 124, 541 \$/y), this is about 8 % reduction in TAC.

7.5 Topics for further research work and recommendations

This section gives an out look of future research by improving the support of process system modeling. A large variety of extensions and further steps are possible. In this steady chemical process modeling was only applied to steady state optimization problems. However the extension of dynamic simulation models is an interesting open issue, as it would allow providing models for further important application areas such as process control or disturbance rejection capabilities of different design alternatives.

For optimization, the estimation of investment and operational cost is necessary. In this work TAC is used as an economic objective function, an integrated model for extended environmental related cost can be included. Ranking of energy / exergy optimization alternatives of distillation unit considering life cycle aspects like operability and safety risk in addition is also another area of process optimization that needs serious attention.

In the environmental model, the other impact categories such as noise pollution, effluent streams of chemical plants can be integrated in the optimization by means of an integrated simulation tool.

Integration of solar heat into industrial production process is a challenge to both the process engineer and the solar expert [solar heat for industrial processes]. A simulation tool can be used to develop a solar collector that convert solar irradiation into thermal heat and a power conversion system that convert the heat to electricity.

The impact on TAC of a credit for reduced emissions is studied in this thesis using a price of CO_2 credits of 7 \$/tCo_2. This price did have only a small effect on TAC. However improvement in TAC was achieved by considering the future price of Co_2 which was predicted by the World Bank [108] to be 10 to 40 \$/tCo_2. In this study even though the future price of 40 \$/tCo_2 was used to predict the future TAC, other factors such as better integration with the power plant and higher collector operating temperatures can reduce LEC which will also reduce TAC.

Appendix A

A.1 Simulation results of activity coefficients of components

Feed						
.	LIQUID GAMMA METHANOL	LIQUID GAMMA ACETALDE	LIQUID GAMMA ME-FORM	LIQUID GAMMA ETHANOL	LIQUID GAMMA ACETONE	LIQUID GAMMA ME-ACET
Temp 68°C						
Gamma γ_{jF}	1,750178	4,061799	2,597631	3,379736	5,116403	10,34922
	LIQUID MOLEFRAC METHANOL	LIQUID MOLEFRAC ACETALDE	LIQUID MOLEFRAC ME-FORM	LIQUID MOLEFRAC ETHANOL	LIQUID MOLEFRAC ACETONE	LIQUID MOLEFRAC ME-ACET
$\tilde{x}_{jF}$	0,0113826	0,0110858	0,0138581	0,00507689	0,0498314	0,00698564
$\sum_j \tilde{x}_{jF} \cdot \ln(\gamma_{jF} \cdot \tilde{x}_{jF})$	-0,04457371	-0,03437113	-0,04606828	-0,02063887	-0,0681025	-0,01835119

Feed							
LIQUID GAMMA MEK	LIQUID GAMMA ETH-ACET	LIQUID GAMMA DEK	LIQUID GAMMA WATER	LIQUID GAMMA ACETIC	LIQUID GAMMA FORMIC	LIQUID GAMMA PROPAC	
15,33713	15,79977	25,52214	1,029954	1,647423	0,5391458	4,489763	
LIQUID MOLEFRAC MEK	LIQUID MOLEFRAC ETH-ACET	LIQUID MOLEFRAC DEK	LIQUID MOLEFRAC WATER	LIQUID MOLEFRAC ACETIC	LIQUID MOLEFRAC FORMIC	LIQUID MOLEFRAC PROPAC	
0,00173083	0,00061588	0,00025199	0,8905586	0,00644157	0,00177433	0,00040614	
-0,00628097	-0,00285304	-0,00127169	-0,07693734	-0,0292819	-0,01233532	-0,00256153	**-0,36362748**

Head						
	LIQUID GAMMA METHANOL	LIQUID GAMMA ACETALDE	LIQUID GAMMA ME-FORM	LIQUID GAMMA ETHANOL	LIQUID GAMMA ACETONE	LIQUID GAMMA ME-ACET
Temp. 46.81°C						
Gamma γ_{jD}	1,381174	0,9729276	0,9845607	1,552184	1,016438	1,151657
	LIQUID MOLEFRAC METHANOL	LIQUID MOLEFRAC ACETALDE	LIQUID MOLEFRAC ME-FORM	LIQUID MOLEFRAC ETHANOL	LIQUID MOLEFRAC ACETONE	LIQUID MOLEFRAC ME-ACET
$\tilde{x}_{jD}$	0,0280465	0,1168256	0,1460408	0,0199721	0,5251364	0,0736165
$\sum_j \tilde{x}_{jD} \cdot \ln(\gamma_{jD} \cdot \tilde{x}_{jD})$	-0,09117798	-0,25403945	-0,28323576	-0,0693782	-0,32967689	-0,18166228

Head							
LIQUID GAMMA MEK	LIQUID GAMMA ETH-ACET	LIQUID GAMMA DEK	LIQUID GAMMA WATER	LIQUID GAMMA ACETIC	LIQUID GAMMA FORMIC	LIQUID GAMMA PROPAC	
0,985073	0,9438754	1,146263	4,0853	0,8212856	1,463371	0,7574876	
LIQUID MOLEFRAC MEK	LIQUID MOLEFRAC ETH-ACET	LIQUID MOLEFRAC DEK	LIQUID MOLEFRAC WATER	LIQUID MOLEFRAC ACETIC	LIQUID MOLEFRAC FORMIC	LIQUID MOLEFRAC PROPAC	
0,0182399	0,0064903	0,00265557	0,0629762	5,84E-13	2,58E-11	1,30E-14	
-0,0733095	-0,03306943	-0,01538794	-0,08549669	-1,6565E-11	-6,1975E-10	-4,1908E-13	-1,41643412

Base						
	LIQUID GAMMA METHANOL	LIQUID GAMMA ACETALDE	LIQUID GAMMA ME-FORM	LIQUID GAMMA ETHANOL	LIQUID GAMMA ACETONE	LIQUID GAMMA ME-ACET
Temp. 101.34°C						
Gamma γ_{jB}	2,057379	4,548151	3,43708	5,313202	11,11657	
	LIQUID MOLEFRAC METHANOL	LIQUID MOLEFRAC ACETALDE	LIQUID MOLEFRAC ME-FORM	LIQUID MOLEFRAC ETHANOL	LIQUID MOLEFRAC ACETONE	LIQUID MOLEFRAC ME-ACET
$\tilde{x}_{jB}$	0,00800922	1,46E-13	1,27E-10	0,00292192	1,18E-11	0
$\sum_j \tilde{x}_{jB} \cdot \ln(\gamma_{jB} \cdot \tilde{x}_{jB})$	-0,03288369	-4,0917E-12	-2,7336E-09	-0,01217073	-2,6802E-10	

Base							
LIQUID GAMMA MEK	LIQUID GAMMA ETH-ACET	LIQUID GAMMA DEK	LIQUID GAMMA WATER	LIQUID GAMMA ACETIC	LIQUID GAMMA FORMIC	LIQUID GAMMA PROPAC	
24,82228		52,78272	1,000677	2,520308	0,6993992	7,234673	
LIQUID MOLEFRAC MEK	LIQUID MOLEFRAC ETH-ACET	LIQUID MOLEFRAC DEK	LIQUID MOLEFRAC WATER	LIQUID MOLEFRAC ACETIC	LIQUID MOLEFRAC FORMIC	LIQUID MOLEFRAC PROPAC	
1,27E-14	0	2,18E-14	0,9811508	0,00591566	0,00162946	0,00037298	
-3,6571E-13		-6,002E-13	-0,01800641	-0,02487991	-0,01104292	-0,00220621	-0,10118988

Appendix B

B.1 Input data for Parabolic trough assembly

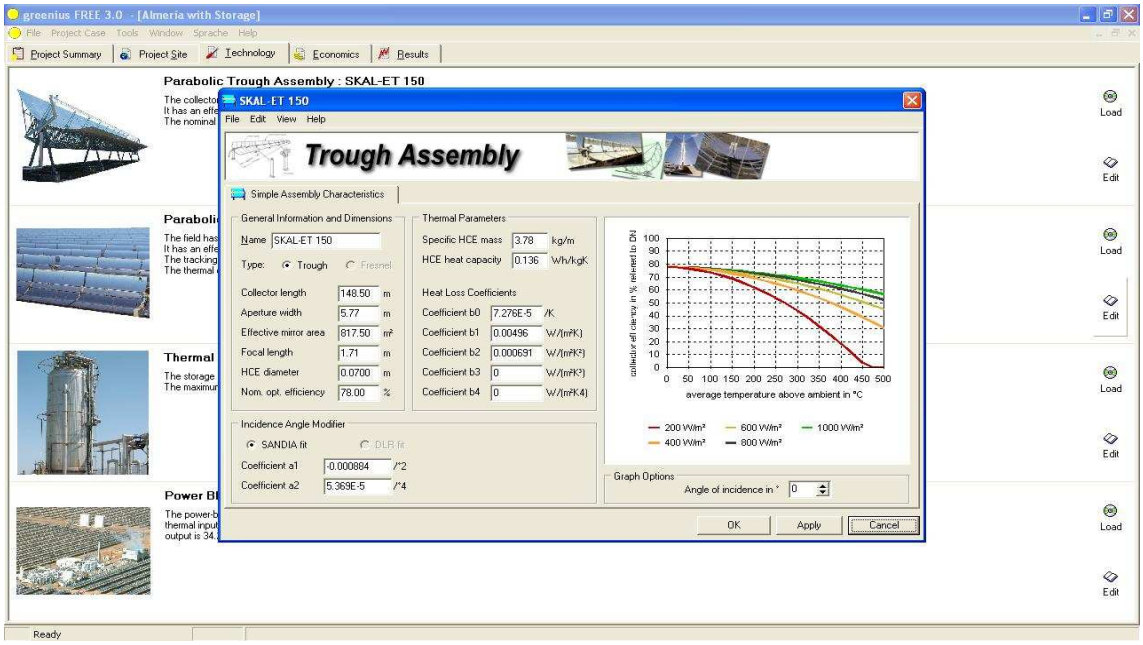

Figure B.1. Parabolic Trough Assembly Input data

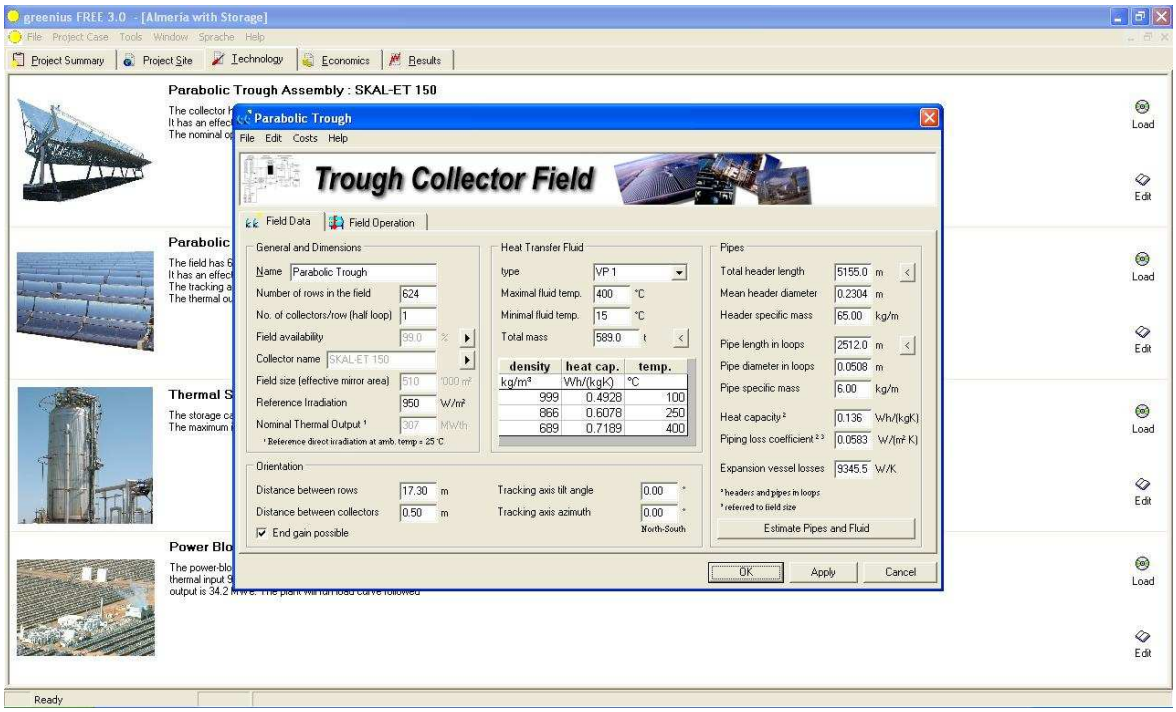

Figure B.2. Parabolic Trough Field Input data

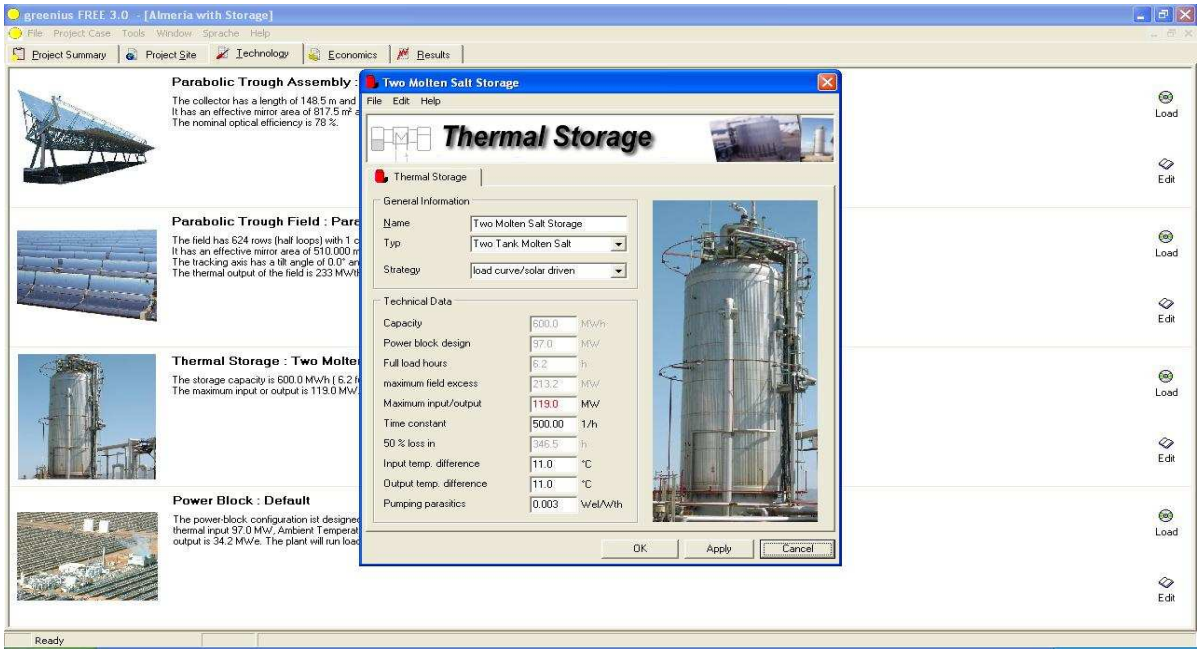

Figure B.3. Thermal Storage Input data

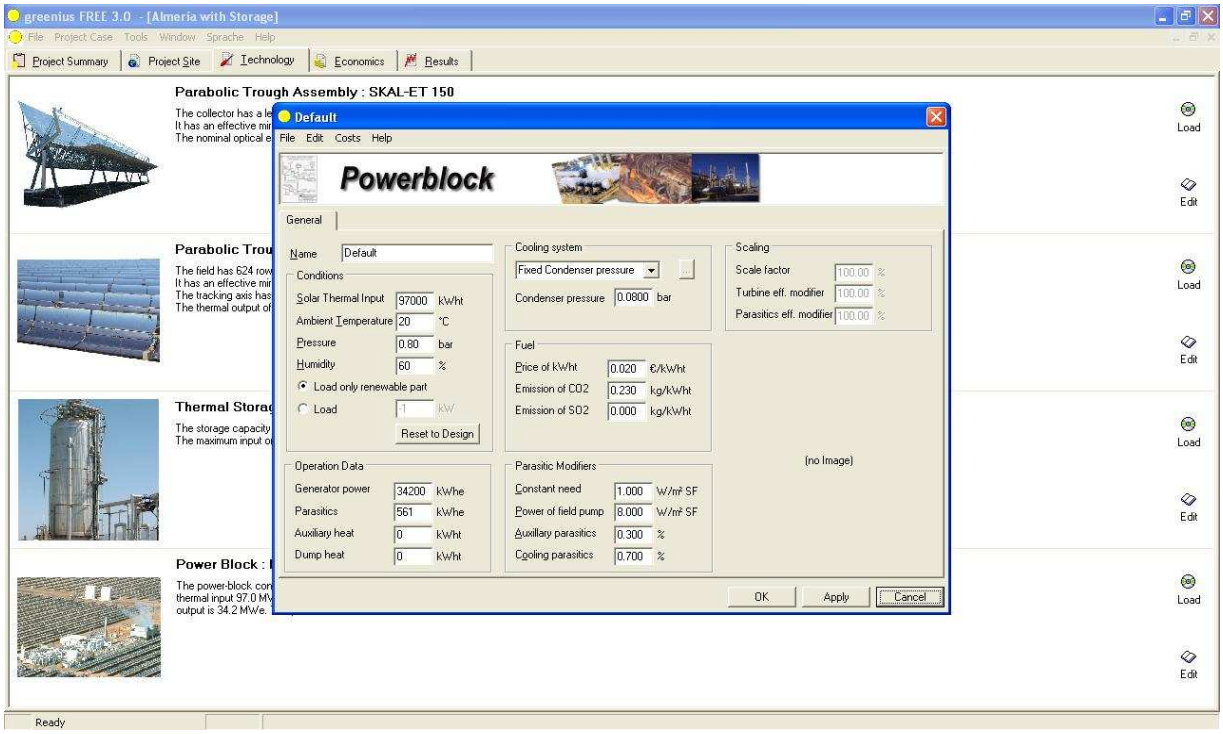

Figure B.4. Power Block Input data

Appendix C

C.1 Integration of tools for process simulation

Process modeling tools are software environments that support the high-level definition of process models. They are used to analyse the physical behaviour of a plant. The most widely used commercial process modeling tools are the tools of Aspen Engineering Suite™ [110]. These tools can be classified as all general purpose tools, since they are used for simulation and several optimization-based model-base applications and can be applied for the modeling of a wide range of chemical processes [111]. This section is structured as follows: The first part of this section focuses on the brief discussion of the Aspen Engineering Suite™ tools. The second part presents the integration of the main commercial tools to this work.

C.2 Aspen Engineering Suite™ tools

Aspen Engineering Suite™ comprises a number of tools for chemical process modeling [112] - [114]. Some of these tools are shown in figure C.2. Even though they all support simulation and optimization only two of the tools have been applied in this work.

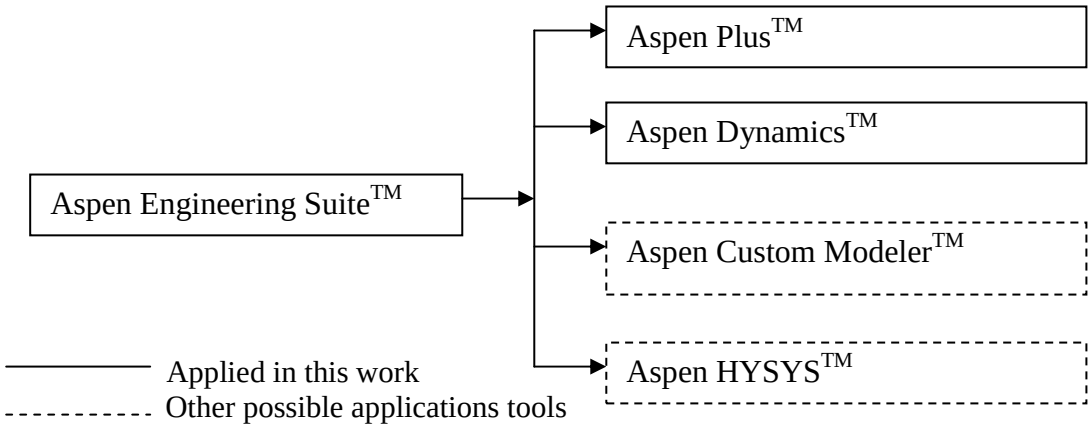

Figure C.1. Process simulation tools

C.3 Aspen Plus™

Aspen Plus™ is a steady state modeling tool that is based on extensive library of process unit models for chemicals processing. Through a graphical user interface (GUI), the user can create process model by selecting unit models from the library and defining their connections.

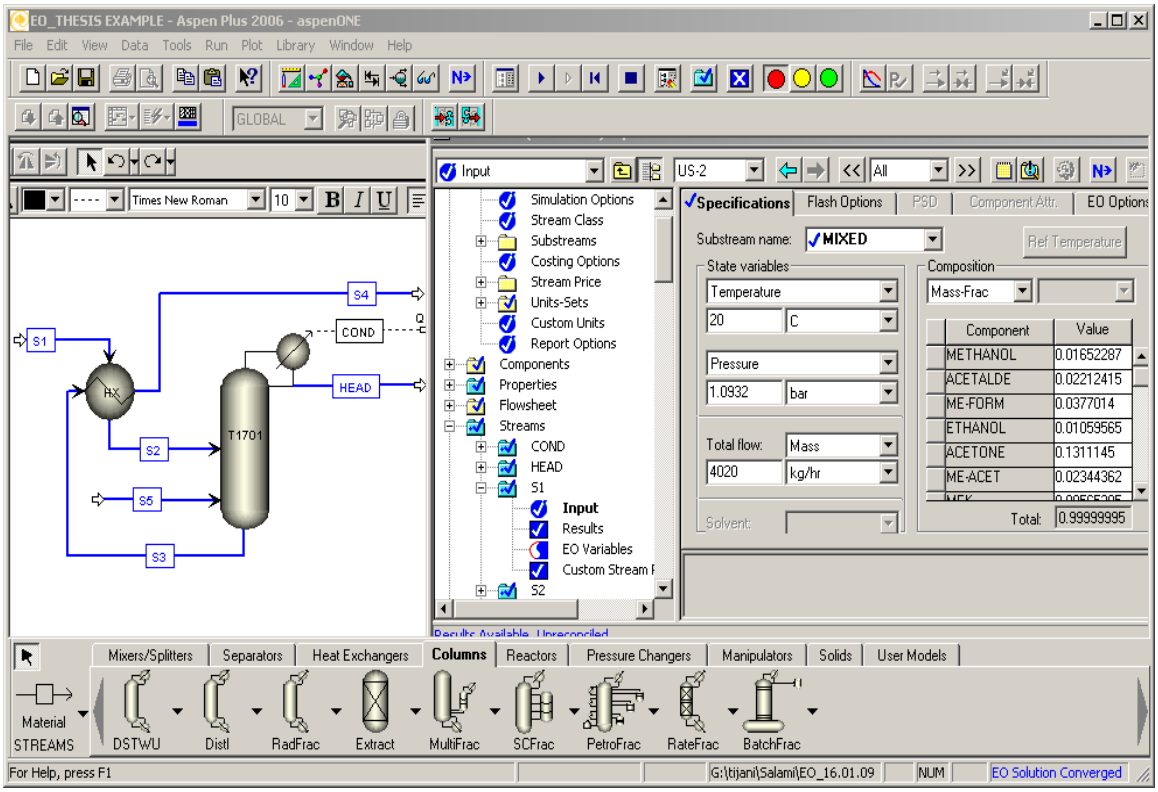

Figure C.2. The main window of Aspen Plus™ GUI

Figure C.2 shows the main window of the Aspen Plus™ GUI for the flowsheet specification. It consists of three sections: the left section shows the Process Flowsheet window where the appropriate models to be simulated are created and displayed.

The right section shows the Data Browser sheet and form viewer with a hierarchical tree view of the available simulation input, results, and objects that have been defined. The parameters of the selected models are provided in this section. The third section is the Model Library which appears at the bottom of the Aspen Plus™ main window.

C.4 Process Simulation

Process simulation is used to predict the behaviour of a process by using basic engineering relationships, such as mass and energy balances, and phase and chemical equilibrium. Given reliable thermodynamic data, realistic operating conditions, and rigorous equipment models, it

is possible to simulate actual plant behaviour. Process simulation can be used to run many cases, conduct "what if" analyses, and perform optimization runs [115] .

Today major chemical plants are built by first simulating the process on a computer. Commercially available software systems such as Aspen Plus™, HYSYS and CHEMCAD are widely used for this purpose. Several researches such as Douglas et. al [116] and Araujo et al [117] have used Aspen Plus™ for steady state simulation of distillation processes. The input and out put to typical flowsheeting program such as Aspen Plus™ is shown in figure C.3.

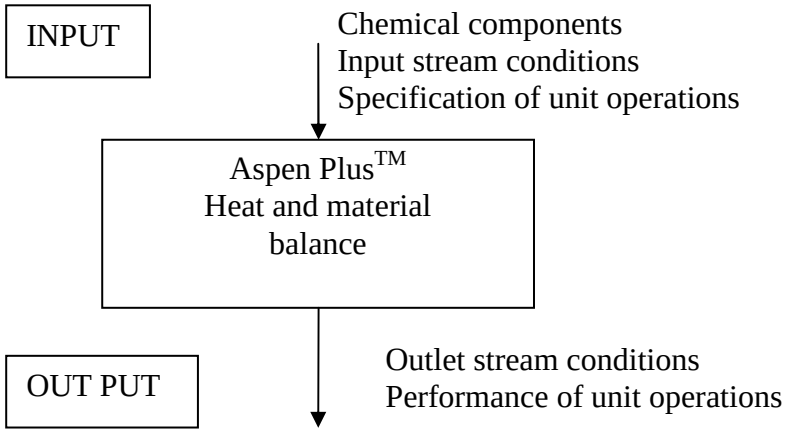

Figure C.3. Input and output to Aspen Plus™ flow sheet program

The input consists of information from the process flowsheet whiles the output consist of the stream conditions such as (temperature, pressure, composition and flow rate) of all the product streams and the performance of the major units, the sizes of equipments and the process economics. In the next section, background on the model-based applications in Aspen Plus™, namely steady state and dynamic simulation models are discussed.

C.5 Steady state (Aspen Plus™) and Dynamics (Aspen Dynamics™)

Steady state model are used for simulating stable operating point. Steady state process simulation model serves to support both operation and design, including revamping and debottlenecking (see figure C.4). In this work, steady state optimization as well as heat integration and potential environmental impact of different design alternatives where analysed

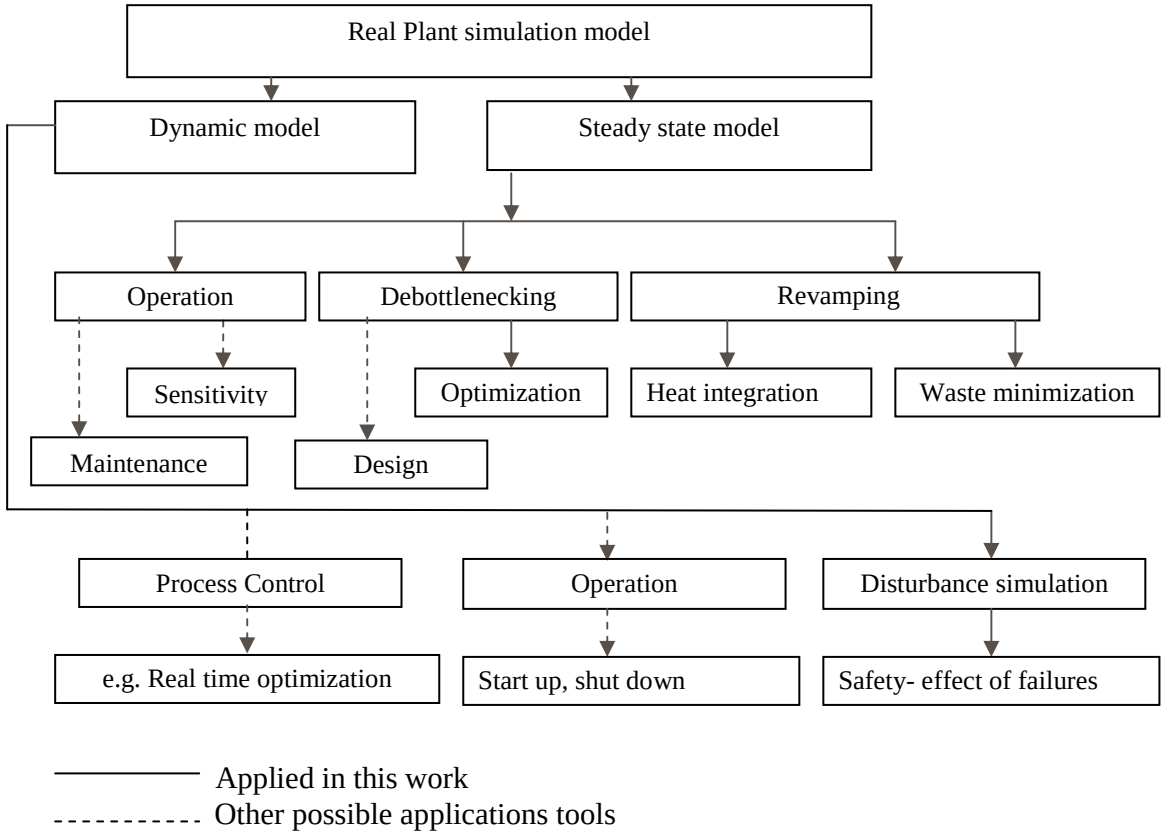

Figure C.4. Application of steady state and dynamic plant simulation model

Dynamic model based applications are used for dynamic models which describe the transient process behaviour. In dynamic simulation, it is important to understand the nature of the disturbances that are likely to upset the distillation column unit, e.g. studying the effect of failures of pumps and compressors of a plant. Accurate predictions of feed rate and feed composition disturbances are a key element to developing a good control structure.

Dynamic simulations can be used to compare the disturbance rejection capabilities of different design alternative (see figure C.4).

For the simulation of steady state models, typically a Newton-type algorithm is used for the solution of the nonlinear algebraic equations [118]. In the case of dynamic models, an integration algorithm is used for the numerical integration of the differential equations [119]. Detail discussions of these algorithms are however not presented in this work.

C.6 Computational approach of Aspen Plus™

This section presents the two main solution approaches adopted for process simulation in Aspen Plus. Once a process model is designed in Aspen Plus™, Equation Oriented (EO) modelling is available as a solution technique in addition to the usual Sequential Modular

(SM) option for running the simulation. These solution approaches are presented in the following sections.

C.7 Sequential Modular (SM)

The SM strategy solves each unit model in the flow sheet in sequence, the output of an already computed unit is used as an input for the next unit to be computed. This approach is straight forward as long as there are no recycles in the process model. When recycles are present, flowsheet iteration solution method is required (Biegler et al. [72]). Figure C.5b shows the block structure for the Aspen Plus simulation flowsheet.

In order to solve a SM problem the system performs the following steps (Smith [66]:

- Partition the flow sheet

Partitioning identifies those sets of blocks that must be solved together. For example, the units in figure C.5b (HX, T1701 and COND) that have to be solved as a group is called partition

- Tear streams

A tear stream is a recycle stream with component flows, total mole flow, pressure, and enthalpy all determined by iteration. It can be any stream in a loop. The SM solution technique is to tear one of the streams in the recycle loop, that is to guess or estimate the variables of that stream [120]. It is best to tear a stream for which a good initial estimate can be provided. Considering the flow sheet in figure C.5b, the process feed stream is S1, which must be specified before the heat exchanger unit (HX) is calculated. The set of units T1701 and COND constitutes a recycle loop. Stream S7 together with its information flow (component flows, total mole flow, pressure, and enthalpy) represent a tear stream (see figure C.5b).

- Convergence

Convergence blocks are defined to converge the tear streams. Convergence blocks determine how guesses for a tear stream are updated from iteration to iteration.

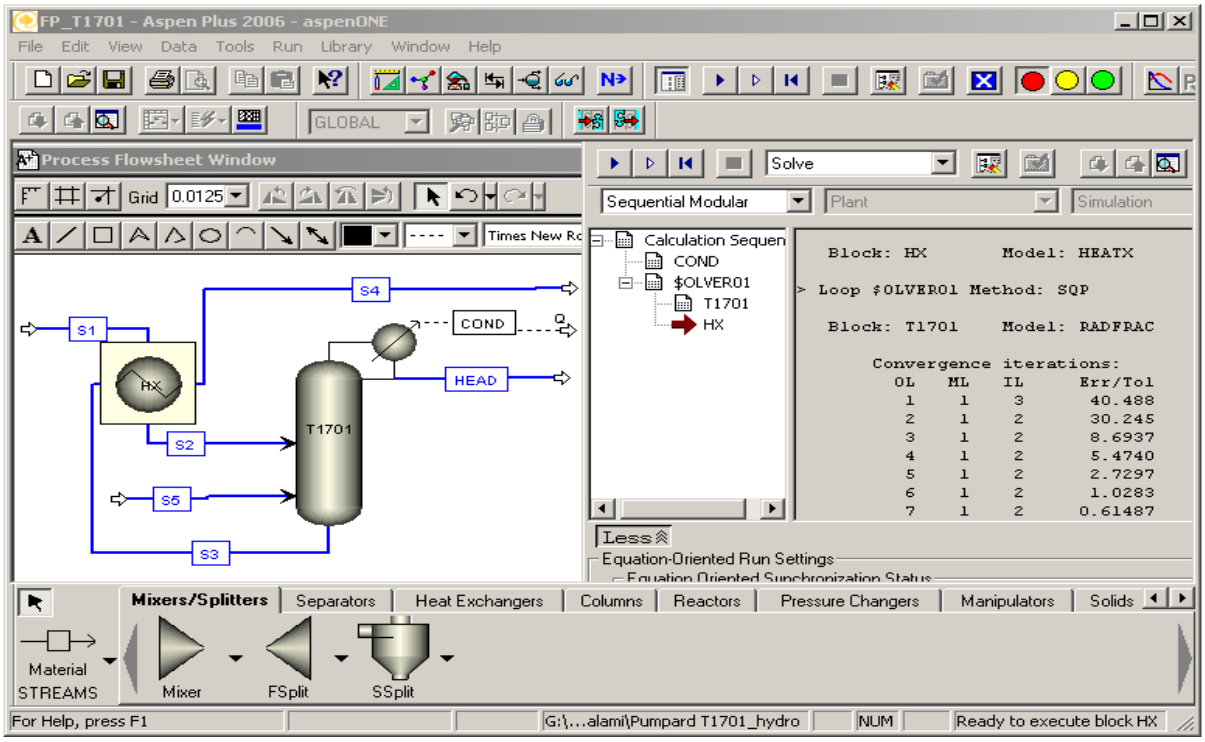

Figure C.5a. Aspen Plus simulation flowsheet of sequential modular calculation

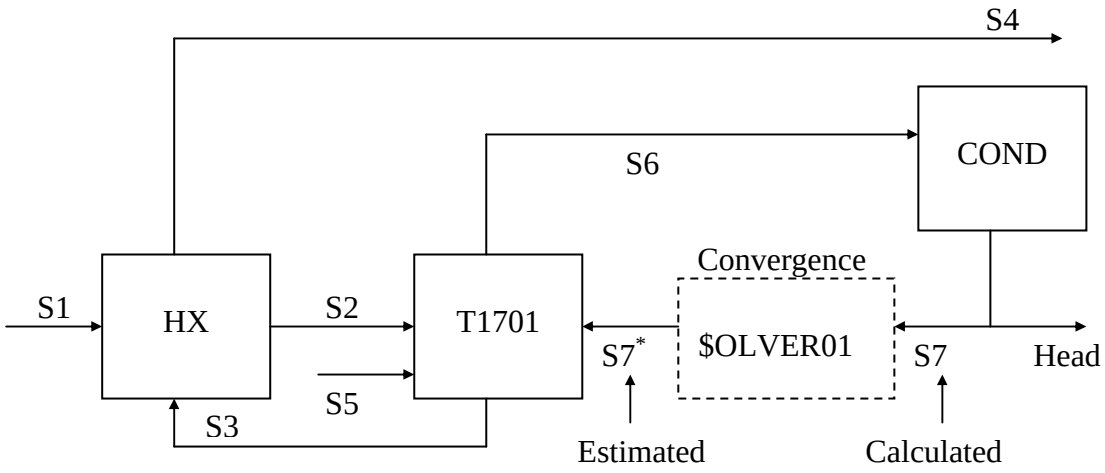

Figure C.5b. Block structure of sequential modular calculation

The units T1701 and COND in figure C.5b constitute a recycle loop, a convergence unit or $OLVER01 is inserted in the tear stream (i.e. in between stream S7* and S7). In a recycle loop, calculations begin with the stream leaving the convergence unit. This allows the material and energy balance in the distillation column (T1701) to be solved. Each of the units in the loop is then computed, returning to the convergence unit, where convergence is checked. When convergence is not achieved, the simulator repeats the loop calculation until the convergence criteria is achieved. Aspen names the convergence unit as $OLVER01. The

name of the convergence unit is reported in the calculation sequence output which is illustrated below for the flowsheet in figure C.5a:

Calculation sequence: COND, $OLVER01, T1701, HX

Stream S7* denotes the vector of estimated variables (e.g. component flows, total mole flow, pressure, and enthalpy) of the tear stream, and S7 denotes the vector of calculated stream variable, i.e. after the units in the recycle loop have been simulated. Although the Aspen Plus simulation flowsheet in figure C.5a does not show S7* and S7, the user should know that they are implemented.

Most widely used recycle convergence methods available in Aspen plus^{TM} are (Wegstine [121], Mayers et al. [122], Westberger et al. [123]):

- WEGSTEIN
- DIRECT
- Secant
- BROYDEN
- NEWTON
- COMPLEX
- SQP

The classical bounded Wegstein method is usually the quickest and most reliable method for tear stream convergence. Each of these methods determine whether the relative difference between the estimated variable (e.g. S7* in figure C.5b) and the calculated variable (e.g. stream S7 figure C.5b) are all less than a specified tolerance. If not, the convergence subroutine computes new estimates for it's output stream variables and iterates until the loop is converged.

Advantages of Sequential Modular (SM)

- The approach is easy to understand
- Errors are straighter forward to understand
- Easy control of convergence, both at the unit and flowsheet level
- Effective for many types of simulations

Disadvantages of Sequential Modular (SM)

- Large problems may be difficult to converge.
- SM strategy can be very time-consuming for certain types of problems.

C.8 Equation Oriented (EO)

Equation Oriented (EO) modelling is an alternate strategy for solving flowsheet simulations. Instead of solving each block in sequence, EO gathers all the model equations together and solves them at the same time. For this reason, EO modeling is sometimes called equation-based or simultaneous equation modeling.

The new version of Aspen Plus™ (Aspen Plus™ 2006-Aspen^{ONE}) supports both sequential-modular simulation and equation oriented approach [124]. It has a mixed mode approach that uses the sequential-modular approach for the first iteration steps and then continues with the equation oriented approach, this step is known as synchronization (see figure C.6).

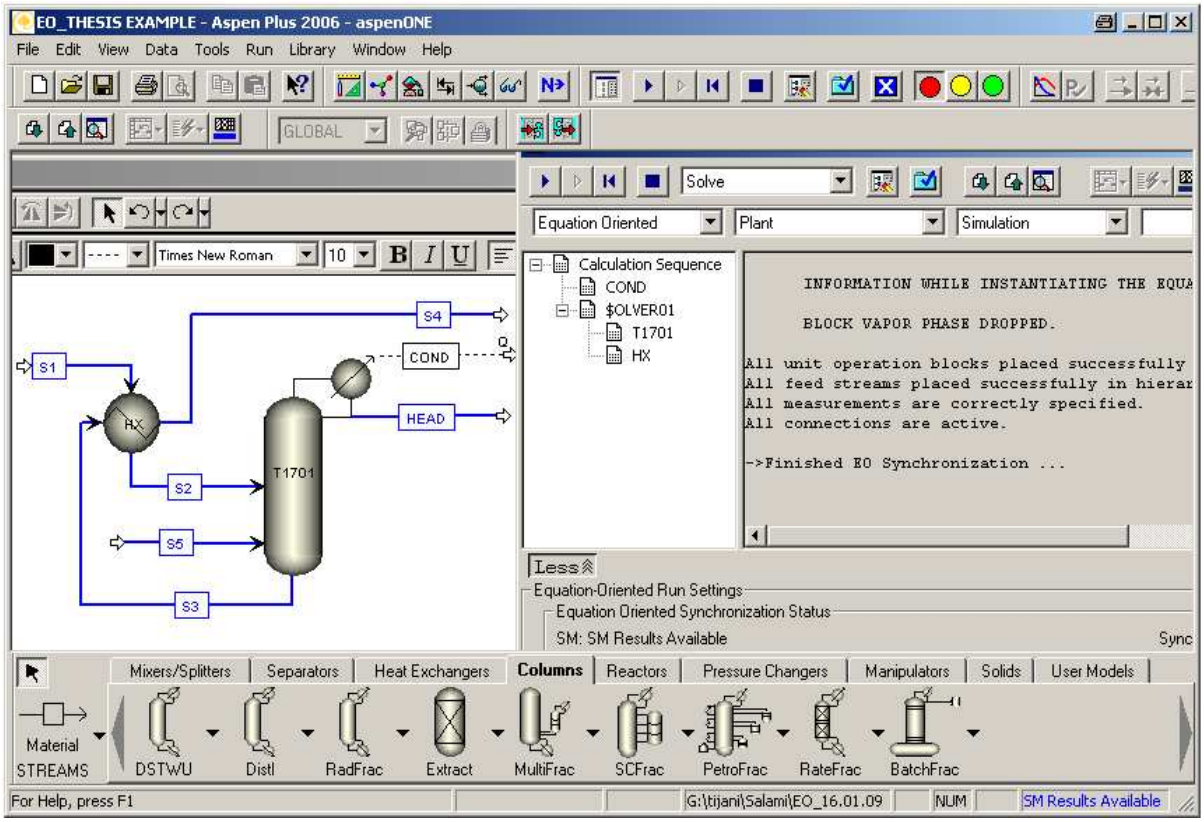

Figure C.6. Aspen Plus simulation flowsheet showing EO synchronization status

Equation Oriented Modeling is a very effective way of solving certain problems [124], such as:

- highly heat-integrated processes
- highly recycled processes
- processes with many design specifications
- process optimization

Normally, these types of problems are difficult to solve with SM strategy, because they may contain many convergence loops. Although the number of variables and equations can be very large, EO solves the entire flowsheet simultaneously without nested convergence loops and utilizes analytical first order derivatives. Nesting determines which tear streams are to be converged simultaneously and in which order collections of tear streams are to be converged. As a result, EO strategy can solve much larger problems using the same computational effort.

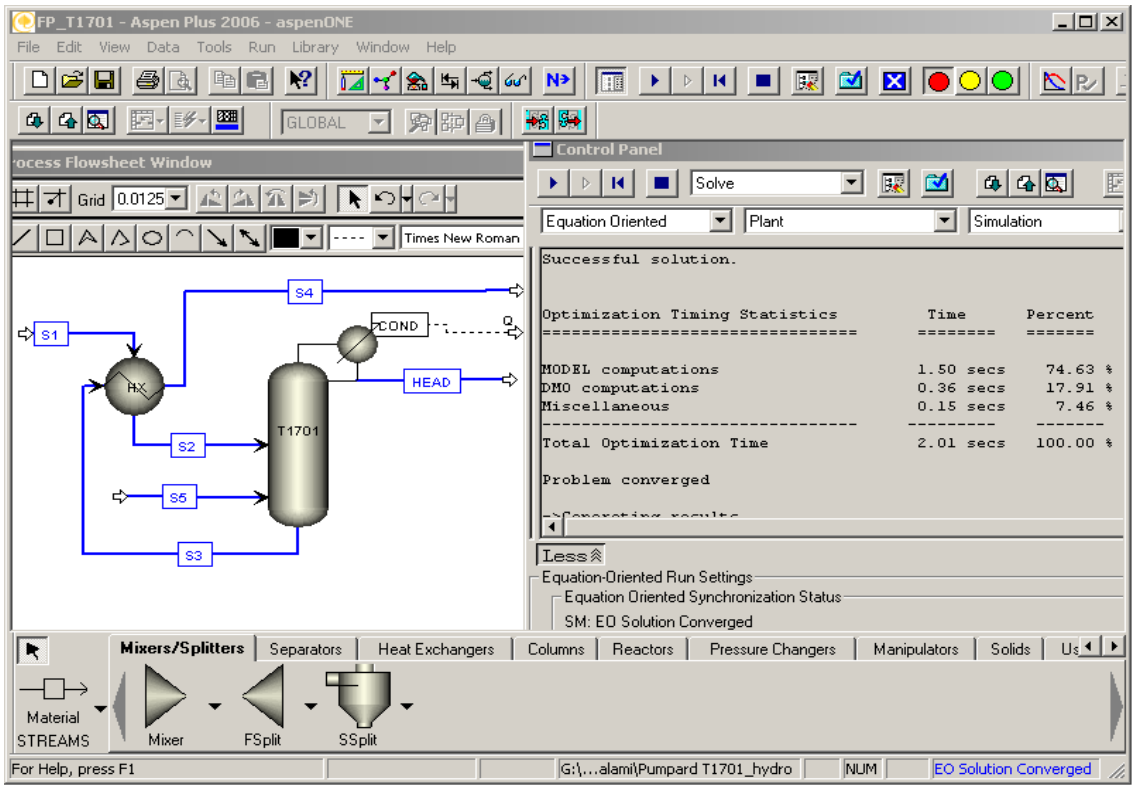

Figure C.7. Aspen Plus™ 12.1 simulation flowsheet of Equation Oriented (EO) mode

C.9 Initialization and Solution

The Equation Oriented modelling strategy works well when all variables are “near” the solution. EO strategy is not generally suited to solving a simulation without good estimates for all variables. Therefore, before you solve your flowsheet in EO, you must initialize it in SM. SM initialization does not require completely converging the SM problem. The minimum requirement is that each block be solved once.

When using the Sequential Modular (SM) strategy, Aspen Plus normally runs in a single mode of operation. SM also has an optimization feature. However, the SM approach to parameter estimation, reconciliation, and optimization generally suffers from long execution

times, particularly in complex flowsheets. Consequently, relatively few users have used those SM features to their fullest extent, (see table C.1 for details).

T**able C.1. Operation mode of SM Source** [124]**.**

SM Solution Mode	Description
Simulation*	Model inputs and parameters are fixed. All the other model quantities are calculated. For given feed conditions and operating parameters, the products are computed. This type of problem has no degrees of freedom. The solver cannot change the variable value. It is a fixed input.

The Equation Oriented (EO) strategy can operate in four different modes as shown in table **C.2**:

Table C.2. Operation mode of EO Source [124]

SM Solution Mode	Description
Simulation*	This type of problem has no degrees of freedom. For given feed conditions and operating parameters, compute the products.
Optimization*	This mode usually involves the manipulation of plant operating conditions (set points) to maximize and objective function (e.g. TAC). It has degrees of freedom, i.e. the solver is free to move the variable to adjust the objective function. Any value that is given before the solution begins is used as an initial guess.
Parameter Estimation**	This mode is a model-tuning mode. It also has no degrees of freedom. Inputs and certain outputs are fixed and model parameters are computed. Parameter Estimation requires one measured variable for each estimated parameter.
Reconciliation**	This mode usually involves the manipulation of plant operating conditions (set points) to maximize profit, and thus, has degrees of freedom. Parameters determined from a model tuning mode are fixed during this mode.

*Applied in this work
**Other possible applications

Advantages of Equation Oriented (EO)

- It has the ability to formulate the problem as an optimization problem
- It is easy to specify variables and constraints
- It can handle highly integrated systems since all equations are solved simultaneously

Disadvantages of Equation Oriented (EO)

- The method requires good initial estimate of variables

- It may be difficult to handle highly nonlinear relations required to represent physical properties.

C.10 Structure of the software package used

Figure C.8 shows a graphical representation of the structure of the software package. The normal way of using a simulator in a stand-alone mode is shown in figure C.8. The engineer prepares an input file for the simulator (ASPEN PLUS^{TM} in this example). The simulator produces an output report and also saves a problem data file which can be used to modify and run the problem. The output results are further transfered into other application programs.

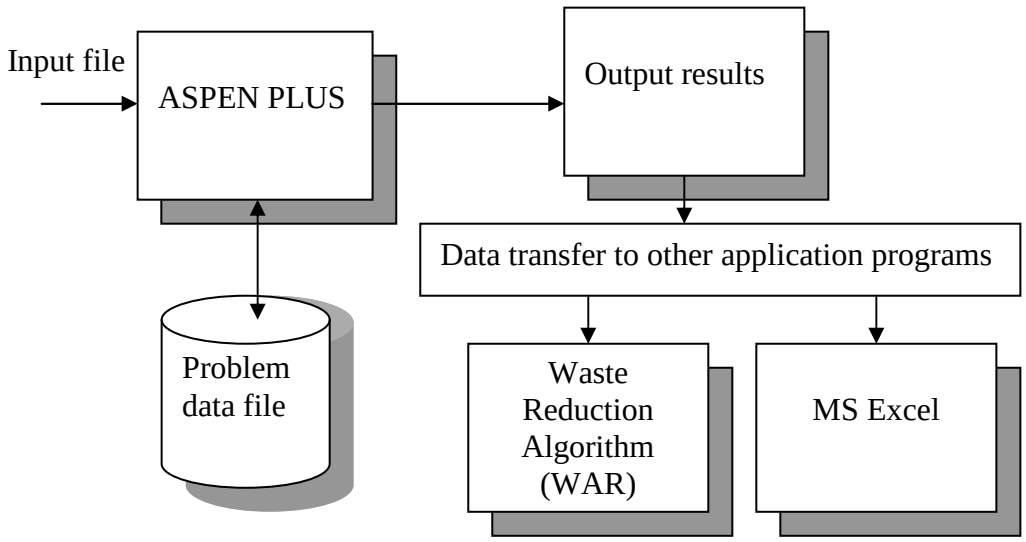

Figure C.8. Structure of the software package

D.1 Simulation features of pumparound

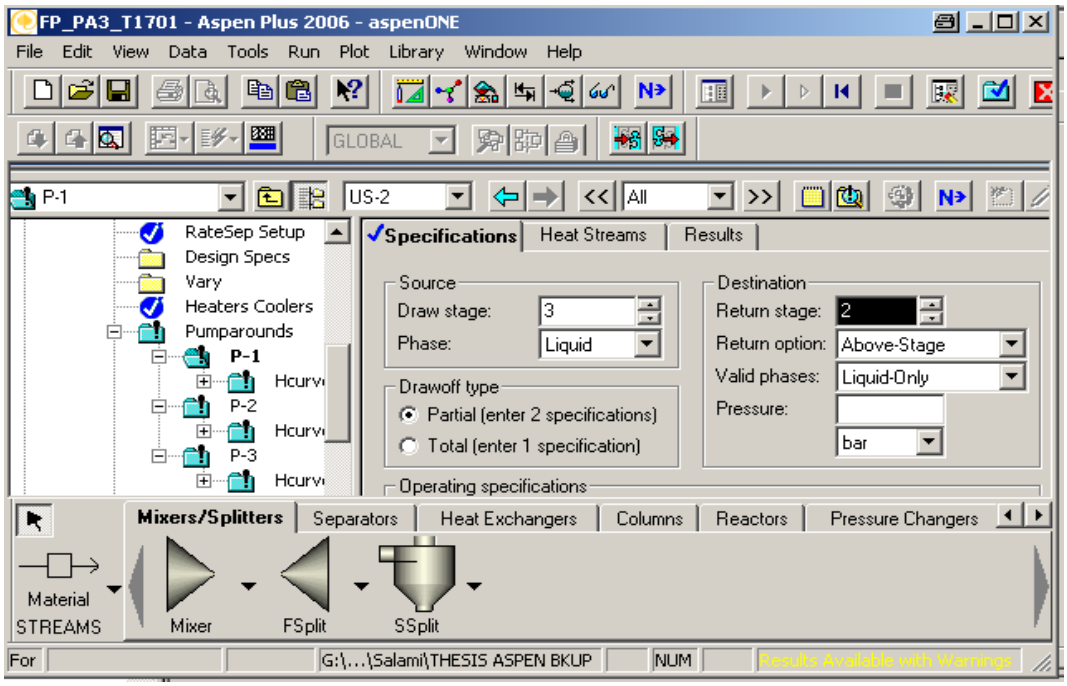

Figure D.1.simulation features of liquid from tray

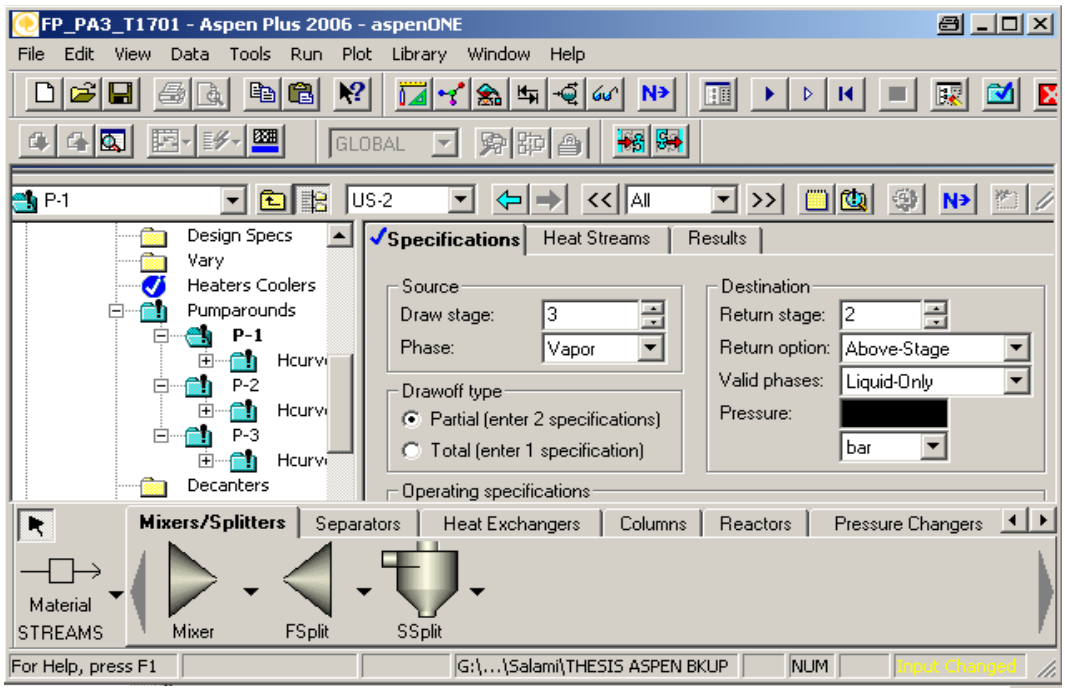

Figure D.1.simulation features of vapour from tray

References

[1] Al-Muslim H., Dincer I., (2005). Thermodynamic analysis of crude oil distillation systems. *International Journal of Energy Research,* 29, 637–655

[2] Teresa M. M., Smith, R. L., Douglas M. Young, Carlos A.V. Costa, (2003), Evaluating the environmental friendliness, economics and energy efficiency of chemical processes: heat integration, *Clean Techn Environ Policy* 5, 302–309

[3] Marc A. R., Dincer, I., (2001). Exergy as the confluence of energy, environment and sustainable development. *Exergy Int. J*. 1, 3–13

[4] Leonardo S. V., Joao L. D., Manuel E. Cruz., (2005). Exergoeconomic Improvement: an Alternative to Conventional Mathematical Optimization of Complex Thermal Systems, Rio de Janeiro, 30 May - 03 June 2005, Brazil

[5] Van der Helm, D. U.; High, K. A. Waste Minimization by Process Modification. *Envir. Prog.* 1996, 56-61.

[6] Datus, M.; High, K. A. Economic evaluation for the Retrofit of Chemical Processes through Waste minimization and Process Integration. *Ind. Eng.Chem. Res* 1996, 35, 4566-4578.

[7] Ciric , A. R.; Huchette, S. G.; (1993). Multiobjective Optimization Approach to sensitivity Analysis: Waste treatment cost in Discrete Process Synthesis and Optimization Problems. *Ind. Eng Chem. Res.* 32, 2636-2646

[8] Cano-Ruiz, J. A.; McRae, G. J. (1998). Environmentally conscious chemical process design. Annu. Rev. *Energy Environ*. 23, 499-536.

[9] Finn A. J., Tomlinson T. R., Johnson G. L., 2000, Oil Gas J.,

[10] Jang W., Hahn R., Hall R. K., 2005, *Comp. Chem. Eng*. 30, 285

[11] Konukman A., Akman U., 2005, *Chem. Eng Sci, 60, 7057*

[12] Cammarata G., Fichera A., Gugliemino D., 2001, *Appl. Energy, 68,19.*

[13] Yan X.F., Chen D.Z., Hu S. X., 2003, Comp. Chem. Eng, 27,1

[14] Skogestad, S. 1994. Controllabilty analysis of SISO systems. Pages 471-476 of: prints of the IFAC Symposium ADCHEM´94.

[15] Evans, L.B. 1994 Steady-State simulation: A state-of-the-Art Review. Pages 953-967 of: Proceedings of the 5th International Symposium on Process Systems Engineering PSE 94.

[16] Humphery, J.L., & Seibert, A.F 1992. Separation technologies: An opportunity for energy Savings. CEP, 88(3), 32-41.

[17] Rivero R., Koeijer G, 2003, Entropy production and exergy loss in experimental distillation columns, *Chemical Engineering Science*, 58, 1587 – 1597

[18] Kister H. Z., (1992). Distillation Design, McGraw-Hill, New York

[19] Olujic, Z., Fakhri, F., de Rijke, A., de Graauw J., Jansens, P.J., Internal heat integration – the key to an energy-conserving distillation column., *Journal of Chemical Technology and Biotechnology.*, 78, 2003, p. 241–248

[20] Flores, O. A., Cardenas, C., Hernandez, S., Rico-Ramırez, V., Thermodynamic Analysis of Thermally Coupled Distillation Sequences, *Ind. Eng. Chem. Res., 42*, 2003, p**.** 5940-5945

[21] Null, H. R., Heat Pump in Distillation, Chemical Engineering Process, 7, No 72, 58-64 (1976

[22] Henley, E. J. and Seader, J. D., Equilibrium-Stage Separation Operations in Chemical Engineering. John Wiley and Sons Inc., New York (1981).

[23] King, C.J., 1980, Separation Processes, 2nd ed., McGraw-Hill

[24] Demirel, Y., (2004), Thermodynamic Analysis of Separation Systems, Department of Chemical Engineering, Virginia Polytechnic Institute and State University,

24061, Blacksburg, Virginia, USA, Volume 39, Number 16 / 2004, page 3897 – 3942, DOI: 10.1081/SS-200041152

[25] Zemp, R.J., and Maia, M. L.O., (2002) Thermodynamic analysis of multicomponent distillation columns, identifying optimal feed conditions, Braz. J. Chem. Eng. vol.17 n.4-7

[26] Faria, S. H. B., and Zemp, R. J., (2005), using exergy loss profiles and enthalpy-temperature profiles for the evaluation of thermodynamic efficiency in distillation columns (Thermal Engineering), Vol. 4 · No. 1 · p.76-82

[27] Chamchine, A., 2005 Exergy Life Cycle Analysis, Proceedings of COST Action 628, Tampere, Finland.

[28] Yunus Cerci, Yunus Cengel, Byard Wood, Nafiz Kahraman, and E. Sinan Karakas (2003), Improving the Thermodynamic and Economic Efficiencies of Desalination Plants: Minimum Work Required for Desalination and Case Studies of Four Working Plants, Mechanical Engineering, University of Nevada, Reno, Nevada, Report No. 78

[29] Fratzscher, W., Picht, P., Szolcsanyi, P., Fonyo, Z., Földes, P., (1980), Energetische Analysis von Stoffuebertragungsprozessen, VEB Deutscher verlag fuer Grundstoffindustrie, Leipzig, VLN 152-915/78/80

[30] Robinson, C. S., Gilliland, E. R., (1950), Elements of Fractional Distillation, 4th edition, McGRAW-HILL BOOK COMPANY, New York, Toronto and London

[31] Rivero R., Szargut Z., Kolenda G.,Tsatsaronis & Ziebik A., 1993, Tridimentional exergy diagram in Energy Systems and Ecology, American Soceity of Mechanical Engineers.Vol. 1, J. pp. 305-312

[32] Ozokwelu, D., Porcelli, J., Akinjiola, P., (2006), Exergy Analysis: A Powerful Tool for Identifying Process Inefficiencies in the U.S. Chemical Industry, Office of Energy Efficiency and Renewable Energy U.S. Department of Energy.

[33] Tirandazi B., Mehrpooya M., Vatani A., (2008), Effect of Valve Pressure Drop in Exergy Analysis of C2 + Recovery Plants Refrigeration Cycles, International Journal of Electrical Power and Energy Systems Engineering.

[34] Sato. N., 2004. Chemical energy and exergy, an introduction to chemical thermodynamics, ELSEVIER, New York.

[35] Douglas. J. M., Richard. S., Cabezas, H., (2000). The waste reduction (WAR) algorithm: environmental impacts, energy consumption, and engineering economics, Waste Management 20 605 ± 615

[36] Douglas. J. M., Cabezas, H., (1999). Designing sustainable processes with simulation: the waste reduction (WAR) algorithm. Computers and Chemical Engineering, 23, 1477–1491

[37] Portha J.F., Jaubert J.N,, Louret S., Pons M.N., (2008), Definition of a Thermodynamic Parameter to Calculate Carbon Dioxide Emissions in a Catalytic forming Process, Int. J. of Thermodynamics, Vol. 11 (No. 2), pp. 81-89,

[38] Hilaly, A. K., & Sikdar, S. K. (1994). Pollution balance: a new method for minimizing waste production in manufacturing processes. Journal of the Air and Waste Management Association, 44, 1303–1308

[39] Cabezas H, Bare JC, Mallick SK. Pollution prevention with chemical process simulators: the generalized waste (WAR) algorithm, full version. Comp Che Eng 1999;23:623±34.

[40] Kim, K., Smith, R. L (.2005), Systematic Procedure for Designing Processes with Multiple Environmental Objectives, Environ. Sci. Technol, 39,2394-2405

[41] USEPA (1997). Profile of the fossil fuel electric power generation industry. Washington, D.C.: United States Environmental Protection Agency, EPA 310-R-97-007.

[42] Price, H. 2003. A Parabolic Trough Solar Power Plant Simulation Model. International Solar Energy Conference NREL/CP-550-33209.

[43] Kelly, B. D. Kearney 2006 Thermal Storage Commercial Plant Design Study for a 2-Tank Indirect Molten Salt System, Subcontract Report, NREL/SR-550-40166.
[44] Bakos GC, Adamopoulos D, Tsagas NF, Soursos M. 1999. Design and construction of a line-focus parabolic trough solar concentrator for electricity generation. In: Proceedings of ISES Solar World Congress. ISES, Jerusalem, Israel.
[45] Kalogirou S. Parabolic trough collector system for low temperature steam generation: design and performance characteristics. Appl Energy 1996;55(1):1–19.
[46] Quaschning, V., Ortmanns, W., Kistner, R., Geyer, M. (2001) greenius – A new Simulation Environment for Technical and Economical Analysis of Renewable Independent Power Projects. Proceedings of ASME International Solar Energy Conference Solar Forum 2001, 22-25 April, Washington DC, pp. 413-417
[47] Quaschning, V.; Ortmanns, W., (2003), Specific cost development of photovoltaic and concentrated solar thermal systems depending on the global irradiation- a study performed with the simulation environment Greenius, ISES Solar World Congress 2003 · Göteborg, Sweden.
[48] Autodesk® Ecotect (2008). Solar Radiation. http://squ1.org/wiki/Solar_Radiation (Accessed on 06.01.2009).
[49] European Solar Thermal Technology Platform "ESTTP" (2006). Solar Thermal Vision 2030.
[50] Nava, Paul (2004). FLAGSOL. The AndaSol Projects.
[51] Goswami, D. Yogi (2008). Energy Conversion.
[52] Winter, C. J., R. Sizmann, and L. Vant-Hull, eds., 1991. Solar Power Plants Fundamentals, Technology, Systems, Economics. Springer-Verlag, Berlin, 1990, ISBN 3-540-18897-5.
[53] Romero-Alvarez, M., Zarza, E. 2008. Concentrating solar thermal power. Energy conversion
[54] Arasu, A. V., Sornakumar S. T., (2006), Performance characteristics of the solar parabolic trough collector with hot water generation system. Thermal Science: Vol. 10, No. 2, pp. 167-17
[55] Reddy, T. A., Battisti, R., Schweiger, H., Weiss, W., Morehouse, H. J., Vijayaraghavan, S., Gaswomi, Y. D., 2008. Solar Themal Energy Conversion. Energy conversion
[56] Fischer, S., Heidemann, W., Steinhagen, H., Test and Simulation of Solar Thermal Collectors with Multi-axial Incident Angle behavior, Universität Stuttgart, Institut für Thermodynamik und Wärmetechnik (ITW) Pfaffenwaldring 6, 70550 Stuttgart Germany
[57] Brooks, M., Mills, I., Harms, T., Design, construction and testing of a parabolic trough solar collector for a developing-country application
[58] Nava, Paul (2004). FLAGSOL. The AndaSol Projects.
[59] World Bank, 1999. Cost reduction study for solar thermal power plants. Prepared by the World Bank
[60] IAEA (1984).Expansion planning for Electrical Generating Systems. A Guidebook
[61] European Commission, 2005, European Concentrated solar Thermal Road mapping,
[62] Kolb, 1997. Economic Evaluation of Solar-Only and Hybrid Power Towers Using Molten-Salt Technology. Prepared for Elsevier Science Ltd., Great Britain. Prepared by Gregory J. Kolb
[63] Stockburger, D., und Bartmann, L., Chem.-1ng.-Tech. 50 (1978) Nr. 7, S. 497-502 Verlag Chemie, GmbH, D-6940 Weinheim
[64] McConkey, A., Eastop, T.D., (1993) Applied thermodynamics for engineering technologist, Longman Group UK Ltd.
[65] Wang J., Henke G. E., (1966), Hydrocarb. Proc. 45(8), p. 155.
[66] Smith, R. (2005), Chemical Process Design and Integration, JOHN WILEY &

SONS, LTD, UK
[67] Brusis D., 2003, Synthesis optimization of distillation processes with MINLP techniques. VDI- Verlag GmbH, Düsseldorf
[68] Lewis W K., Matheson G. L., 1932, Studies Distillation, Design of Rectification Columns FOR Natural and Refinery Gasoline, Industrial Engineering Chemistry 24, No. 5 pp. 494/498
[69] Bauer, M.H., (1997) Synthesis und Optimierung nichtidealer Rektifizierprozess, Fortschr.-Ber. VDI, Reihe 3, Nr. 496, VDI Verlag, Düsseldorf, 1997
[70] Douglas, J. M., Conceptual Design of Chemical Processes. McGraw-Hill Book Company, New York (1988).
[71] Peters, M.S., Timmerhaus; K.D., (1991) Plant Design and Economics for Chemical Engineers, 4th edition, McGRAW-Hill, New York,
[72] Biegler L. T., Grossmann, I.; E and Westerberg A.W., (1997) Systematic methods of chemical Process Design, Prentice-Hall, New Jersey
[73] Colson G, Bruyn CD. (1989) Models and methods in multiple objectives decision making. Math. Comput. Modelling 12:1201–11.
[74] Zeleny M. (1982) Multiple criteria decision making. New York: McGraw-Hill.
[75] Hobbs, B.F., (1986), "What can we learn from experiments in multiobjective decision analysis," IEEE Trans. On Systems Management and Cybernetics, 16, pp. 384-394.
[76] Zanakis, S., A. Solomon, N. Wishart, and S. Dublish, (1998), "Multi-Attribute Decision Making: A Comparison of Select Methods," European Journal of Operational Research, 107,
[77] Triantaphyllou, E., (2000), Multi-Criteria Decision Making Methods: A Comparative Study, Kluwer Academic Publishers, Boston, MA, U.S.A.
[78] linkov, I., Varghese, A., Jamil, S., Seager, T.P., Kiker, G., Bridges, T., (2004) Multi-criteria Decision analysis: a framework for structuring remedial decisions at contaminated sites, Comparative Risk Assessment and Environmental Decision Making" Kluwer, , p. 15-54
[79] Hwang CL, Masud AS. Multiple objective decision making: methods and applications. Berlin: Springer; 1979.
[80] Zhou P., Ang B.W., Poh K.L., 2005 Decision analysis in energy and environmental modeling: An update Elsevier Ltd. doi:10.1016/journal.energy.2005.10.023
[81] Hwang, C.L., Yoon, K., 1981. Multiple Attribute Decision Making. In: Lecture Notes in Economics and Mathematical Systems 186. Springer-Verlag, Berlin.
[82] Benayoun, R., Roy, B., Sussman, N., (1966). Manual de Reference du Programme Electre. Note de synthese et Formation, 25.
[83] Saaty, T.L., (1980), "The Analytic Hierarchy Process," McGraw-Hill, New York, NY, USA
[84] Zimmermann, H. J., (1996), Fuzzy Set Theory and it´s application, Kluwer Academic Publishers, Third Revised Edition, Boston, MA, USA
[85] Janssen, R. 1992. Multiobjective decision support for environmental management. Dordrecht, the Netherlands: Kluwer Academic Publishers..
[86] Forman, E. H., Selly, M. A. (2001). Decision by Objectives. World Scientific. USA
[87] Volker H. Hoffmann , Konrad Hungerbu1 hler, and Gregory J. McRae, 2001, Multiobjective Screening and Evaluation of Chemical Process Technologies, Ind. Eng. Chem. Res., 40, 4513-4524
[88] Rajesh J. K., Gupta S. K., Rangaiah G. P., Ray A. K., 2001 Multi-objective optimization of industrial hydrogen plants, Chemical Engineering Science 56, 999-010
[89] Edgar T.F., Himmelblau D.M., 2001. Optimization of Chemical Processes; McGraw-Hill, New York
[90] Deb K., (20039, Multi-Objective Optimization using Evolutionary Algorithms, JOHN WILEY & SONS, LTD, New York
[91] Pareto V. (1971), Manual of political Economy, The MacMillan Press Ltd.
[92] Diwekar U., 2003, Introduction to Applied Optimization, Kluwer Academic

Publishers, Norwell Massachusetts.
[93] Morosyuk, T. V. "The conceptual selection model of a household heat pump," No 200Uk-94, Deposited in Ukrainian State Scientific and Technical Library on 01.25.1994
[94] Comos® innotec GmbH, 2004, Quick start Basic - http://www.innotec.de
[95] Douglas, J. M. AZChE 1985,31, 353.
[96] Douglas, J. M. Synthesis of Multistep Reaction Processes. In Foundations of Computer-Aided Design; Siirola, J. J., Grossmann, I. E., Stephanopoulos, G., Eds.; Elsevier: New York, 1990; pp 74-105
[97] Rossiter, A. P.; Douglas, J. M. Chem. Eng. Process Des. 1986, 64, 27, 2071-2078. 175-183
[98] Kirkwood, R. L.; Locke, M. H.; Douglas, J. M. Comput. Chem. Eng. 1988, 12,329
[99] Rajagopal, S..Ng, K. M.; Douglas: J. M. Znd. Eng. Chem. Res. 1988, 27,2071-2078
[100] Grossmann, I. E. MINLP Optimization Strategies andAlgorithms for Process Synthesis. In Foundations of Computer-Aided Process Design; Siirola, J. J., Grossmann, I. E., Stefanopoulos, G., Eds.; Elsevier Science Publishers: New York, 1990.
[101] El-Halwagi, M. M.; Manousiouthakis, V. Simultaneous synthesis of reactive mass-exchange and regeneration networks. AIChE J. 1990, 36 (8), 1209-1219.
[102] Papalexandri, K. P.; Pistikopoulos, E. N.; Floudas, C. Mass exchange networks for waste minimization: a simultaneous approach. Trans. Inst. Chem. Eng. 1994, 72A, 279-294.
[103] Y.D. Lang, L. T. Biegler , Comp. Chem. Eng. 1987, 11, 143
[104] Ahmad Hamad, Russell F. Dunn, 2002., Energy Optimization of Pressure-Swing azeotropic Distillation Systems, Ind. Eng. Chem.Re 2002, 41,6082
[105] Seider, W. D., Seader, J.D., Lewin, D.R., 2003, Product and Process Design principles, Synthesis, Analysis and Evaluation, John Willey & Sons, Inc., New York.
[106] Taprap, R., Ishida, M., Graphic Exergy Analysis of Processes in Distillation Column by Energy-Utilization Diagrams, AIChE Journal,Vol. 42, no. 6, 1996, p. 1633-1641
[107] European Commission (2007). Concentrating Solar Power.
[108] World Bank, 1998. Commodity Markets and the Developing Countries. Prepared by the World Bank, Washington, D.C
[109] Franka Herold, (2006), Master arbeit BTU Cottbus
[110] Aspen Engineering SuiteTM, (2006), product information version 2006, Aspen Technology, Inc.
[111] Schopfer G., (2006), A Frame Work for Tool Integration in Chemical Process Modeling Fortschr.-Ber. VDI, Reihe 3, Nr. 868, VDI Verlag GmbH, Düsseldorf.
[112] Aspen DynamicsTM 2006 Getting Started Guide, Aspen Technology, Inc., Cambridge, MA.
[113] Aspen Custom Modeler, Getting Started Guide, Aspen Technology, Inc., Cambridge, MA
[114] Aspen HYSYS, (2006) user's guide, Aspen Technology, Inc., Cambridge, MA
[115] Aspen PlusTM 2006-aspenONE, Getting Started Building and Running a Process Model, Aspen Technology, Inc., Cambridge, MA.
[116] Douglas. J. M., Richard. S., Cabezas, H., (2000). The waste reduction (WAR) algorithm: environmental impacts, energy consumption, and engineering economics, Waste Management 20 605 ± 615
[117] Araujo. A. C. B., Vasconcelos, L. G. S., Fossy. M. F., Brito. R. P., (2007). Exergetic and Economic Analysis of an Industrial Distillation Column. Brazilian Journal of Chemical Engineering, Vol. 24, No. 03, pp. 461 - 469,
[118] Riggs J. B., (1994), An Introduction to Numerical Methods for Chemical

Engineers. Texas Tech University Press, Lubbock.
[119] Ascher U.M., Petzold L.R., (1998) Computer Methods for Ordinary Differential Equations and Differential- Algebraic Equations SIAM, Philadelphia.
[120] Henley E.J., Rosen E.M., (1969), Material and Energy Balance Computations, Wiley, New York.
[121] Wegstein J.H., (1958), “Accelerating convergence of Iterative Processes” Commun. Assoc. Comp. Machinery, 1(6), 9.
[122] Myers A.L., Seider W.D., (1976) Introduction to Chemical Engineering and Computer Calculations, Prentice-Hall, Englewood Cliffs, New Jersey
[123] Westerberg A.W., Hutchison H.P., Motard R.L., Winter P., (1979) Process Flowsheeting, Cambridge University Press, Cambridge
[124] Aspen PlusTM 2006-aspenONE, Getting Started Using Equation Oriented Modeling, Aspen Technology, Inc., Cambridge, MA.

List of publications

- Tijani, A. S., Witt, W., Dietzsch, L., (2007). Process and Plant Improvement Using Extended Exergy Analysis, a Case Study. *Revista de Chimie volume 4 pp 392-396.*
- Tijani, A. S., Witt, W., Multiobjective Optimization of Distillation Column Unit in Respect with Economic and Environmental Targets:
    I. Part I- Fundamentals and case study of power plant (*in progress*)
    II. Part II- Case study of distillation unit (*in progress*)
- Tijani, A. S., Naveed Ramzan, Witt, W. Integration of Solar Thermal Energy into Chemical Processes: Case Study of a Distillation Unit. *(in progress)*
- Tijani, A. S., Witt, W., Exergy analysis of Combine Distillation and Coal Power Plant. *(in progress)*

All papers in progress will be submitted in Chemical engineering Science *journal*

Supervision of master thesis and study project

- Rafael A. C. L., Werner Witt, Jörg Schmul, (2009) Combination of Solar Thermal Power with Distillation Process.
- Takoeta S., Werner W., Tijani, A. S., (2006) Energy Optimization and Pollution Control Measures in Petrochemical Industry, a Case Study of a Unit of British Petroleum Plant.

Supervision of bachelor thesis

- Elvis M. P., Werner W., Tijani, A. S., (2008). Combination of Solar Thermal Power Plant with Distillation Unit.